COPYRIGHT STATEMENT

The author hereby certifies that the use of any copyrighted material in the thesis

manuscript entitled:

" Pathogenesis of eastern equine encephalitis virus in mice and development of a second

generation vaccine "

is appropriately acknowledged and, beyond brief excerpts, is with the permission of the

copyright owner.

Shelley P. Honnold

Department of Pathology

Uniformed Services University of the Health Sciences

31 January 2012

ABSTRACT

Title of Dissertation: Pathogenesis of eastern equine encephalitis virus in mice and development of a second generation vaccine

Shelley P. Honnold, Ph.D., 2012

Thesis directed by: Dr. Radha Maheshwari, Professor, Pathology Department

Eastern equine encephalitis virus (EEEV), an *Alphavirus* in the family *Togaviridae*, is an important human and veterinary pathogen, and is considered the most deadly of the mosquito-borne alphaviruses due to the high case fatality rate associated with clinical infections, reaching as high as 75% in humans and 90% in horses. In patients that survive, the neurologic sequelae are often devastating. Although natural infections are acquired by mosquito bite, EEEV is also highly infectious by aerosol. This fact, along with the relative ease of production and stability of this virus, has led it to being identified as a potential agent of bioterrorism.

Characterizing the early events in the pathogenesis of EEEV (FL93-939) by various routes of infection is an important first step in developing a vaccine to prevent disease. We hypothesize that when mice are challenged with EEEV either intranasally or via aerosol that the virus will enter the brain rapidly using the olfactory system, which will have important implications for therapeutic and vaccine development.

The goal of vaccine development is to produce a product that closely mimics natural infection; thereby stimulating an appropriate and effective immune response. However, new EEEV vaccine candidates should protect against both subcutaneous and aerosol exposure to virulent virus, which can be challenging. Formalin, INA, and gamma-irradiation have been used to inactivate viruses and have recently been used to inactivate V3526. Inactivating an attenuated-live virus provides an additional layer of safety in the formulation of the vaccine candidate. We hypothesize that formalin, INA, and gamma-irradiation will inactivate a genetically modified strain of EEEV (CVEV1219) but will maintain its antigenic epitopes, thereby creating a valid vaccine candidate that will result in protective immune responses in mice when challenged by the parental virus (EEEV FL93-939).

EEEV is listed as a category B agent by the National Institute of Allergy and Infectious Diseases (NIAID) due to its virulence, its potential use as a biological weapon, and the lack of a licensed vaccine or effective antiviral treatment for human infections. Therefore, research directed towards the development of a safe and effective vaccine and antiviral treatment for humans is essential.

PATHOGENESIS OF EASTERN EQUINE ENCEPHALITIS VIRUS IN MICE

AND

DEVELOPMENT OF A SECOND GENERATION VACCINE

By

Shelley P. Honnold

Dissertation submitted to the Faculty of the
Pathology Graduate Program
Uniformed Services University of the Health Sciences
in partial fulfillment of the requirements for the degree of
Doctor of Philosophy 2012

ACKNOWLEDGEMENTS

First and foremost, I thank the Lord, for through Him all things are possible. I am very grateful to the U.S. Army, USUHS and the Pathology Department, as well as USAMRIID and the Virology Division for giving me the opportunity to pursue my goals. I express my thanks to all the USUHS faculty and staff for their time and dedication in developing and supporting the graduate program curriculum, it was a great learning experience. A special thanks to Dr. Radha Maheshwari, my advisor, and his lab, especially, Anuj Sharma, Paridhi Gupta, and Manish Bhomia, who mentored and supported me from the first day to the last, providing advice, technical guidance, and most importantly friendship. I thank all of my committee members: Dr. Kagan, for being willing to chair this committee, as well as Drs. Radha Maheshwari, Pam Glass, Keith Steele, and Robert Friedman for their time and effort, their mentorship, and enduring support. I especially thank Dr. Steele for his thoughtful discussions on infectious disease pathology.

My deepest gratitude to Drs. Mike Parker and Pam Glass at USAMRIID for their willingness to support this research in their BSL3 laboratory. Pam, I am forever grateful for the opportunity to work with you. Thank you for being an outstanding mentor, for sharing your knowledge, expertise, and enthusiasm, and for always being available to discuss issues, big and small. I will cherish our many discussions and will miss the spontaneous scientific reflections. Above all, thank you for your support and friendship, which has been invaluable over the last several years, and I look forward to the many exciting collaborations that lay ahead. I could not have done this work without the help

of the Glass lab, including Dr. Kevin Spurgers, Russ Bakken, Jeff Cohen, Cathy Lind, Lori Rowan, and Laura Prugar. Russ, your animal skills are unmatched! Cathy, thank you for teaching me the ropes in the laboratory, from large scale virus preparation to the numerous and very large plaque assays and PRNTs, you were always ready and eager to help. Jeff, Lori, and Laura, I am incredibly grateful your assistance with the various studies, I could not have done it without you! I thank Dr. Stephen Bradfute for his help and guidance with the cytokine study. A special thanks to the Aerobiology Division, especially Rebecca Erwin-Cohen, for teaching me the ins-and-outs of the aerosol exposure system, for the many intellectually stimulating and thought provoking scientific discussions, but especially for your friendship and support.

Most of all, I thank my friends and family. To all my friends, thank you for your endless support and encouragement! I am forever grateful to my mom and dad, who have taught me to work hard, to pursue my dreams and willingly accept the sacrifices, and to always be grateful for all the Lord has provided. Thank you both for your unwavering support, it has constantly given me strength when I needed it most. My deepest gratitude to my husband, Cary, who has been my biggest supporter for over 17 years. Thank you for your never-ending encouragement, your numerous sacrifices, and most of all for your steadfast friendship. I could not have done this without you! I am so extraordinarily blessed to have you as my husband and my best friend. To my son Jacob, who at 3 years old is too young to realize all that he has given me. Thank you for always putting a smile on my face, no matter how long or difficult the day. Your hugs and kisses, laughter and joy, and endless sweet expressions were a constant source of strength.

TABLE OF CONTENTS

LIST OF FIGURES

Chapter 1

General Introduction

Overview of Alphaviruses

Alphaviruses are single-stranded, enveloped, positive-sense RNA viruses that belong to the *Togaviridae* family. There are currently 28 virus species in the *Alphavirus* genus, which can be classified into at least 7 groups based on antigenic complex homology. Alphaviruses cycle between invertebrate insect vectors and vertebrate reservoir hosts. For most alphaviruses, the insect vectors are mosquitoes; however, lice and mites can also serve as vectors for some alphaviruses. The vertebrate hosts are generally birds and mammals; however, fish and primates can serve as vertebrate hosts for select alphaviruses. Although the alphaviruses have worldwide geographic distribution, they have classically been described as Old World or New World viruses based on their predominant distribution. The Old World alphaviruses, typically found in Africa and Asia, primarily cause a rash and arthritis, while the New World alphaviruses, typically found in North and South America, often cause encephalitis. However, based on phylogenetic analysis, alphaviruses most likely originated in the Americas and later spread to the rest of the world (Griffin DE 2007). Sindbis virus is the type-member of the alphavirus genus and has been extensively studied due to its ease of growth in culture and its relatively low virulence in humans.

The alphavirus virion is spherical, 60-70 nm in diameter, and is composed of a single plus-strand of RNA, which is surrounded by a capsid formed by a single protein arranged as an icosahedron with T=4 symmetry. This nucleocapsid is surrounded by a lipid envelope composed of the host cell plasma membrane that is rich in cholesterol,

sphingolipid, the viral-encoded glycoproteins E1and E2, as well as smaller amounts of a membrane associated protein called 6K (Gaedigk-Nitschko K and MJ 1990; Paredes AM, Brown DT et al. 1993; Cheng RH, Kuhn RJ et al. 1995; Griffin DE 2007). There are 240 copies of the E1 and E2 transmembrane glycoproteins. These form heterodimers and are further grouped as trimers, resulting in the formation of 80 knobs on the virion surface. E1 is the more conserved glycoprotein of the alphaviruses (Strizki and Repik 1995), the E2 glycoprotein contains the most significant epitopes for neutralizing antibody (Griffin DE 2007).

The alphavirus genome is generally 11-12 kilobases in size (Griffin DE 2007). The replication or nonstructural proteins (nsP) are located in the 5' two-thirds of the genome, while the virion or structural proteins are located in the 3' one-third of the genome. There are 4 nonstructural proteins (nsP1, nsP2, nsP3, nsP4) and five structural proteins (capsid (C), E1, E2, E3, and 6K) (Griffin DE 2007). And while the nonstructural proteins are translated from the genomic RNA, the structural proteins are translated from a subgenomic mRNA (Simmons DT and JH 1972).

The alphaviral lifecycle is depicted in Figure 1.1. Binding of the virus to the cell surface and entry into the cell is a complex process which depends on both viral and host cell factors including virus glycoproteins E1 and E2, cell surface molecules, low pH in the endosome, and fusion of membrane lipids (Griffin DE 2007). After attachment, the virus in endocytosed utilizing a clathrin-dependent pathway (Helenius A, Kartenbeck J et al. 1980; Marsh M, Bolzau E et al. 1983; DeTulleo L and T 1998; Griffin DE 2007). Acidification of the vesicle then triggers membrane fusion, releasing the genomic RNA
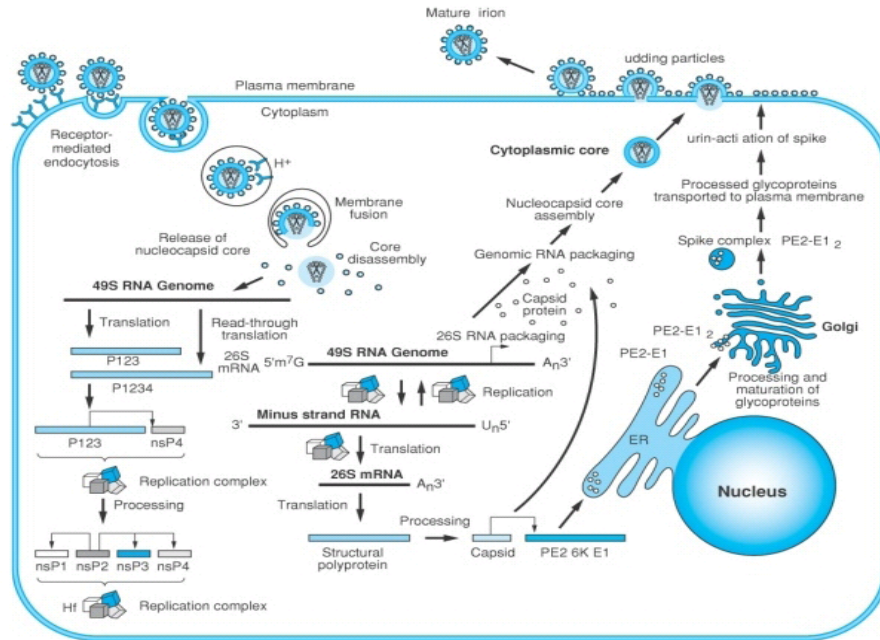
Figure 1.1. Alphavirus lifecycle (Kuhn RJ 2007)

into the cytoplasm (White J, J et al. 1980; Glomb-Reinmund S and M 1988). Upon

release into the cytoplasm, the nucleocapsid is uncoated and the genomic RNA serves as

a messenger RNA for the synthesis of the nonstructural or replication proteins.

Translation results in two polyproteins, either P123, which is smaller but more abundant,

or P1234, which is larger, but only accounts for 10-20 percent of the polyprotein found in

the cell (Hardy RW and JH 1988; Ding M and MJ 1989). The nonstructural proteins

(nsP1, nsP2, nsP3, and nsP4) are the primary mediators of viral replication and also

perform a number intracellular functions which have mostly been elucidated using SINV

and SFV (Table 1.1) (Reichert, Clase et al. 2009). While the nonstructural proteins

continue to be translated as the minus strand is synthesized. As with other plus strand

RNA viruses, synthesis is asymmetric with minus strand synthesis accounting for only

Table 1.1. Identified functions and enzymatic activities of Alphaviral nonstructural proteins*

Protein	Function/Enzymatic Activity
nsP1	Methyltransferase
	Guanyltransferase
	Minus strand RNA sythesis
nsP2	Protease
	Helicase
	NTPase
	5'triphosphatase activity
	Host transcription inhibition
nsP3	Minus strand RNA sythesis
nsP4	RNA-dependent RNA polymerase
	Adenlytransferase

*Adapted from Reichert et. al., 2009.

about 2-5 percent of the level of plus strand genomic RNA (Wang YF, Sawicki SG et al. 1991). The structural polyprotein is translated in a specific order: capsid, PE2 (E3+E2), 6K, E1 and is then processed by host and viral proteases to form the final structural proteins that will make up the virion (Frolov I and S 1996). Most alphaviruses package their genomes with high efficiency and the development of alphaviruses as gene expression vectors has lead to more studies in this area. The final stage of the virus life cycle is virus budding, which requires effective interaction between the capsid protein and the glycoproteins (Kuhn RJ 2007).

The alphavirus genus is composed of a group of antigenically related viruses that cycle between a variety of invertebrate insect vectors, primarily mosquitoes, and vertebrate reservoir hosts, which may include mammals, birds, and even fish. While, the geographic distribution of the specific invertebrate vectors and reservoir hosts largely determines the distribution of the specific alphaviral disease, alphaviruses have been found on all of the major continents. And although the alphaviruses can generally be

broken down into two major groups, the Old World group that mainly manifests primarily as a rash and arthritis, and the New World group that mainly causes encephalitis, it is becoming increasingly clear that the outcome of infection with any one alphavirus depends on a wide variety of host and viral factors. Understanding the pathogenesis of each of the alphaviruses at the molecular, cellular, tissue and organism level will aid in identifying, understanding, and controlling as many of the host and viral factors as possible, and ultimately will be instrumental in developing effective vaccines and therapeutics.

History and Epidemiology of EEEV

The first recorded epidemic of equine encephalitis, resulting in the death of 75 horses, occurred in Massachusetts in 1831. However, it was not until 1933 that eastern equine encephalitis virus (EEEV) was isolated from the brains of horses in New Jersey and Virginia (Tenbroeck, Hurst et al. 1935). And it was not until five years later, in 1938, that EEEV was linked to a human outbreak that resulted in fatal encephalitis in 30 children (Webster and Wright 1938). Since then approximately 5-8 human cases have been reported to the CDC each year (2006).

The EEEV complex is divided into four distinct lineages, I-IV which differ in geographic, epidemiologic, phylogenetic, and pathogenic characteristics (Brault, Powers et al. 1999; Arrigo, Adams et al. 2010). Group I is composed of the strains enzootic along the eastern seaboard and Gulf Coast of North America (NA) and the Caribbean. The strains in this group are highly conserved, monophyletic, and temporally-related, and are responsible for the majority of human cases, with significant mortality rates in

humans and equines. Groups II, III, and IV are composed of the strains enzootic in Central America, along the north and east coasts of South America (SA), and in the Amazon River Basin. The strains in these groups are highly divergent, polyphyletic, co-circulating, geographically-associated, and primarily result in equine disease (Arrigo, Adams et al. 2010).

In North America, the enzootic cycle of NA EEEV is maintained in shaded swamps, where the virus cycles between ornithophilic mosquitoes, primarily *Culiseta melanura*, and passerine birds. Humans, horses and other mammals are considered dead-end hosts and generally only become infected when bridge vectors, zoophilic mosquitoes such as *Aedes* sp. and *Coquillettidia* sp., feed on an infected bird and then a mammal. Outbreaks in humans, often seen in the late summer or early fall, are frequently preceded by cases of equine encephalitis and are usually associated with heavy rainfall and warmer water temperatures (Letson, Bailey et al. 1993; Griffin DE 2007).

In Central and South America, the enzootic cycle of SA EEEV is less understood due to lack of human pathogenicity and limited research. SA EEEV has been isolated from *Culex* (*Melanoconion*) spp., which are found primarily in tropical forest habitats. However, the vertebrate ecology of SA EEEV is not well understood and serological associations with wild birds, ground-dwelling rodents, marsupials, and reptiles have been reported (Monath, Sabattini et al. 1985; Arrigo, Adams et al. 2010). SA EEEV has caused sporadic epizootics in horses, and although seroconversion in humans has been documented in these regions, there have been only 2 reported fatal human encephalitis cases in more than 50 years, compared to over 180 documented EEE cases in North America (Corniou, Ardoin et al. 1972; Aguilar, Robich et al. 2007).

Disease in Humans and Animals

EEEV is the most virulent of the encephalitic alphaviruses, resulting in fatal encephalitis in 30-75% of human patients (Calisher 1994; Deresiewicz, Thaler et al. 1997). Both sexes are equally susceptible to EEEV infection; however, disease in children less than 15 years old and adults over 55 years old is more likely to result in encephalitis and death. The patient's clinical history often involves exposure to wooded areas adjacent to swamps or marshes. EEEV infection can be asymptomatic, or result in systemic or encephalitic disease. In one study, during the 1959 outbreak in New Jersey, the ratio of apparent to inapparent infection was 1:23 (Goldfield, Welsh et al. 1968). Generally, the incubation period in humans is short, usually 4-10 days. Systemic infection is often characterized by abrupt onset of chills and fever followed by malaise, arthralgia, and myalgia. Illness usually lasts 1-2 weeks with complete recovery. Clinical signs of encephalitis include abrupt onset of severe fever, intense headache, irritability, restlessness, drowsiness, anorexia, nausea, vomiting, diarrhea, cyanosis, convulsions, and coma. Children often present with generalized, facial, or periorbital edema. Death usually occurs within 2-14 days after the onset of clinical signs (Calisher 1994). Of the individuals that survive, approximately 50-75% have severe neurologic sequelae, such as seizure disorders, hemi- or quadriplegia, and profound mental retardation and many patients with severe sequelae die within a few years (Przelomski, O'Rourke et al. 1988; Letson, Bailey et al. 1993; Calisher 1994; Deresiewicz, Thaler et al. 1997; 2006). Gross lesions include edema, meningeal congestion, hemorrhage, and encephalomalacia. Histopathologic lesions include vasculitis, thrombosis, perivascular cuffing, neutrophilic

and histiocytic infiltrates, neuronal cell death, neuronophagia, focal necrosis, demyelination, and gliosis. The basal ganglia, thalamus, and brain stem are preferentially affected and antemortem neuroradiographic abnormalities are often identified using CT or MRI (Deresiewicz, Thaler et al. 1997).

EEEV infection has been documented in a number of animal species, including horses (Ross and Kaneene 1996; Del Piero, Wilkins et al. 2001), cattle (Pursell, Mitchell et al. 1976), camels, llamas and alpacas (Nolen-Walston, Bedenice et al. 2007), sheep (Bauer, Gill et al. 2005), pigs (Pursell, Peckham et al. 1972; Elvinger, Liggett et al. 1994), emus (Veazey, Vice et al. 1994), dogs (Farrar, Miller et al. 2005), white tailed deer (Tate, Howerth et al. 2005; Schmitt, Cooley et al. 2007), black bears (Dunbar, Cunningham et al. 1998), African penguins (Tuttle, Andreadis et al. 2005), a harbor seal (McBride, Sims et al. 2008), turkeys (Guy, Siopes et al. 1995), chickens (Day and Stark 1996), pheasants (Williams, Fulton et al. 2000), and a variety wading birds (Spalding, McLean et al. 1994; McLean, Crans et al. 1995; Gottdenker, Howerth et al. 2003). In areas where EEEV is endemic, cases of encephalitis in horses are often diagnosed before those in humans. Horses may present with fever, acute neurologic signs including ataxia, profound changes in sensorium, hyperexcitability, restlessness, depression, or abdominal signs such as colic. The prognosis for EEE in horses is poor and many animals are euthanized. Gross lesions are often unremarkable; however, histopathologic lesions are similar to those seen in humans. Lesions include diffuse polioencephalomyelitis and leptomeningitis, often with moderate numbers of perivascular and parenchymal neutrophils. The cerebral cortex, thalamus, hypothalamus, and mesencephalon were

preferentially affected in one report (Del Piero, Wilkins et al. 2001). Often there is

neuronal degeneration and death, neuronophagia, and gliosis.

Animal Models of EEEV

Although EEEV has not been as well studied as other alphaviruses such as VEEV,

there have been several animals models utilized over the years, including mice (Liu, Voth

et al. 1970; Mathews and Roehrig 1989; Aguilar, Paessler et al. 2005; Vogel P, Kell WM

et al. 2005; Aguilar PV, Adams AP et al. 2008; Gardner, Burke et al. 2008; Gardner, Yin

et al. 2009), hamsters (Dremov, Solyanik et al. 1978; Paessler, Aguilar et al. 2004),

guinea pigs (Roy, Reed et al. 2009), rabbits (Dremov and Solianik 1977), and nonhuman

primates (Hurst 1936; Pratt, Hart et al. 2006; Reed, Lackemeyer et al. 2007; Adams,

Aronson et al. 2008; Espinosa, Weaver et al. 2009). In a recent review, the pathology of

the various animal models has been described (Steele and Twenhafel 2010), and as with

many diseases, the mouse model, while not perfect, has been the best characterized and

most frequently utilized.

As with other alphaviruses, newborn mice are the most susceptible to EEEV, with

resistance to peripheral infection occurring between 4-8 weeks of age (Morgan 1941; Liu,

Voth et al. 1970; Vogel P, Kell WM et al. 2005; Pratt, Hart et al. 2006; Steele and

Twenhafel 2010). In a recent study by Vogel et. al., 5-week-old female mice exhibited a

biphasic disease course, similar to that seen in humans, where the virus initially

replicated in peripheral tissues, followed by viremia, CNS invasion and eventually

encephalitis after peripheral inoculation with EEEV (FL91-4679). Mice began to show

clinical signs, such as lethargy and ruffled fur, 1 day post-infection (p.i.). By 4 days p.i.

clinical signs included hunching, tremors, seizures, and prostration. Animals succumbed to infection or were sacrificed 4 days after peripheral inoculation. In this study, primary viral replication occurred in fibroblasts, osteoblasts, and skeletal myocytes, with little to no viral replication in lymphoid tissues. Virus was first detected in the brain 1 day p.i. with rapid interneuronal spread resulting in death by day 4 p.i.. In this study, there was simultaneous multifocal infection of neurons and fewer glial cells, with minimal involvement of the olfactory neuroepithelium, suggesting invasion of the CNS occurred by the vascular route. Lesions in these mice included widespread neuronal necrosis that preferentially affected the caudate nucleus/putamen, thalamus, and the pons. In addition, there was rarefaction of the adjacent neuropil and some white matter tracts, and mild inflammation with infiltrates of neutrophils and eosinophils. However, unlike some human cases of EEE, mice did not appear to have vasculitis associated with infection (Vogel P, Kell WM et al. 2005).

The golden hamster has recently been studied as a possible animal model for EEEV (Paessler, Aguilar et al. 2004; Pratt, Hart et al. 2006; Steele and Twenhafel 2010). Paessler et. al. inoculated 6-8 week-old female hamsters with NA EEEV strain 79-2138 subcutaneously. These animals developed a fever within 24 hours and other clinical signs such as head-pressing, vomiting, lethargy, and anorexia by 2-3 days p.i.. This was followed by respiratory signs and stupor and coma by 4-5 days p.i., with all animals succumbing to infection by 5-6 days p.i. Virus was present in the brain, lung, liver, kidney, spleen, and skeletal and cardiac muscle. Histologic lesions included vasculitis, characterized by infiltration of vessel walls by mononuclear cells and neutrophils with associated hemorrhage, neuronal destruction, neuronophagia, and mild lymphocytic,

neutrophilic, and histiocytic inflammation, with early involvement of the basal ganglia and brainstem.

EEEV causes encephalitis in guinea pigs when administered intracranially, intramuscularly, subcutaneously, or intradermally. In a recent study by Roy et. al., 8-10 week-old Hartley guinea pigs were challenged by aerosol with two regionally distinct EEEV strains, NA strain NJ1959 or SA strain ArgM. There was no significant difference in clinical signs, time to death, viral titer, or histological lesions between strains. Clinical signs in guinea pigs included decreased activity and dorsal tremors that progressed to head tilt, circling, lateral recumbency, coma, and death. Virus was isolated from the liver, lung, brain, and blood in all animals. Virus isolation and immunohistochemistry indicated that both strains invaded the brain within one day post-exposure via the olfactory system, which then lead to rapid widespread infection. Neurons were the main cellular target and histologic lesions included neuronal necrosis, perivascular cuffs, mild heterophilic and histiocytic infiltrates in the neuropil, and vasculitis in some late-stage cases (Roy, Reed et al. 2009; Steele and Twenhafel 2010).

EEEV has also been studied in several NHP species, including juvenile rhesus macaques (Nathanson, Stolley et al. 1969), cynomolgus macaques (Reed, Lackemeyer et al. 2007), common marmosets (Adams, Aronson et al. 2008), and owl monkeys (Espinosa, Weaver et al. 2009). Reed et al. conducted a study to examine the disease course of aerosolized EEEV (FL91-4679) in adult cynomolgus macaques and the majority of animals developed fever, viremia, and neurologic signs (recumbancy and coma), and succumbed 5-9 days post-infection (Reed, Larsen et al. 2005). The major histopathologic lesions included severe meningoencephalomyelitis with widespread

neuronal necrosis, satellitosis, gliosis, perivascular cuffs, vasculitis, edema, and

hemorrhage (Steele and Twenhafel 2010). In a recently published study by Adams et al.,

common marmosets (*Callithrix jacchus*) were challenged with either NA EEEV (FL93-

939) or SA EEEV (BeAr436087) intranasally. The animals challenged with the NA

strain of EEEV succumbed to infection or were euthanized by day 4-5 p.i., while those

challenged with the SA strain of EEEV did not develop clinical disease. Interestingly,

those challenged with the NA strain did not develop a detectable viremia, yet virus was

detected in the brain, liver, and muscle, and all animals developed meningoencephalitis

and perivascular hemorrhage in the cerebral cortex. Lastly, in the most recent study,

Espinosa et al. investigated the suitability of owl monkeys as an animal model for EEEV.

Two to four year old owl monkeys were challenged either subcutaneously (SC) or

intranasally (IN) with 10^4 pfu of virulent EEEV (EEEV FL93-939). None of the animals

from either group exhibited clinical signs. Only the SC inoculated group developed

viremia and mounted an immune response. Two animals from each group were

necropsied on day 6 p.i. and neither had gross or histologic lesions (Espinosa, Weaver et

al. 2009).

Pathogenesis of EEEV (FL93-939)

There is little known about the pathogenesis of NA EEEV (FL93-939), a strain that

was initially isolated from a mosquito pool in Florida in 1993 (Aguilar, Paessler et al.

2005). Unlike many of the NA EEEV strains, this strain is virulent in adult mice when

inoculated peripherally. It has recently been used in an attempt to elucidate the

mechanism(s) by which the NA strains of EEEV cause such significant disease in

humans and mammals compared to the SA strains of EEEV, which rarely result in encephalitis. Aguilar et al. hypothesized that the difference in virulence was due to a greater ability of NA strains to evade the innate immune system. They found that *in vitro*, human IFN-α, -β, and –γ generally exhibited less effect on replication of NA (FL93-939) than SA (BeAr436087) strains of EEEV in Vero cells. However, in the murine model, they found no significant difference in IFN induction between the strains, nor did they find a significant difference in viremia levels or survival times in mice deficient in either IFN-α/β or - γ receptors compared to wild-type mice (Aguilar, Paessler et al. 2005).

Gardner et al. also assessed the role of Type I IFN responses in NA (FL93-939) versus SA (BeAr436087) EEEV strains; however, their results differed from those found by Aguilar et al.. In this study the strains were similarly sensitive to IFN-α/β priming *in vitro* but FL93-939 induced a significantly lower systemic IFN-α/β release compared to BeAr436087 *in vivo*. The results of this study showed that FL93-939 initially replicated less efficiently than BeAr436087 in lymphoid and other tissues in 6-week-old CD1 mice. And importantly, while BeAr432087 was cleared from the brain by 120 hours p.i., FL93-939 virus titers continued to rise. Additionally, BeAr436087 was more virulent than FL93-939 in IFN- α/β deficient mice, confirming that Type I IFNs play an important role in the attenuation of this SA strain (Gardner, Yin et al. 2009).

The importance of initial cellular tropism and induction of a systemic Type I IFN response is also highlighted in another paper by Gardner et al. where they compared the cellular tropism *in vitro* and *in vivo* between VEEV (ZPC738) and EEEV (FL93-939). They demonstrated that the infectivity of EEEV for dendritic cells and macrophages was

dramatically reduced compared to VEEV, whereas both viruses replicated efficiently in osteoblasts and fibroblasts *in vitro*. They confirmed these results *in vivo* using 6- to 8-week-old CD1 mice and found that the reduced ability of EEEV to replicate in lymphoid tissue directly correlated with an almost complete avoidance of a systemic Type I IFN response (Gardner, Burke et al. 2008).

Significance and Military Relevance

EEEV is listed as a category B priority agent by the National Institute of Allergy and Infectious Diseases (NIAID) because of its virulence, its potential use as a biological weapon, and the lack of a licensed vaccine or an effective treatment for human infections. Developing an effective vaccine against a peripheral challenge is an important initiative of the CDC as mosquito transmitted EEEV, although uncommon, is a devastating and costly disease. Developing an effective vaccine against an aerosol challenge is an important initiative for the Department of Defense due to its potential use as a biological weapon. Creating a single vaccine that is effective against both subcutaneous and aerosol challenge is a universal objective that has yet to be achieved.

Summary and Specific Aims

Eastern equine encephalitis virus (EEEV), an arbovirus (arthropod-borne), is an important human and veterinary pathogen belonging to one of seven antigenic complexes in the genus *Alphavirus*, family *Togaviridae*. It is considered the most deadly of the mosquito-borne alphaviruses due to the high case fatality rate associated with clinical infections, reaching as high as 75% in humans and 90% in horses. In patients that

survive, the neurologic sequelae are often devastating and include severe mental retardation, seizures, and paralysis.

There are four antigenic subtypes of EEEV, one that circulates in North America (NA EEEV) and the Caribbean, and three that circulate in Central and South America (SA EEEV). The strains differ in their geographic, epidemiologic, pathogenic, phylogenetic, and evolutionary characteristics. While NA EEEV results in approximately 5-8 human cases yearly in the United States, often with devastating outcomes; SA EEEV has little to no association with human disease, despite evidence of human exposure in endemic areas. Understanding the molecular differences between these strains will provide useful information in therapeutic and vaccine development.

EEEV is also listed as a category B agent by the National Institute of Allergy and Infectious Diseases (NIAID) due to its virulence, its potential use as a biological weapon, and the lack of a licensed vaccine or effective antiviral treatment for human infections. Therefore, research directed towards understanding the pathogenesis of EEEV, the difference in virulence between NA EEEV and SA EEEV strains, and the development of a safe and effective vaccine and antiviral treatment for humans is pertinent and essential. Recently, a NA EEEV strain (FL93-939) has been used in several studies because of its uniform virulence in adult mice. However, little is known about the early events in the pathogenesis of this strain, which are important to understand prior to challenging animal models in vaccine development protocols.

New vaccine candidates should protect against both subcutaneous and aerosol exposure to virulent virus, which can be challenging. While genetically-modified live viruses often induce a strong immune response, they are not without safety concerns,

which was recently experienced when V3526 was transitioned to phase-I clinical trials.

Inactivating a genetically-modified live virus provides an additional layer of safety as

these vaccines are unable to replicate in the host. Several chemical compounds that have

historically been used to inactivate viruses include formalin and gamma-irradiation.

Additionally, more recently, INA (1,5-iodonaphthylazide) has also been used

successfully to inactivate enveloped viruses. It is unique in that it preserves membrane

protein structural integrity and therefore is potentially useful for vaccine applications.

Using these methods to inactivate a genetically-modified strain of EEEV (CVEV1219)

may provide a much needed second-generation vaccine candidate for further evaluation.

To address the need for further understanding of the pathogenesis of NA EEEV

(FL93-939), and to address the need for an effective vaccine against subcutaneous and

aerosol exposure to NA EEEV strains, the specific aims of these studies were the

following:

Specific Aim 1: Characterize and compare the pathogenesis of EEEV (FL93-939) in
BALB/c mice infected by the aerosol, subcutaneous and intranasal routes of
infection

1. A time course study was performed to characterize the pathogenesis of EEEV

   FL93-939. Mice were infected by the intranasal, aerosol, or subcutaneous route

   and animals were euthanized at specified time points, including 6 hours post-

   infection (p.i), 12 hours p.i., 1 day p.i., 2 days p.i., 3 days p.i., 4 days p.i., and 5

   days p.i.. For the subcutaneous route of exposure, collection time points also

   included 6 days p.i, 7 days p.i. and 8 days p.i.

2. Immunohistochemistry (IHC) of tissues was performed to identify virally infected cells at the various time points to elucidate target cells/tissues over the course of infection and identify cells/sites of viral amplification when animals are exposed by different routes.

3. Histopathological evaluation of select tissues was performed to characterize the light microscopic changes in infected tissues.

4. Viral titer of target tissues by standard plaque assay was performed in order to determine peak viral titer over the course of infection and to correlate viral titers with IHC and histologic findings.

5. Immunohistochemical analysis was performed on mouse brain tissue from the aerosol study to evaluate the mechanism of neuronal cell death using antibodies to detect apoptosis and autophagy.

Specific Aim 2: Optimize the inactivation of CVEV1219 using formalin, INA, and gamma-irradiation; and validate the inactivation of CVEV1219 *in vitro* and *in vivo*

1. Protocols were optomized to inactivate various amounts of CVEV1219 using formalin (fCVEV1219), INA (iCVEV1219), and gamma-irradiation (gCVEV1219).

2. Residual infectivity of inactivated CVEV1219 virus (iEEEV) was determined *in vitro* by using a multi-system approach (cell passage, standard plaque assay, and indirect immunofluorescence).

3. Residual infectivity of iEEEV was determined *in vivo* by using the suckling mouse model.

Specific Aim 3: Determine the immunogenicity and protective efficacy of inactivated CVEV1219 (iEEEV) vaccine candidates

1. Mice were given varying doses (0.1 µg – 5 µg) of iEEEV subcutaneously, intramuscularly, or intranasally, either once or twice using various vaccination protocols. Serum was collected 21 days after each immunization to analyze the immune response.

2. Serum and vaginal flush samples were analyzed for immunoglobulin responses: serum neutralizing antibody responses were measured by PRNT; virus-specific total IgG levels and the isotype specific antibodies (IgG1, IgG2a, IgG2b) were measured by ELISA to evaluate systemic antibody-mediated immune responses. Vaginal flush virus-specific IgA levels were measured by ELISA to evaluate mucosal antibody-mediated immune responses.

3. Splenocytes were analyzed for T and B cell responses: measurement of ex vivo T and B cell activation and immune function by flow cytometry using intracellular cytokine and surface antibody detection was used to evaluate the role of humoral and cell-mediated immunity (CMI)

4. Animals were aerosol challenged with wild-type virus EEEV strain FL93-939 after either the first or second immunization and monitored for 28 days for clinical signs of disease.

REFERENCES

(2006). "Eastern equine encephalitis--New Hampshire and Massachusetts, August-September 2005." MMWR Morb Mortal Wkly Rep **55**(25): 697-700.

Adams, A. P., J. F. Aronson, et al. (2008). "Common marmosets (Callithrix jacchus) as a nonhuman primate model to assess the virulence of eastern equine encephalitis virus strains." J Virol **82**(18): 9035-9042.

Aguilar PV, Adams AP, et al. (2008). "Structural and nonstructural protein genome regions of eastern equine encephalitis virus are determinants of interferon sensitivity and murine virulence." J Virol **82**(10): 4920-4930.

Aguilar, P. V., S. Paessler, et al. (2005). "Variation in interferon sensitivity and induction among strains of eastern equine encephalitis virus." J Virol **79**(17): 11300-11310.

Aguilar, P. V., R. M. Robich, et al. (2007). "Endemic eastern equine encephalitis in the Amazon region of Peru." Am J Trop Med Hyg **76**(2): 293-298.

Arrigo, N. C., A. P. Adams, et al. (2010). "Evolutionary patterns of eastern equine encephalitis virus in North versus South America suggest ecological differences and taxonomic revision." J Virol **84**(2): 1014-1025.

Bauer, R. W., M. S. Gill, et al. (2005). "Naturally occurring eastern equine encephalitis in a Hampshire wether." J Vet Diagn Invest **17**(3): 281-285.

Brault, A. C., A. M. Powers, et al. (1999). "Genetic and antigenic diversity among eastern equine encephalitis viruses from North, Central, and South America." Am J Trop Med Hyg **61**(4): 579-586.

Calisher, C. H. (1994). "Medically important arboviruses of the United States and Canada." Clin Microbiol Rev **7**(1): 89-116.

Cheng RH, Kuhn RJ, et al. (1995). "Nucleocapsid and glycoprotein organization in an enveloped virus." Cell **80**(4): 621-630.

Corniou, B., P. Ardoin, et al. (1972). "First isolation of a South American strain of Eastern Equine virus from a case of encephalitis in Trinidad." Trop Geogr Med **24**(2): 162-167.

Day, J. F. and L. M. Stark (1996). "Transmission patterns of St. Louis encephalitis and eastern equine encephalitis viruses in Florida: 1978-1993." J Med Entomol **33**(1): 132-139.

Del Piero, F., P. A. Wilkins, et al. (2001). "Clinical, pathologic, immunohistochemical, and virologic findings of eastern equine encephalomyelitis in two horses." Vet Pathol **38**(4): 451-456.

Deresiewicz, R. L., S. J. Thaler, et al. (1997). "Clinical and neuroradiographic manifestations of eastern equine encephalitis." N Engl J Med **336**(26): 1867-1874.

DeTulleo L and K. T (1998). "The clathrin endocytic pathway in viral infection." EMBO J **17**(16): 4585-4593.

Ding M and S. MJ (1989). "Evidence that Sindbis virus nsP2 is an autoprotease which processes the virus nonstructural polyprotein." Virology **171**: 280-284.

Dremov, D. P. and R. G. Solianik (1977). "[Use of rabbits for study of the neurovirulence of attenuated variants of eastern equine encephalomyelitis virus]." Virologie **28**(4): 263-269.

Dremov, D. P., R. G. Solyanik, et al. (1978). "Attenuated variants of eastern equine encephalomyelitis virus: pathomorphological, immunofluorescence and virological studies of infection in Syrian hamsters." Acta Virol **22**(2): 139-145.

Dunbar, M. R., M. W. Cunningham, et al. (1998). "Seroprevalence of selected disease agents from free-ranging black bears in Florida." J Wildl Dis **34**(3): 612-619.

Elvinger, F., A. D. Liggett, et al. (1994). "Eastern equine encephalomyelitis virus infection in swine." J Am Vet Med Assoc **205**(7): 1014-1016.

Espinosa, B. J., S. C. Weaver, et al. (2009). "Susceptibility of the Aotus nancymaae owl monkey to eastern equine encephalitis." Vaccine **27**(11): 1729-1734.

Farrar, M. D., D. L. Miller, et al. (2005). "Eastern equine encephalitis in dogs." J Vet Diagn Invest **17**(6): 614-617.

Frolov I and S. S (1996). "Translation of Sindbis virus mRNA: analysis of sequences downstream of the initiating AUG codon that enhance translation." J Virol **70**: 1182-1190.

Gaedigk-Nitschko K and S. MJ (1990). "The Sindbis virus 6K protein can be detected in virions and is acylated with fatty acids." Virology **175**(1): 274-281.

Gardner, C. L., C. W. Burke, et al. (2008). "Eastern and Venezuelan equine encephalitis viruses differ in their ability to infect dendritic cells and macrophages: impact of altered cell tropism on pathogenesis." J Virol **82**(21): 10634-10646.

Gardner, C. L., J. Yin, et al. (2009). "Type I interferon induction is correlated with attenuation of a South American eastern equine encephalitis virus strain in mice." Virology **390**(2): 338-347.

Glomb-Reinmund S and K. M (1988). "The role of low pH and disulfide shuffling in the entry and fusion of Semliki Forest virus and Sindbis virus." Virology **248**(2): 372-381.

Goldfield, M., J. N. Welsh, et al. (1968). "The 1959 outbreak of Eastern encephalitis in New Jersey. 5. The inapparent infection:disease ratio." Am J Epidemiol **87**(1): 32-33.

Gottdenker, N. L., E. W. Howerth, et al. (2003). "Natural infection of a great egret (Casmerodius albus) with eastern equine encephalitis virus." J Wildl Dis **39**(3): 702-706.

Griffin DE (2007). Alphaviruses. Fields Virology. Knipe DM, Griffin DE, Lamb RAet al. Philadelphia, Lippincott Williams & Wilkins**:** 1024-1067.

Guy, J. S., T. D. Siopes, et al. (1995). "Experimental transmission of eastern equine encephalitis virus and Highlands J virus via semen of infected tom turkeys." Avian Dis **39**(2): 337-342.

Hardy RW and S. JH (1988). "Processing of the nonstructural polyproteins of Sindbis virus: study of the kinetics in vivo using monospecific antibodies." J Virol **62**: 998-1007.

Helenius A, Kartenbeck J, et al. (1980). "On the entry of Semliki Forest virus into BHK-21 cells." J Cell Biol **84**: 404-420.

Hurst, E. W. (1936). "Infection of the rhesus monkey (Macaca mulatta) and the guinea-pig with the virus of equine encephalomyelitis." J Path Bact **42**: 371-402.

Kuhn RJ (2007). Togaviridae: The viruses and their replication. Fields Virology. Knipe DM, Griffin DE, Lamb RAet al. Philadelphia, Lippincott Williams & Wilkins**:** 1001-1022.

Letson, G. W., R. E. Bailey, et al. (1993). "Eastern equine encephalitis (EEE): a description of the 1989 outbreak, recent epidemiologic trends, and the association of rainfall with EEE occurrence." Am J Trop Med Hyg **49**(6): 677-685.

Liu, C., D. W. Voth, et al. (1970). "A comparative study of the pathogenesis of western equine and eastern equine encephalomyelitis viral infections in mice by intracerebral and subcutaneous inoculations." J Infect Dis **122**(1): 53-63.

Marsh M, Bolzau E, et al. (1983). "Penetration of Semliki Forest virus from acidic prelysosomal vacuoles." Cell **32**: 931-940.

Mathews, J. H. and J. T. Roehrig (1989). "Specificity of the murine T helper cell immune response to various alphaviruses." J Gen Virol **70 (Pt 11)**: 2877-2886.

McBride, M. P., M. A. Sims, et al. (2008). "Eastern equine encephalitis in a captive harbor seal (Phoca vitulina)." J Zoo Wildl Med **39**(4): 631-637.

McLean, R. G., W. J. Crans, et al. (1995). "Experimental infection of wading birds with eastern equine encephalitis virus." J Wildl Dis **31**(4): 502-508.

Monath, T. P., M. S. Sabattini, et al. (1985). "Arbovirus investigations in Argentina, 1977-1980. IV. Serologic surveys and sentinel equine program." Am J Trop Med Hyg **34**(5): 966-975.

Morgan, I. M. (1941). "INFLUENCE OF AGE ON SUSCEPTIBILITY AND ON IMMUNE RESPONSE OF MICE TO EASTERN EQUINE ENCEPHALOMYELITIS VIRUS." J Exp Med **74**(2): 115-132.

Nathanson, N., P. D. Stolley, et al. (1969). "Eastern equine encephalitis. Distribution of central nervous system lesions in man and Rhesus monkey." J Comp Pathol **79**(1): 109-115.

Nolen-Walston, R., D. Bedenice, et al. (2007). "Eastern equine encephalitis in 9 South American camelids." J Vet Intern Med **21**(4): 846-852.

Paessler, S., P. Aguilar, et al. (2004). "The hamster as an animal model for eastern equine encephalitis--and its use in studies of virus entrance into the brain." J Infect Dis **189**(11): 2072-2076.

Paredes AM, Brown DT, et al. (1993). "Three-dimensional structure of a membrane-containing virus." Proc Natl Acad Sci USA **90**(19): 9095-9099.

Pratt, W., M. K. Hart, et al. (2006). Alphaviruses. Biodefense Research Methodology and Animal Models. J. R. Swearengen. Boca Raton, Florida, CRC Taylor & Francis**:** 181-206.

Przelomski, M. M., E. O'Rourke, et al. (1988). "Eastern equine encephalitis in Massachusetts: a report of 16 cases, 1970-1984." Neurology **38**(5): 736-739.

Pursell, A. R., F. E. Mitchell, et al. (1976). "Naturally occurring and experimentally induced eastern encephalomyelitis in calves." J Am Vet Med Assoc **169**(10): 1101-1103.

Pursell, A. R., J. C. Peckham, et al. (1972). "Naturally occurring and artificially induced eastern encephalomyelitis in pigs." J Am Vet Med Assoc **161**(10): 1143-1147.

Reed, D. S., M. G. Lackemeyer, et al. (2007). "Severe encephalitis in cynomolgus macaques exposed to aerosolized Eastern equine encephalitis virus." J Infect Dis **196**(3): 441-450.

Reed, D. S., T. Larsen, et al. (2005). "Aerosol exposure to western equine encephalitis virus causes fever and encephalitis in cynomolgus macaques." J Infect Dis **192**(7): 1173-1182.

Reichert, E., A. Clase, et al. (2009). "Alphavirus antiviral drug development: scientific gap analysis and prospective research areas." Biosecur Bioterror **7**(4): 413-427.

Ross, W. A. and J. B. Kaneene (1996). "Evaluation of outbreaks of disease attributable to eastern equine encephalitis virus in horses." J Am Vet Med Assoc **208**(12): 1988-1997.

Roy, C. J., D. S. Reed, et al. (2009). "Pathogenesis of aerosolized Eastern Equine Encephalitis virus infection in guinea pigs." Virol J **6**(1): 170.

Schmitt, S. M., T. M. Cooley, et al. (2007). "An outbreak of Eastern equine encephalitis virus in free-ranging white-tailed deer in Michigan." J Wildl Dis **43**(4): 635-644.

Simmons DT and S. JH (1972). "Replication of Sindbis virus. I. Relative size and genetic content of the 26S and 49S RNA." J Mol Biol **71**: 599-613.

Spalding, M. G., R. G. McLean, et al. (1994). "Arboviruses in water birds (Ciconiiformes, Pelecaniformes) from Florida." J Wildl Dis **30**(2): 216-221.

Steele, K. E. and N. Twenhafel (2010). "Review paper: Pathology of animal models of alphavirus encephalitis." Vet Pathol **45**(7): 790-805.

Strizki, J. M. and P. M. Repik (1995). "Differential reactivity of immune sera from human vaccinees with field strains of eastern equine encephalitis virus." Am J Trop Med Hyg **53**(5): 564-570.

Tate, C. M., E. W. Howerth, et al. (2005). "Eastern equine encephalitis in a free-ranging white-tailed deer (Odocoileus virginianus)." J Wildl Dis **41**(1): 241-245.

Tenbroeck, C., E. W. Hurst, et al. (1935). "EPIDEMIOLOGY OF EQUINE ENCEPHALOMYELITIS IN THE EASTERN UNITED STATES." J Exp Med **62**(5): 677-685.

Tuttle, A. D., T. G. Andreadis, et al. (2005). "Eastern equine encephalitis in a flock of African penguins maintained at an aquarium." J Am Vet Med Assoc **226**(12): 2059-2062, 2003.

Veazey, R. S., C. C. Vice, et al. (1994). "Pathology of eastern equine encephalitis in emus (Dromaius novaehollandiae)." Vet Pathol **31**(1): 109-111.

Vogel P, Kell WM, et al. (2005). "Early events in the pathogenesis of eastern equine encephalitis virus in mice." Am J Pathol **166**(1): 159-171.

Wang YF, Sawicki SG, et al. (1991). "Sindbis virus nsP1 functions in negative-strand RNA synthesis." J Virol **65**: 985-988.

Webster, L. T. and F. H. Wright (1938). "RECOVERY OF EASTERN EQUINE ENCEPHALOMYELITIS VIRUS FROM BRAIN TISSUE OF HUMAN CASES OF ENCEPHALITIS IN MASSACHUSETTS." Science **88**(2283): 305-306.

White J, K. J, et al. (1980). "Fusion of Semliki Forest virus with the plasma membrane can be induced by low pH." J Cell Biol **87**(264-272).

Williams, S. M., R. M. Fulton, et al. (2000). "Diagnosis of eastern equine encephalitis by immunohistochemistry in two flocks of Michigan ring-neck pheasants." Avian Dis **44**(4): 1012-1016.

Chapter 2

Pathogenesis of Eastern Equine Encephalitis Virus in BALB/c mice

Abstract

Eastern equine encephalitis virus (EEEV), an arbovirus, is an important human and

veterinary pathogen belonging to one of seven antigenic complexes in the genus

Alphavirus, family *Togaviridae*. EEEV is considered the most deadly of the mosquito-

borne alphaviruses due to the high case fatality rate associated with clinical infections,

reaching as high as 75% in humans and 90% in horses. In patients that survive, the

neurologic sequelae are often devastating (Griffin DE 2007). Although natural infections

are acquired by mosquito bite, EEEV is also highly infectious by aerosol. This fact,

along with the relative ease of production and stability of this virus, has led it to being

identified as a potential agent of bioterrorism.

To characterize the early events in the pathogenesis of EEEV strain FL93-939, we

compared the clinical parameters, viral titers in the blood and target tissues, and

histologic and immunohistochemical findings in mice exposed to this virus by various

routes. Twelve-week-old female BALB/c mice were infected by the intranasal, aerosol,

or subcutaneous route. Mice were then euthanized at specified time points (6 hpi through

8 dpi) and tissues harvested for viral titer determination and histopathological analysis.

Although all groups of animals exhibited similar clinical signs after inoculation, the onset

and severity were different, with the majority of those exposed by the aerosol route

developing severe clinical signs by 4 dpi. Significant differences were also found in the

viral titers of target tissues as well as the presence of viral antigen as determined by

immunohistochemistry. Virus was detected in the brain by titer at 6 hpi in the aerosol

study. Additionally, viral antigen was detected by immunohistochemistry at early times post-infection in the nasal cavity and olfactory bulb in both the intranasal and aerosol studies confirming that EEEV enters the brain through the olfactory system when mice are exposed by these routes of infection. In contrast, the clinical signs of disease, viral titers, and histopathologic lesions were delayed in the subcutaneous group and it appears the virus may utilize both the vascular and olfactory routes to enter the brain when mice are exposed to EEEV subcutaneously.

Introduction

Eastern equine encephalitis virus (EEEV) is considered the most deadly of the mosquito-borne alphaviruses due to the high case fatality rate associated with clinical infections. There are four antigenic subtypes of EEEV, one that circulates in North America and the Caribbean (NA EEEV), and three that circulate in Central and South America (SA EEEV). The strains differ in their geographic, epidemiologic, pathogenic, phylogenetic, and evolutionary characteristics. NA EEEV strains are highly conserved, monophyletic, and temporally related, while SA EEEV strains are highly divergent, polyphyletic, co-circulating, and geographically associated (Arrigo, Adams et al. 2010). NA EEEV results in approximately 5-8 human cases yearly, often with devastating outcomes, while SA EEEV has little to no association with human disease, despite evidence of human exposure in endemic areas (2006).

NA EEEV is also listed as a category B agent by the National Institute of Allergy and Infectious Diseases (NIAID) due to its virulence, its potential use as a biological weapon, and the lack of a licensed vaccine or effective antiviral treatment for human

infections. Therefore, research directed towards understanding the pathogenesis of EEEV, the difference in virulence between NA EEEV and SA EEEV strains, and the development of a safe and effective vaccine and antiviral treatment for humans is essential. However, research has been hampered by the fact that mice develop age-dependent resistance to peripheral infection. Recently, a North American (NA) strain of EEEV, FL 93-939, has been shown to be virulent in adult mice when administered peripherally, but there is limited information regarding the pathogenesis of this strain, with most studies focusing on how Type I IFN induction is decreased in mice infected with FL93-939 (Aguilar, Paessler et al. 2005; Gardner, Burke et al. 2008; Gardner, Yin et al. 2009). Characterizing the early events in the pathogenesis of EEEV strain FL93-939 in mice using various routes of infection is an important first step in developing a vaccine to prevent the disease.

We chose to compare the intranasal (IN) and aerosol (AE) routes of exposure to the more well characterized subcutaneous (SC) route of exposure for several reasons. First, many investigators utilize the IN route in place of the AE route of exposure due to the lack of equipment necessary to carry out an AE exposure. Secondly, as a potential military bioweapon, EEEV would most likely be formulated for AE exposure. Lastly, we hypothesized that the pathogenesis would differ depending on the route of exposure, which would be important in vaccine development.

EEEV strain FL93-939 LD$_{50}$ Studies

In order to develop equivalent pathogenesis studies by the various routes of exposure, the LD$_{50}$ of EEEV strain FL93-939 had to first be determined for each of the

routes. This was done using a stair-step approach such that each group of mice received logarithmic increases in viral dose by each route of infection (IN, AE, SC).

Materials and Methods

Mice

Specific pathogen free 6-8-week-old female BALB/c mice (NCI, Frederick, MD) were housed in cages equipped with microisolators and were provided food and water *ad libitum* throughout the study. The room temperature was 23 ± 1 ^{o}C and periods of light and dark were maintained on a 12 h cycle. Mice were acclimated for 1 week before challenge. For the portions of the study involving live EEEV, mice were housed in a biosafety level 3 (BSL-3) facility. Research was conducted at the United States Army Medical Research Institute of Infectious Diseases (USAMRIID) under an IACUC approved protocol in compliance with the Animal Welfare Act and other Federal statutes and regulations relating to animals and experiments involving animals and adheres to principles stated in the Guide for the Care and Use of Laboratory Animals, National Research Council, 1996. The facility is fully accredited by the Association for Assessment and Accreditation of Laboratory Animal Care International.

Virus

EEEV strain FL93-939 was obtained from Dr. Scott Weaver, UTMB, Galveston, TX. A sucrose-purified working stock was prepared from seed stock (P1) through an additional passage (P2) in Vero cells. Virus titer was determined by standard plaque assay on Vero cell monolayers. Challenge virus was diluted in either Eagle's minimum

essential medium (EMEM) (USAMRIID, Fort Detrick, MD) or sterilized phosphate

buffered saline (PBS) (GIBCO Invitrogen Corp., Grand Island, NY).

Experimental Design

Groups of 10 mice were exposed to increasing amounts of EEEV strain FL93-939

by either the intranasal (IN), aerosol (AE) or subcutaneous (SC) route. For the intranasal

route of exposure, virus doses were prepared in a 20 µL volume in PBS. Mice were

briefly anesthetized with isoflurane using an integrated multi-patient anesthesia machine

(IMPAC[6]) (VetEquip, Pleasanton, CA), were restrained in dorsal recumbency, and were

given predetermined virus concentrations in a total volume of 10 µL per nostril. For the

aerosol route of exposure, virus doses were prepared in 10 ml volumes in EMEM.

Control mice were exposed to diluent only. Aerosol exposures were conducted by

placing mice in wire cages into a chamber where they were exposed to aerosolized virus

for 10 min. Virus collected in an all-glass impinger (AGI) was titrated to determine the

concentration of virus (pfu/L) in air by standard plaque assay and the volume inhaled per

mouse was calculated using Guyton's formula (Guyton 1947). For the subcutaneous

route of exposure, virus doses were prepared in a 200 µL volume in sterilized PBS. Mice

were inoculated subcutaneously between the shoulder blades. Challenge virus

preparations were back-titrated by standard plaque assay. Mice were monitored daily for

14 days for clinical signs of disease and early endpoints were employed when animals

became moribund. Two iterations were performed for some routes in order to determine

the LD_{50} and the LD_{99}. Dose response curves were constructed and LD_{50} and LD_{99}

values were determined by Probit analysis with 95% fiducial limits using SAS Version
9.2 (SAS Institute Inc., Cary, NC).

Results

Using the data and the descriptive statistics shown in Table 2.1, the LD_{50} for the
intranasal route of exposure was determined to be 9.32 pfu, with a mean-time-to-death
(MTTD) between 6-6.5 days; while the LD_{99} was determined to be 1485 pfu, with a
MTTD between 4.5-6 days. Using the data and descriptive statistics shown in Table 2.2,
the LD_{50} for the aerosol route of exposure was determined to be 2.70 pfu with a MTTD
between 5-6 days; while the LD_{99} was determined to be 17.15 pfu with a MTTD between
4.6-6 days. Using the data and descriptive statistics shown in Table 2.3, the LD_{50} for the
subcutaneous route of exposure was determined to be 32 pfu, with MTTD of
approximately 6 days. The LD99 was not able to be determined.

Table 2.1. Descriptive statistics for intranasal exposure LD_{50} determination

Dose (pfu)	Log_{10} Dose	# Alive	# Dead	% Death	Mean TTD	SD TTD
0.01	-2.00	10	0	0	--	--
0.1	-1.00	10	0	0	--	--
0.4	-0.40	10	0	0	--	--
2.9	0.46	5	5	50	6.60	2.30
116	2.06	2	8	80	6.00	1.69
4300	3.63	0	10	100	4.50	0.71

Table 2.1. Data for determining LD_{50} and mean-time-to-death (MTTD) for the intranasal route of
exposure. Six-eight week old female BALB/c mice (n=10) were given increasing amounts of virus
intranasally. Mice were monitored daily for 14 days for clinical signs of disease and death. SD TTD,
standard deviation time to death.

Table 2.2. Descriptive statistics for aerosol exposure LD_{50} determination

Dose (pfu)	Log$_{10}$ Dose	# Alive	# Dead	% Death	Mean TTD	SD TTD
0.164	-0.785	10	0	0	--	--
0.967	-0.015	9	1	10	5.00	--
4.10	0.613	3	7	70	6.00	2.16
55.7	1.746	0	10	100	4.60	0.52
3220	3.508	0	10	100	3.90	0.32

Table 2.2. Data for determining LD_{50} and mean-time-to-death (MTTD) for the aerosol route of exposure. Six-eight week old female BALB/c mice (n=10) were given increasing amounts of virus by aerosol. Mice were monitored daily for 14 days for clinical signs of disease and death. SD TTD, standard deviation time to death.

Table 2.3. Descriptive statistics for subcutaneous exposure LD_{50} determination

Dose (pfu)	Log$_{10}$ Dose	# Alive	# Dead	% Death	Mean TTD	SD TTD
0.01	-2.00	9	0	0	--	--
0.10	-1.00	9	1	10	11.00	--
1	0.00	8	2	20	8.00	1.41
4	0.60	3	7	70	7.86	1.57
29	1.46	5	5	50	6.60	0.89
1160	3.06	4	6	60	6.33	0.52

Table 2.3. Data for determining LD_{50} and mean-time-to-death (MTTD) for the subcutaneous route of exposure. Six-eight week old female BALB/c mice (n=9-10) were given increasing amounts of virus by subcutaneous inoculation. Mice were monitored daily for 14 days for clinical signs of disease and death. SD TTD, standard deviation time to death.

Conclusion

We were able to determine the LD_{50} for each route of exposure. As expected, the LD_{50} for the aerosol route of exposure was the lowest, followed closely by the intranasal route. The LD_{50} for the subcutaneous route of exposure was higher. Interestingly, the LD_{99} for the aerosol exposure was significantly lower than that for the intranasal route of exposure, which can be explained by the difference in the shape of the curves determined by Probit Analysis. This may be a result of the variance in particle size between the IN and AE routes. For the IN study, the virus was delivered in a total volume of 20 μL, 10 μL per nostril. It is possible that some virus did not make it into the nostril or that it may have been swallowed. For the AE study, the particle size generated during aerosolization is approximately 1 μm. Such a small particle size is expected to have better particle-to-olfactory epithelial cell contact, which would likely facilitate attachment and viral entry. We were unable to determine the LD_{99} for the subcutaneous route because there were not any groups in which there was 100% mortality. Additionally, we repeated the subcutaneous route of exposure at increasing doses ranging from 6.4E+3 to 1.12E+8 pfu/ml and were only able to obtain 90% death at the lowest dose and 80% death at the highest dose. Therefore, a dose-response curve was not observed in this study. As noted in the literature with other alphaviruses (Morgan 1941; Griffin, Levine et al. 1994; Steele, Davis et al. 1998; Labrada, Liang et al. 2002; Vogel P, Kell WM et al. 2005), these results suggest there may be an age and/or strain dependent resistance in mice when exposed to EEEV FL93-939 by the subcutaneous route.

EEEV strain FL93-393 Pathogenesis Studies

Understanding the pathogenesis of a disease is an important first step in vaccine or therapeutic development. Determining the primary site of viral replication, target organ(s), target cell(s), and cause of death aid in determining the type of vaccine or therapeutic that must be developed in order to prevent disease and/or death. Based on the data from the LD_{50} studies, three experiments were designed to elucidate the pathogenesis of EEEV strain FL93-939 in BALB/c mice. The goal for each of the studies was to expose the mice to $100LD_{50}$ in order to ensure that majority of the mice would receive a lethal dose of the virus.

Materials and Methods

Mice

Specific pathogen free 8-10-week-old female BALB/c mice (NCI, Frederick, MD) were housed in cages equipped with microisolators and were provided food and water *ad libitum* throughout the study. The room temperature was 23 ± 1 ^{o}C and periods of light and dark were maintained on a 12 h cycle. Mice were acclimated for 1 week after which 10 animals in each study were surgically implanted with intraperitoneal telemetry devices (TA-F20, Data Sciences International, St. Paul, MN) to monitor body temperature and activity. Animals received 1 week post-operative recovery, weighed approximately 20 gm, and were 12-13 weeks old at the time of exposure. For the portions of the study involving live EEEV, mice were housed in a biosafety level 3 (BSL-3) facility. Research was conducted at the United States Army Medical Research Institute of Infectious

Diseases (USAMRIID) in compliance with the Animal Welfare Act and other Federal

statutes and regulations relating to animals and experiments involving animals and

adheres to principles stated in the Guide for the Care and Use of Laboratory Animals,

National Research Council, 1996. The facility is fully accredited by the Association for

Assessment and Accreditation of Laboratory Animal Care International.

Virus

EEEV strain FL93-939 was obtained from Dr. Scott Weaver, UTMB, Galveston,

TX. A sucrose-purified working stock was prepared from seed stock (P1) through an

additional passage (P2) in Vero cells. Virus titer was determined by standard plaque

assay on Vero cell monolayers. Virus was aliquoted and frozen at -70 to -80 $^{\circ}$C prior to

use.

Experimental Design

Groups of 10 mice were exposed to approximately $100LD_{50}$ of EEEV strain FL93-

939 by either the intranasal, aerosol or subcutaneous route. For the intranasal route of

exposure, virus dose was prepared in a 20 μL volume in sterilized PBS. Control mice

received only sterilized PBS. Mice were briefly anesthetized with isoflurane using the

IMPAC[6] and given 10 μL of challenge virus per nostril. For the aerosol route of

exposure, virus dose was prepared in a 10 ml volume in EMEM. Control mice were

exposed to diluent only. Aerosol exposures were conducted in a whole-body bioaerosol

exposure system. A Collison nebulizer (BGI, Inc., Waltham, MA) was used to generate

small (1μm mass median aerodynamic diameter) diameter particles for each acute 10 min

exposure. Briefly, mice were placed in wire cages, which were then placed into a

chamber where they were exposed to aerosolized virus for 10 min. 'Presented' dose was

estimated by calculating the respiratory minute volume (V_m) using Guyton's formula

(Guyton 1947), expressed as $Vm = 2.10 \times W_b^{0.75}$ where W_b = body weight (gm) based on

the average group weights the day of exposure. The presented dose was then calculated

by multiplying the estimated total volume (V_t) of experimental atmosphere inhaled by

each animal ($V_t = V_m \times$ length of exposure) by the empirically determined exposure

concentration (C_e) ('presented dose' = $C_e \times V_t$). Exposure concentration, expressed in

plaque-forming units (PFU)/L, was determined by isokinetic sampling of the chamber

with an all-glass impinger (AGI) (Ace Glass, Vineland, NJ). Samples were titrated by

standard plaque assay on Vero cell monolayers (Roy, Reed et al. 2009). For the

subcutaneous route of exposure, virus dose was prepared in a 10 µL volume in EMEM.

Mice were inoculated in the left foot pad in order to track viral replication in the

surrounding tissue and draining lymph node (popliteal lymph node). Control mice

received diluent only. Challenge virus preparations were back-titrated by standard plaque

assay using Vero cells. Mice from the intranasal and aerosol studies were euthanized at

pre-determined time points: 6, 12, 24, 48, 72, 96, and 120 hours post-infection (hpi). In

addition to the previous listed time points, mice in the subcutaneous study were also

euthanized at 144, 168, and 192 hpi. At the time of euthanasia, mice were anesthetized

with mouse K-A-X (50 mg ketamine 100 mg/ml (Fort Dodge Animal Health, Fort

Dodge, IA), 0.5 mg acepromazine 10 mg/ml (Boehringer Ingelheim, Ridgefield, CT), and

5.5 mg xylazine 20 mg/ml (Lloyd Laboratories, Walnut, CA)) given intraperitoneally at a

dose of 0.2 ml per 20 gm. Mice were euthanized by exsanguination via cardiac puncture

and whole blood samples were collected for CBC analysis, while serum samples were
collected for viral titer and cytokine analysis. Five mice from each time point were
perfused with PBS and tissues were individually collected and frozen for viral titer
analysis. Five mice from each time point were perfused with 10% neutral buffered
formalin (NBF) (LabChem, Inc., Pittsburg, PA) and tissues were harvested for
histopathologic analysis.

Acquisition and analysis of telemetry data

All telemetry data was collected using the DSI DataQuest ARTM[TM] software. The
system was programmed to sample body temperature and physical activity for a 20 sec
period every 30 min. Baseline data was collected for 2 days. Data collection continued
until euthanasia or the end of the study. Pre-exposure temperature data was used to
develop a baseline period to fit an autoregressive integrated moving average (ARIMA)
model. Forecasted values for the post-exposure period were based on the baseline
extrapolated forward in time using SAS ETS (vers. 9.2). Residual changes were
determined by subtracting the predicted value from the actual value recorded for each
time point. For temperature, residual changes greater than two standard deviations were
used to compute fever duration (number of hours of significant temperature elevation),
fever hours (sum of the significant temperature elevations), and average fever elevation
(fever hours divided by fever duration in hours). Only time periods consisting of two or
more consecutive time points of elevated temperature were used in the analysis.

CBC analysis

A complete blood count (CBC) was determined on whole blood samples collected at the time of euthanasia. Samples were run on an Abbott CELL-DYN 3700 with veterinary package (Abbott Laboratories, Abbott Park, IL) on the same day as collection. T-tests with stepdown Bonferroni adjustment were used to compare mean levels of blood parameters between infected groups and uninfected control groups at various time points.

Cytokine analysis

Cytokines/chemokines were measured on selected serum samples using BD™ Cytometric Bead Array mouse soluble protein flex sets (BD Biosciences, San Jose, CA) read on a BD FACSCanto II flow cytometer as per manufacturer's instructions. Twenty-five soluble proteins were measured (CD62E, CD62L, G-CSF, GM-CSF, IFN-γ, IL-1α, IL-1β, IL-2, I L-3, IL-4, IL-5, IL-6, IL-9, IL-10, IL-12/IL23p40, IL-13, IL-17A, IL-21, KC, MCP-1, MIG, MIP-1α, MIP-1β, RANTES, and TNF) and results were analyzed using FCAP Array software (BD Biosciences, San Jose, CA).

Mucosal secretions

A bronchoalveolar lavage (BAL) and nasopharyneal flush (NF) were performed using 0.5 ml of sterile PBS for each. Briefly, under deep anesthesia, the trachea was exposed and an 18-g needle was inserted toward the lower or upper respiratory tract, respectively. PBS was flushed into the lungs and aspirated for BALs or through the nares and/or oropharynx for nasopharyneal flushes. Mice were then euthanized by exsanguination via cardiac puncture.

Virus titrations

For determination of EEEV titers, tissue samples were homogenized using a mini-bead beater and 1-2 stainless steel beads (3.2 mm diameter) (BioSpec Products, Inc., Bartlesville, OK) and 500 µL of complete medium. Homogenized samples were centrifuged for 10 min at 10,000 rpm in a table-top centrifuge and supernatants were collected and stored at -70 to -80 ^{o}C until virus titration. Titration of virus was performed by standard plaque assay on Vero cell monolayers. Briefly, supernatant from homogenized tissues, serum, BAL, nasal flush, or AGI samples were serially diluted in EMEM (USAMRIID, Fort Detrick, MD) containing 5% fetal bovine serum (FBS) (GIBCO Invitrogen Corp., Grand Island, NY), 1% penicillin (20,000 IU/ml)-streptomycin sulfate (20,000 µg/ml), 1% non-essential amino acids (NEAA) (Sigma Aldrich Company, Inc., St. Louis, MO), 1% 200mM L-glutamine (Thermo Scientific, Logan, UT), and 0.1% gentimicin solution (Sigma Aldrich Company, Inc., St. Louis, MO). Diluted samples were then added in duplicate to 6-well plates containing confluent monolayer of Vero cells (African green monkey kidney cells) which were incubated at 37 ^{o}C for 1 hour, with rocking every 15 min. Following the incubation period, a 0.5% agarose overlay in 2x EBME solution (USAMRIID, Fort Detrick, MD) with HEPES and 10% FBS, 1% L-glutamine, 1% NEAA, 1% penicillin -streptomycin sulfate, and 0.1% gentimicin was added, and plated were incubated at 37 ^{o}C at 5% CO_2 for 24 hr. Thereafter, a second agarose overlay in 2x EBME containing supplements and 5% neutral red was added. The plates were again incubated at 37 ^{o}C at 5% CO_2 for 24 hr. Defined plaques (neutral red exclusion areas) were then counted.

Pathology

Animal tissues collected for pathology were fixed in 10% neutral buffered formalin (NBF) (LabChem, Inc., Pittsburg, PA) for a minimum of 21 days prior to removal from the BSL-3 containment lab for processing. Skulls were decalcified in 10% ethylenediamenetetraacetic acid (EDTA) in Tris buffer solution (pH 6.95) (Sigma Chemical Co., St. Louis, MO). Tissues were trimmed and processed according to standard protocol and embedded in paraffin blocks. Histologic sections were trimmed at 5-6 μm thickness, mounted on positively charged glass slides (Superfrost Plus, Fischer Scientific, Pittsburg, PA), and stained with hematoxylin (PolyScientific, Bay Shore, NY) and eosin (PolyScientific, Bay Shore, NY).

Serial sections were stained for viral antigen using a polyclonal rabbit antiserum directed against several alphaviruses , followed by a horseradish peroxidase-labeled polymer conjugated to goat anti-rabbit immunoglobulins. Briefly, tissue sections were deparaffinized using Xyless (LabChem, Inc., Pittsburg, PA) and rehydrated using sequentially less concentrated alcohol solutions ranging from 100% to 70%. Endogenous peroxidases were blocked using a methanol/hydrogen peroxide solution. To increase staining intensity, antigen retrieval was performed by immersing slides in Tris/EDTA buffer for 30min at 97°C. Endogenous proteins were blocked by incubating the slides in serum-free protein block (Invitrogen, Carlsbad, CA) plus 5% normal goat serum (Vector Labs, Burlingame, CA) for 30 min at room temperature. Sections were incubated with the primary antibody, a polyclonal rabbit antiserum directed against EEEV, WEEV, VEEV and Sindbis virus (Applied Diagnostic Branch, Diagnostic Systems Division, USAMRIID) diluted 1:8000, for 30 min at room temperature. Sections were then

incubated with a secondary antibody, horseradish peroxidase-labeled polymer conjugated to goat anti-rabbit immunoglobulins (DAKO, Carpenteria, CA), and incubated for 30 min at room temperature. Staining was completed by adding the substrate-chromagen, diaminobenzidine (DAB) (DAKO, Carpenteria, CA) and incubating slides for 5 min at room temperature. Tissues were counterstained with hematoxylin for 2 min at room temperature and then dehydrated in sequentially more concentrated alcohol solutions, cleared using Xyless II, and coverslip was mounted using Permount (Fisher Scientific, Pittsburg, PA). Non-immune (normal) rabbit serum (Vector Labs, Burlingame, CA) was used as a negative control for the primary antibody. Sections of confirmed EEE virus-infected mouse brain were used as a positive control.

Serial sections were stained for cleaved caspase-3, a marker for apoptosis, using a monoclonal rabbit antiserum, followed by a horseradish peroxidase-labeled polymer conjugated to goat anti-rabbit immunoglobulins. Briefly, tissue sections were processed as described above. Sections were then incubated with the primary antibody, a monoclonal rabbit antiserum directed against cleaved caspase-3 (Asp175) (51AE) (Cell Signaling Technology, Danvers, MA) diluted 1:100, for 60 min at room temperature. Sections were then incubated with a secondary antibody, horseradish peroxidase-labeled polymer conjugated to goat anti-rabbit immunoglobulins (DAKO, Carpenteria, CA), and incubated for 30 min at room temperature. Staining was completed by adding the substrate-chromagen, diaminobenzidine (DAB) (DAKO, Carpenteria, CA) and incubating slides for 5 min at room temperature. Tissues were counterstained with hematoxylin for 2 min at room temperature and then dehydrated in sequentially more concentrated alcohol solutions, cleared using Xyless II, and coverslip was mounted using

Permount (Fisher Scientific, Pittsburg, PA). Non-immune (normal) rabbit serum (Vector Labs, Burlingame, CA) was used as a negative control for the primary antibody. Sections of confirmed VEE virus-infected mouse spleen were used as a positive control.

Serial sections were also stained for LC3B II, a marker of autophagy, using a monoclonal rabbit antiserum, followed by a horseradish peroxidase-labeled polymer conjugated to goat anti-rabbit immunoglobulins. Briefly, tissue sections were processed as described above. Sections were then incubated with the primary antibody, a monoclonal rabbit antiserum directed against LC3B (DII) x P (R) (Cell Signaling, Danvers, MA) diluted 1:500, for 60 min at room temperature. Sections were then incubated with a secondary antibody, horseradish peroxidase-labeled polymer conjugated to goat anti-rabbit immunoglobulins (DAKO, Carpenteria, CA), and incubated for 30 min at room temperature. Staining was completed by adding the substrate-chromagen, diaminobenzidine (DAB) (DAKO, Carpenteria, CA) and incubating slides for 5 min at room temperature. Tissues were counterstained with hematoxylin for 2 min at room temperature and then dehydrated in sequentially more concentrated alcohol solutions, cleared using Xyless II, and coverslip was mounted using Permount (Fisher Scientific, Pittsburg, PA). Non-immune (normal) rabbit serum (Vector Labs, Burlingame, CA) was used as a negative control for the primary antibody.

Results

To evaluate the pathogenesis of EEEV strain FL93-939 mice were inoculated with 30-100LD$_{50}$ of virus. The absolute amount of virus used for the inoculation varied by route according to the results of the previously performed LD$_{50}$ studies. For the

intranasal (IN) study, mice received 1300 pfu, approximately $130LD_{50}$ (1LD99), while the mice in the aerosol (AE) study received 250 pfu, approximately $80LD_{50}$ ($5LD_{99}$). Mice in the subcutaneous (SC) study received 1000 pfu, approximately $30LD_{50}$.

Weight variance and clinical signs

Overall, the results from the IN and AE studies are similar when comparing post-exposure weight variance and onset of clinical signs (Figure 2.1), which differed from the SC study. Both groups of mice continued to gain weight up to 2 dpi. However, the IN group began to lose weight by 3 dpi, while the AE group had minimal increases in weight over the same time period. For both groups, there was rapid weight loss from 3 dpi to 4 dpi and the IN group continued to lose weight through the end of the study, 5 dpi. The AE study was terminated at 4 dpi due to the fact that 90% of the animals in the 5 dpi group were showing moderate to severe signs of clinical disease. In both the IN and AE studies, mice began showing clinical signs of disease (ruffled fur, lethargy, hunched posture) at 3 dpi and both the percentage of animals affected and the severity of clinical signs increased from 3 dpi to the study endpoints. More severe clinical signs of disease included weight loss, dehydration, head tilt, circling, head tremors, focal muscle twitching, lateral recumbency, and rarely seizures.

For the SC study, mice initially lost some weight at 1 dpi but then gradually gained weight over the following 5 days. Mice began losing weight after 5 dpi, which coincided with the onset of clinical signs in most animals. Three animals from the 8 dpi group were moribund and were euthanized on either 6 dpi or 7 dpi. The 7 remaining animals in the 8dpi group were clinically normal and gaining weight at 8 dpi. Overall, the clinical signs

A.

B.
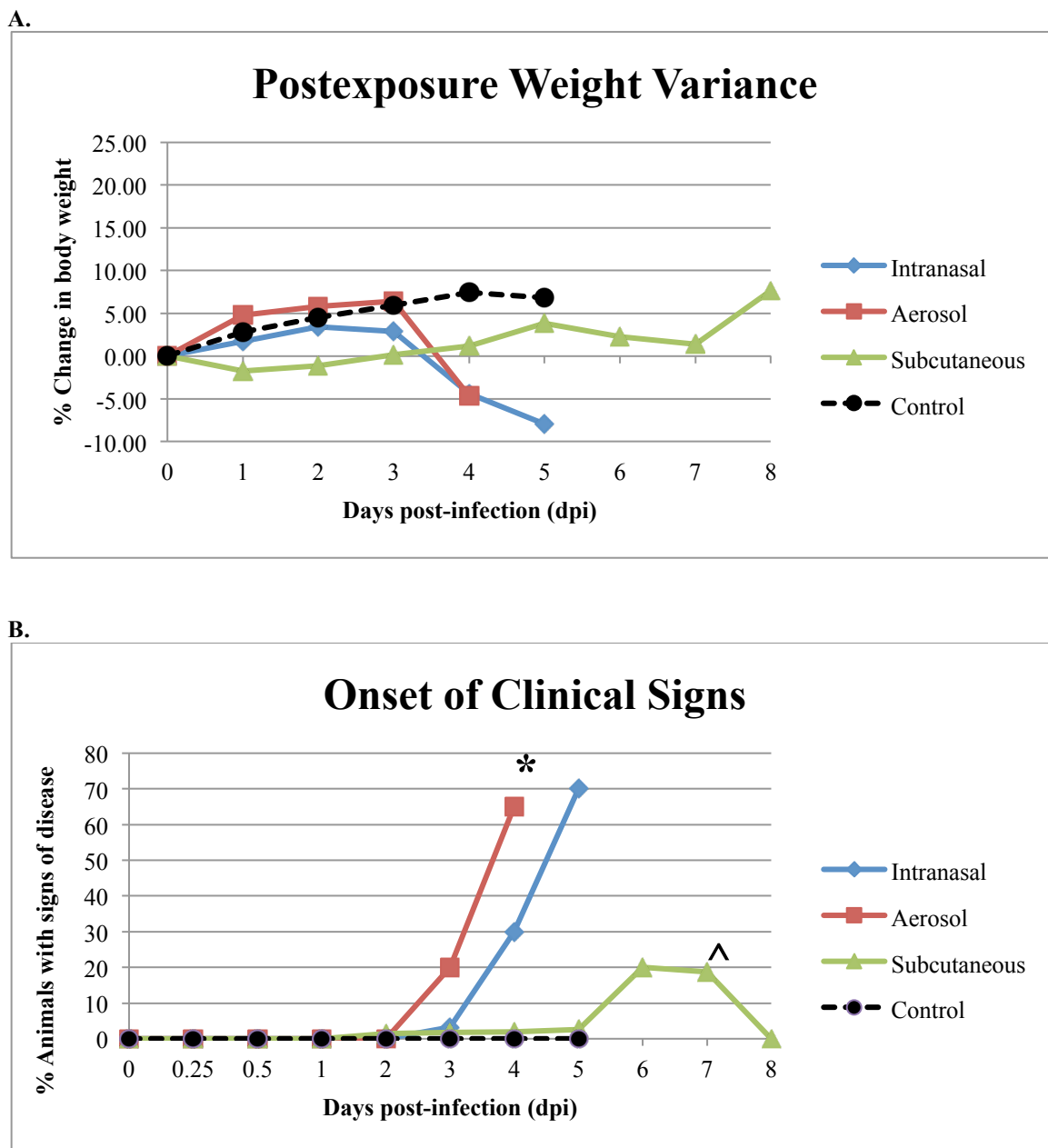
Figure 2.1. Change in mean body weight **(A)** and percent of BALB/c mice that either showed clinical signs of disease or were moribund **(B)** after intranasal, aerosol, or subcutaneous infection with NA EEEV strain FL93-939. Mice were monitored daily after infection and percent change in weight was determined from the day of infection (day 0). Values in graph A represent the mean body weight within that cohort (intranasal n=5; aerosol n=5; subcutaneous n= 9; control n=15) and percent change the mean. The values in graph B represent the number of animals affected compared to all animals evaluated at that time point.

(*)The aerosol study was terminated at 4 dpi because 90% of the animals in the 5dpi group had moderate to severe signs of clinical disease

(^) Three animals in the subcutaneous study from the 8 dpi group were euthanized prematurely due to the onset of severe clinical disease

of disease observed in the SC study were similar to those noted in the IN and

AE studies but occurred in fewer animals and generally were not noted until 6 dpi.

However, one animal in the 8 dpi group did show clinical signs of disease starting on 2

dpi. The disease progressed slowly and the animal was euthanized on 7 dpi due to severe

clinical signs of disease.

Temperature and activity

In each study, temperature and activity data were collected from infected and

uninfected BALB/c mice to evaluate differences between various routes of infection

compared to age-matched controls. Distinct diurnal patterns were observed over a 24 hr

period in all groups, with temperatures peaking during nocturnal activity and reaching

daily lows during daylight hours. The average daily range in temperature was 35.2 -

37.8°C. The mean temperature profile for each group is shown in Figure 2.2a. For the

IN and AE studies, the diurnal temperature pattern in EEEV infected mice began to

deviate from the pattern observed in control mice approximately 3-4 dpi, which coincided

with onset of clinical signs. For the SC study, the diurnal temperature pattern was

unchanged until 6-7 dpi, which coincided with the time at which the highest percentage

of animals showed clinical signs. The fever detected by telemetry at 3 dpi for the IN and

AE studies and 5 dpi in the SC study (Table 2.4) was the first indication that telemetric

analysis coincided with the daily cage-side observations in detecting onset of disease.

However, when comparing infected to uninfected mice within each study, only the

infected animals in the AE and SC studies showed a significant difference in the duration

and total fever hours as compared to uninfected controls ($p<0.05$), which is likely a result

of the small group numbers. In the AE study, 4/5 animals had a fever of significant

duration; however, in the IN study only 3/5 animals had a fever for 2 or more consecutive

time points. Nonetheless, the p-value in the IN study was just slightly abover 0.05 for

both duration and total fever hours (p=0.08 for duration and p=0.09 for total fever hours).

There were also distinct diurnal patterns in activity that were recorded over a 24 hr

period in all groups, with activity generally peaking during nocturnal time points and

reaching daily lows in the morning hours. The mean activity profile for each group is

shown in Figure 2.2b. When compared to the controls, mice in both the IN and AE

studies deviated from the pattern observed in control mice between 3-5 dpi, again

coinciding with the onset of clinical signs. It is difficult to draw conclusions regarding

the SC study, as the control mice were only monitored for 5 days in the first experiment.

We did not see any clinical signs in infected animals in this study due to the low viral

dose given, approximately $3LD_{50}$ (data not shown). This experiment was repeated;

however, control animals were not included in order to minimize the overall animals used

for the study. In the second study, we increased the viral dose given to approximately

30LD50 and did not see significant clinical signs of disease until 5-6 dpi.

CBC analysis

When an adequate volume of blood was collected at euthanasia, a complete blood

count was performed on individual animals from the AE and SC studies and the group

mean results are shown in Figure 2.3. There were some significant individual animal

differences, which resulted in large standard deviations in some groups. However, in the

A.

B.
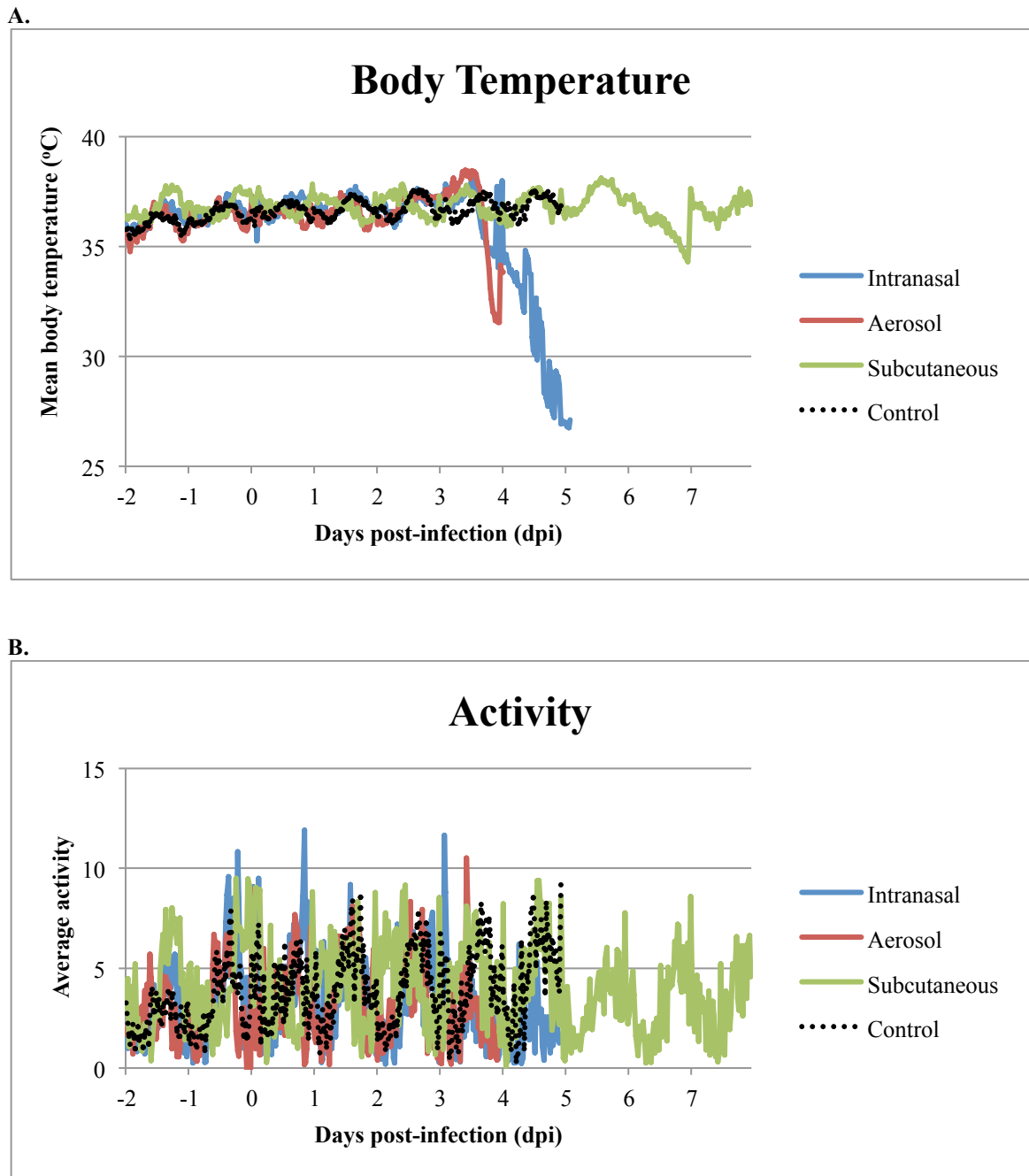
Figure 2.2. Change in average body temperature **(A),** and activity **(B)** after intranasal, aerosol, or subcutaneous infection with NA EEEV strain FL93-939. Mice were monitored daily after infection. Body temperatures and activity were recorded for a 20 sec period every 30 min via an intraperitoneal telemetry device before and after infection with NA EEEV strain FL93-939. Values represent the average within the cohort (intranasal n=5; aerosol n=5; subcutaneous n= 9; control n=15).

(*)The aerosol study was terminated at 4 dpi because 90% of the animals in the 5dpi group were showing moderate to severe signs of clinical disease

Table 2.4 Summary of fever data for IN, AE, and SC studies

	Group	Onset[a]	$\Delta T_{max},\,^0C$	Duration, h[b]	Fever hours[c]	Average elevation[d]
	Infected	3.0	1.9	11.3	28.2	1.9
IN	Controls	--	1.1	0.6	1.1	1.1
	p-value	--	0.2972	0.0822	0.0913	0.3166
	Infected	3.0	2.3	11.6	26.5	1.8
AE	Controls	--	0.5	0.4	0.9	0.4
	p-value	--	**0.0405**	**0.0302**	**0.0350**	0.0670
	Infected	5.0	1.8	5.9	12.9	1.6
SC	Controls	--	0.7	0.2	0.4	0.7
	p-value	--	0.1000	**0.0436**	**0.0485**	0.1144

Table 2.4. Summary of fever data. Temperature was recorded for 20 sec every 30 minutes, beginning 2-3 days prior to exposure and continuing 4-8 days post-exposure. Pre-exposure temperature data was used to develop a baseline period. Residual changes were determined by subtracting the predicted value from the actual value recorded for each time point. For temperature, residual changes greater than 2 standard deviations (SD) were used to compute fever duration (number of hours of significant temperature elevation), fever hours (sum of the significant temperature elevations), and average fever elevation (fever hours divided by fever duration in hours). Only time periods consisting of two or more consecutive time points of elevated temperature were used in the analysis.

Notes:
ΔT_{max} is the maximum change in temperature
[a] Defined as the first day with >8 hours of significant temperature elevation (as determined by ARIMA modeling)
[b] Calculated as the number of hours of significant temperature elevation
[c] Calculated as the sum of the significant temperature elevations
[d] Calculated by dividing fever hours by fever duration in hours
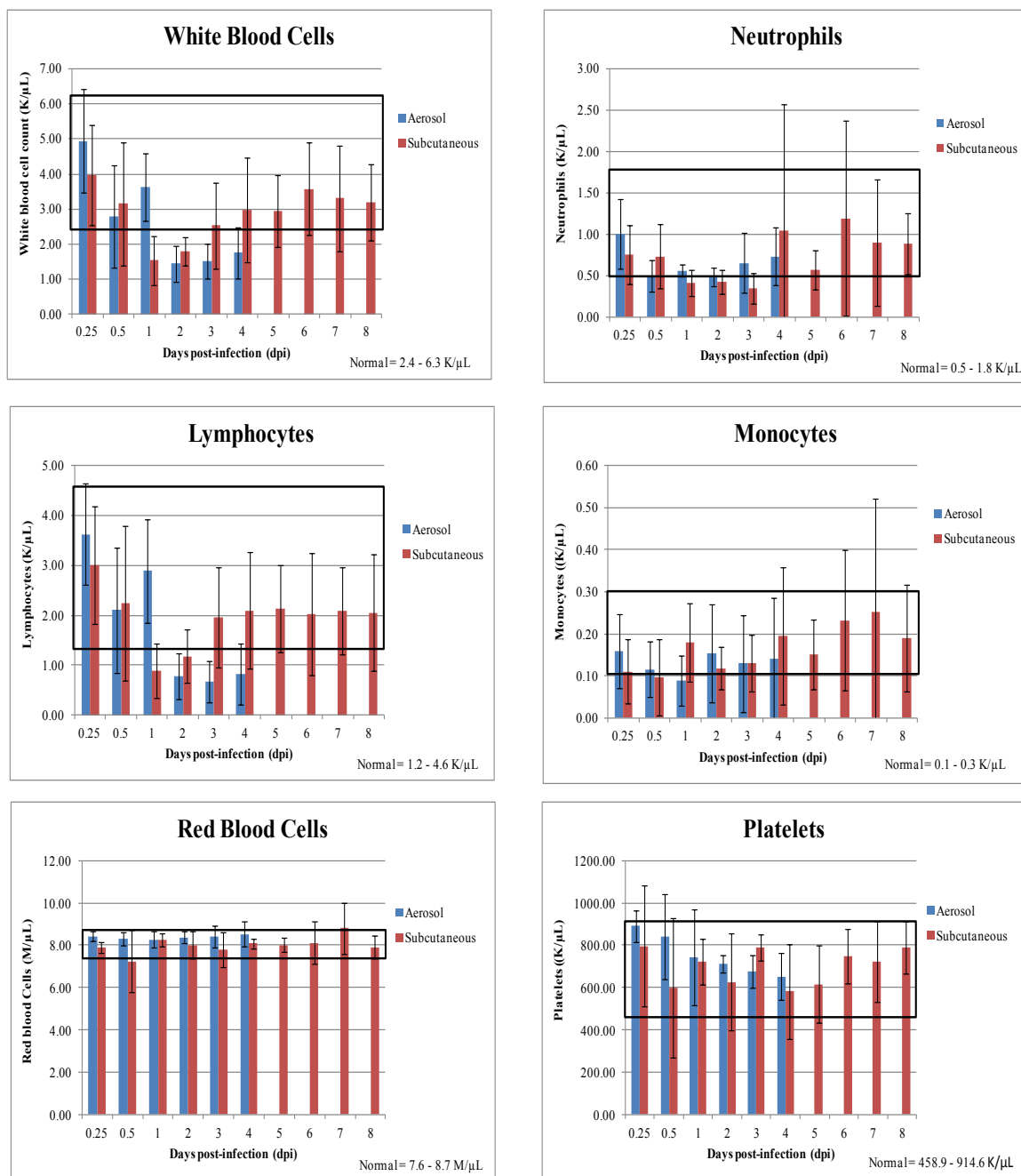
Figure 2.3. Results of complete blood counts in animals exposed to EEEV strain FL93-939 either by the aerosol or subcutaneous routes (N=10 per route). Normal ranges were determined from control animals (n=20) combined from both routes of exposure. Red and blue bars represent the group mean for each time point with the standard deviation indicated by the black bars. The black box indicates the normal range as determined from uninfected control animals. The aerosol study was terminated at 4 dpi because 90% of the animals in the 5dpi group were showing moderate to severe signs of clinical disease

AE study, there was a general decrease in the total number of white blood cells (WBC) (leukopenia) at 2 dpi, with the group mean value dropping below the normal range and remaining low through the end of the study. This decrease in WBCs was characterized by a decrease in lymphocytes (lymphopenia) as the number of neutrophils and monocytes, as well as the number of eosinophils and basophils (data not shown), remained within the normal range. There were statistically significant differences ($p<0.05$) in total WBC and number of lymphocytes between infected and uninfected animals from 12 hpi through the end of the study (Table 2.5). Interestingly, while the mean total number of neutophils in infected animals never fell below the normal range at any time point, there were statistically significant differences in the total number of neutrophils present in infected and uninfected animals at every time point. There were also differences in the number of platelets at 0.25 dpi and 0.5 dpi hpi. In the SC study, there was also a leukopenia; however, this occurred earlier, at 1 dpi, and when evaluating group means, was characterized by both a lymphopenia as well as a neutropenia (decrease in neutrophils). These values remained low through 2 dpi for lymphocytes and 3 dpi for neutrophils, after which time all mean values were within the normal range for the remainder of the study. There were no statistically significant differences between infected and uninfected animals at any of the time points. The group mean values for red blood cells remained within the normal range throughout in both the AE and SC studies and there were no significant differences noted.

Table 2.5. P-values for the pairwise comparisons of mean blood parameters

		Days post-exposure (dpi)									
Study	Blood Parameter	0.25	0.5	1	2	3	4	5	6	7	8
AE study	WBC #	0.0563	<0.0001	<0.0001	<0.0001	<0.0001	<0.0001	<0.0001	--	--	--
	Neutrophil #	0.0366	<0.0001	<0.0001	<0.0001	0.0001	0.0002	0.021	--	--	--
	Lymphocyte #	0.1292	<0.0001	0.0038	<0.0001	<0.0001	<0.0001	<0.0001	--	--	--
	Monocyte #	1	0.784	0.2948	1	1	0.2948	1	--	--	--
	Eosinophil #	1	1	1	1	0.7126	1	1	--	--	--
	Basophil #	0.0086	0.9014	0.8748	0.0473	0.1029	0.2591	0.7711	--	--	--
	Hermatocrit	0.1232	0.6098	0.7575	0.703	0.6373	0.7575	0.0297	--	--	--
	Platelet #	0.0016	0.0058	0.2013	0.4579	0.6875	0.8702	0.8702	--	--	--
SC Study	WBC #	0.5959	1	0.1037	0.3519	1	1	1	1	1	1
	Neutrophil #	1	1	0.9472	0.9975	0.7343	1	1	1	1	1
	Lymphocyte #	0.0557	1	0.6456	1	1	1	1	1	1	1
	Monocyte #	0.2604	0.232	1	0.3549	0.4931	1	0.8363	1	1	1
	Eosinophil #	1	1	1	1	1	1	1	0.1933	1	1
	Basophil #	1	1	0.5224	1	1	1	1	1	1	0.9507
	Hermatocrit	1	0.0886	1	1	1	1	1	1	1	1
	Platelet #	1	0.7499	1	0.9118	1	0.4313	0.8769	1	1	1

Table 2.5. P-values for the pairwise comparisons of mean blood parameters in the AE and SC studies. Whole blood was collected at the time of euthanasia and processed on the same day. T-tests with stepdown Bonferroni adjustment were used to compare mean levels of blood parameters between infected and uninfected animals in each study (n=10).

Cytokine analysis

In order to further elucidate the role of inflammatory and immunomodulatory cytokines and chemokines, we analyzed a subset of serum samples from the IN, AE, and SC studies for the presence of 25 soluble proteins (CD62E, CD62L, G-CSF, GM-CSF, IFN-γ, IL-1α, IL-1β, IL-2, I L-3, IL-4, IL-5, IL-6, IL-9, IL-10, IL-12/IL23p40, IL-13, IL-17A, IL-21, KC, MCP-1, MIG, MIP-1α, MIP-1β, RANTES, and TNF). Significant increases were observed in serum levels of IFN-γ at 1 dpi in the SC study and 2 dpi in the IN and AE studies compared to baseline controls (Figure 2.4). Other pro-inflammatory cyto/chemokines were upregulated in sera, depending on the infection route. Intranasal infection induced increased CD62E (E-selectin), which plays a role in leukocyte

transmigration, at 6 hpi. At 2 dpi, there was an increase in RANTES (regulated upon activation, normal T-cell expressed and secreted), a chemokine for T-cells, eosinophils and basophils as well as an activator of NK cells; MIP-1β (macrophage inflammatory protein), which is a chemoattractant for monocytes and NK cells; and MIG (monokine induced by IFN-γ), which attracts and activates T-cells. At 4 dpi there was an increase in MCP-1 (macrophage chemoattractant protein), a chemoattractant for monocytes, but not neutrophils. Aerosol infection induced increased RANTES throughout most of study, at 6 hpi and 1, 2 and 4 dpi; IL-9, an interleukin that generally stimulates cell proliferation and inhibits apoptosis, at 12 hpi; MIP-1β at 2 and 3 dpi; G-CSF (granulocyte colony-stimulating factor), a growth factor and cytokine that stimulates the bone marrow to produce granulocytes and stem cells, at 2-4 dpi; and MIG at 2-3 dpi. Subcutaneous infection induced increased levels of CD62L (L-selectin), which is a cell adhesion molecule found on leukocytes, throughout most of the study at 6 hpi and 1, 3,4, and 8 dpi; RANTES at 12 hpi; and IL-6, which can act as both a pro-inflammatory and anti-inflammatory cytokine at 8dpi. Although these changes were all statistically significant relative to saline-treated control animals, most of the elevated cyto/chemokine levels were only slightly increased from baseline. There was no change in the levels of IL-2, IL-3, IL-4, KC (orthologue of IL-8), IL-21, IL-13, GM-CSF, IL-10, IL-17A, MIP-1α, TNF, IL-12/23p70, IL-1 α, IL-1β, and IL-5 induced in any of the infection routes relative to saline-treated mice. Overall, these data suggest a mild induction of certain pro-inflammatory cytokines and chemokines after infection.
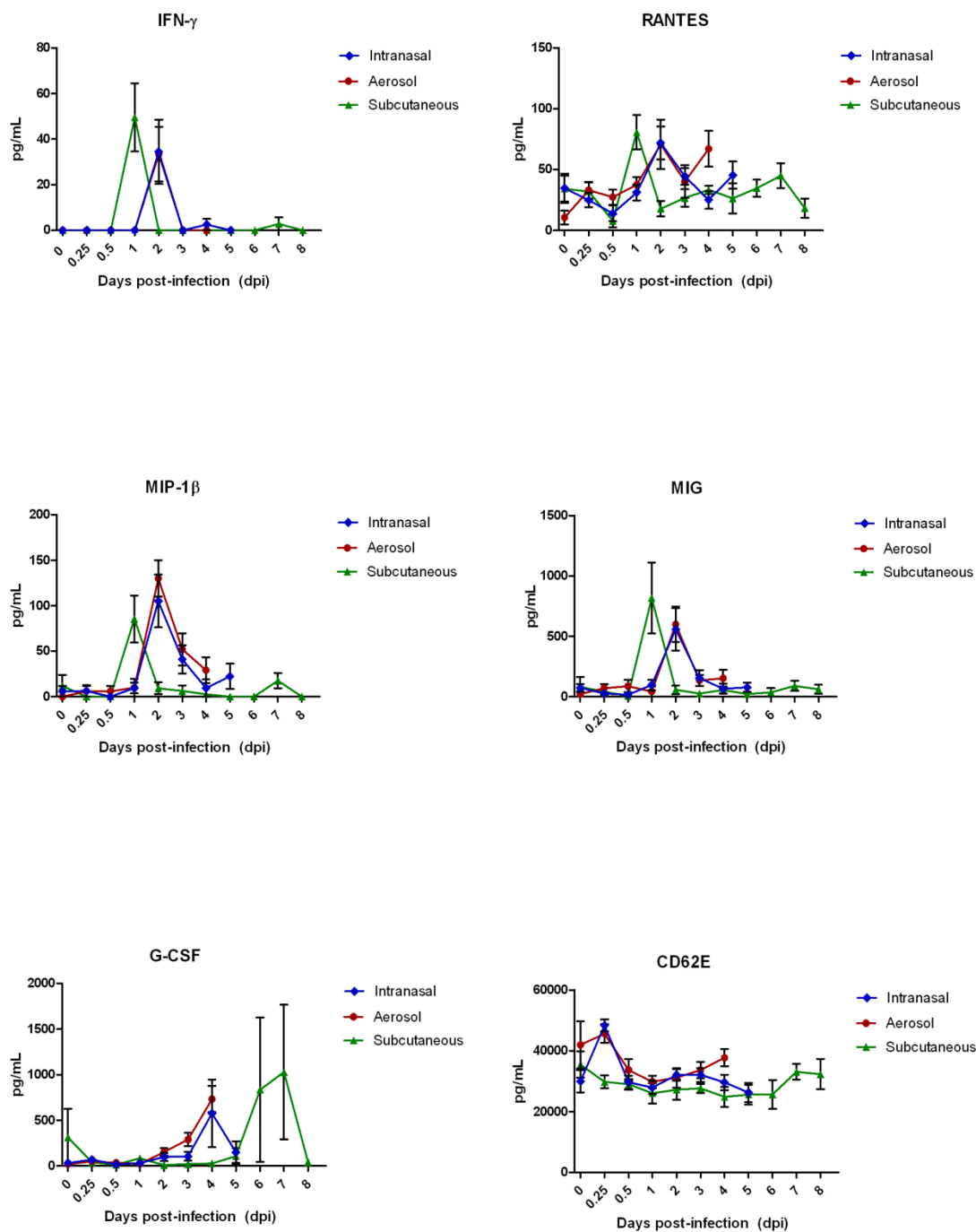
Figure 2.4. Serum analysis of soluble proteins in mice infected with EEEV strain FL93-939 by the intranasal, aerosol, or subcutaneous route. Mice were infected with approximately $30\text{-}100LD_{50}$ and were euthanized at specified time points (n=10). Soluble proteins in the serum were determined using BD^{TM} Cytometric Bead Array mouse soluble protein flex sets and results were analyzed using FCAP Array software. Values represent the group mean at each time point (n=6), bars represent the standard deviation. Mean baseline values (0 dpi) were determined from uninfected controls (n=6).

Comparison of cytokine levels between different infection routes at each time point revealed some interesting findings. There were no statistically significant differences in any of the 25 cytokines and chemokines tested between aerosol and intranasal infection at any time point. However, there were many differences between subcutaneous and intranasal or aerosol infections. Subcutaneous infection resulted in an increase of IFN-γ, MIP-1β, RANTES, and MIG at 1 dpi compared to aerosol or intranasal infection, followed by a return to baseline at 2 dpi. However, these same cyto/chemokines were increased in aerosol and intranasal infection at 2 dpi relative to subcutaneous infection. These differences could be a result of the route of infection or the variation in dose given in each study.

Virus titrations

Viral titers in the serum, bronchoalveolar lavage (BAL), nasopharyngeal flush (NF), and several tissues were determined by standard plaque assay. Significant differences in viral load were detected in most samples based on the route of infection. However, substantial variability was noted between animals in any one group. For this reason, the data shown is for both individual animals as well as group mean titers.

Interestingly, viremia was first detected in the SC study at 12 hpi, while virus was not detected until 1 dpi in either the IN or AE studies (Figure 2.5). This was likely due to the route of infection and rapid viral replication at the inoculation site. However, the viremia remained low in the SC study and was not detected after 4 dpi. In contrast, while the viremia appeared at 1 dpi in both the IN and AE studies, it peaked at 2 dpi, was significantly higher than the SC study, and was present until the study endpoint.

As expected, no virus was detected in the BAL or NF during the early time points in the SC study (Figures 2.6 and 2.7). Significantly more virus was present in the BAL at 6 hpi and 12 hpi in the AE study as compared to the IN study, and virus levels remained higher throughout the study (Figure 2.6). Virus was not present in the NF until 1 dpi in the AE study and 2 dpi in the IN study. Similar to the titers in the BAL, those in the NF were higher in AE study throughout all time points, although the overall titers were lower and the differences less distinct (Figure 2.7). These observations are likely due to the difference in delivery method. The collison nebulizer used for the AE study is designed to generate small 1µm particles, many of which are small enough to be delivered into the terminal bronchioles, while some particles are likely to remain in direct contact with olfactory nasal epithelium, allowing for attachment, entry, and replication. Virus in the IN study was delivered in liquid form, 10 µL per nostril, some may have remained outside the nostril and some may have been swallowed or inhaled.

Viral titers in the tissues followed similar trends. Although the mice in the IN and AE studies received similar LD_{50} doses of virus, virus was present in the brain 6 hpi in the AE study, but did not appear until 1 dpi in the IN study (Figure 2.8). Viral titers in the brain continued to increase in both groups, with mice of the AE group consistently having higher titers than mice in the IN group at all time points, peaking with very high titers at 4 dpi in the AE study and 5 dpi in the IN study. In the SC study, virus was first detected in the brain at 1 dpi, similar to the IN study; however, titers remained lower in the SC study, as compared to the AE and IN studies, for all time points, with virus titer

A.

B.

Figure 2.5. Geometric mean viral titer in the serum of individual mice **(A),** and mean viral titer of the groups **(B)** from BALB/c mice infected with NA EEEV strain FL93-939. Mice were infected with approximately 30-100X LD_{50} and were then euthanized at specified time points (n=5). Viral titers were determined by standard plaque assay. Symbols represent individual animals with values calculated from the geometric mean titer of all dilutions which had at least one visible pfu. The mean for the group is shown in the colored line (A). Bars represent the mean titer of the group for each time point (B). Limit of detection of the assay is 5 pfu/ml.

A.

B.

Figure 2.6. Geometric mean viral titer in the bronchoalveolar lavage (BAL) of individual mice **(A),** and mean viral titer of the groups **(B)** from BALB/c mice infected with NA EEEV strain FL93-939. Mice were infected with approximately 30-100X LD$_{50}$ and were then euthanized at specified time points (n=5). Viral titers were determined by standard plaque assay. Symbols represent individual animals with values calculated from the geometric mean titer of all dilutions which had at least one visible pfu. The mean for the group is shown in the colored line (A). Bars represent the mean titer of the group for each time point (B). Limit of detection of the assay is 5 pfu/ml.

A.

B.
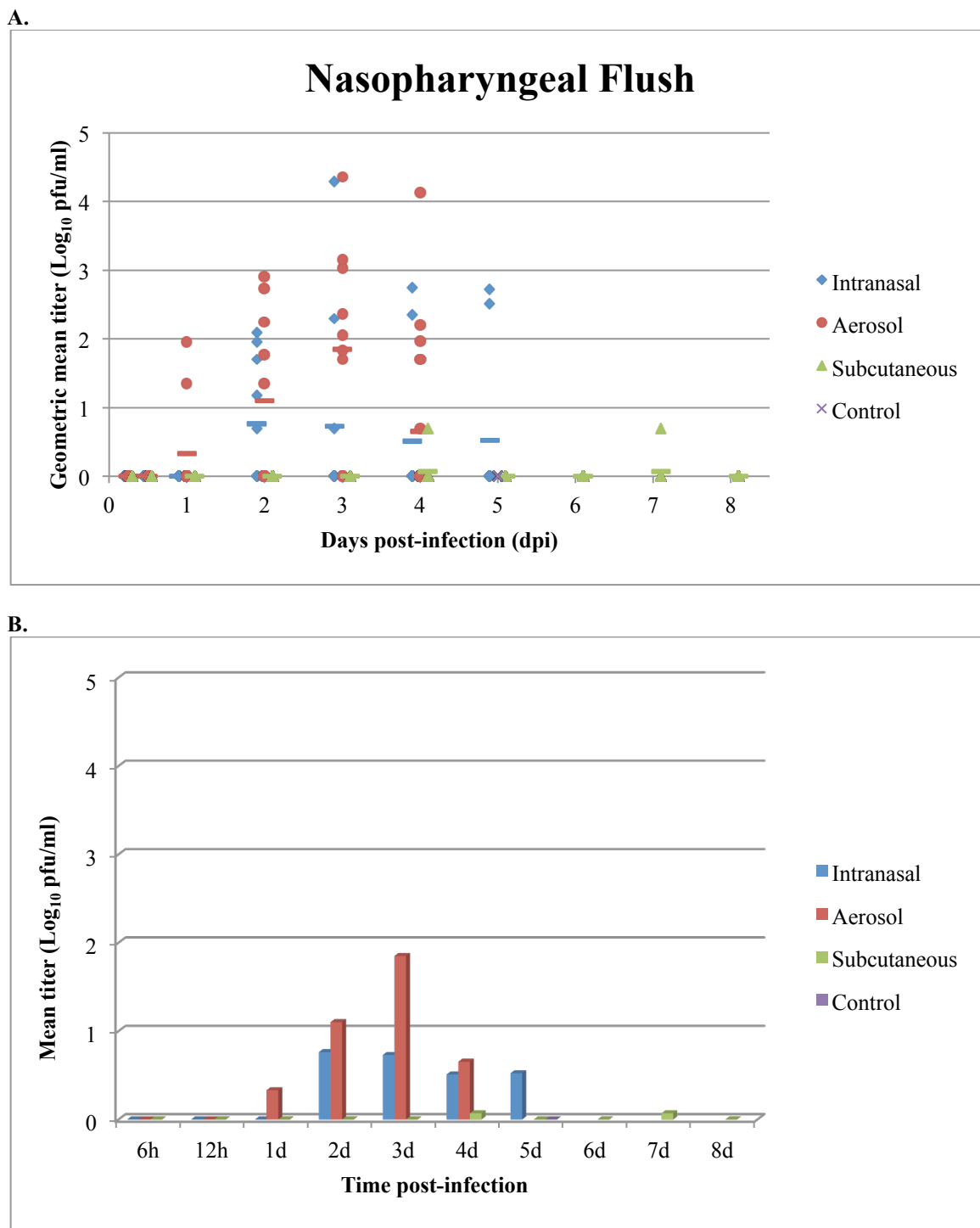
Figure 2.7. Geometric mean viral titer in the nasopharyngeal flush (NF) of individual mice **(A),** and mean viral titer of the groups **(B)** from BALB/c mice infected with NA EEEV strain FL93-939. Mice were infected with approximately 30-100X LD_{50} and were then euthanized at specified time points (n=5). Viral titers were determined by standard plaque assay. Symbols represent individual animals with values calculated from the geometric mean titer of all dilutions which had at least one visible pfu. The mean for the group is shown in the colored line (A). Bars represent the mean titer of the group for each time point (B). Limit of detection of the assay is 5 pfu/ml.

A.

B.
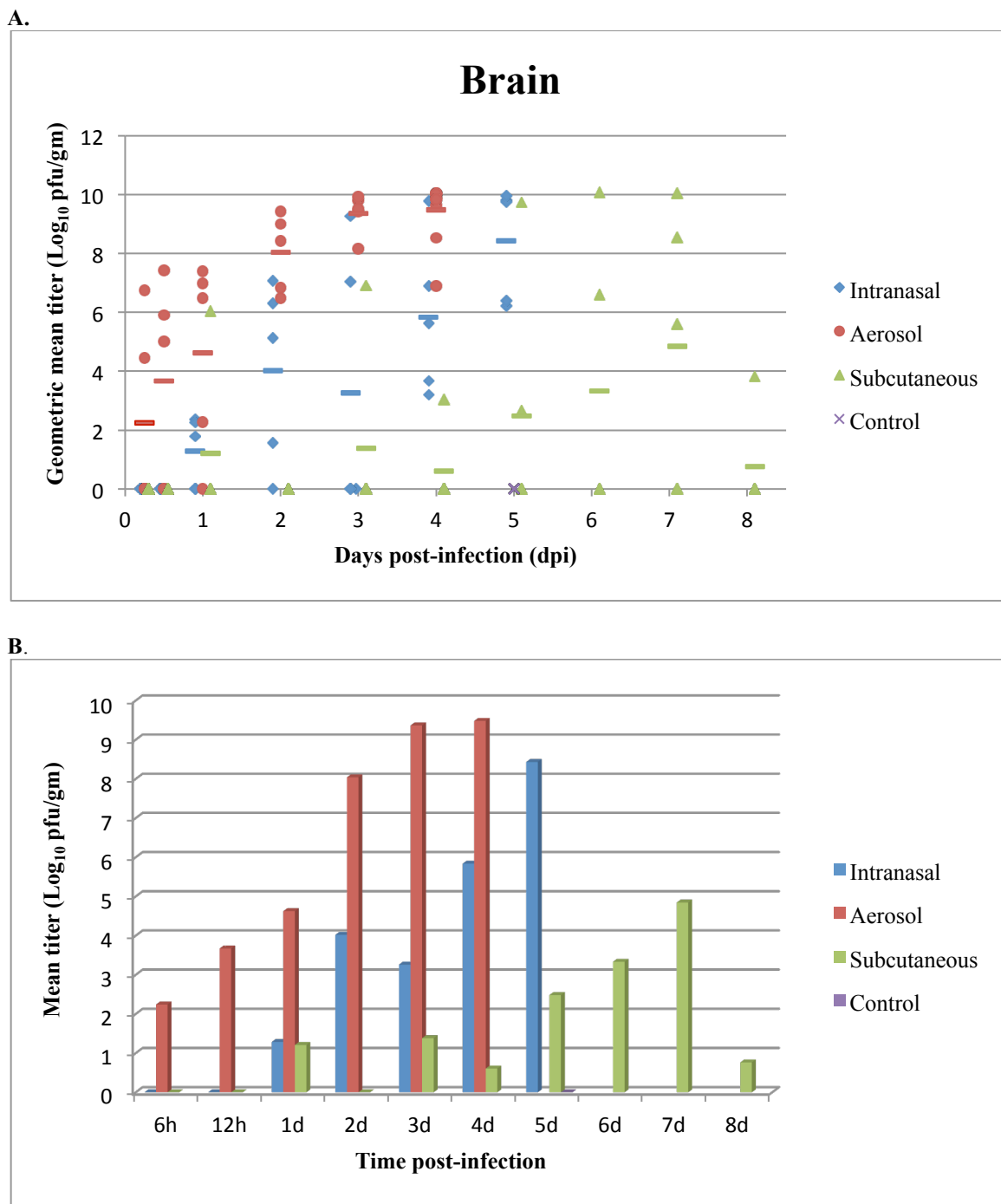
Figure 2.8. Geometric mean viral titer in the brain of individual mice **(A),** and mean viral titer of the groups **(B)** from BALB/c mice infected with NA EEEV strain FL93-939. Mice were infected with approximately 30-100X LD_{50} and were then euthanized at specified time points (n=5). Viral titers of tissue supernatants were determined by standard plaque assay. Symbols represent individual animals with values calculated from the geometric mean titer of all dilutions which had at least one visible pfu. The mean for the group is shown in the colored line (A). Bars represent the mean titer of the group for each time point (B).

peaking later, at 7 dpi. Viral titers in the lung (Figure 2.9) in the IN and AE studies were

similar at 6 hpi, and in both studies continued to rise to fairly high titers through 2 dpi;

however, the titers in the AE study were significantly higher than those in the IN study

from 2-4 dpi. Virus was not present in the lung in the SC study until 4 dpi and titers

remained low even at 6-7 dpi. The mandibular salivary gland and lymph nodes were

collected and analyzed together due to their intimate association anatomically. The

mandibular lymph nodes, also known as the mandibular and accessory mandibular lymph

node, submandibular lymph nodes, or superficial cervical lymph nodes (Van den Broeck,

Derore et al. 2006), are a small group of lymph nodes that drain the structures of the

muzzle (Dyce, Sack et al. 1987) and were therefore of interest in the IN and AE studies.

As might be expected, virus was present at low levels in the mandibular lymph nodes in

both the IN and AE studies at 1 dpi (Figure 2.10) and titers slowly increased throughout

the remaining time points, peaking at 5 dpi and 4 dpi, respectively. In the SC study, virus

was not present in the mandibular lymph nodes until 4 dpi and remained at relatively low

levels through 7 dpi. Virus at this site could be the result of drainage from the nasal

cavity or seeding from viremia. Viral titers in the spleen (Figure 2.11) followed similar

trends, with virus first appearing in the spleen at 1 dpi in the AE study and at 2 dpi in the

IN study; titers increased throughout the study and peaked at 4 dpi and 5 dpi,

respectively. In the SC study, virus appeared at 3 dpi, peaked at 4 dpi and slowly

decreased over the remaining time points. The mesenteric lymph node, which drains the

digestive tract, is a distant lymph node for all routes of infection, and virus present in this

lymph node may be indicative of distant viral spread by either blood or lymph. The viral

A.

B.
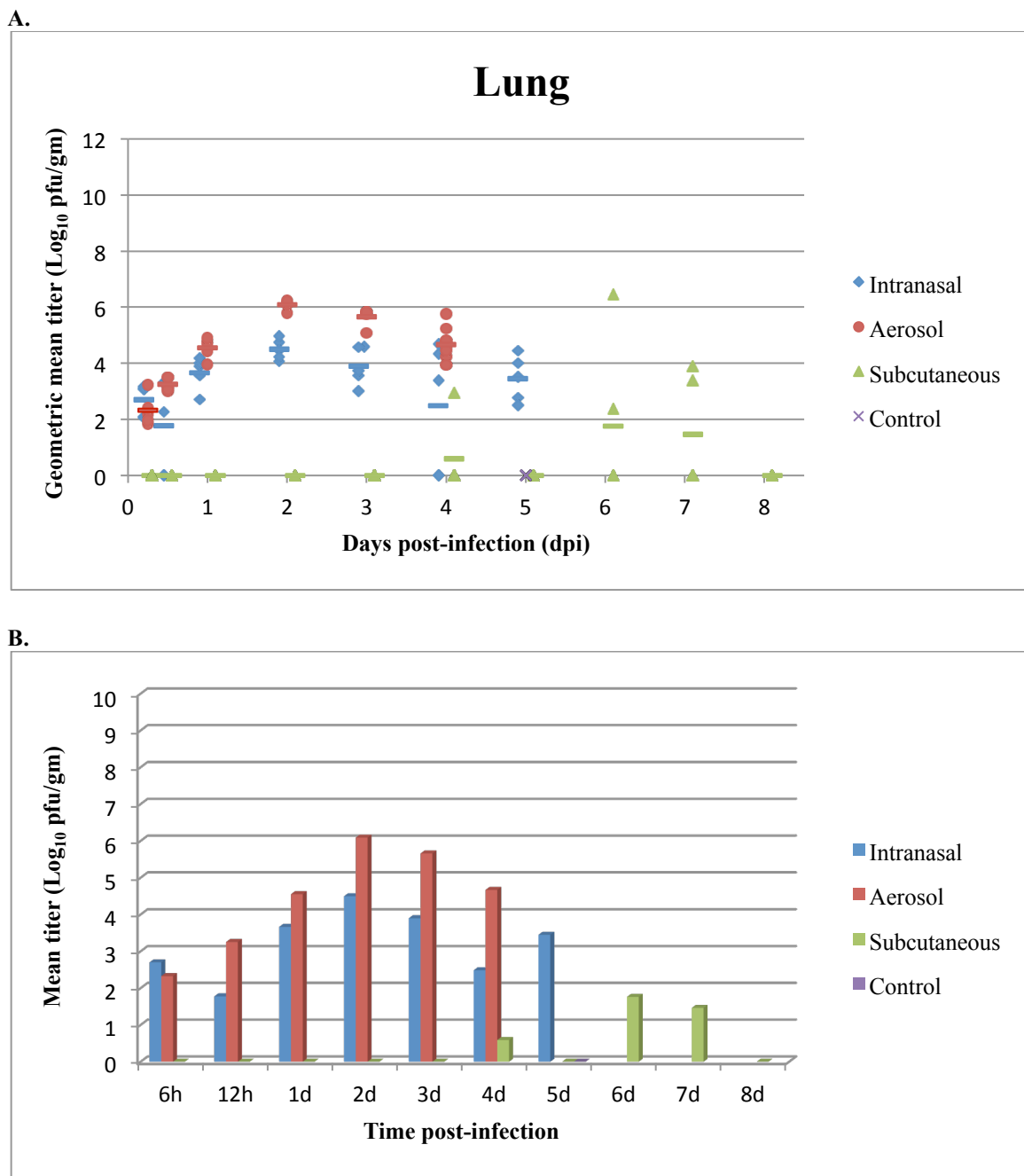
Figure 2.9. Geometric mean viral titer in the lung of individual mice **(A),** and mean viral titer of the groups **(B)** from BALB/c mice infected with NA EEEV strain FL93-939. Mice were infected with approximately 30-100X LD_{50} and were then euthanized at specified time points (n=5). Viral titers of tissue supernatants were determined by standard plaque assay. Symbols represent individual animals with values calculated from the geometric mean titer of all dilutions which had at least one visible pfu. The mean for the group is shown in the colored dashed line (A). Bars represent the mean titer of the group for each time point (B).

A.

B.
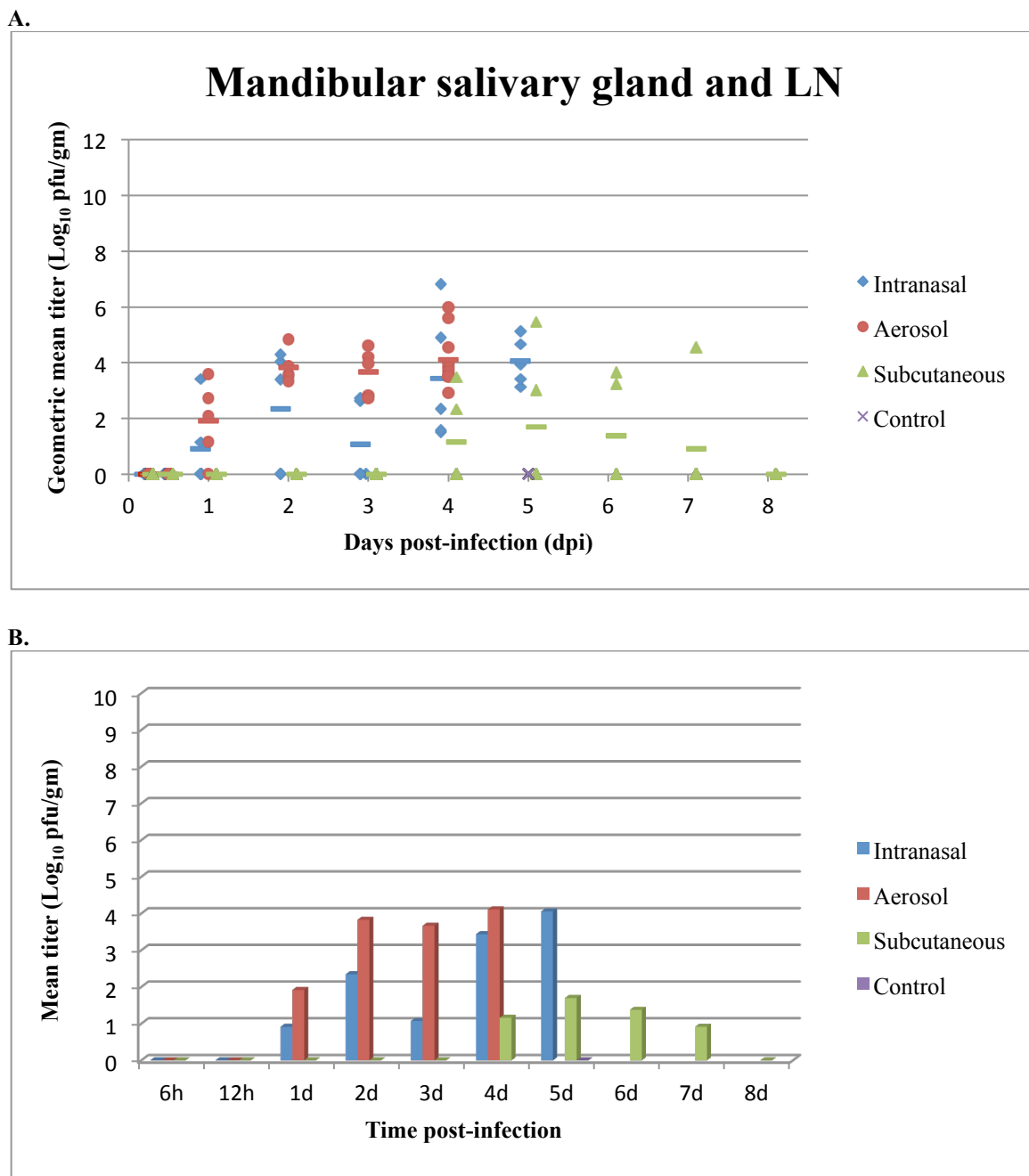
Figure 2.10. Geometric mean viral titer in the submandibular salivary gland and lymph node of individual mice **(A),** and mean viral titer of the groups **(B)** from BALB/c mice infected with NA EEEV strain FL93-939. Mice were infected with approximately 30-100X LD_{50} and were then euthanized at specified time points (n=5). Viral titers of tissue supernatants were determined by standard plaque assay. Symbols represent individual animals with values calculated from the geometric mean titer of all dilutions which had at least one visible pfu. The mean for the group is shown in the colored dashed line (A). Bars represent the mean titer of the group for each time point (B).

A.

B.
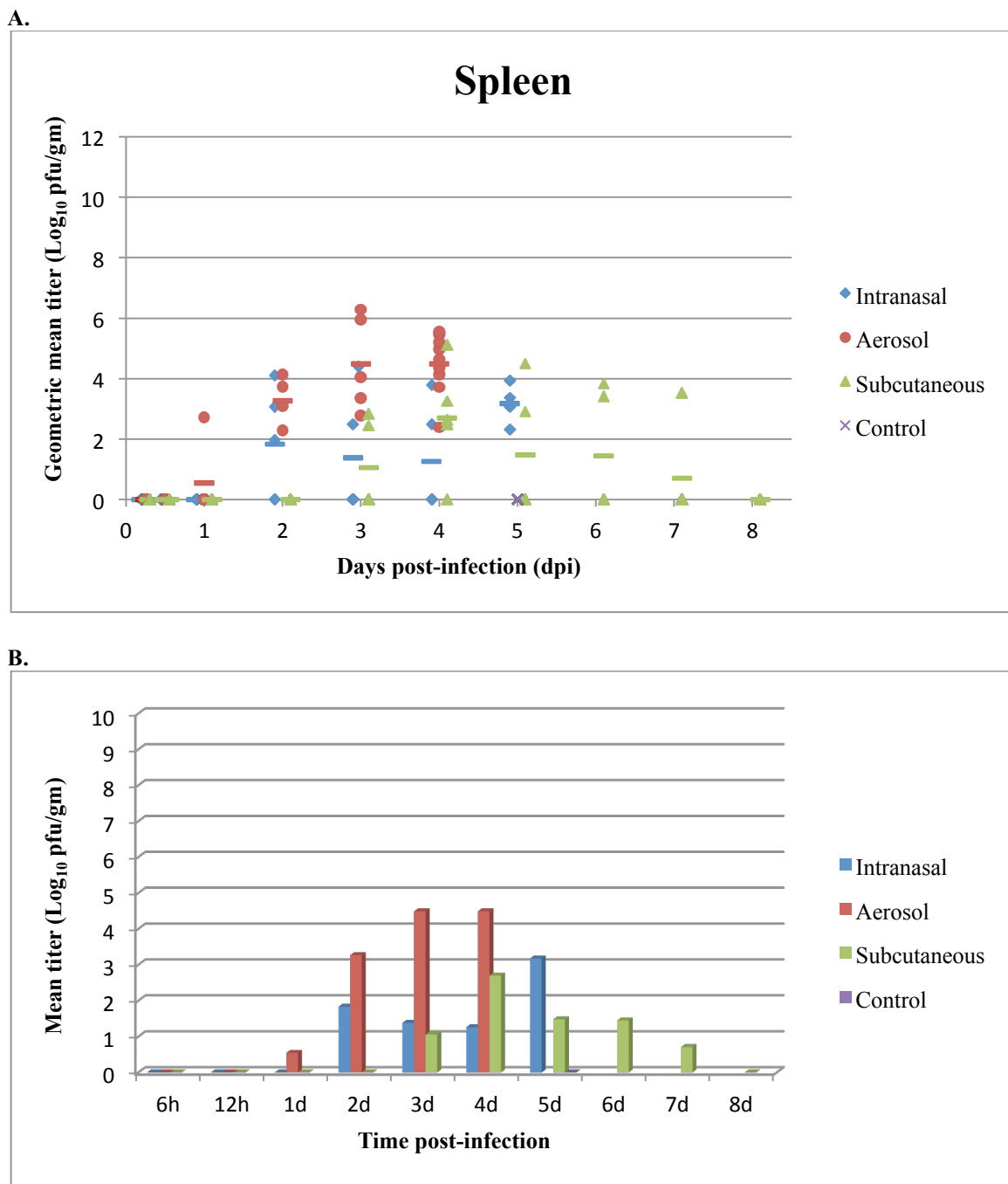
Figure 2.11. Geometric mean viral titer in the spleen of individual mice **(A),** and mean viral titer of the groups **(B)** from BALB/c mice infected with NA EEEV strain FL93-939. Mice were infected with approximately 30-100X LD_{50} and were then euthanized at specified time points (n=5). Viral titers of tissue supernatants were determined by standard plaque assay. Symbols represent individual animals with values calculated from the geometric mean titer of all dilutions which had at least one visible pfu. The mean for the group is shown in the colored dashed line (A). Bars represent the mean titer of the group for each time point (B).

titers in this tissue were low for all routes of infection and peaked at 3 dpi in the AE study, 5 dpi in the IN study, and 7 dpi in the SC study (Figure 2.12). Mean group viral titers of the remaining tissues (liver, heart, kidneys, adrenal glands, and pancreas) evaluated in all three studies are shown in Figure 2.13. No virus was present in any of these tissues until 1 dpi and virus titers remained very low throughout most time points. The slight increase in titer in the heart and kidneys could be due to poor perfusion of these vascular organs with PBS prior to tissue collection. Overall, the differences in viral titer in the various tissues are likely due to the variation in delivery method and viral dose. In the IN and AE studies, in which mice received approximately $100LD_{50}$, virus was present early on and at high titer in the serum, BAL, brain, and lung. The viral titer in the remaining tissues was lower and peaked later in the time course. While in the SC study, in which mice received approximately 30LD50, the viral titer in tissues was generally lower and peaked later in the course of disease.

In order to more accurately trace the path of the virus in the SC study, mice were inoculated in the left rear footpad and subsequent samples were collected from both the left and right footpad, foot, gastronemius muscle, and popliteal lymph node for viral titer. As expected, the viral titer was high in the left footpad and left foot early in infection (6 hpi) and remained high throughout all time points, whereas virus appeared at low levels in the right footpad and right foot after 12 hpi and 2 dpi and peaked at 4 dpi and 3 dpi respectively (Figure 2.14). There was significant viral replication at the site of inoculation (left footpad and foot) as the mice received approximately 1000 pfu/footpad and the titers reached 6 log10 pfu/gm by 1 dpi.

A.

B.
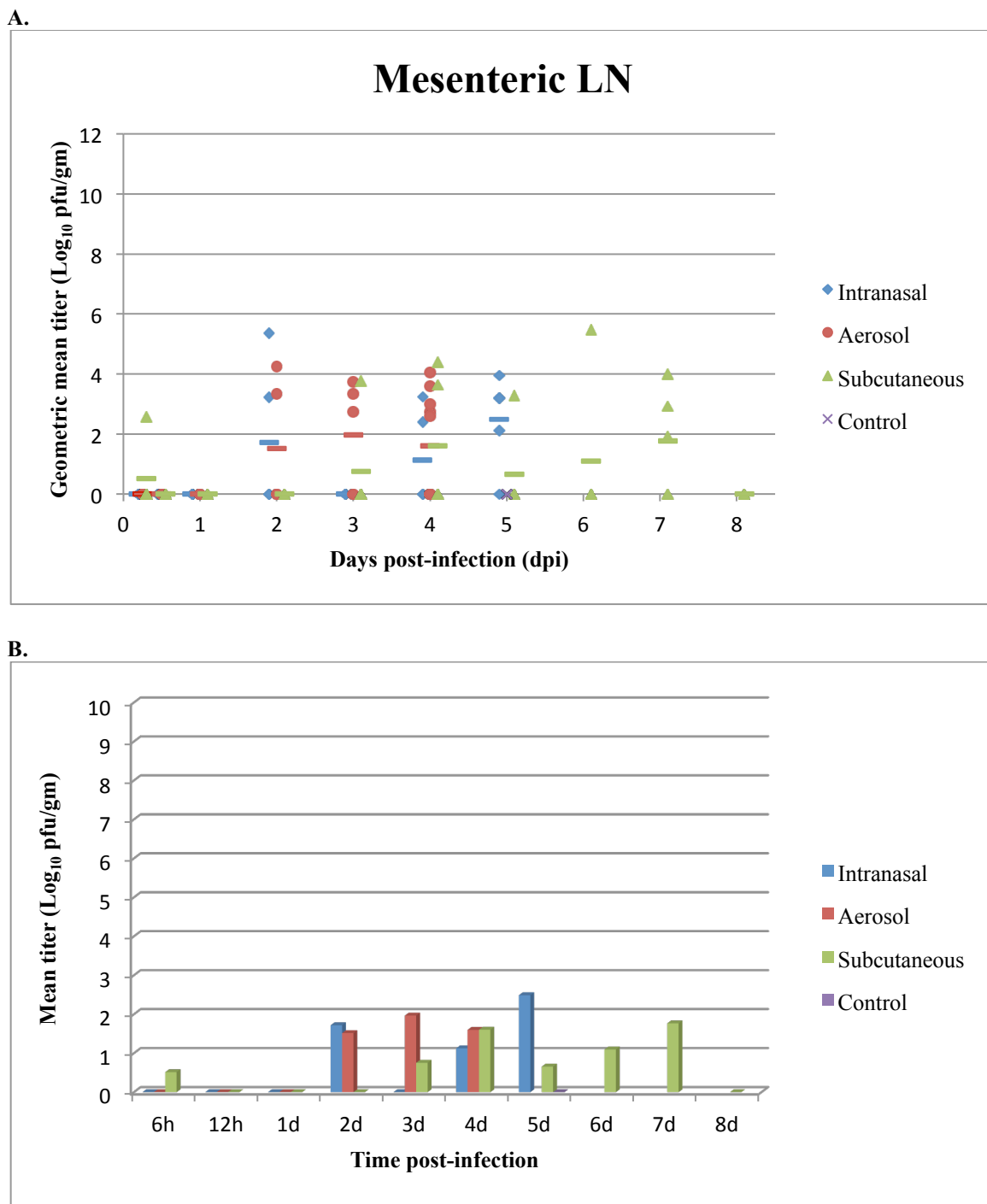
Figure 2.12. Geometric mean viral titer in the mesenteric lymph node of individual mice **(A),** and mean viral titer of the group **(B)** from BALB/c mice infected with NA EEEV strain FL93-939. Mice were infected with approximately 30-100X LD_{50} and were then euthanized at specified time points (n=5). Viral titers of tissue supernatants were determined by standard plaque assay. Symbols represent individual animals with values calculated from the geometric mean titer of all dilutions which had at least one visible pfu. The mean for the group is shown in the colored dashed line (A). Bars represent the mean titer of the group for each time point (B).
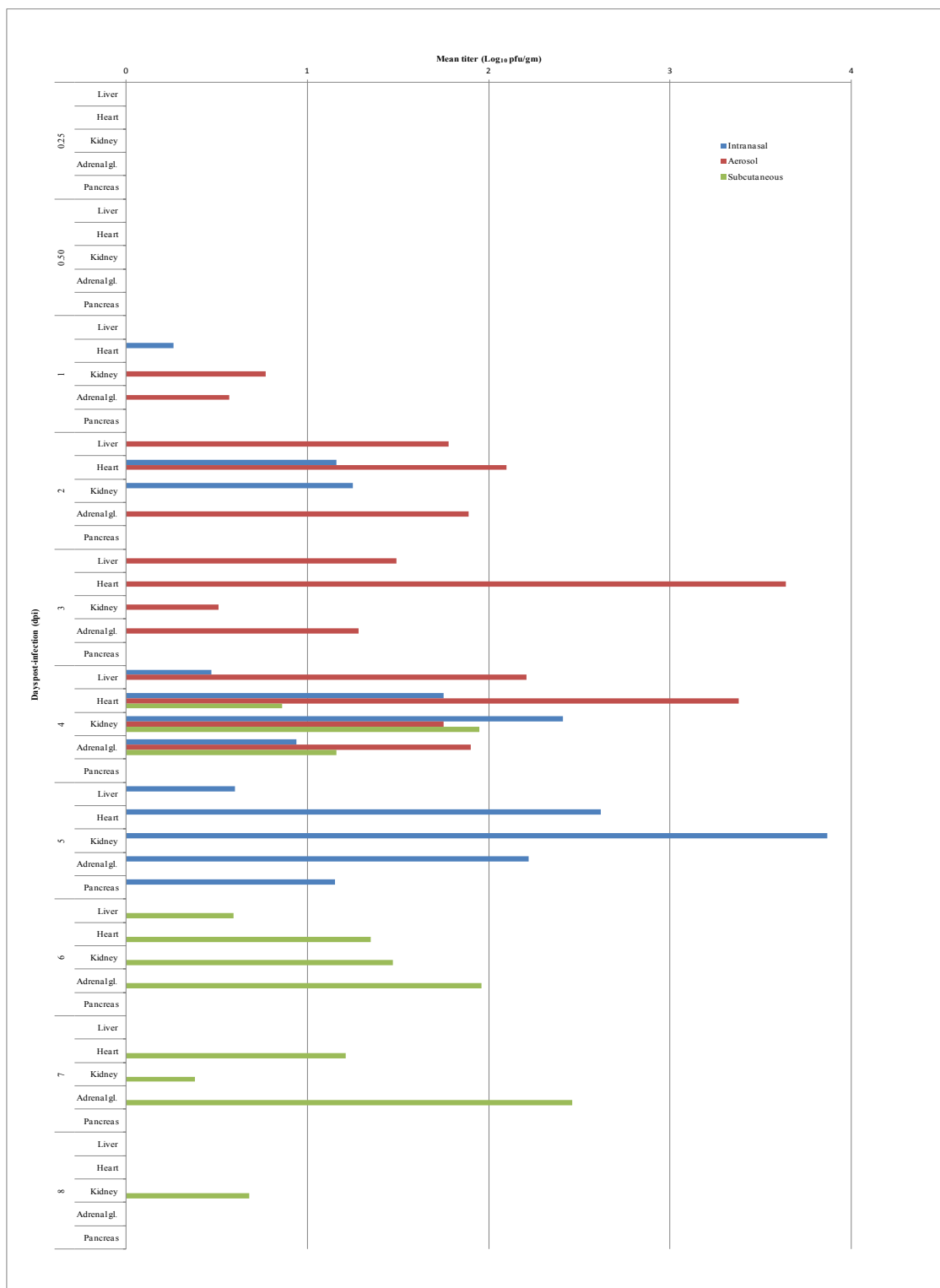
Figure 2.13. Mean viral titer in the liver, heart, kidney, adrenal gland, and pancreas of the groups from BALB/c mice infected with NA EEEV strain FL93-939. Mice were infected with approximately 30-100X LD_{50} and were then euthanized at specified time points (n=5). Viral titers of tissue supernatants were determined by standard plaque assay. Bars represent the mean titer of the group for each time point.

Viral titers were determined for the left and right gastrocnemius muscle (calf muscle), a large muscle group in the lower leg, as it has been previously reported that EEEV replicates in skeletal muscle (Vogel P, Kell WM et al. 2005). The mean viral titer of left gastrocnemius muscle remained low throughout the study and virus did not appear in the right gastrocnemius muscle until 5 dpi (Figure 2.15). Viral titers were also determined for the left and right popliteal lymph nodes, the draining lymph nodes of the inoculation site. Mean viral titer of the left popliteal lymph node rose rapidly post-inoculation and remained at high levels until 6 dpi. While virus was detected in the right popliteal lymph node 1 dpi, viral titers remained low throughout the study.

Pathology

Five mice from each time point were euthanized and perfused with 10% NBF and routine tissues were collected for histologic and immunohistochemical analysis. Significant immunohistochemical findings and histologic lesions from the IN study are summarized in tables 2.6 and 2.7, respectively. In the IN study, viral antigen was first detected in the nasal cavity of one mouse at 1 dpi (Figure 2.16). At this time viral antigen also was detected in both the olfactory epithelium (Figure 2.16B, arrow) and lamina propria as well as the odontoblasts of a tooth. However, no histologic lesions were noted at these sites. By 2 dpi, viral antigen was present in the nasal cavity of 3 mice (Figure 2.16C). Viral antigen was only detected in the olfactory epithelium and underlying lamina propria (Figure 2.16C, arrows) and not within the respiratory epithelium (Figure 2.16C, arrow head). Two of the mice also had viral antigen present in the olfactory bulb (Figure 2.16D), and in one of these mice there was also viral antigen present in low

A.

B.
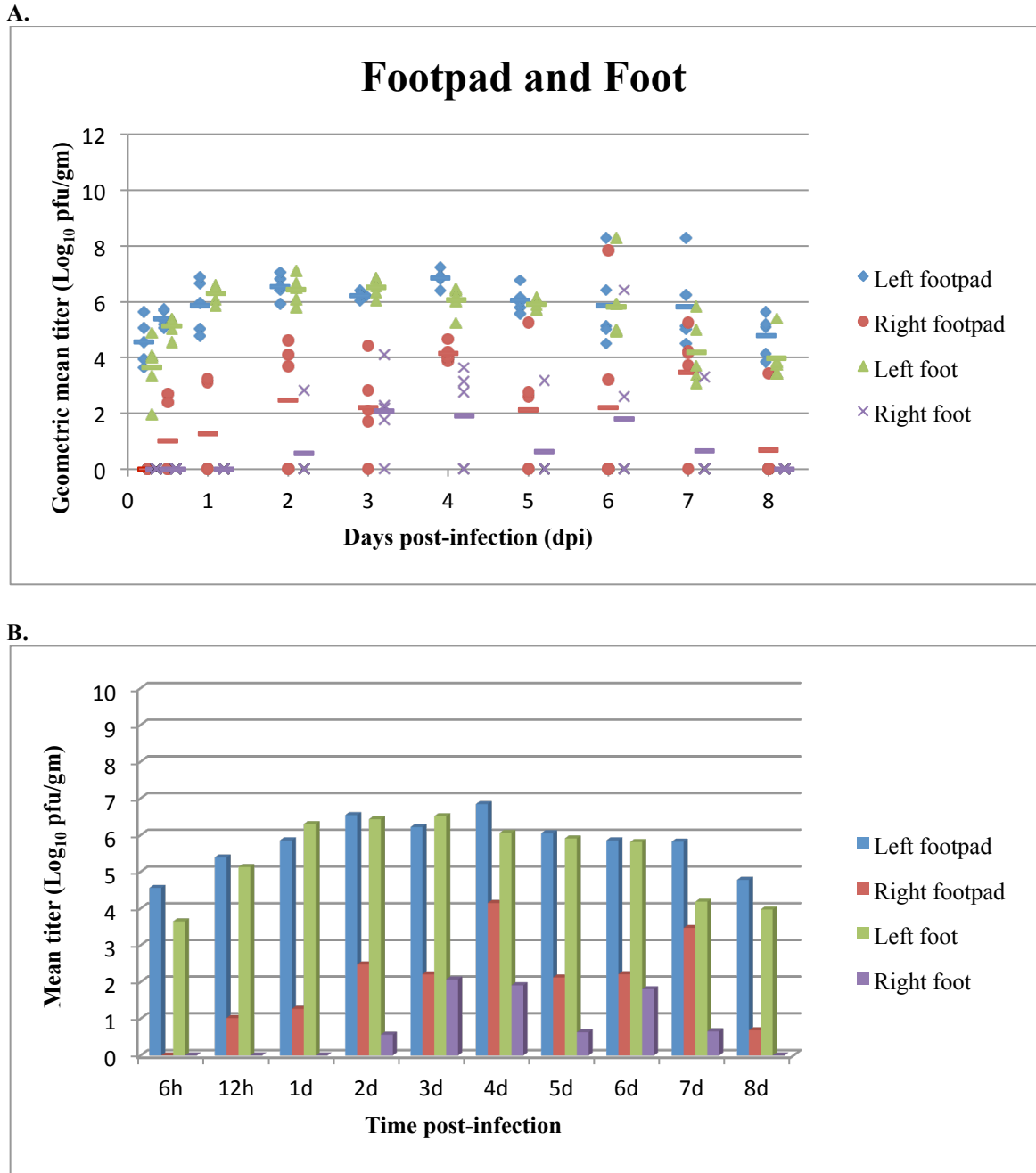
Figure 2.14. Geometric mean viral titer in the left and right footpad and foot of individual mice **(A),** and mean viral titer of the groups **(B)** from BALB/c mice infected with NA EEEV strain FL93-939. Mice were infected with approximately 30-100X LD_{50} and were then euthanized at specified time points (n=5). Viral titers of tissue supernatants were determined by standard plaque assay. Symbols represent individual animals with values calculated from the geometric mean titer of all dilutions which had at least one visible pfu. The mean for the group is shown in the colored dashed line (A). Bars represent the mean titer of the group for each time point (B).

A.

B.
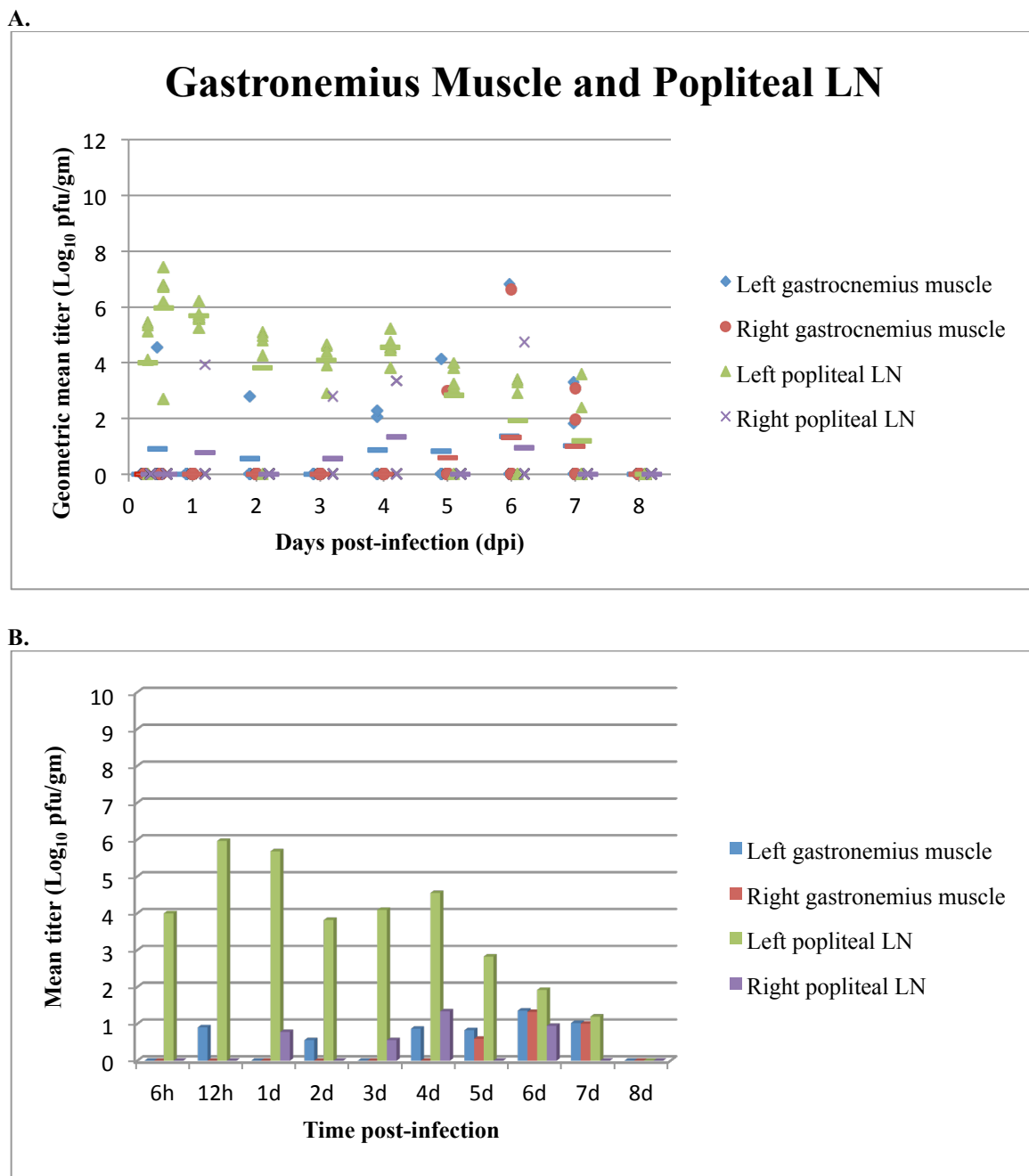
Figure 2.15. Geometric mean viral titer in the left and right gastrocnemius muscle and popliteal lymph node of individual mice **(A),** and mean viral titer of the groups **(B)** from BALB/c mice infected with NA EEEV strain FL93-939. Mice were infected with approximately 30-100X LD_{50} and were then euthanized at specified time points (n=5). Viral titers of tissue supernatants were determined by standard plaque assay. Symbols represent individual animals with values calculated from the geometric mean titer of all dilutions which had at least one visible pfu. The mean for the group is shown in the colored dashed line (A). Bars represent the mean titer of the group for each time point (B).

numbers of neurons in the cerebrum, primarily in the piriform cortex. Additionally, one mouse had minimal viral antigen present in the lungs, within the alveolar septa in close proximity to a terminal bronchiole. Two mice also had viral antigen in the mandibular lymph node, one of the draining lymph nodes of the nasal cavity. The antigen was found only in mononuclear cells, histocytes or dendritic cells, within the subcapsular sinus, and not within the follicles of the cortex. In most sites where antigen was present, except the lymph node, there was single cell death, characterized by pyknosis and eosinophilic cellular and karyorrhectic debris without inflammation, suggestive of apoptosis. Both the immunohistochemical and histologic findings at 3 dpi were similar to those seen at 2 dpi, with viral antigen present in the nasal cavity, olfactory bulb, and cerebrum of 2 mice, accompanied by single cell death in a small number of cells in the areas where antigen was present. At both 4 and 5 dpi; however, viral antigen was noted multifocally in the nasal cavity, teeth, as well as throughout the olfactory bulb, frontal cortex, midbrain (Figure 2.16E), cerebellum, brain stem, and spinal cord. Additionally, there was vacuolation, both intracytoplasmic and within the neuropil (spongiosis), within the olfactory bulb and spinal cord of some animals. Varying amounts of single cell death were noted in all sites where viral antigen was present, and a significant number of neurons in the hippocampus were apoptotic or absent (Figure 2.16F, arrow). There was also mild leptomeningitis with occasional perivascular infiltrates (minimal encephalitis) in a few mice. In later time points, viral antigen was also noted in ganglion cells of the retina (eye), osteoblasts and fibroblasts lining the trabecular bone surrounding the nasal cavity, pituitary gland, renal pelvic tubules (kidney), and myometrium (uterus).

The findings in the AE study were similar; however, there were some important

differences. Significant immunohistochemical findings and histologic lesions from the

AE study are summarized in Tables 2.8 and 2.9, respectively. While viral antigen was

also first detected in the olfactory epithelium and lamina propria of the nasal cavity at 1

dpi (Figure 2.17A), it was found in 3 of the 5 mice, all of which also had histologic

evidence of apoptosis in the areas where antigen was present. One of these mice also had

minimal viral antigen present in the olfactory nerve within the nasal cavity as well as the

olfactory bulb (Figure 2.17B), the first indication of neural invasion. By 2 dpi, 4 of the 5

mice had viral antigen present multifocally within the nasal cavity (Figure 2.17C) and

within the olfactory nerve (Figure 2.17C, inset), while 3 of these mice also had viral

antigen in the teeth (odontoblasts) and/or olfactory bulb and frontal cortex. In one of

these mice, viral antigen was also present in the cerebrum at the level of the hippocampus

(midbrain). In all of the mice that had viral antigen present in the brain, it was primarily

located in the piriform cortex and sporadically within the thalamus (Figure 2.17D). In the

nasal cavity of all of the mice with viral antigen there was varying amount of apoptosis.

At 3 dpi, viral antigen was present in the nasal cavity, olfactory bulb, frontal cortex, and

midbrain of all mice, and within the brain stem of 2 animals. Viral antigen was also

found in the teeth (odontoblasts or ameloblasts) and lungs (alveolar septa/interstitium) of

4 mice. Single cell death was easily recognized within the nasal cavity, olfactory bulb,

and cerebrum and was variably present in other areas where viral antigen was located.

Additionally, there was focally extensive moderate inflammation (rhinitis) within the

nasal cavity of two mice. Within the brain, there were variable amounts of neuronal
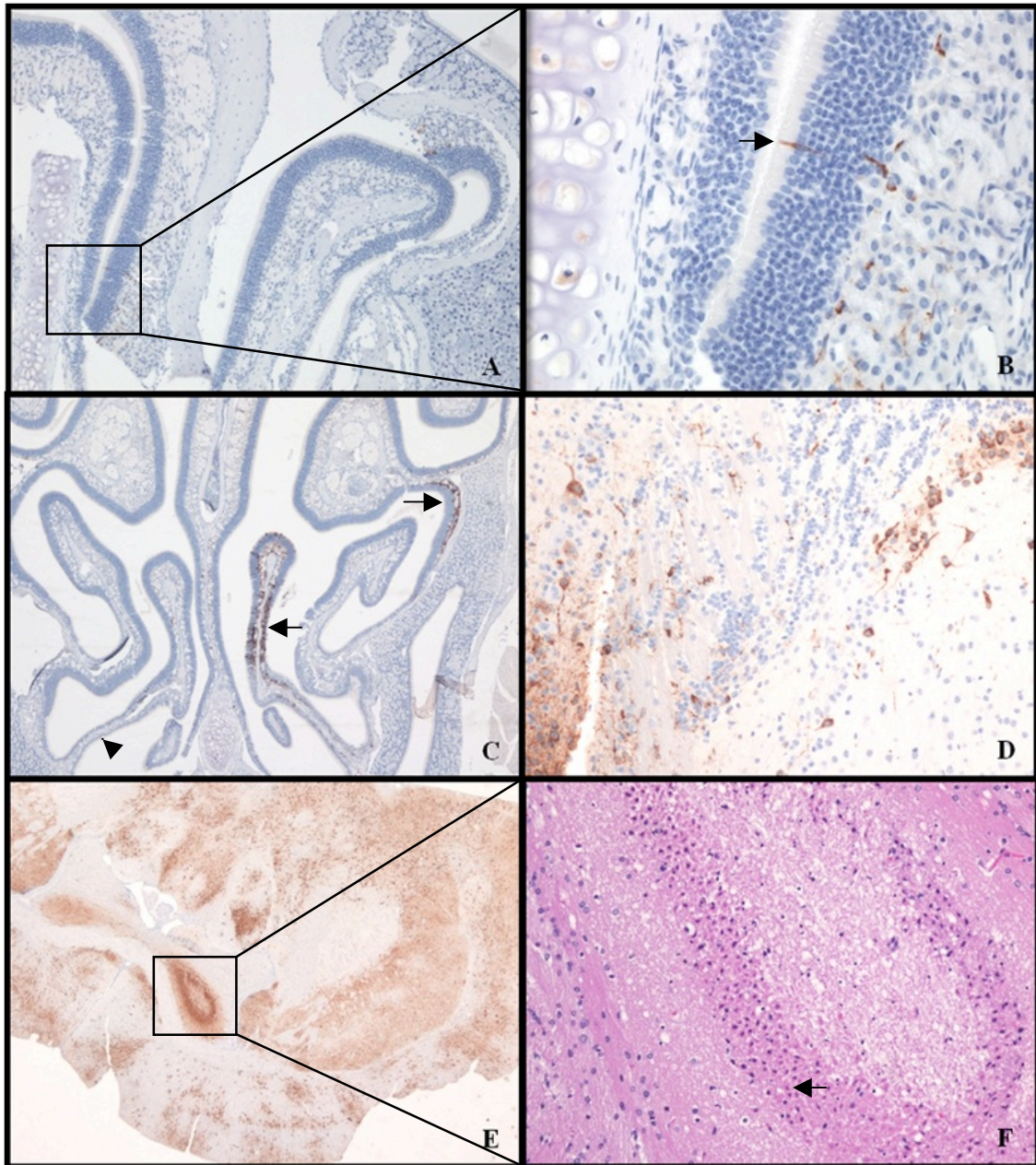
Figure 2.16. Immunohistochemical and histologic findings in mice after IN infection with EEEV strain FL93-939. Mice were infected with approximately $100LD_{50}$ and were euthanized at specified time points (n=5). Viral antigen was first detected in the nasal cavity at1 dpi (box) (A; magnification X100), specifically the olfactory epithelium and underlying lamina propria (arrow) (B; magnification X400). A significant amount of viral antigen was present in the nasal cavity by 2 dpi, but was restricted to the olfactory epithelium (arrows), the respiratory epithelium was not involved (arrow head) (C; magnification X40). Viral antigen was first detected in the olfactory bulb at 2 dpi (D; magnification X400). Viral antigen was present throughout the brain by 5 dpi (E; magnification X20) and there was significant neuronal cell death (hypereosinophilic, shrunken neurons with pyknosis or karyorrhexis, arrow) in the hippocampus (F; magnification X200)

Table 2.6. Significant immunohistochemical findings observed in mice after IN challenge with EEEV

Tissue		6 hpi					12 hpi					1 dpi					2 dpi					3 dpi					4 dpi					5 dpi				
		IN6	IN7	IN8	IN9	IN10	IN6	IN7	IN8	IN9	IN10	IN6	IN7	IN8	IN9	IN10	IN6	IN7	IN8	IN9	IN10	IN6	IN7	IN8	IN9	IN10	IN6	IN7	IN8	IN9	IN10	IN6	IN7	IN8	IN9	IN10
Head	Nasal cavity	-	-	-	-	-	-	-	-	-	-	++	-	-	-	-	++	++	++	-	-	++	-	-	++	-	++	++	++	++	-	++	++	-	++	++
	Teeth	-	-	-	-	-	-	-	-	-	-	++	-	-	-	-	++	-	++	-	-	++	-	-	++	-	++	++	++	-	-	++	++	-	++	++
	Bone	-	-	-	-	-	-	-	-	-	-	-	-	-	-	-	-	++	-	-	-	++	-	-	++	-	-	-	-	-	-	-	-	-	-	-
	Eyes	-	-	-	-	-	-	-	-	-	-	-	-	-	-	-	-	-	-	-	-	-	-	-	-	-	-	++	++	-	-	++	++	-	-	-
Brain	Olfactory bulb	-	-	-	-	-	-	-	-	-	-	++	-	++	-	-	++	-	-	++	-	++	-	++	-	-	++	++	++	++	-	++	++	-	-	++
	Frontal cortex	-	-	-	-	-	-	-	-	-	-	++	-	-	-	-	++	-	-	++	-	++	-	-	++	-	++	++	++	++	-	++	++	-	-	++
	Midbrain	-	-	-	-	-	-	-	-	-	-	++	-	-	-	-	++	-	-	++	-	++	-	-	++	-	++	++	++	++	-	++	++	-	-	++
	Cerebellum	-	-	-	-	-	-	-	-	-	-	-	-	-	-	-	-	-	-	-	-	-	-	-	-	-	++	++	-	++	-	++	++	-	-	++
	Brain stem	-	-	-	-	-	-	-	-	-	-	-	-	-	-	-	-	-	-	-	-	-	-	-	-	-	++	++	-	++	-	++	++	-	-	++
	Pituitary gland	-	-	-	-	-	tnp	-	-	tnp	tnp	-	-	-	-	-	-	tnp	tnp	tnp	tnp	tnp	tnp	tnp	tnp	-	-	-	tnp	++	tnp	tnp	tnp	-	tnp	tnp
Spinal cord		-	-	-	-	-	-	-	-	-	-	-	-	-	-	-	-	-	-	-	-	++	-	-	++	-	++	++	-	++	-	++	++	-	-	++
Salivary gland	Mandibular	-	-	-	-	-	-	-	-	-	-	-	-	-	-	-	-	-	-	-	-	++	-	-	-	-	-	-	-	-	-	-	-	-	-	-
Haired skin		-	-	-	-	-	-	-	-	-	-	-	-	-	-	-	-	-	-	-	-	-	-	-	-	-	-	-	-	-	-	-	-	-	-	-
Lung		-	-	-	-	-	-	-	-	-	-	-	-	-	-	-	-	++	-	-	-	++	++	-	-	++	-	++	-	-	-	-	-	-	-	++
Heart		-	-	-	-	-	-	-	-	-	-	-	-	-	-	-	-	-	-	-	-	-	-	-	-	-	-	-	-	-	-	-	-	-	-	-
Spleen		-	-	-	-	-	-	-	-	-	-	-	-	-	-	-	-	-	-	-	-	-	-	-	-	-	-	-	-	-	-	-	-	-	-	-
Liver		-	-	-	-	-	-	-	-	-	-	-	-	-	-	-	-	-	-	-	-	-	-	-	-	-	-	-	-	-	-	-	-	-	-	-
Lymph node	Mandibular	-	-	-	-	-	-	-	-	-	-	-	-	-	-	-	-	++	-	-	++	-	-	-	-	-	-	++	++	-	-	++	-	-	-	-
	Tracheobronchial	-	-	-	-	-	-	-	-	-	-	-	-	-	-	-	-	-	-	-	-	-	-	-	tnp	tnp	-	-	-	-	-	-	-	-	-	-
	Axillary, left	-	tnp	-	-	-	-	-	-	-	-	-	-	-	-	-	-	-	-	tnp	-	-	-	-	-	tnp	-	-	-	-	-	tnp	tnp	tnp	-	-
	Axillary, right	-	-	-	-	-	tnp	-	-	-	-	-	-	-	-	-	-	tnp	-	tnp	-	tnp	tnp	tnp	-	-	-	-	-	-	tnp	tnp	tnp	tnp	-	tnp
	Mesenteric	-	-	-	-	-	-	-	-	-	-	-	-	-	-	-	-	-	-	-	-	-	-	-	-	-	-	-	-	-	-	-	-	-	-	-
	Inguinal, left	-	-	-	-	-	-	-	-	-	-	-	-	-	-	-	-	-	-	-	-	-	tnp	tnp	tnp	-	tnp	-	tnp	-	-	tnp	tnp	-	-	-
	Inguinal, right	-	tnp	tnp	tnp	tnp	tnp	-	tnp	tnp	tnp	-	-	-	-	-	-	-	-	-	-	-	-	tnp	-	-	-	-	-	tnp	-	-	-	tnp	-	tnp
	Popliteal, left	-	-	-	-	-	-	-	-	-	-	-	-	-	-	-	-	tnp	-	-	tnp	-	tnp	-	tnp	-	tnp	tnp	-	-	-	-	-	-	-	-
	Popliteal, right	-	-	-	-	tnp	-	-	-	tnp	-	-	-	-	-	-	-	-	-	-	-	-	tnp	-	-	-	-	-	-	tnp	-	tnp	tnp	tnp	-	-
Thymus		-	-	-	-	-	-	-	-	-	-	-	-	-	-	-	-	-	-	-	-	-	-	-	-	-	-	-	-	-	-	-	-	-	-	-
Thyroid gland		-	-	-	-	-	-	-	-	-	-	-	-	-	-	-	-	-	-	-	-	-	-	-	-	-	-	-	-	-	-	-	-	-	tnp	-
Pancreas		-	-	-	-	-	-	-	-	-	-	-	-	-	-	-	-	-	-	-	-	-	-	-	-	-	-	-	-	-	-	-	-	-	-	-
GI tract		-	-	-	-	-	-	-	-	-	-	-	-	-	-	-	-	-	-	-	-	-	-	-	-	-	-	-	-	-	-	-	-	-	-	-
Kidneys		-	-	-	-	-	-	-	-	-	-	-	-	-	-	-	-	-	-	-	-	-	-	-	-	-	-	-	-	-	-	++	-	-	-	-
Urinary bladder		-	-	-	-	-	-	tnp	tnp	-	-	-	-	-	-	-	-	-	-	-	-	-	-	-	-	-	-	-	-	-	-	-	-	-	-	-
Adrenal glands		-	-	-	-	-	-	-	-	-	-	-	-	-	-	-	-	-	-	-	-	-	-	-	-	-	-	-	-	-	-	-	-	-	-	-
Uterus	Myometrium	-	-	-	-	-	-	-	-	-	-	-	-	-	-	-	-	-	-	-	-	++	-	-	-	-	-	-	-	-	-	-	-	-	-	-
Ovaries		-	-	-	-	-	-	-	-	-	-	-	-	-	-	-	-	-	-	-	-	-	-	-	-	-	-	-	-	-	-	-	-	-	-	-
Rear leg, left		-	-	-	-	-	-	-	-	-	-	-	-	-	-	-	-	-	-	-	-	-	-	-	-	-	-	-	-	-	-	-	-	-	-	-
Rear foot, left		-	-	-	-	-	-	-	-	-	-	-	-	-	-	-	-	-	-	-	-	-	-	-	-	-	-	-	-	-	-	-	-	-	-	-
Rear leg, right		-	-	-	-	-	-	-	-	-	-	-	-	-	-	-	-	-	-	-	-	-	-	-	-	-	-	-	-	-	-	-	-	-	-	-
Rear foot, right		-	-	-	-	-	-	-	-	-	-	-	-	-	-	-	-	-	-	-	-	-	-	-	-	-	-	-	-	-	-	-	-	-	-	-

Table 2.6. Significant immunohistochemical findings observed in mice after IN challenge with EEEV. Symbols (++, ±, -) indicate that viral antigen was present and easily recognized (++); variably present throughout the tissue (±); or not detected histologically (-). Tnp= tissue not present on slide.

Table 2.7. Significant histologic lesions noted in mice after IN challenge with EEEV.

Tissue	Lesion	6 hpi					12 hpi					1 dpi					2 dpi					3 dpi					4 dpi					5 dpi				
		IN6	IN7	IN8	IN9	IN10	IN6	IN7	IN8	IN9	IN10	IN6	IN7	IN8	IN9	IN10	IN6	IN7	IN8	IN9	IN10	IN6	IN7	IN8	IN9	IN10	IN6	IN7	IN8	IN9	IN10	IN6	IN7	IN8	IN9	IN10
Nasal cavity	Inflammation	-	-	-	-	-	-	-	-	-	-	-	-	-	-	-	-	-	-	-	-	-	-	-	-	-	-	-	-	-	-	-	-	-	-	-
	Single cell death	-	-	-	-	-	-	-	-	-	-	-	-	-	-	-	++	++	++	-	-	++	-	-	++	-	++	++	++	-	-	++	++	-	++	++
Tooth	Inflammation	-	-	-	-	-	-	-	-	-	-	-	-	-	-	-	-	-	-	-	-	-	-	-	-	-	-	-	-	-	-	-	-	-	-	-
	Single cell death	-	-	-	-	-	-	-	-	-	-	-	-	-	-	-	-	-	-	-	-	-	-	-	±	-	++	-	±	-	-	-	±	-	±	±
Bone	Single cell death	-	-	-	-	-	-	-	-	-	-	-	-	-	-	-	-	-	-	-	-	±	-	-	±	-	-	-	-	-	-	-	-	-	-	-
Eyes	Ganglion cell loss	-	-	-	-	-	-	-	-	-	-	-	-	-	-	-	-	-	-	-	-	-	-	-	-	-	-	±	-	-	-	-	-	-	-	-
Olfactory bulb	Vacuolation	-	-	-	-	-	-	-	-	-	-	-	-	±	-	±	-	-	-	-	-	-	-	-	-	-	-	-	-	++	-	++	++	-	-	++
	Single cell death	-	-	-	-	-	-	-	-	-	-	-	-	-	-	-	-	-	-	-	-	±	-	-	±	-	++	±	±	++	-	++	++	-	-	++
Cerebrum	Inflammation	-	-	-	-	-	-	-	-	-	-	-	-	-	-	-	-	-	-	-	-	-	-	-	-	-	-	-	-	2,mf	-	2,mf	-	-	-	2,mf
	Single cell death	-	-	-	-	-	-	-	-	-	-	-	-	-	-	-	-	-	-	-	-	±	-	-	±	-	++	±	±	++	-	++	++	-	-	++
Cerebellum	Inflammation	-	-	-	-	-	-	-	-	-	-	-	-	-	-	-	-	-	-	-	-	-	-	-	-	-	-	-	-	-	-	-	-	-	-	-
	Single cell death	-	-	-	-	-	-	-	-	-	-	-	-	-	-	-	-	-	-	-	-	-	-	-	-	-	++	±	-	±	-	++	++	-	-	++
Brain stem	Inflammation	-	-	-	-	-	-	-	-	-	-	-	-	-	-	-	-	-	-	-	-	-	-	-	-	-	-	-	-	-	-	-	-	-	-	-
	Single cell death	-	-	-	-	-	-	-	-	-	-	-	-	-	-	-	-	-	-	-	-	-	-	-	-	-	-	-	-	-	-	-	-	-	-	++
Spinal cord	Vacuolation	-	-	-	-	-	-	-	-	-	-	-	-	-	-	-	-	-	-	-	-	-	-	-	-	-	-	-	-	-	-	-	-	-	-	++
	Single cell death	-	-	-	-	-	-	-	-	-	-	-	-	-	-	-	-	-	-	-	-	-	-	-	-	-	-	±	-	-	-	++	++	-	-	±
Lung	Hemorrhage	-	-	-	-	-	±	-	±	±	-	±	±	±	-	±	±	-	-	-	-	±	-	-	-	±	±	±	-	-	±	±	±	±	±	±
	Inflammation	-	-	-	-	-	-	-	-	-	-	-	-	-	-	-	-	-	-	-	2,mf	-	2,f	2,f	-	-	-	2,mf	-	-	-	-	-	-	-	-
	Single cell death	-	-	-	-	-	-	-	-	-	-	-	-	-	-	-	-	±	-	-	-	±	±	-	-	-	-	±	-	-	-	-	-	-	-	-
Repro Tract	Single cell death	-	-	-	-	-	-	-	-	-	-	-	-	-	-	-	-	-	-	-	-	±	-	-	-	-	-	-	-	-	-	-	-	-	-	-

Table 2.7. Significant histologic lesions noted in mice after IN challenge with EEEV. Symbols (++, ±, -) indicate if the entity was present and easily recognized (++); variably present throughout the tissue (±); or not detected histologically (-). A score of 1-5 indicates the severity of the inflammation: 1 (minimal); 2 (mild); 3 (moderate); 4 (marked); 5 (severe). Distribution of the lesion: f (focal); fe (focally extensive); mf (multifocal); d (diffuse).

vacuolation, spongiosis, and moderate meningoencephalitis in some mice. This study was terminated on 4 dpi because a majority of mice remaining had severe clinical disease. Therefore, the 4 dpi group consisted of 10 mice. In 9 of these mice, viral antigen was multifocally to diffusely present throughout nasal cavity, olfactory bulbs, frontal cortex, midbrain (Figure 2.17E), cerebellum, and brain stem, as well as the spinal cord, lung and pituitary gland of most mice. Again, single cell death without inflammation (apoptosis) was easily recognized in all tissues, including the cerebrum (Figure 2.17F, arrow), in which viral antigen was present. Similar to the lesions noted at 3 dpi, there was variable neuronal vacuolation, spongiosis, and moderate meningoencephalitis (Figure 2.17F) in the brain of some mice. And similar to the findings in the IN study, viral antigen was variably present after 1 dpi in the lung (alveolar septa, adjacent to terminal bronchioles), eye (ganglion cells of the retina), reproductive tract (myometrium and/or ovary), and renal pelvic epithelium.

In comparison, the results of the SC (left footpad) study were quite different. Significant immunohistochemical findings and histologic lesions from the SC study are summarized in Tables 2.10 and 2.11, respectively. As expected, viral antigen was present at the inoculation site (left footpad) from 6 hpi, and remained within the left foot to varying degrees throughout the study (Figure 2.18). Cells most commonly positive for viral antigen included connective tissue fibroblasts (Figure 2.18C), synovial cells (Figure 2.18B), and skeletal myocytes; however, antigen was also present in and around hair follicles, within the epidermis and mononuclear inflammatory cells near the inoculation site. No significant histologic lesions were noted in the left foot until 1 dpi when there was scattered single cell death. However, by 2 dpi, there was mild to moderate cellulitis
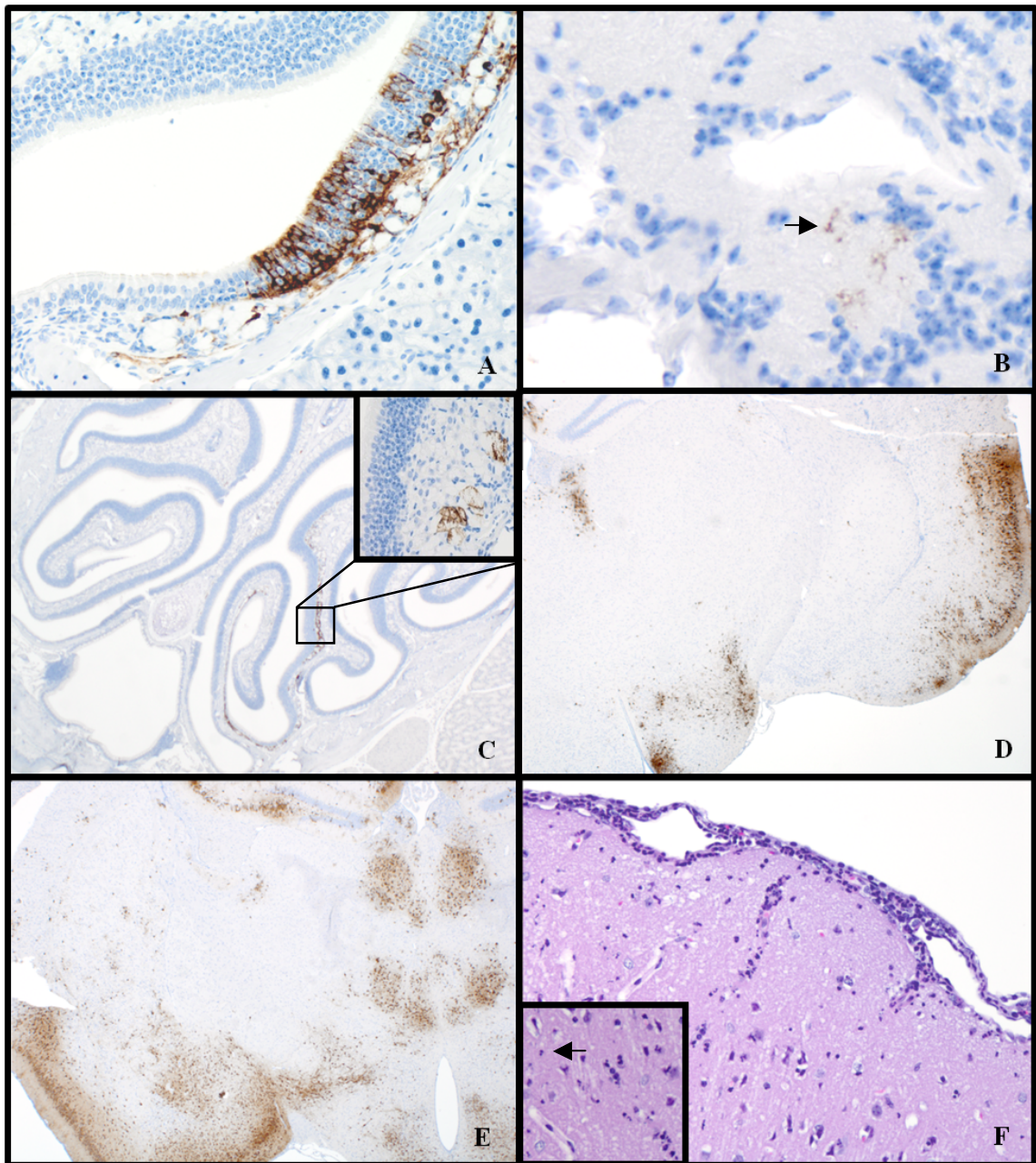
Figure 2.17. Immunohistochemical and histologic findings in mice after AE infection with EEEV strain FL93-939. Mice were infected with approximately $100LD_{50}$ and were euthanized at specified time points (n=5, except 4dpi n=10). Viral antigen was first detected in the olfactory nasal epithelium, lamina propria, and olfactory nerve (A; magnification X200), as well as the olfactory bulb at 1 dpi (B; magnification X200). Multifocally, viral antigen was present in the nasal cavity (C; magnification X20), the olfactory nerve (C; inset, magnification X400), and cerebrum, especially the piriform cortex, by 2 dpi (D; magnification X20). Viral antigen was present throughout the brain by 3 dpi (E; magnification X20) and there was meningoencephalitis in the cerebrum (F; magnification X200) and multifocal neuronal cell death (hypereosinophilic, shrunken neurons with pyknosis or karyorrhexis; inset, arrow).

Table 2.8. Significant immunohistochemical findings observed in mice after AE challenge with EEEV

Tissue		6 hpi AE6	AE7	AE8	AE9	AE10	12 hpi AE6	AE7	AE8	AE9	AE10	1 dpi AE6	AE7	AE8	AE9	AE10	2 dpi AE6	AE7	AE8	AE9	AE10	3 dpi AE6	AE7	AE8	AE9	AE10	4 dpi AE6	AE7	AE8	AE9	AE10	5 dpi AE6	AE7	AE8	AE9	AE10
Head	Nasal cavity	-	-	-	-	-	-	-	-	-	-	-	++	++	-	++	++	++	-	++	++	++	++	++	++	++	++	++	++	-	-	++	++	++	++	++
	Teeth	-	-	-	-	-	-	-	-	-	-	-	-	-	-	-	++	++	-	-	++	++	++	-	-	++	++	++	++	-	-	++	++	++	++	++
	Bone	-	-	-	-	-	-	-	-	-	-	-	-	-	-	-	-	-	-	-	-	-	-	-	-	-	-	-	-	-	-	-	-	-	-	-
	Eyes	-	-	-	-	-	-	-	-	-	-	-	-	-	-	-	-	-	-	-	-	-	-	-	-	-	++	++	++	-	-	-	-	-	++	++
Brain	Olfactory bulb	-	-	-	-	-	-	-	-	-	-	-	++	++	-	++	-	++	++	-	++	++	++	++	++	++	++	++	++	++	-	++	-	++	++	++
	Frontal cortex	-	-	-	-	-	-	-	-	-	-	-	-	-	-	-	++	++	-	++	-	++	++	++	++	++	++	++	++	++	-	++	-	++	++	++
	Midbrain	-	-	-	-	-	-	-	-	-	-	-	-	-	-	-	++	-	-	-	-	++	++	++	++	++	++	++	++	++	-	++	++	++	++	++
	Cerebellum	-	-	-	-	-	-	-	-	-	-	-	-	-	-	-	-	-	-	-	-	-	-	-	-	-	++	++	++	++	-	++	++	++	++	++
	Brain stem	-	-	-	-	-	-	-	-	-	-	-	-	-	-	-	-	-	-	-	-	++	-	++	-	tnp	++	++	++	++	-	++	++	++	++	++
	Pituitary gland	-	tnp	-	-	tnp	-	tnp	-	-	tnp	-	-	-	-	-	++	-	-	-	-	-	-	-	-	++	++	++	++	-	-	tnp	tnp	++	++
Spinal cord		-	-	-	-	-	-	-	-	-	-	-	-	-	-	-	-	-	-	-	-	-	-	-	-	-	++	++	++	++	-	++	++	++	++	++
Salivary gland	Mandibular	-	-	-	-	-	-	-	-	-	-	-	-	-	-	-	-	-	-	-	-	-	-	-	-	-	-	-	-	-	-	-	-	-	-	-
Haired skin		-	-	-	-	-	-	-	-	-	-	-	-	-	-	-	-	-	-	-	-	-	-	-	-	-	-	-	-	-	-	-	-	-	-	-
Lung		-	-	-	-	-	-	-	-	-	-	-	++	++	-	-	-	++	++	-	++	++	++	++	++	++	++	++	++	++	++	++	++	++	++	++
Heart		-	-	-	-	-	-	-	-	-	-	-	-	-	-	-	-	-	-	-	-	-	-	-	-	-	-	-	-	-	-	-	++	-	-	-
Spleen		-	-	-	-	-	-	-	-	-	-	-	-	-	-	-	-	-	-	-	-	-	-	-	-	-	-	-	-	-	-	-	-	-	-	-
Liver		-	-	-	-	-	-	-	-	-	-	-	-	-	-	-	-	-	-	-	-	-	-	-	-	-	-	-	-	-	-	-	-	-	-	-
Lymph node	Mandibular	-	-	-	-	-	-	-	-	-	-	-	-	-	-	-	tnp	-	-	-	-	-	-	-	-	-	-	-	-	-	-	-	-	-	-	-
	Tracheobronchial	-	-	-	-	-	-	-	-	-	-	-	-	-	-	-	-	-	-	-	-	-	-	-	-	-	-	-	-	-	-	-	-	-	-	-
	Axillary, left	-	-	tnp	-	tnp	-	-	-	-	tnp	-	-	tnp	-	-	-	-	-	-	-	-	-	-	-	-	-	-	-	-	-	-	-	-	-	-
	Axillary, right	-	-	-	-	-	-	-	-	-	-	-	-	-	-	-	tnp	-	-	-	-	-	-	-	-	-	-	-	-	tnp	-	-	-	-	-	-
	Mesenteric	-	-	-	-	-	-	-	-	-	-	-	-	-	-	-	-	-	-	-	-	-	-	-	-	-	-	-	-	-	-	-	-	-	-	-
	Inguinal, left	-	-	-	-	-	-	-	-	-	-	-	tnp	-	-	-	-	tnp	tnp	tnp	-	-	-	-	-	-	-	tnp	-	tnp	tnp	-	-	-	-	-
	Inguinal, right	-	tnp	tnp	-	-	-	-	-	-	-	-	-	-	-	-	-	-	-	tnp	-	-	-	-	-	-	tnp	tnp	tnp	-	tnp	-	-	-	-	-
	Popliteal, left	-	-	-	tnp	-	tnp	tnp	-	tnp	-	tnp	-	tnp	-	-	-	tnp	tnp	-	tnp	-	tnp	tnp	-	-	-	-	-	tnp	-	-	-	-	tnp	tnp
	Popliteal, right	tnp	-	tnp	-	-	tnp	tnp	-	tnp	tnp	tnp	tnp	-	-	-	-	-	-	tnp	-	tnp	-	tnp	-	tnp	tnp	-	-	tnp	-	-	-	-	-	-
Thymus		-	-	-	-	-	-	-	-	-	-	-	-	-	-	-	-	-	-	-	-	-	-	-	-	-	-	-	-	-	-	-	-	-	-	-
Thyroid gland		tnp	-	-	-	-	-	tnp	-	tnp	tnp	tnp	-	-	-	-	-	-	tnp	tnp	-	tnp	tnp	-	tnp	tnp	-	tnp	tnp	tnp	tnp	-	tnp	tnp	-	-
Pancreas		-	-	-	-	-	-	-	-	-	-	-	-	-	-	-	-	-	-	-	-	tnp	-	-	-	-	-	-	-	-	-	-	-	-	-	-
GI tract		-	-	-	-	-	-	-	-	-	-	-	-	-	-	-	-	-	-	-	-	-	-	-	-	-	-	-	-	-	-	-	-	-	-	-
Kidneys		-	-	-	-	-	-	-	-	-	-	-	-	-	-	-	-	-	-	-	-	-	-	-	-	-	-	-	-	-	-	-	-	-	-	++
Urinary bladder		-	-	-	-	-	-	-	-	-	-	-	-	-	-	-	-	-	-	-	-	-	-	-	-	-	-	-	-	-	-	-	-	-	-	-
Adrenal glands		-	-	-	-	-	-	-	-	-	-	-	-	-	-	-	-	-	-	-	-	-	-	-	-	-	-	-	-	-	-	-	-	-	-	-
Uterus	Myometrium	-	-	-	-	-	-	-	-	-	-	-	-	-	-	-	++	-	-	-	++	-	-	-	-	++	-	-	++	++	++	-	++	-	-	-
Ovaries		-	-	-	-	-	-	-	-	-	-	-	-	-	-	-	++	++	-	-	++	-	-	++	-	-	-	-	-	-	-	-	++	-	-	-
Rear leg, left		-	-	-	-	-	-	-	-	-	-	-	-	-	-	-	-	-	-	-	-	-	-	-	-	-	-	-	-	-	-	-	-	-	-	-
Rear foot, left		-	-	-	-	-	-	-	-	-	-	-	-	-	-	-	-	-	-	-	-	-	-	-	-	-	-	-	-	-	-	-	-	-	-	-
Rear leg, right		-	-	-	-	-	-	-	-	-	-	-	-	-	-	-	-	-	-	-	-	-	-	-	-	-	-	-	-	-	-	-	-	-	-	-
Rear foot, right		-	-	-	-	-	-	-	-	-	-	-	-	-	-	-	-	-	-	-	-	-	-	-	-	-	-	-	-	-	-	-	-	-	-	-

Table 2.8. Significant immunohistochemical findings observed in mice after AE challenge with EEEV. Symbols (++, ±, -) indicate that viral antigen was present and easily recognized (++); variably present throughout the tissue (±); or not detected histologically (-). Tnp= tissue not present on slide.

Table 2.9. Significant histologic lesions observed in mice after AE challenge with EEEV

Tissue	Lesion	6 hpi AE6	AE7	AE8	AE9	AE10	12 hpi AE6	AE7	AE8	AE9	AE10	1 dpi AE6	AE7	AE8	AE9	AE10	2 dpi AE6	AE7	AE8	AE9	AE10	3 dpi AE6	AE7	AE8	AE9	AE10	4 dpi AE6	AE7	AE8	AE9	AE10	5 dpi AE6	AE7	AE8	AE9	AE10
Nasal cavity	Inflammation	-	-	-	-	-	-	-	-	-	-	-	-	-	-	-	-	-	3,mf	-	-	3,fe	-	-	3,fe	-	-	-	-	-	-	3,mf	-	-	3,fe	3,mf
	Single cell death	-	-	-	-	-	-	-	-	-	-	-	++	±	-	±	++	++	-	++	++	++	++	++	++	++	++	++	++	++	-	++	++	++	++	++
Tooth	Inflammation	-	-	-	-	-	-	-	-	-	-	-	-	-	-	-	-	-	-	-	-	-	-	-	-	-	-	-	-	-	-	-	-	-	-	-
	Single cell death	-	-	-	-	-	-	-	-	-	-	-	-	-	-	-	-	-	-	-	±	±	±	-	±	±	±	±	±	-	-	±	±	±	-	±
Bone	Single cell death	-	-	-	-	-	-	-	-	-	-	-	-	-	-	-	-	-	-	-	-	-	-	-	-	-	-	-	-	-	-	-	-	-	-	-
Eyes	Ganglion cell loss	-	-	-	-	-	-	-	-	-	-	-	-	-	-	-	-	-	-	-	-	-	-	-	-	-	-	-	-	-	-	-	-	-	-	-
Olfactory bulb	Vacuolation	-	-	-	-	-	-	-	-	-	-	-	-	-	-	-	±	-	-	-	-	-	±	±	-	±	±	-	±	-	-	±	-	±	±	±
	Single cell death	-	-	-	-	-	-	-	-	-	-	-	-	-	-	-	±	±	-	-	-	++	++	++	++	++	++	++	++	++	-	++	-	++	++	++
Cerebrum	Vacuolation	-	-	-	-	-	-	-	-	-	-	-	-	-	-	-	-	-	-	-	-	-	-	-	-	++	±	±	±	-	-	++	-	++	±	±
	Hemorrhage	-	-	-	-	-	-	-	-	-	-	-	-	-	-	-	-	-	-	-	-	-	++	-	-	-	-	-	-	-	-	-	-	-	-	-
	Inflammation	-	-	-	-	-	-	-	-	-	-	-	-	-	-	-	-	-	-	-	-	3,d	-	2,mf	-	4,mf	-	-	3,d	3,d	-	3,d	-	3,d	-	3,mf
	Single cell death	-	-	-	-	-	-	-	-	-	-	-	-	-	-	-	±	-	-	-	-	++	±	++	±	++	++	++	++	++	-	++	-	++	++	++
Cerebellum	Inflammation	-	-	-	-	-	-	-	-	-	-	-	-	-	-	-	-	-	-	-	-	-	-	-	-	-	-	-	-	-	-	-	-	-	-	-
	Single cell death	-	-	-	-	-	-	-	-	-	-	-	-	-	-	-	-	-	-	-	-	±	-	±	-	-	±	±	±	±	-	±	±	±	±	±
Brain stem	Inflammation	-	-	-	-	-	-	-	-	-	-	-	-	-	-	-	-	-	-	-	-	-	-	-	-	-	-	-	-	-	-	-	-	-	3,mf	-
	Single cell death	-	-	-	-	-	-	-	-	-	-	-	-	-	-	-	-	-	-	-	-	-	-	-	-	-	±	±	±	±	-	±	±	±	±	-
Spinal cord	Vacuolation	-	-	-	-	-	-	-	-	-	-	-	-	-	-	-	-	-	-	-	-	-	-	-	-	-	±	-	-	-	-	-	-	-	-	-
	Single cell death	-	-	-	-	-	-	-	-	-	-	-	-	-	-	-	-	-	-	-	-	-	-	-	-	-	±	±	±	±	-	±	±	±	±	-
Lung	Hemorrhage	-	-	-	-	-	-	-	-	-	-	±	-	±	-	-	-	-	-	-	-	-	-	-	-	-	-	-	-	-	-	-	-	-	-	-
	Inflammation	-	-	-	-	-	-	-	-	-	-	-	-	-	-	-	2,fe	-	-	-	-	2,fe	-	2,mf	-	-	-	-	-	-	-	-	-	-	-	-
	Single cell death	-	-	-	-	-	-	-	-	-	-	-	-	-	-	-	±	-	-	-	-	±	±	-	±	±	±	±	±	±	-	±	±	±	±	-
Repro Tract	Single cell death	-	-	-	-	-	-	-	-	-	-	-	-	-	-	-	++	-	-	-	++	-	±	-	±	±	-	-	++	++	++	-	++	-	-	-

Table 2.9. Significant histologic lesions observed in mice after AE challenge with EEEV. Symbols (++, ±, -) indicate that the entity was present and easily recognized (++); variably present throughout the tissue (±); or not detected histologically (-). A score of 1-5 indicates the severity of the inflammation: 1 (minimal); 2 (mild); 3 (moderate); 4 (marked); 5 (severe). Distribution of the lesion: f (focal); fe (focally extensive); mf (multifocal); d (diffuse).

and single cell death was easily identified. Additionally, myocyte degeneration/necrosis was noted in one mouse. Single cell death (apoptosis), cellulitis, and myocyte degeneration, necrosis and regeneration were noted in most mice, to varying degrees, in the left foot from 2 dpi through the end of the study. Viral antigen was noted in the left popliteal lymph node, the draining lymph node of the foot and lower leg, from 6 hpi (Figure 2.18A) through 2 dpi. Similar to the results of the IN study, the antigen was only found in histocytes and/or cells with morphologic features of dendritic cells within the subcapsular sinus, not within the follicles of the cortex. Viral antigen was first noted in one mouse in the nasal cavity olfactory epithelium/lamina propria and teeth (odontoblasts) at 3 dpi (Figure 2.18D) and was detected in a low number of mice through 7 dpi. From 4 dpi through 8 dpi viral antigen was detected in either the olfactory epithelium/lamina propria and/or the teeth in only 8 of 25 mice; viral antigen was also detected in the olfactory bulb or cerebrum in 7 of those 8 animals, 4 of which had viral antigen throughout the cerebrum, cerebellum (Figure 2.18E), and brain stem. Significantly, these 4 mice also had moderate-marked neuronal apoptosis, spongiosis, meningoencephalitis, vasculitis, thrombosis, and perivascular hemorrhage (Figure 2.18F, arrows), which was not seen in either the IN or AE studies. Interestingly, viral antigen was not closely associated with the areas of vasculitis or thrombosis (Figure 2.18F, inset, between arrows). In one mouse at 7 dpi, viral antigen was detected throughout the brain, but was not detected in either the nasal cavity or teeth. However, histologically there was a significant mucosal hyperplastic response along with a marked secondary bacterial rhinitis.
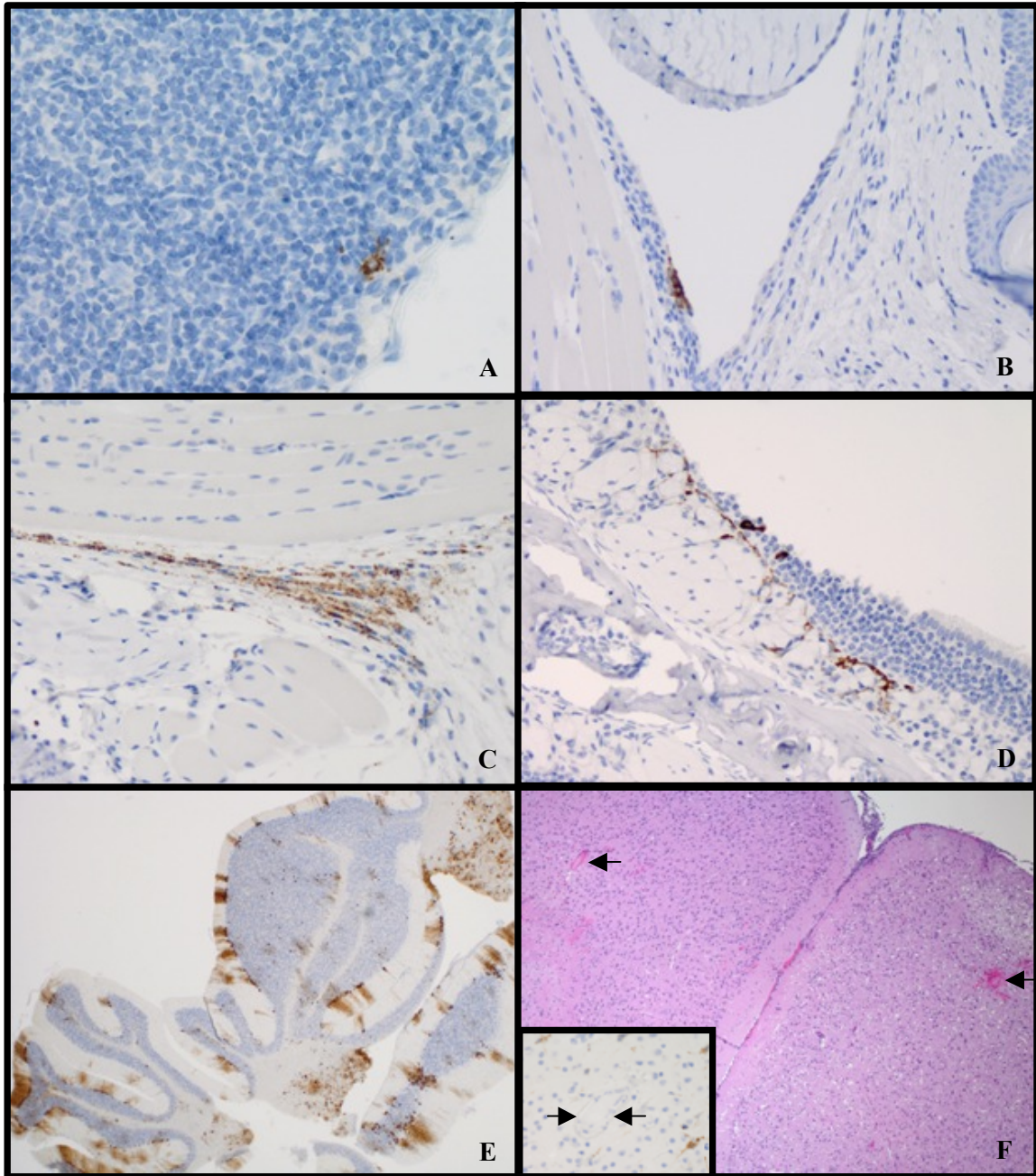
Figure 2.18. Immunohistochemical and histologic findings in mice after SC (left footpad) infection with EEEV strain FL93-939. Mice were infected with approximately 30LD$_{50}$ and were euthanized at specified time points (n=5). Viral antigen was first detected in the left popliteal (draining) lymph node at 6 hpi (A; magnification X400). At the inoculation site, viral antigen was present in synovial cells at 12 hpi (B; magnification X200). Viral antigen was found in numerous fibroblasts in the left foot at 2 dpi (C; magnification X200). Viral antigen was first detected in the olfactory epithelium at 3 dpi (D; magnification X200) and was present throughout the brain, including the cerebellum by 4 dpi (E; magnification X20). Within the cerebrum there was meningoencephalitis with vasculitis, thrombosis, hemorrhage (arrows), and spongiosis by 6 dpi (F; magnification X40); however, viral antigen was not present around thrombotic vessels (inset, between arrows)

Table 2.10. Significant immunohistochemical findings observed in mice after SC challenge with EEEV

Tissue		6 hpi S6	S7	S8	S9	12 hpi S6	S7	S8	S9	S10	1 dpi S6	S7	S8	S9	S10	2 dpi S6	S7	S8	S9	S10	3 dpi S6	S7	S8	S9	S10	4 dpi S6	S7	S8	S9	S10	5 dpi S6	S7	S8	S9	S10	6 dpi S6	S7	S8	S9	S10	7 dpi S6	S7	S8	S9	S10	8 dpi S6	S7	S8	S9	S10
Head	Nasal cavity	-	-	-	-	-	-	-	-	-	-	-	-	-	-	-	-	-	-	-	-	-	-	-	++	-	++	-	-	-	-	-	-	-	++	-	-	++	++	-	-	-	-	++	-	-	-	-	-
	Teeth	-	-	-	-	-	-	-	-	-	-	-	-	-	-	-	-	-	-	-	++	++	++	++	++	-	-	-	-	-	-	-	-	-	-	-	-	-	-	-	-	-	-	-	-	-	-	-	-
	Bone	-	-	-	-	-	-	-	-	-	-	-	-	-	-	-	-	-	-	-	-	-	-	-	-	-	-	-	-	-	-	-	-	-	-	-	-	-	-	-	-	-	-	-	-	-	-	-	-
	Eyes	-	-	-	-	-	-	-	-	-	-	-	-	-	-	-	-	-	-	-	-	-	-	-	-	-	-	-	-	-	-	-	-	-	-	-	-	-	-	-	-	++	-	-	-	-	-	-	-
Brain	Olfactory bulb	-	-	-	-	-	-	-	-	-	-	-	-	-	-	-	-	-	-	-	-	-	-	-	-	++	++	-	-	++	-	-	-	-	++	++	++	-	-	++	-	-	-	-	-
	Frontal cortex	-	-	-	-	-	-	-	-	-	-	-	-	-	-	-	-	-	-	-	-	-	-	-	-	-	++	++	-	-	-	-	++	++	++	-	-	++	-	-	-	-	-
	Midbrain	-	-	-	-	-	-	-	-	-	-	-	-	-	-	-	-	-	-	-	-	-	-	-	-	-	++	-	-	-	-	++	++	++	-	-	++	-	-	-	-	-
	Cerebellum	-	-	-	-	-	-	-	-	-	-	-	-	-	-	-	-	-	-	-	-	-	-	-	-	-	++	-	-	-	-	++	++	++	-	-	++	-	-	-	-	-
	Brain stem	-	-	-	-	-	-	-	-	-	-	-	-	-	-	-	-	-	-	-	-	-	-	-	-	-	++	-	-	-	-	++	++	++	-	-	++	-	-	-	-	-
	Pituitary gland	-	-	tnp	-	-	-	tnp	-	-	-	tnp	-	tnp	-	-	-	-	tnp	-	-	-	-	-	tnp	tnp	tnp	tnp	-	-	tnp	tnp	-	tnp	-	-	-	-	tnp	-	-	++	tnp	-
Spinal cord		-	-	-	-	-	-	-	-	-	-	-	-	-	-	-	-	-	-	-	-	-	-	-	-	-	-	-	-	-	-	-	-	++	++	++	-	-	++	-	-	-	-	-
Salivary gland	Mandibular	-	-	-	-	-	tnp	-	-	-	-	-	-	-	-	-	-	-	-	-	-	-	-	-	-	-	-	-	-	-	-	-	-	-	-	-	-	-	-	-	-	-	-	-
Haired skin		-	-	-	-	-	-	-	-	-	-	-	-	-	-	-	-	-	-	-	-	-	-	-	-	-	-	-	-	-	-	-	-	-	-	-	-	-	-	-	-	-	-	-
Lung		-	-	-	-	-	-	-	-	-	-	-	-	-	-	-	-	-	-	-	-	-	-	-	-	-	-	-	-	-	-	-	-	-	-	-	-	-	-	-	-	-	-	-
Heart		-	-	-	-	-	-	-	-	-	-	-	-	-	-	-	-	-	-	-	-	-	-	-	-	-	-	-	-	-	-	-	-	-	-	-	-	-	-	-	-	-	-	-
Spleen		-	-	-	-	-	-	-	-	-	-	-	-	-	-	-	-	-	-	-	-	-	-	-	-	-	-	-	-	-	-	-	-	-	-	-	-	-	-	-	-	-	-	-
Liver		-	-	-	-	-	-	-	-	-	-	-	-	-	-	-	-	-	-	-	-	-	-	-	-	-	-	-	-	-	-	-	-	-	-	-	-	-	-	-	-	-	-	-
Lymph node	Mandibular	-	-	-	-	-	-	-	-	-	-	-	-	-	-	-	-	-	-	++	-	-	-	-	-	-	-	++	-	-	-	-	-	-	-	-	-	-	-	-	-	-	-	tnp
	Tracheobronchial	-	-	-	-	-	-	-	-	-	-	-	-	-	-	-	-	-	tnp	-	tnp	-	-	-	-	-	-	-	-	-	-	-	-	-	-	-	-	-	-	-	-	tnp	-
	Axillary, left	-	-	tnp	-	-	-	-	tnp	-	-	tnp	-	-	-	-	tnp	-	tnp	-	-	-	-	-	-	-	-	-	tnp	-	-	-	-	-	-	-	tnp	-	-	-	-	-
	Axillary, right	-	-	-	-	-	-	-	tnp	-	-	tnp	-	tnp	tnp	-	-	-	-	tnp	-	-	-	-	tnp	-	-	-	-	-	tnp	-	-	-	-	-	-	-
	Mesenteric	-	-	-	-	-	-	-	-	-	-	-	-	-	-	-	-	-	-	-	-	-	-	-	-	-	-	-	-	-	-	-	-	-	-	-	-	-	-	-	-	-	-
	Inguinal, left	-	-	-	-	-	-	-	-	-	-	-	-	-	tnp	-	tnp	-	-	-	-	-	-	-	-	-	-	-	-	-	-	-	-	-	-	-	-	-	-	-	-	tnp
	Inguinal, right	tnp	-	tnp	tnp	tnp	tnp	-	tnp	-	-	tnp	tnp	tnp	tnp	-	-	-	-	tnp	-	-	-	-	-	-	-	-	-	-	-	-	-	-	-	-	-	-	-	tnp
	Popliteal, left	++	-	-	tnp	++	tnp	++	++	++	++	tnp	tnp	++	++	-	tnp	-	-	-	-	-	-	-	-	-	-	-	-	-	-	-	-	-	tnp	-	tnp	tnp	-	-
	Popliteal, right	-	-	tnp	tnp	tnp	-	tnp	-	+++	tnp	tnp	tnp	tnp	-	-	-	-	-	-	tnp	tnp	-	-	-	-	-	-	-	-	-	-	-	tnp	-	tnp	tnp	-	-
Thymus		-	-	-	-	-	-	-	-	-	-	-	-	-	-	-	-	-	-	-	tnp	-	-	-	-	-	tnp	-	-	-	-	-	-	-	-	-	-	-	-	-	-	-
Thyroid gland		tnp	tnp	-	-	-	-	-	-	tnp	-	tnp	-	-	tnp	tnp	-	tnp	-	-	-	-	tnp	-	-	tnp	-	-	-	-	tnp	-	-	-	tnp	-	tnp	tnp	-	tnp	-	tnp	tnp	-
Pancreas		-	-	-	-	-	-	-	-	-	-	-	-	-	-	-	-	-	-	-	-	-	-	-	-	-	-	-	-	-	-	-	-	-	-	-	-	-	-	-	-	-	-	-
GI tract		-	-	-	-	-	-	-	-	-	-	-	-	-	-	-	-	-	-	-	-	-	-	-	-	-	-	-	-	-	-	-	-	-	-	-	-	-	-	-	-	-	-	-
Kidneys		-	-	-	-	-	-	-	-	-	-	-	-	-	-	-	-	-	-	-	-	-	-	-	-	-	-	-	-	-	-	-	-	-	-	-	-	-	-	-	-	-	-	-
Urinary bladder		-	-	-	-	-	-	-	-	-	-	-	-	-	-	-	-	-	-	-	-	-	-	-	-	-	-	-	-	-	-	-	-	-	-	-	-	-	-	-	-	tnp	-	-
Adrenal glands		-	-	-	-	-	-	-	-	-	-	-	-	-	-	-	-	-	-	-	-	-	-	-	-	-	-	-	-	-	-	-	-	-	-	-	-	-	-	-	-	-	-	tnp
Uterus	Myometrium	-	-	-	-	-	-	-	-	-	-	-	-	-	-	-	-	-	-	-	-	-	-	-	-	-	-	-	-	-	-	-	-	-	-	-	-	-	-	-	-	-	-	-
Ovaries		-	-	-	-	-	-	-	-	-	-	-	-	-	-	-	-	-	-	-	-	tnp	-	-	-	-	-	tnp	-	-	-	-	-	-	-	-	-	-	-	-	-	-	-	-
Rear leg, left		-	-	-	-	-	-	-	-	-	-	-	-	-	-	-	-	-	-	-	-	-	-	-	-	-	-	-	-	-	-	-	-	-	-	-	-	-	-	-	-	-	-	-
Rear foot, left		++	-	-	-	++	++	++	++	++	++	++	++	++	++	++	++	++	++	++	++	++	++	++	++	++	++	++	++	++	++	++	++	++	++	++	++	++	++	++	++	++	-	-	++	-
Rear leg, right		-	-	-	-	-	-	-	-	-	-	-	-	-	-	-	-	-	-	-	-	-	-	-	-	-	-	-	-	-	-	-	-	-	-	-	-	-	-	-	-	-	-	-
Rear foot, right		-	-	-	-	-	-	-	-	-	-	-	-	-	-	-	-	-	-	-	-	-	-	-	-	-	-	-	-	-	-	-	-	-	-	-	-	-	-	-	-	-	-	-

Table 2.10. Significant immunohistochemical findings observed in mice after SC challenge with EEEV. Symbols (++, ±, -) indicate that viral antigen was present and easily recognized (++); variably present throughout the tissue (±); or not detected histologically (-). Tnp= tissue not present on slide.

Table 2.11. Significant histologic lesions observed in mice after SC challenge with EEEV

Tissue	Lesion	6 hpi S6	S7	S8	S9	12 hpi S6	S7	S8	S9	S10	1 dpi S6	S7	S8	S9	S10	2 dpi S6	S7	S8	S9	S10	3 dpi S6	S7	S8	S9	S10	4 dpi S6	S7	S8	S9	S10	5 dpi S6	S7	S8	S9	S10	6 dpi S6	S7	S8	S9	S10	7 dpi S6	S7	S8	S9	S10	8 dpi S6	S7	S8	S9	S10
Nasal cavity	Inflammation	-	-	-	-	-	-	-	-	-	-	-	-	-	-	-	-	-	-	-	-	-	-	-	-	-	-	-	-	-	-	-	-	-	-	-	-	-	5,mf	5,mf	5,mf	-	-	-	3,mf	-	-	-	-	-
	Single cell death	-	-	-	-	-	-	-	-	-	-	-	-	-	-	-	-	-	-	-	-	±	-	++	-	-	-	-	-	-	-	-	-	-	-	++	-	-	++	++	++	-	-	-	++	-	-	-	-	-
Tooth	Inflammation	-	-	-	-	-	-	-	-	-	-	-	-	-	-	-	-	-	-	-	-	-	-	-	-	-	-	-	-	-	-	-	-	-	-	-	-	-	-	-	-	-	-	-	-	-	-	-	-	-
	Single cell death	-	-	-	-	-	-	-	-	-	-	-	-	-	-	-	-	-	-	-	-	±	-	++	-	-	-	-	-	-	-	-	-	-	-	-	-	-	-	-	-	-	-	-	-	-	-	-	-	-
Olfactory bulb	Vacuolation	-	-	-	-	-	-	-	-	-	-	-	-	-	-	-	-	-	-	-	-	-	-	-	-	-	-	-	-	-	-	-	-	-	-	-	-	-	-	-	-	++	-	-	-	++	-	-	-	-	-
	Single cell death	-	-	-	-	-	-	-	-	-	-	-	-	-	-	-	-	-	-	-	-	±	±	-	-	-	-	-	-	±	-	-	-	-	++	++	++	-	-	++	-	-	-	-	-
Cerebrum	Vacuolation	-	-	-	-	-	-	-	-	-	-	-	-	-	-	-	-	-	-	-	-	-	-	-	-	-	-	-	-	-	-	-	-	-	++	++	++	-	-	++	-	-	-	-	-
	Hemorrhage	-	-	-	-	-	-	-	-	-	-	-	-	-	-	-	-	-	-	-	-	-	-	-	-	-	-	-	-	-	-	-	-	++	++	++	-	-	++	-	-	-	-	-
	Vasculitis/thrombosis	-	-	-	-	-	-	-	-	-	-	-	-	-	-	-	-	-	-	-	-	-	-	-	-	-	-	-	-	-	-	-	++	++	++	-	-	++	-	-	-	-	-
	Inflammation	-	-	-	-	-	-	-	-	-	-	-	-	-	-	-	-	-	-	-	-	-	-	-	-	-	-	-	-	-	-	-	-	4,d	4,d	4,d	-	-	-	4,d	-	-	-	-
	Single cell death	-	-	-	-	-	-	-	-	-	-	-	-	-	-	-	-	-	-	-	±	±	-	-	-	-	-	-	++	++	++	-	-	++	-	-	-	-	-
Cerebellum	Inflammation	-	-	-	-	-	-	-	-	-	-	-	-	-	-	-	-	-	-	-	-	-	-	-	-	-	-	-	-	-	-	-	-	-	-	-	-	-	-	-	-	-	-	-
	Single cell death	-	-	-	-	-	-	-	-	-	-	-	-	-	-	-	-	-	-	-	±	-	-	-	-	-	-	-	±	±	±	-	-	±	-	-	-	-	-
Brain stem	Inflammation	-	-	-	-	-	-	-	-	-	-	-	-	-	-	-	-	-	-	-	-	-	-	-	-	-	-	-	-	-	-	-	-	-	-	-	-	-	-	-	-	-	-	-
	Single cell death	-	-	-	-	-	-	-	-	-	-	-	-	-	-	-	-	-	-	-	±	-	-	-	-	-	-	-	±	±	±	-	-	±	-	-	-	-	-
Spinal cord	Inflammation	-	-	-	-	-	-	-	-	-	-	-	-	-	-	-	-	-	-	-	-	-	-	-	-	-	-	-	-	-	-	3,mf	2,mf	-	-	2,mf	-	-	-	-	-
	Single cell death	-	-	-	-	-	-	-	-	-	-	-	-	-	-	-	-	-	-	-	±	-	-	++	++	-	-	-	++	-	-	-	-	-	-	-	-	-
Foot, left	Inflammation	-	-	-	-	-	-	-	-	-	-	-	-	-	-	3,mf	2,mf	2,mf	2,mf	3,mf	2,mf	4,mf	3,mf	4,mf	-	3,mf	2,mf	2,mf	2,fe	2,mf	2,fe	-	2,mf	2,mf	-	3,mf	-	2,mf	3,mf	4,mf	2,fe	2,fe	-	3,mf	3,mf	3,fe
	Single cell death	-	-	-	-	-	-	-	-	±	±	±	±	±	++	++	±	±	±	±	±	++	++	++	++	±	++	++	±	±	±	-	±	-	-	-	±	-	-	-	-	-
	Muscle degen/regen	-	-	-	-	-	-	-	-	-	-	-	-	-	-	-	-	-	-	-	-	-	-	-	-	-	-	-	-	-	-	-	-	-	±	±	±	-	±	±	±
Popliteal LN, left	Inflammation	-	-	-	±	-	-	-	-	-	-	-	-	-	-	-	-	-	-	-	-	-	-	-	-	-	-	-	-	-	-	-	-	-	-	-	-	-	-	-	-
	Single cell death	-	-	-	-	-	-	-	-	-	±	±	-	-	-	-	-	-	-	-	-	-	-	-	-	-	-	-	-	-	-	-	-	-	-	-	-	-	-	-
Lung	Hemorrhage	-	-	-	±	±	-	±	±	-	±	-	-	±	-	-	-	-	±	-	-	-	±	-	-	-	±	-	-	±	±	-	±	±	-	-	±	±	-
	Thrombosis	-	-	-	-	-	-	-	-	-	-	-	-	-	-	-	-	-	-	-	-	-	-	-	-	-	-	-	++	-	-	-	-	-	-	-	-	-	-
	Single cell death	-	-	-	-	-	-	-	-	-	-	-	-	-	-	-	-	-	-	-	-	-	-	-	-	-	-	-	-	-	-	-	-	-	-	-	-	-	-
Heart	Inflammation	-	-	-	-	-	-	-	-	-	-	-	-	2,mf	-	3,fe	-	-	2,fe	3,fe	-	-	-	2,fe	-	2,fe	2,fe	-	-	2,fe	-	-	-	-	-	-	-	2,fe

Table 2.11. Significant histologic lesions observed in mice after SC challenge with EEEV. Symbols (++, ±, -) indicate that the entity was present and easily recognized (++); variably present throughout the tissue (±); or not detected histologically (-). A score of 1-5 indicates the severity of the inflammation: 1 (minimal); 2 (mild); 3 (moderate); 4 (marked); 5 (severe). Distribution of the lesion: f (focal); fe (focally extensive); mf (multifocal); d (diffuse).

In an attempt to further elucidate the mechanism of neuronal cell death, brain sections from the AE study were evaluated immunohistochemically for the presence of cleaved-caspase-3 antigen as a marker of apoptosis as well as LC3BII antigen as a marker of autophagy. While there were very few cells in the control animals that had intracytoplasmic staining for cleaved-caspase-3 antigen (Figure 2.19A), there was a marked increase in the number of cells staining for the apoptotic marker in the olfactory bulb of EEEV infected mice, especially after 2 dpi (Figure 2.19B), this trend continued through 4 dpi (Figure 2.19C). The c-caspase 3 antigen was also found within the cerebrum, especially within the piriform cortex (Figure 2.19D) and within cells with karyorrhexis (Figure 2.19D, inset, arrow) as well as within some inflammatory cells within the meninges. The antigen remained present within the cerebrum, especially the piriform cortex, at low levels through 4 dpi, the study endpoint.

LC3BII is typically noted as cytoplasmic punctate staining in cells undergoing autophagy. While autophagy can be part of normal cellular turnover in the brain, staining was not evident in uninfected control animals. Overall, there were only a few neurons containing intracytoplasmic punctate staining; however, these were in areas that were positive for viral antigen. LC3BII antigen was noted in 3/5 mice in the olfactory bulb, in both the external plexiform and internal granular layers, at 3 dpi.   At 4 dpi, 6/10 animals had low numbers of neurons in the olfactory bulb, frontal cortex (Figure 2.19E), and midbrain which contained intracytoplasmic punctate staining (Figure 2.19F, arrow) for LC3BII. This suggests that while autophagy occurs in EEEV infected mice, it does not occur until later in the disease and that only a small number of neurons are removed by this process.
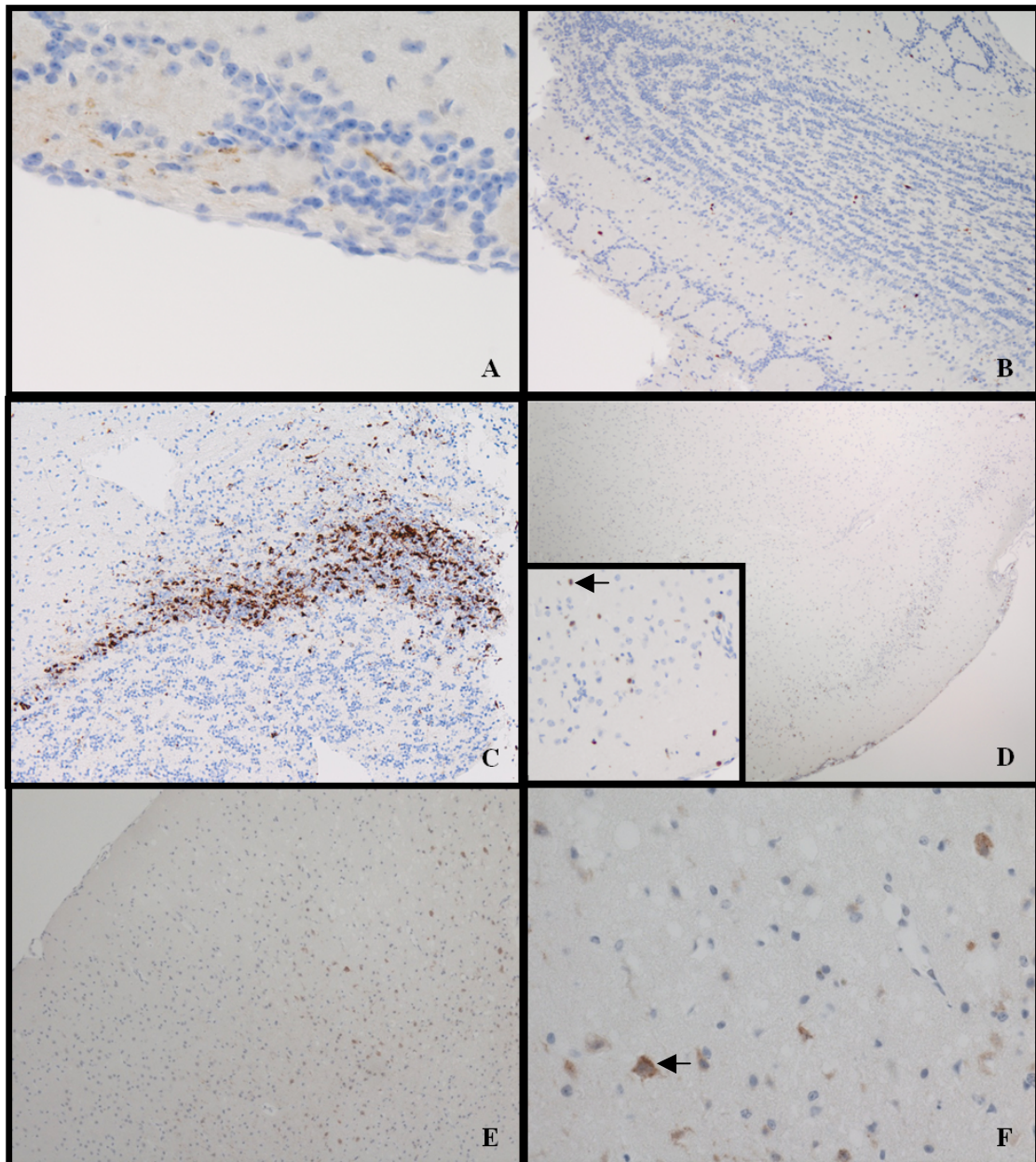
Figure 2.19. Immunohistochemical findings for c-caspase 3 (A-D) and LC3BII (E-F) in mice after AE infection with EEEV strain FL93-939. Mice were infected with approximately $100LD_{50}$ and were euthanized at specified time points (n=5). While c-caspase 3 antigen was detected in very few cells in the olfactory bulb in controls (A; magnification X400), there was an increase antigen detected in the olfactory bulb by 2 dpi (B; magnification X100). The increase in c-caspase 3 antigen detection in the olfactory bulb continued through the study and was present in clusters of cells at 4 dpi (C; magnification X100). Cleaved-caspase 3 antigen was present within the cerebrum, primarily within the piriform cortex (D; magnification X40) and specifically within cells with karyorrhexis (D; inset, arrow) as well as within some inflammatory cells within the meninges. The LC3BII antigen was detected in low numbers of neurons within the olfactory bulb, frontal cortex (E; magnification X100), and midbrain at 3-4 dpi. The antigen was cytoplasmic and punctate in affected cells (F, magnification X400, arrow)

Conclusion

In order to better understand the pathogenesis of EEEV strain FL93-939 we conducted several studies to evaluate the differences between 3 routes of infection: intranasal, aerosol, and subcutaneous. Although the intranasal and aerosol routes were similar, there were important differences noted clinically and pathologically. While animals in both groups lost weight between 3-4 dpi, those animals in the AE study showed clinical signs of disease at 3 dpi compared to 4 dpi in the IN study. The clinical signs were so severe in the majority of animals in the AE study at 4 dpi that the study was terminated early. Clinical signs of disease did not appear until 5 dpi in the SC study. This may be due to the fact that the animals in the SC study only received approximately $30LD_{50}$, compared to $100LD_{50}$ in both the IN and AE studies. Interestingly though, the absolute dose given per mouse was similar between the IN and SC routes, 1300 pfu and 1000 pfu respectively, yet the outcome was drastically different. This is likely due to differences in inoculation site and the resultant immune response. The clinical signs noted in these studies were similar to those reported by Vogel et. al. (Vogel P, Kell WM et al. 2005); however, mice in that study had severe clinical signs by 4 dpi. The difference in onset of clinical signs and severity noted in the Vogel study may be attributed to the higher inoculum (10^5 pfu), the mouse strain (C57/BL6), or the age (5-week-old) or most likely a combination of these factors. The clinical findings in our SC study more closely paralleled those noted recently by Gardner et al. (Gardner, Ebel et al. 2011) where they did not observe signs of disease until 6 dpi following a subcutaneous exposure and weight loss was minimal over the course of the study.

Telemetry proved to be a helpful tool in determining onset of clinical disease. Fever was detected at 3 dpi in both the IN and AE studies, which coincided with the onset of mild signs (ruffled fur). Additionally, obvious changes in diurnal patterns in both temperature and activity coincided with the onset of more severe clinical signs of disease. Telemetry has not previously been used to study EEEV infection in mice; however, this study indicated the importance of monitoring such parameters and revealed that the clinical signs in mice, similar to those seen in humans, included fever prior to or at the onset of more obvious clinical signs of disease, such as ruffled fur and lethargy.

A complete blood count was performed on animals from the AE and SC studies; however, the results were not specific or predictive of outcome. Most animals had a leukopenia characterized by a lymphopenia at 2-3 dpi, which can be indicative of a viral infection. These results are similar to those reported by Adams et al. (Adams, Aronson et al. 2008) in which marmosets infected with EEEV had a leukopenia 1 dpi, but a concomitant decrease in neutrophils, lymphocytes and monocytes. In the marmosets, this blood profile rapidly changed to a leukocytosis, characterized by a neutrophilia, lymphocytosis and a monocytosis by 3-4 dpi. While there was a rise in leukocytes in our SC study after 3 dpi, the number of leukocytes remained within the normal range for the study duration. It is difficult to compare CBC results in research models to that observed in human cases, since the infectious dose and time from inoculation to presentation in humans is typically not known.

Cytokine analysis in EEEV infection in research models has not been previously reported. While there were several pro-inflammatory cytokines and chemokines that were elevated to statistically significant levels relative to saline-treated control animals,

most of the elevated cyto/chemokine levels were only mildly increased from baseline. Overall, these data suggest a mild induction of certain pro-inflammatory cytokines and chemokines after infection. However, temporal comparison of cytokine levels between different routes of infection at each time point revealed some interesting findings. There were no statistically significant differences in any of the 25 cytokines and chemokines tested between aerosol and intranasal infection at any time point, suggesting that these routes of infection induced very similar immune responses. However, there were many differences between subcutaneous and intranasal or aerosol infections. Subcutaneous infection resulted in an increase of IFN-γ, MIP-1β, RANTES, and MIG at 1 dpi compared to aerosol or intranasal infection, followed by a return to baseline at 2 dpi. However, these same cyto/chemokines were increased in aerosol or subcutaneous infection at 2 dpi relative to subcutaneous infection. It is possible that the earlier spike in IFN-γ, MIP-1β, RANTES, and MIG levels after subcutaneous infection contributed to the decreased virulence seen in these mice compared to intranasal or aerosol infection. However, this difference could also be due to the variance in LD_{50} dose given; further work is needed to explore this possibility.

In this study, we used both viral titration of tissue homogenates as well as histopathology and immunohistochemistry to better define the pathogenesis of EEEV strain FL93-939 in mice. Not surprisingly, viral titration was much more sensitive than IHC in detecting the presence of virus at early time points. In the IN study, virus was first detected in the blood and the brain homogenate at 1 dpi; however, at this time, viral antigen was only noted in the nasal cavity (olfactory epithelium and lamina propria) and not the olfactory bulb or cerebrum immunohistochemically. The bipolar olfactory

neuron, found in the olfactory epithelium is instrumental as one pole of the cell has cilia that project into the air passages, a likely site of viral contact, and the opposite pole extends an axon that synapses directly with neurons of the olfactory bulb. Therefore, viruses that target olfactory neurons have a direct conduit to the brain. This appeared to be the case in this study, because by 2 dpi, when viremia peaked and titer in the brain rapidly increased, there was viral antigen present multifocally within the nasal cavity and also within the olfactory bulb. In the one animal where viral antigen was detected in the frontal cortex and midbrain, it was present in only a few scattered cells primarily within the piriform cortex. Virus then appeared to spread in a rostral to caudal fashion, infecting neurons of the cerebellum and brain stem only at the later time points. Overall, these findings suggest the virus entered the brain via the olfactory route rather than the vascular route, which is similar to that seen in guinea pigs exposed to aerosolized EEEV (Roy, Reed et al. 2009).

The results for the AE study were very similar to the results of the IN study, with the important exception that virus was detected in the brain by titer at only 6 hpi and viral antigen was present in the olfactory bulb by 1 dpi. The virus appeared to enter the brain through the olfactory tract and spread transneuronally, rostral to caudal, as noted in the IN study. The aerosol delivery method likely allowed more viral contact with olfactory neurons, thus facilitating the earlier viral invasion of the olfactory bulb and subsequent transport to the olfactory tract and beyond. These results support the clinical findings of more rapid and severe disease onset in this study.

The results of the SC study are less clear, which may be due to the dose and/or route of inoculation. Throughout the study we did not see consistent evidence of viral

infection. While virus was first detected in the brain by standard plaque assay at 1 dpi (1/5 animals, 20%), virus was only detected in 10/60 (17%) of animals from 3-8 dpi. Similar inconsistencies were seen on pathological examination of the tissues. Viral antigen was only detected in the nasal cavity and/or brain in 10/60 animals from 3-8 dpi. In some animals viral antigen was seen in the nasal cavity and olfactory bulb, while in others it was detected in the nasal cavity and throughout the brain simultaneously. This could be a result of individual animal variability or the result of vascular spread to the brain. These results are similar to those found by Vogel et al. (Vogel P, Kell WM et al. 2005); however, in their study they found that the virus generally spared the olfactory epithelium. Similar to their study, we also noted viral replication at the inoculation site, in fibroblasts, skeletal myocytes, and synovial cells; however, unlike in their study, we did not note any viral antigen in osteoblasts of the long bones. This is likely due to the age difference of the mice used in each of the studies. In their study the mice were 5-weeks old and the mice were actively growing with open growth plates and high numbers of osteoblasts, whereas in our study the mice were 12-weeks-old, which is considered an adult characterized by closed growth plates and relatively few osteoblasts. Also, in contrast to their study, we had a few animals at 6-7 dpi that had moderate to marked meningoencephalitis with vasculitis, thrombosis, and hemorrhage. Interestingly, viral antigen was not present adjacent to affected vessels, suggesting this lesion could be immune-mediated rather than a direct result of viral infection. Meningoencephalitis and vasculitis have been associated with EEEV infection in humans and guinea pigs (Roy, Reed et al. 2009), but have not been reported in mice. Our findings may be due to the

lower inoculation dose and/or the prolonged study design, which may actually mimic natural human infection more accurately.

In humans, the incubation period following natural infection is short, usually 4-10 days. Systemic infection is often characterized by abrupt onset of chills and fever followed by malaise, arthralgia, and myalgia. Typically these are difficult parameters to measure in animals; however, telemetry did allow us to monitor temperature and activity and we did note fever and decreased activity (lethargy or malaise) in many infected animals. Clinical signs of encephalitis in humans include abrupt onset of severe fever, intense headache, irritability, restlessness, drowsiness, anorexia, nausea, vomiting, diarrhea, cyanosis, convulsions, and coma. Again, while most of these clinical signs cannot be evaluated in mice, we did note marked lethargy and tremors in some infected animals. In humans, death usually occurs within 2-14 days after the onset of clinical signs (Calisher 1994). In the LD_{50} study we noted that mice generally were moribund or succumbed to infection within 2-4 days following the onset of clinical signs. Histopathologic lesions in human cases of EEE include vasculitis, thrombosis, perivascular cuffing, neutrophilic and histiocytic infiltrates, neuronal cell death, neuronophagia, focal necrosis, demyelination, and gliosis. (Deresiewicz, Thaler et al. 1997). While vasculitis, thrombosis, and inflammation were not prominent lesions in our intranasal or aerosol studies, they were noted in several animals, especially after 5 dpi, in our subcutaneous study. Neuronal cell death, regardless of mechanism of cell death, is a universal key feature in this disease and has been noted in all animal models studied (Vogel P, Kell WM et al. 2005; Adams, Aronson et al. 2008; Roy, Reed et al. 2009; Steele and Twenhafel 2010). Again, the lower dose and longer duration used in the

subcutaneous study likely more closely mimics the disease seen in humans. However, it is important to remember that in most human cases of natural infection the exact time of exposure is not likely to be known.

Our results also support the findings in guinea pigs where researchers determined that aerosolized EEEV entered the brain through the olfactory system followed by transneuronal spread to all regions of the brain. In this study, viral antigen was detected immunohistochemically in the olfactory mucosa, the olfactory nerves, and/or lamina propria 1 dpi (Roy, Reed et al. 2009). To date, the NHP studies published have not evaluated the mechanism of neuroinvasion of EEEV following aerosol exposure (Reed, Lackemeyer et al. 2007; Adams, Aronson et al. 2008; Espinosa, Weaver et al. 2009; Steele and Twenhafel 2010). While it is likely that EEEV utilizes the olfactory system to invade the brain in NHP, this is an important question that remains to be answered.

To further elucidate the mechanism of neuronal cell death in the mouse model, we evaluated brain sections from the AE study for the presence of cleaved-caspase 3 antigen as a marker of apoptosis as well as LC3B-II antigen as a marker of autophagy. While there was a low basal level of apoptosis present in control animals, significantly more was present in EEEV infected animals, especially at later time points. Cleaved-caspase 3 antigen was found primarily in the neurons of the olfactory bulb and the piriform cortex of the cerebrum. However, the number of cells staining for c-caspase-3 was lower than expected based on histologic findings. At later time points, a significant number of neurons with condensed cytoplasm and either pyknosis or karyorrhexis, suggestive of apoptosis, were present. This disparity may be due to the fact that c-caspase 3, a marker in the terminal pathway of apoptosis, may not be present in cells that have already

undergone apoptosis with resultant cellular and nuclear fragmentation. On the other hand, it may be that some neurons are not undergoing apoptosis but are dying by another mechanism, such as necrosis or autophagy. Autophagy, also known as type II programmed cell death, has been recognized as a means of cellular death in other alphaviral infections (Orvedahl and Levine 2008; Orvedahl, MacPherson et al. 2010) and can be histologically indistinguishable from apoptosis. We found relatively few neurons that were immunohistochemically positive for LC3B-II antigen, and these were only present at 3-4 dpi. The positive neurons were within viral antigen positive areas within the olfactory bulb, frontal cortex, and midbrain, but specifically not within the piriform cortex. This suggests that neurons in various areas of the brain may respond to viral infection differently and ultimately undergo one of several mechanisms of cell death.

It is important to note that histologically it can be difficult to determine the mechanism of cell death for each individual neuron as apoptosis, necrosis, and autophagy can occur simultaneously in the same tissue. The morphological features of apoptosis are generally characterized by cell shrinkage and convolution, pyknosis and karyorrhexis, intact cell membranes with no inflammation affecting single cells or small clusters of cells, while the morphological features of necrosis are generally characterized by cell swelling, karyolysis, disruption of cell membranes with inflammation affecting contiguous cells. However, pyknosis and karyorrhexis can be seen in necrosis as well as apoptosis (Elmore 2007) and recent studies indicate that necrosis may not only be an accidental form of cell death, but that it may be initiated or modulated by programmed control mechanisms, much like apoptosis and autophagy (Festjens, Vanden Berghe et al. 2006; Zong and Thompson 2006; Golstein and Kroemer 2007; Hotchkiss, Strasser et al.

2009). There is overlap between these two processes, which has been described as the "necrosis-apoptosis continuum" and whether a cell dies by necrosis or apoptosis may be determined by the tissue type, developmental stage of the tissue, cell death signal, as well as the physiologic microenvironment (Fiers, Beyaert et al. 1999; Zeiss 2003). Autophagy is a more recently recognized form of programmed cell death. While autophagy is generally recognized as an adaptive response, there is some controversy as to its role in cell death. It is uncertain if the accumulation of autophagosomes in some dying cells is a consequence of cellular adaptation alone or if these structures actually facilitate cell death (Hotchkiss, Strasser et al. 2009). As the molecular pathways of these processes becomes more defined, it may be revealed that the various mechanisms of cell death work in concert to eliminate unwanted cells in order to preserve tissue and organ function.

It is widely accepted that the brain is composed of numerous morphologically, metabolically, and functionally diverse neuroanatomic regions, which have differential sensitivities to various toxic and infectious insults. While neurons can be broadly classified as "small neurons" and "large neurons", various subtypes of each exist and interact with a number of support cells of varying function (Garman 2011). With the complexity and mutually supportive roles of the numerous cell types within the CNS just beginning to be understood, it is not difficult to imagine that one or more mechanisms of cell death may play an important role in overall maintenance of brain function. As our study suggests, in mice infected with EEEV, neurons in the CNS may undergo cell death by apoptosis, necrosis, or autophagy depending on the neuroanatomic location of the neuron and stage of disease.

While it has long been known that in mice infected with VEEV, regardless of route of exposure, neuroinvasion occurs through the olfactory system (Charles PC, Walters E et al. 1995; Ryzhikov, Ryabchikova et al. 1995; Steele, Davis et al. 1998; Pratt, Hart et al. 2006; Steele and Twenhafel 2010), this study has been crucial in understanding the mechanism of neuroinvasion of EEEV. It is clear from these studies that EEEV enters the brain through the olfactory system when mice are exposed either by the intranasal or aerosol route. The mechanism and rapidity in which the virus enters the brain has important vaccine and therapeutic implications. First, for a vaccine to be effective, it must prevent the virus from infecting olfactory neurons. Since the nasal cavity is a mucosal surface, it would be reasonable to expect that an effective vaccine would induce the production of neutralizing IgA as well as IgG. Secondly, since virus was present within 6 hpi in the aerosol study, a useful therapeutic would need to be administered very soon after exposure and would have to be formulated to easily cross the blood-brain-barrier. These are not insurmountable tasks; however, after years of research, there is still no licensed vaccine or therapeutic available for humans to prevent the often devastating outcome of EEEV infection.

REFERENCES

(2006). "Eastern equine encephalitis--New Hampshire and Massachusetts, August-September 2005." MMWR Morb Mortal Wkly Rep 55(25): 697-700.

Adams, A. P., J. F. Aronson, et al. (2008). "Common marmosets (Callithrix jacchus) as a nonhuman primate model to assess the virulence of eastern equine encephalitis virus strains." J Virol 82(18): 9035-9042.

Aguilar, P. V., S. Paessler, et al. (2005). "Variation in interferon sensitivity and induction among strains of eastern equine encephalitis virus." J Virol 79(17): 11300-11310.

Arrigo, N. C., A. P. Adams, et al. (2010). "Evolutionary patterns of eastern equine encephalitis virus in North versus South America suggest ecological differences and taxonomic revision." J Virol 84(2): 1014-1025.

Calisher, C. H. (1994). "Medically important arboviruses of the United States and Canada." Clin Microbiol Rev 7(1): 89-116.

Charles PC, Walters E, et al. (1995). "Mechanism of neuroinvasion of Venequelan equine encephalitis virus in the mouse." Virology 208: 662-671.

Deresiewicz, R. L., S. J. Thaler, et al. (1997). "Clinical and neuroradiographic manifestations of eastern equine encephalitis." N Engl J Med 336(26): 1867-1874.

Dyce, K. M., W. O. Sack, et al. (1987). Textbook of Veterinary Anatomy. Philadelphia, W.B. Saunders Company.

Elmore, S. (2007). "Apoptosis: a review of programmed cell death." Toxicol Pathol 35(4): 495-516.

Espinosa, B. J., S. C. Weaver, et al. (2009). "Susceptibility of the Aotus nancymaae owl monkey to eastern equine encephalitis." Vaccine 27(11): 1729-1734.

Festjens, N., T. Vanden Berghe, et al. (2006). "Necrosis, a well-orchestrated form of cell demise: signalling cascades, important mediators and concomitant immune response." Biochim Biophys Acta 1757(9-10): 1371-1387.

Fiers, W., R. Beyaert, et al. (1999). "More than one way to die: apoptosis, necrosis and reactive oxygen damage." Oncogene 18(54): 7719-7730.

Gardner, C. L., C. W. Burke, et al. (2008). "Eastern and Venezuelan equine encephalitis viruses differ in their ability to infect dendritic cells and macrophages: impact of altered cell tropism on pathogenesis." J Virol 82(21): 10634-10646.

Gardner, C. L., G. D. Ebel, et al. (2011). "Heparan sulfate binding by natural eastern equine encephalitis viruses promotes neurovirulence." Proc Natl Acad Sci U S A 108(38): 16026-16031.

Gardner, C. L., J. Yin, et al. (2009). "Type I interferon induction is correlated with attenuation of a South American eastern equine encephalitis virus strain in mice." Virology 390(2): 338-347.

Garman, R. H. (2011). "Histology of the central nervous system." Toxicol Pathol 39(1): 22-35.

Golstein, P. and G. Kroemer (2007). "Cell death by necrosis: towards a molecular definition." Trends Biochem Sci 32(1): 37-43.

Griffin DE (2007). Alphaviruses. Fields Virology. Knipe DM, Griffin DE, Lamb RAet al. Philadelphia, Lippincott Williams & Wilkins: 1024-1067.

Griffin, D. E., B. Levine, et al. (1994). "Age-dependent susceptibility to fatal encephalitis: alphavirus infection of neurons." Arch Virol Suppl 9: 31-39.

Guyton, A. C. (1947). "Measurement of the respiratory volumes of laboratory animals." Am J Physiol 150(1): 70-77.

Hotchkiss, R. S., A. Strasser, et al. (2009). "Cell death." N Engl J Med 361(16): 1570-1583.

Labrada, L., X. H. Liang, et al. (2002). "Age-dependent resistance to lethal alphavirus encephalitis in mice: analysis of gene expression in the central nervous system and identification of a novel interferon-inducible protective gene, mouse ISG12." J Virol 76(22): 11688-11703.

Morgan, I. M. (1941). "INFLUENCE OF AGE ON SUSCEPTIBILITY AND ON IMMUNE RESPONSE OF MICE TO EASTERN EQUINE ENCEPHALOMYELITIS VIRUS." J Exp Med 74(2): 115-132.

Orvedahl, A. and B. Levine (2008). "Autophagy and viral neurovirulence." Cell Microbiol 10(9): 1747-1756.

Orvedahl, A., S. MacPherson, et al. (2010). "Autophagy protects against Sindbis virus infection of the central nervous system." Cell Host Microbe 7(2): 115-127.

Pratt, W., M. K. Hart, et al. (2006). Alphaviruses. Biodefense Research Methodology and Animal Models. J. R. Swearengen. Boca Raton, Florida, CRC Taylor & Francis: 181-206.

Reed, D. S., M. G. Lackemeyer, et al. (2007). "Severe encephalitis in cynomolgus macaques exposed to aerosolized Eastern equine encephalitis virus." J Infect Dis 196(3): 441-450.

Roy, C. J., D. S. Reed, et al. (2009). "Pathogenesis of aerosolized Eastern Equine Encephalitis virus infection in guinea pigs." Virol J 6(1): 170.

Ryzhikov, A. B., E. I. Ryabchikova, et al. (1995). "Spread of Venezuelan equine encephalitis virus in mice olfactory tract." Arch Virol 140(12): 2243-2254.

Steele, K. E., K. J. Davis, et al. (1998). "Comparative neurovirulence and tissue tropism of wild-type and attenuated strains of Venezuelan equine encephalitis virus administered by aerosol in C3H/HeN and BALB/c mice." Vet Pathol 35(5): 386-397.

Steele, K. E. and N. Twenhafel (2010). "Review paper: Pathology of animal models of alphavirus encephalitis." Vet Pathol 45(7): 790-805.

Van den Broeck, W., A. Derore, et al. (2006). "Anatomy and nomenclature of murine lymph nodes: Descriptive study and nomenclatory standardization in BALB/cAnNCrl mice." J Immunol Methods 312(1-2): 12-19.

Vogel P, Kell WM, et al. (2005). "Early events in the pathogenesis of eastern equine encephalitis virus in mice." Am J Pathol 166(1): 159-171.

Zeiss, C. J. (2003). "The apoptosis-necrosis continuum: insights from genetically altered mice." Vet Pathol 40(5): 481-495.

Zong, W. X. and C. B. Thompson (2006). "Necrotic death as a cell fate." Genes Dev 20(1): 1-15.

Chapter 3

Inactivation of CVEV1219

Abstract

Eastern equine encephalitis virus (EEEV), an arbovirus, is an important human and veterinary pathogen belonging to one of seven antigenic complexes in the genus *Alphavirus*, family *Togaviridae*. EEEV is considered the most deadly of the mosquito-borne alphaviruses due to the high case fatality rate associated with clinical infections, reaching as high as 75% in humans and 90% in horses (Griffin DE 2007). In patients that survive, the neurologic sequelae are often devastating. Although natural infections are acquired by mosquito bite, EEEV is also highly infectious by aerosol, making it a potential agent of bioterrorism.

Currently, there are no FDA-licensed vaccines or therapeutics for EEEV for human use. To evaluate the ability of formalin, 1, 5-iodonaphthylazide (INA), and gamma-irradiation to inactivate a genetically modified strain of EEEV, CVEV1219, we used a multi-system approach. Here we report the complete inactivation of CVEV1219 by formalin, INA, and gamma-irradiation methodologies. Future experiments will test these inactivated preparations in mice for immunogenicity and protective efficacy against wild-type EEEV.

Introduction

Eastern equine encephalitis virus (EEEV) is considered the most deadly of the mosquito-borne alphaviruses due to the high case fatality rate associated with clinical infections. There are four antigenic subtypes of EEEV, one that circulates in North

America and the Caribbean (NA EEEV), and three that circulate in Central and South America (SA EEEV). The strains differ in their geographic, epidemiologic, pathogenic, phylogenetic, and evolutionary characteristics. NA EEEV strains are highly conserved, monophyletic, and temporally related, while SA EEEV strains are highly divergent, polyphyletic, co-circulating, and geographically associated (Arrigo, Adams et al. 2010). NA EEEV results in approximately 5-8 human cases yearly, often with devastating outcomes, while SA EEEV has little to no association with human disease, despite evidence of human exposure in endemic areas (2006). EEEV is also listed as a category B agent by the National Institute of Allergy and Infectious Diseases (NIAID) due to its virulence, its potential use as a biological weapon, and the lack of a licensed vaccine or effective antiviral treatment for human infections. Therefore, research directed towards the development of a safe and effective vaccine and antiviral treatment for humans is essential.

The goal of vaccine development is to produce a product that closely mimics natural infection; thereby stimulating an appropriate and effective immune response. However, new vaccine candidates should protect against both subcutaneous and mucosal exposure to virulent virus, which can be challenging. CVEV1219 is a genetically modified strain of EEEV, containing the nonstructural proteins of Venezuelan equine encephalitis virus (VEEV) and the structural proteins of EEEV. Additionally, the furin cleavage site within the PE2 glycoprotein was deleted, which significantly attenuated the virus *in vitro*. During cellular processing of the wild-type virus, furin, a cellular protease, cleaves E2 and E3, E3 is then released and E1 and E2 form a heterodimer which is transported to the cell surface. In the mutant virus, the site for cleavage is deleted; therefore, furin is unable

to cleave E2 and E3 and they are transported to the cell surface as their precursor (PE2) (Figure 3.1B). This results in a change in the surface structure, as noted in Figure 3.2, a modified image from Paredes et. al. (Paredes, Heidner et al. 1998). In the wild-type virus, E1 and E2 form a heterodimer which then trimerizes (figure 3.2, left panel); however, in the cleavage mutant PE2 forms a heterodimer with E1 which then trimerizes resulting in an extra surface projection (Figure 3.2, right panel). This is a lethal mutation; however, rescued virus contains compensatory mutations which alter the glycoprotein interactions and resuscitate the virus. This mutant virus is similar to V3526, the furin cleavage deletion mutant of VEEV. The PE2 domain of V3526 has been shown to be immunogenic given that monoclonal antibodies directed to this domain were able to protect mice from lethal VEEV challenge (Parker, Buckley et al. 2010). Additionally, this vaccine candidate showed great promise in animal studies and protected against multiple serotypes of VEEV, while circumventing the vaccine interference that is often observed with alphaviruses (Hart, Caswell-Stephan et al. 2000; Hart, Lind et al. 2001). However, when it was transitioned to phase 1 human clinical trials, V3526 induced unacceptable side effects and was not further pursued.

Inactivating a modified-live virus provides an additional layer of safety in the formulation of the vaccine candidate. Formalin has historically been used in inactivated vaccines licensed by the FDA.   Although it induces cross-linking of proteins, which could affect epitope immunogenicity, it has recently been used to successfully inactivate both V3526 (Martin, Bakken et al. 2010) and Japanese encephalitis virus (JEV)

A.

VEEV **EEEV**

C — | nsp 1 | nsp 2 | nsp 3 | nsp 4 | C | E3 | E2 | 6K | E1 | — polyA

B.

Wild-type cleavage site   **Cleavage site deletion (CVEV1219)**
-12 nucleotides

E3 Protein   E2 Protein   E3 Protein   E2 Protein

..CYS PRO GLY ARG LYS ARG ARG SER THR GLU.   .VAL LYS CYS PRO GLY SER THR GLU GLU PHE.
..TGC CCC GGA AGG AAA AGG AGA TCC ACC GAG.   .GTT AAG TGC CCC GGA TCC ACC GAG GAG CTG.

| E3 | RKRR | E2 | ≡ | E1 | | E3 | E2 | ≡ | E1 |

Trans Golgi Processing

Furin   **Furin**

| E3 | | E2 | ≡ | E1 | | PE2 | ≡ | E1 |

Figure 3.1. CVEV1219 is a genetically modified chimeric virus. The virus is composed of the non-structural proteins (nsP) of VEEV and the structural proteins (capsid, E3, E2, 6K, and E1) of EEEV (A). In addition, the site for furin cleavage is deleted. During cellular processing of the wild-type virus, furin, a cellular protease, cleaves E2 and E3, E3 is then released and E1 and E2 form a heterodimer which is transported to the cell surface. In the mutant virus, the site for cleavage is deleted; therefore, furin is unable to cleave E2 and E3 and they are transported to the cell surface as their precursor (PE2) (B).

Wild Type   **Cleavage Mutant**
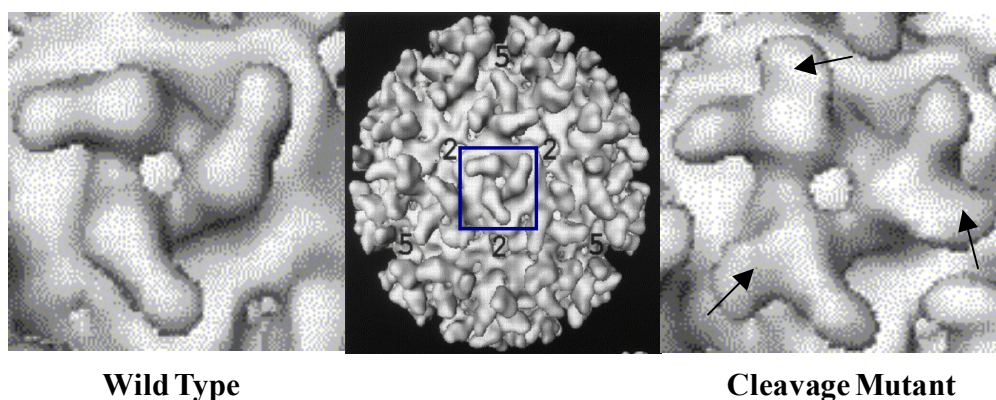
Figure 3.2. Surface structure of a cleavage mutant. The left panel depicts the wild type spike, which is a structure composed of E1 and E2 heterodimers, which then trimerize. The right panel shows the surface spike of the cleavage mutant, which is composed of the PE2 protein that forms a heterodimer with E1, which then trimerizes. This results in an extra projection on the surface (arrows). Modified from Paredes et. al., 1998.

(http://www.fda.gov/BiologicsBloodVaccines/Vaccines/ApprovedProducts/ucm142577.h

tm 2009). Another chemical compound recently used to inactivate enveloped viruses is

INA, which is a hydrophobic photo-reactive probe that binds to transmembrane anchors

of proteins upon photo-activation with UV light (Viard, Ablan et al. 2008). Traditionally,

it has been used for labeling membrane proteins and evaluating their dynamics and fusion

as well as for studying protein-membrane interactions (Raviv, Salomon et al. 1987).

However, with far-UV irradiation (310-360 nm), INA alkylates the transmembrane

domains of viral proteins, resulting in their inactivation, while maintaining the integrity

of the external domains. INA is unique in that it preserves membrane protein structural

integrity and therefore is potentially useful for vaccine applications. INA has recently

been used inactivate V3000 (Sharma, Raviv et al. 2007), V3526 (Sharma, Gupta et al.

2011), HIV (Raviv, Viard et al. 2005), SIV (Raviv, Viard et al. 2005), influenza virus

(Raviv, Blumenthal et al. 2008), and Ebola virus (Warfield, Swenson et al. 2007).

Gamma-irradiation has also been used experimentally to inactivate enveloped viruses.

Gamma-irradiation inactivates viruses by generating strand-breaks in the genetic

material, with little impact on the antigenic structure and biological integrity of proteins

and has been used successfully to inactivate V3526 (Martin, Bakken et al. 2010) and

influenza A virus (Lowy, Vavrina et al. 2001; Alsharifi, Furuya et al. 2009; Furuya,

Regner et al. 2010). Therefore we tested each of these inactivation methods using

CVEV1219 in order to provide an additional layer of safety in the formulation of the

vaccine candidate and to avoid potential unwanted side effects in human vaccinees.

Materials and Methods

CVEV1219

CVEV1219 is a chimeric virus composed of the nonstructural proteins of VEEV and the structural proteins of EEEV. In addition, the site for furin cleavage is deleted; therefore, furin is unable to cleave E2 and E3 and they are transported to the cell surface as their precursor (PE2). PE2 then forms a heterodimer with E1 and these structures then trimerize, resulting in an extra surface projection. This is a lethal mutation; however, compensatory mutations in the rescued virus alter the glycoprotein interactions and resuscitate the virus.

Formalin Inactivation

Sucrose purified CVEV1219 virus stock aliquots with known viral titer and protein concentration were suspended in 1X Dulbecco's PBS (DPBS) (GIBCO^{TM}, Invitrogen Corp., Grand Island, NY) at a protein concentration of 100 µg/ml. One milliliter aliquots of virus, in cyrovial tubes, were treated with 37% Formaldehyde solution stabilized with 10% methanol (Thomas Scientific, Swedesboro, NJ) at a final concentration of 0.1% and 25% Buminate, human serum albumin (Baxter Healthcare Corp., Westlake Village, CA) at a final concentration of 0.5%. Samples were incubated for 18 hours at 37°C in a Forma Scientific orbital shaker at 200 rpm (ThermoFisher Scientific, Waltham, MA). Formalin was removed by pelleting the virus through a 20% sucrose cushion at 40,000 rpm for 4 hours using a Beckman, L7 ultracentrifuge (Beckman Coulter, Inc., Brea, CA). The formalin treated CVEV1219 (fCVEV1219) pellet was suspended in 250-500 µL of 1X DPBS overnight at 4°C. Aliquots were combined and protein concentration was

determined using a BCA Protein Assay kit (Thermo Scientific, Rockford, IL) as per manufacturer's instructions. The fCVEV1219 sample was adjusted to a final concentration of 250-750 µg/ml in 1X DPBS. Aliquots were frozen at -80°C until used for *in vitro* and *in vivo* testing.

INA Inactivation

Sucrose purified CVEV1219 virus stock aliquots with known viral titer and protein concentration were suspended in 1X DPBS at a protein concentration of 500 µg/ml in a clear transparent tube, and from this point on, reduced lighting conditions were used. INA (Biotium, Hayward, CA) was added to the virus suspension to a final concentration of 200 µM in 5 installments with vortexing and then samples were incubated for 20 min in the dark at room temperature (RT). Samples were then centrifuged at 1000 rpm for 1 min to remove precipitated INA crystals. Supernatant was transferred to new tube and glutathione was added to a final concentration of 20 mM. The virus suspension was irradiated using a BLAK-Ray^R B-100 series longwave ultraviolet lamp with a 100 watt bulb (UVP, Upland, CA) using the following setup: A 3 mm thick, clear glass plate was placed immediately in front of the lamp in order to filter lower UV wavelengths of light; a water filled 75 cm^2 transparent tissue culture flask, used as a heat filter, was placed approximately 5 cm from the glass plate; samples were placed 5 cm away from the flask such that samples were completely illuminated with the light passing through the flask (Figure 3.3). Samples were irradiated for a total of 10 min with vortexing at 2 min intervals. Thereafter full light conditions were used and aliquots were stored at -80 ^{o}C until used for *in vitro* and *in vivo* testing.

Figure 3.3. Setup for INA inactivation of CVEV1219. Ultraviolet light was filtered through a 3 mm thick, clear glass plate to filter lower wavelengths and then through a transparent tissue flask filled with water used as a heat filter. There was approximately 10 cm between the UV source and the sample.

UV Lamp (100 W) *Glass Plate* (300 nm cut-off filter) *Water* (heat shield) *Sample*

Gamma-irradiation

Sucrose purified CVEV1219 virus stock aliquots with known viral titer and protein concentration were frozen at -80°C and sent for gamma-irradiation. Samples were irradiated with 10 million rads (100,000 Gy) of gamma-irradiation in a 484R AECL gammacell cobalt irradiator (J.L. Shepherd and Assoc., San Fernando, CO). Samples were aliquoted and stored at -80°C until used for *in vitro* and *in vivo* testing.

Testing for residual infectivity in vitro

Serial passage

Inactivated virus preparations were tested for residual infectivity by five serial passages of 72-96 hours each on BHK-21 cells. Briefly, inactivated vaccine candidates were diluted 1:5 in supplemented EMEM (USAMRIID, Fort Detrick, MD) containing 5% fetal bovine serum (FBS) (GIBCO Invitrogen Corp., Grand Island, NY), 1% penicillin (20,000 IU/ml)-streptomycin sulfate (20,000 μg/ml), 1% non-essential amino acids (NEAA) (Sigma Aldrich Company, Inc., St. Louis, MO), 1% 200 mM L-glutamine

(Thermo Scientific, Logan, UT), and 0.1% gentamicin solution (Sigma Aldrich Company, Inc., St. Louis, MO). One hundred microliters of the diluted vaccine candidate was added to one well of a 6 well plate (Costar) containing BHK-21 cells at 50% confluency. Samples were tested in duplicate. Plates were incubated for 1 hour at 37°C, 5% CO_2 with humidity with rocking every 15 min. One to two milliliters of supplemented EMEM was added to each well and plates were incubated for 3-4 days at 37°C, 5% CO_2 with humidity (pass 1). After incubation, wells were evaluated for the presence of cytopathology. If no cytopathic effect (CPE) was observed 200 µL of supernatant was transferred to new plates containing BHK-21 cells at 50% confluency. Plates were incubated for 1 hour at 37°C, 5% CO_2 with humidity and then 1-2 ml of supplemented EMEM was added to each well. Plates were then incubated for 3-4 days at 37°C, 5% CO_2 with humidity (pass 2). This procedure was repeated for a total of 5 passes. Supernatant from the 5th passage was collected and stored at -80°C for further *in vitro* testing by standard plaque assay and indirect immunofluroescent analysis.

Standard Plaque Assay

A standard plaque assay on Vero cell monolayers was used to determine if any infectious particles remained in each of the inactivated virus preparations. Briefly, supernatant from the 5th passage on BHK-21 cells was serially diluted with supplemented EMEM. Diluted samples were then added in duplicate to 6-well plates containing a confluent monolayer of Vero cells (African green monkey kidney cells). Plates were incubated at 37°C for 1 hour, with rocking every 15 min. Following the incubation period, wells were overlaid with 0.5% agarose in EBME media (USAMRIID,

Fort Detrick, MD) containing HEPES and 10% FBS, 1% L-glutamine, 1% NEAA, 1% penicillin -streptomycin sulfate, and 0.1% gentimicin, and plates were incubated at 37 °C at 5% CO_2 for 24 hr. Thereafter, cells were stained by the addition of a second agarose overlay prepared as above containing 5% neutral red. The plates were incubated at 37°C at 5% CO_2 for 24 hr. Residual infectivity was quanititated by counting defined plaques (neutral red exclusion areas).

Immunofluorescent Assay

Indirect immunofluorescent assay was also used to determine if any infectious particles remained in each of the inactivated virus preparations. Briefly, 100 µL of supernatant from the 5th passage on BHK-21 cells was added in duplicate to a chamber of a Lab-Tek 8-well chamber slide system (Nalge Nunc International, Rochester, NY) containing confluent BHK-21 cells. Slides were incubated for 1 hour at 37°C, 5% CO_2 with humidity and then 300 µL of supplemented EMEM was added. Slides were incubated overnight at 37°C, 5% CO_2 with humidity. The following day, the chamber was removed and the slide was rinsed in DPBS and air dried at RT. Cells were fixed in ice cold acetone for 10 min at RT after which the slides were air dried. In order to visualize viral proteins, slides were incubated with EEE hyperimmune mouse acites fluid, EEE-HMAF, in 50% glycerol diluted 1:500 in PBS with 5% FBS for 1 hour at RT in a humidified chamber. After incubation, the slide was rinsed in DPBS and incubated with the secondary antibody (FITC labeled goat anti-mouse antibody diluted 1:80 in DPBS with 5% FBS) in the dark for 30 min at RT in a humidified chamber. The slide was then rinsed in DPBS and coverslip mounted using Vectashield mounting medium for

fluorescence with DAPI (Vector Laboratories, Inc., Burlingame, CA). Slides were

evaluated using a Nikon Eclipse E800 fluorescent microscope.

Testing for residual infectivity in vivo

Inactivated virus preparations were tested *in vivo* by intracranial inoculation of

suckling mice. Briefly, specific pathogen free late-pregnant female BALB/c mice (NCI,

Frederick, MD) were housed a biosafety level 3 (BSL-3) facility in cages equipped with

microisolators and were provided food and water *ad libitum* throughout the study. The

room temperature was $23 \pm 1^{o}C$ and periods of light and dark were maintained on a 12 h

cycle. Newborn suckling mice were allowed to acclimate for 1 day prior to inoculation.

Suckling mice were inoculated by the intracranial route (IC) with 10µL of inactivated

CVEV1219 or sterile saline (negative control) using a 50 or 100 µl Hamilton syringe

with a 22-26 gauge needle. The mice were observed twice daily for 14 days for clinical

signs of illness, cannibalization, and death. Surviving mice were euthanized on day 14

and the brains removed and homogenized. Ten microliters of the supernatant from the

homogenate was then injected IC into a second group of suckling mice. These mice were

observed twice daily for 14 days for clinical signs of illness, cannibalization and death.

The brain from any suckling mouse that died or was euthanized due to illness was

homogenized and frozen for viral titer analysis.

Research was conducted at the United States Army Medical Research Institute of

Infectious Diseases (USAMRIID) under an IACUC approved protocol in compliance

with the Animal Welfare Act and other Federal statutes and regulations relating to

animals and experiments involving animals and adheres to principles stated in the Guide

for the Care and Use of Laboratory Animals, National Research Council, 1996. The facility is fully accredited by the Association for Assessment and Accreditation of Laboratory Animal Care International.

Results

Several experiments were conducted in order to optimize the protocol for each inactivation method. For formalin inactivation, a series of experiments were conducted using 100 µg/ml of CVEV1219 and formalin at a concentration of 0.1, 0.25, or 0.5% with incubation periods ranging from 18-48 hours. For INA inactivation, a series of experiments were conducted using 50-500 µg/ml of CVEV1219 with INA concentrations ranging from 50-400 µM and UV exposures ranging from 5-12 minutes. For gamma-irradiation of CVEV1219, virus concentration ranged from 800-1000 µg/ml and received either 8 million or 10 million Rad (80,000 or 100,000 Gy). The optimal inactivation methods that resulted from these experiments are shown in Table 3.1.

Table 3.1. Inactivation methods optimized for CVEV1219

	Virus (µg/ml)	Method of Inactivation
Formalin (fCVEV1219)	100	0.1% formalin $\rightarrow$ incubate 18 hr 37°C with shaking $\rightarrow$ purify through a 20% sucrose cushion
INA (iCVEV1219)	500	200 µM INA $\rightarrow$ incubate in the dark for 20 min at RT $\rightarrow$ 10 min UV, vortex every 2 min
Gamma-irradiation (gCVEV1219)	939	Sample frozen $\rightarrow$ 10 M Rad (100,000 Gy) in a cobalt irradiator

Table 3.1. Three methods of inactivation were optimized and tested using CVEV1219, a genetically modified chimeric virus composed of the nonstructural proteins of VEEV and the structural proteins of EEEV, in which the site for furin cleavage is deleted. The three methods of inactivation included formalin-inactivation, INA-inactivation, and gamma-irradiation.

CVEV1219 was completely and consistently inactivated when treated with 0.1% formalin after an 18 hour incubation period at 37°C with shaking. After purification through a 20% sucrose cushion, 75-80% of the starting protein concentration was recovered as determined by the BCA method. After inactivated samples were serially passed 5 times using BHK-21 cells with no CPE detected, the supernatant from the 5th passage was tested for residual infectivity using the standard plaque assay and immunofluorescent assay (IFA) (Figure 3.4A). No virus was detected using the standard plaque assay (data not shown) and no viral antigen was detected by IFA (Figure 3.4B).

Higher concentrations of CVEV1219 (500 µg/ml) were completely and consistently inactivated using 200 µM of INA combined with 10 min of UV exposure. Individual samples were serially passed 5 times using BHK-21 cells and no CPE was detected, the supernatant from the 5th passage was tested for residual infectivity using the standard plaque assay and immunofluorescent assay (IFA) (Figure 3.4A). No virus was detected using the standard plaque assay (data not shown) and no viral antigen was detected by IFA (Figure 3.4B).

High concentrations (800-1000 µg/ml) of CVEV1219 were completely and consistently inactivated with exposure to 8 M or 10 M Rad. Samples were inactivated in bulk quantities, usually 20-30 ml and an aliquot was then tested for residual infectivity *in vitro* using the serial passage on BHK-21 cells, standard plaque assay, and immunofluorescent assay (IFA) (Figure 3.4A). No virus was detected using the standard plaque assay (data not shown) and no viral antigen was detected by IFA (Figure 3.4B).

A.

B.

CVEV1219 (positive control)   EMEM+ (negative control)

fCVEV1219   iCVEV1219   gCVEV1219
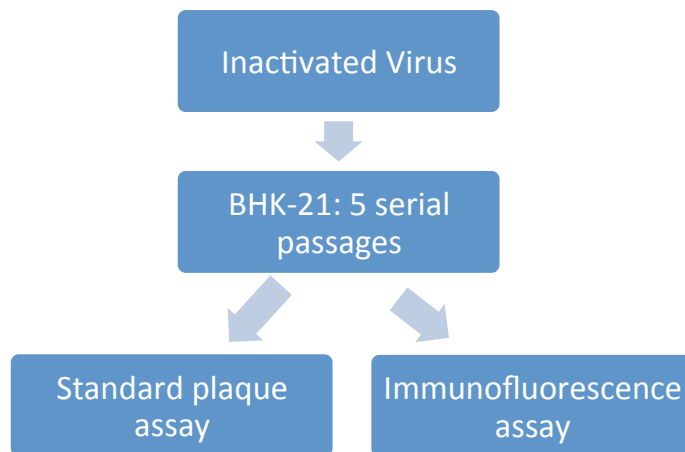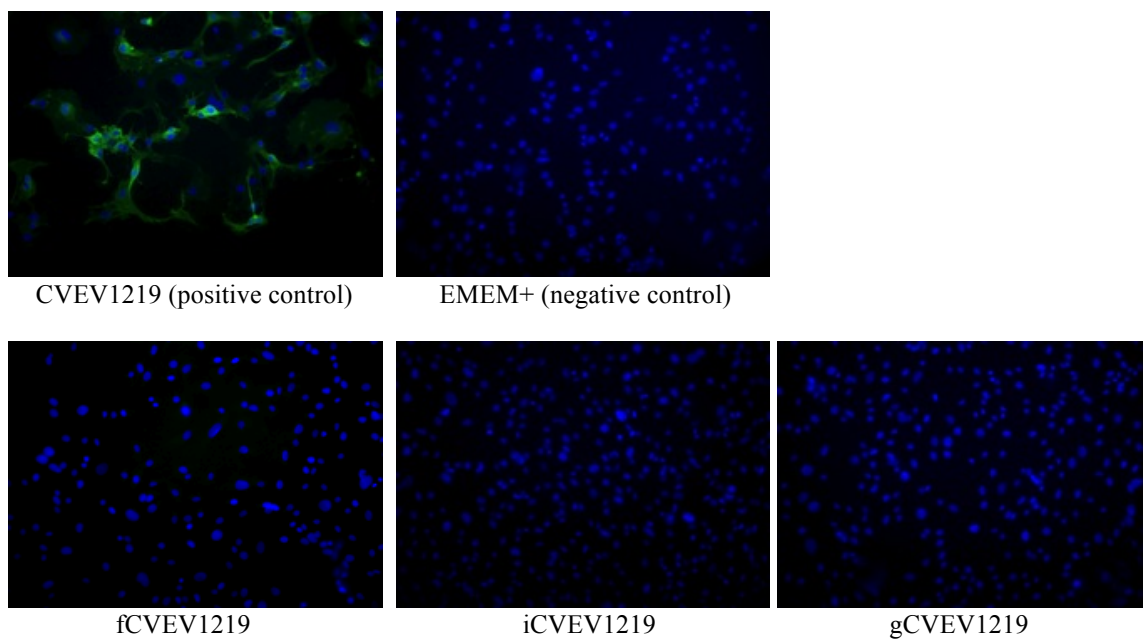
Figure 3.4. (A) A multi-system approach was used to verify complete inactivation *in vitro*. Samples were passed five times on BHK-21 cells. The supernatant from the 5th passage was evaluated by standard plaque assay and (B) immunofluorescent assay to determine residual infectivity.

After all methods of inactivation (formalin, INA, gamma-irradiation) were optimized, sufficiently large quantities of CVEV1219 were inactivated by each method and tested for residual infectivity *in vitro* using the multi-system approach described above. These samples were then tested for residual infectivity *in vivo* (Figure 3.5). Although the *in vitro* assessment of viral inactivation is sensitive, intracranial inoculation of suckling mice has been shown to be a more sensitive indicator and is considered the "gold-standard" for assessing inactivation/attenuation of alphaviruses (Labrada, Liang et al. 2002; Paessler, Fayzulin et al. 2003).
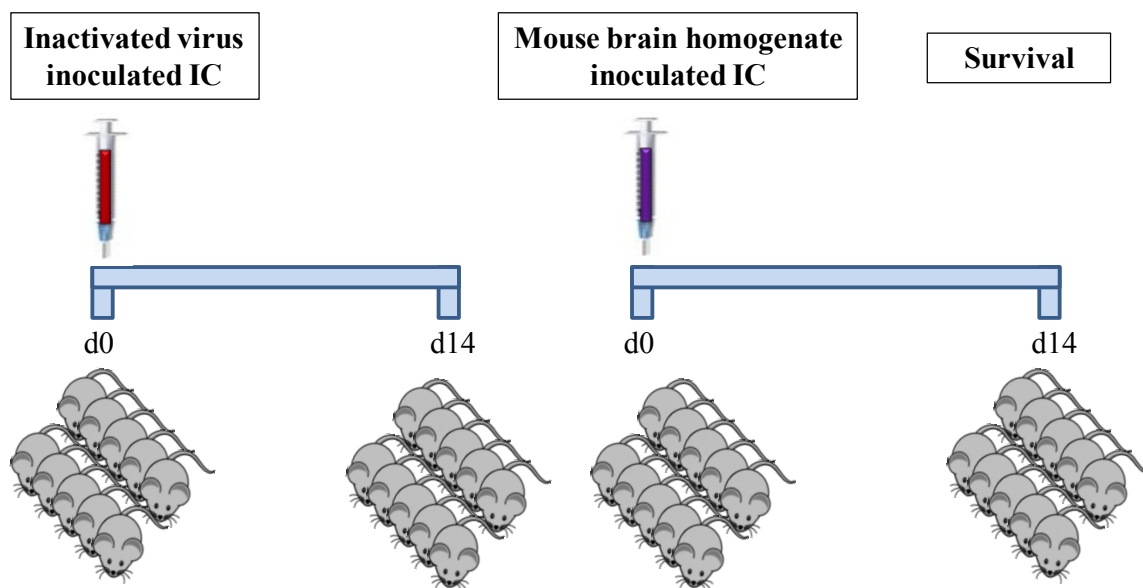
Figure 3.5. Residual viral infectivity was assessed by intracranial inoculation of BALB/c suckling mice with 10 µL of inactivated virus. Controls for the assay included suckling mice intracranially inoculated with live CVEV1219 or PBS. The brains from mice surviving 14 days post-inoculation were removed upon euthanasia and homogenized; the supernatant was collected and frozen at -80C. A second set of suckling mice were inoculated intracranially with 10 µL of the brain homogenate supernatant from the corresponding group and observed for an additional 14 days.

Interestingly, while the formalin-inactivated CVEV1219 (fCVEV1219) and the INA-inactivated CVEV1219 (iCVEV1219) passed both the *in vitro* and *in vivo* testing for residual infectivity, the gamma-irradiated CVEV1219 (gCVEV1219) that received 8 M Rad passed all of the *in vitro* testing; however, 2/12 suckling mice died after intracranial inoculation (Table 3.2). The brains from these mice were homogenized and virus was detected by plaque assay. A new preparation of CVEV1219 was gamma-irradiated with10 M Rad and these samples passed both the *in vitro* and *in vivo* testing for residual infectivity (Table 3.2).

Table 3.2. Results of suckling mouse studies.

Groups	Suckling mouse study #1		Suckling mouse study #2	
	% Survival	# died/total	% Survival	# died/total
fCVEV1219	100	0/13	100	0/11
iCVEV1219	100	0/11	100	0/13
gCVEV1219 (8M Rad)	83.3	2/12		
gCVEV1219 (10M Rad)	100	0/11	100	0/16
PBS	100	0/8	100	0/8
CVEV1219	0	5/5	0	7/7

Table 3.2. Residual viral infectivity was assessed by intracranial inoculation of BALB/c suckling mice with 10 µL of inactivated virus. Controls for the assay included suckling mice intracranially inoculated with live CVEV1219 or PBS. The brains from mice surviving 14 days post-inoculation were removed upon euthanasia and homogenized; the supernatant was collected and frozen at -80C. A second set of suckling mice were inoculated intracranially with 10 µL of the brain homogenate supernatant from the corresponding group and observed for an additional 14 days.

Conclusion

The goal of vaccine development is to produce a product that closely mimics natural infection; thereby stimulating an appropriate and effective immune response. However, because EEEV is a NIAID Category B agent due to its virulence and potential use as a biological weapon, new vaccine candidates should protect against both subcutaneous and mucosal exposure to virulent virus, which can be challenging.

Modified live vaccines often induce a stronger and longer lasting immune response; nonetheless, they are not without problems, as was recently seen when V3526 was tested in phase I clinical trials. V3526 protected mice from both subcutaneous and aerosol challenge (Hart, Caswell-Stephan et al. 2000). Additionally, V3526 provided protection within one week of vaccination and protection persisted for at least one year against both homologous and heterologous VEEV (Hart, Lind et al. 2001). However, when it was transitioned to phase 1 human clinical trials it induced unacceptable side effects and was not further pursued.

Inactivating an attenuated-live virus provides an additional layer of safety in the formulation of the vaccine candidate. Since there is no virus replication during immunization with inactivated vaccines, the virus cannot revert to virulence, as can occur with modified-live vaccines. We utilized formalin, INA, and gamma-irradiation to inactivate a genetically modified strain of EEEV. Since all three of these methods were successful in inactivating V3526 and most induced significant immune responses and were at least partially protective against an aerosol challenge (Sharma, Raviv et al. 2007; Martin, Bakken et al. 2010; Martin, Bakken et al. 2010; Sharma, Gupta et al. 2011), these inactivation methods were used in the preparation of a second-generation inactivated

EEEV vaccine candidate using CVEV1219. CVEV1219 was completely and consistently inactivated by formalin, INA, and gamma-irradiation methodologies. As was shown in this study, it is important to use a multi-system approach with both *in vitro* and *in vivo* methodologies, to determine residual infectivity and ensure complete and consistent inactivation. The inactivated CVEV1219 preparations were further investigated to determine immunogenicity and protective efficacy using several vaccine routes and schedules.

REFERENCES

(2006). "Eastern equine encephalitis--New Hampshire and Massachusetts, August-September 2005." MMWR Morb Mortal Wkly Rep **55**(25): 697-700.

Alsharifi, M., Y. Furuya, et al. (2009). "Intranasal flu vaccine protective against seasonal and H5N1 avian influenza infections." PLoS One **4**(4): e5336.

Arrigo, N. C., A. P. Adams, et al. (2010). "Evolutionary patterns of eastern equine encephalitis virus in North versus South America suggest ecological differences and taxonomic revision." J Virol **84**(2): 1014-1025.

Furuya, Y., M. Regner, et al. (2010). "Effect of inactivation method on the cross-protective immunity induced by whole 'killed' influenza A viruses and commercial vaccine preparations." J Gen Virol **91**(Pt 6): 1450-1460.

Griffin DE (2007). Alphaviruses. Fields Virology. Knipe DM, Griffin DE, Lamb RAet al. Philadelphia, Lippincott Williams & Wilkins**:** 1024-1067.

Hart, M. K., K. Caswell-Stephan, et al. (2000). "Improved mucosal protection against Venezuelan equine encephalitis virus is induced by the molecularly defined, live-attenuated V3526 vaccine candidate." Vaccine **18**(26): 3067-3075.

Hart, M. K., C. Lind, et al. (2001). "Onset and duration of protective immunity to IA/IB and IE strains of Venezuelan equine encephalitis virus in vaccinated mice." Vaccine **20**(3-4): 616-622.

http://www.fda.gov/BiologicsBloodVaccines/Vaccines/ApprovedProducts/ucm142577.htm. (2009). "Japanese Encephalitis Virus Vaccine, Inactivated, Adsorbed Approval Letter."   Retrieved November, 29, 2011, 2011.

Labrada, L., X. H. Liang, et al. (2002). "Age-dependent resistance to lethal alphavirus encephalitis in mice: analysis of gene expression in the central nervous system and identification of a novel interferon-inducible protective gene, mouse ISG12." J Virol **76**(22): 11688-11703.

Lowy, R. J., G. A. Vavrina, et al. (2001). "Comparison of gamma and neutron radiation inactivation of influenza A virus." Antiviral Res **52**(3): 261-273.

Martin, S. S., R. R. Bakken, et al. (2010). "Comparison of the immunological responses and efficacy of gamma-irradiated V3526 vaccine formulations against subcutaneous and aerosol challenge with Venezuelan equine encephalitis virus subtype IAB." Vaccine **28**(4): 1031-1040.

Martin, S. S., R. R. Bakken, et al. (2010). "Evaluation of formalin inactivated V3526 virus with adjuvant as a next generation vaccine candidate for Venezuelan equine encephalitis virus." Vaccine **28**(18): 3143-3151.

Paessler, S., R. Z. Fayzulin, et al. (2003). "Recombinant sindbis/Venezuelan equine encephalitis virus is highly attenuated and immunogenic." J Virol **77**(17): 9278-9286.

Paredes, A. M., H. Heidner, et al. (1998). "Structural localization of the E3 glycoprotein in attenuated Sindbis virus mutants." J Virol **72**(2): 1534-1541.

Parker, M. D., M. J. Buckley, et al. (2010). "Antibody to the E3 glycoprotein protects mice against lethal venezuelan equine encephalitis virus infection." J Virol **84**(24): 12683-12690.

Raviv, Y., R. Blumenthal, et al. (2008). "Hydrophobic inactivation of influenza viruses confers preservation of viral structure with enhanced immunogenicity." J Virol **82**(9): 4612-4619.

Raviv, Y., Y. Salomon, et al. (1987). "Selective labeling of proteins in biological systems by photosensitization of 5-iodonaphthalene-1-azide." Proc Natl Acad Sci U S A **84**(17): 6103-6107.

Raviv, Y., M. Viard, et al. (2005). "Inactivation of retroviruses with preservation of structural integrity by targeting the hydrophobic domain of the viral envelope." J Virol **79**(19): 12394-12400.

Sharma, A., P. Gupta, et al. (2011). "Safety and protective efficacy of INA-inactivated Venezuelan equine encephalitis virus: implication in vaccine development." Vaccine **29**(5): 953-959.

Sharma, A., Y. Raviv, et al. (2007). "Complete inactivation of Venezuelan equine encephalitis virus by 1,5-iodonaphthylazide." Biochem Biophys Res Commun **358**(2): 392-398.

Viard, M., S. D. Ablan, et al. (2008). "Photoinduced reactivity of the HIV-1 envelope glycoprotein with a membrane-embedded probe reveals insertion of portions of the HIV-1 Gp41 cytoplasmic tail into the viral membrane." Biochemistry **47**(7): 1977-1983.

Warfield, K. L., D. L. Swenson, et al. (2007). "Ebola virus inactivation with preservation of antigenic and structural integrity by a photoinducible alkylating agent." J Infect Dis **196 Suppl 2**: S276-283.

Chapter 4

Immunogenicity and Protective Efficacy of Inactivated CVEV1219

Abstract

Eastern equine encephalitis virus (EEEV), an arbovirus, is an important human and veterinary pathogen belonging to one of seven antigenic complexes in the genus *Alphavirus*, family *Togaviridae*. EEEV is considered the most deadly of the mosquito-borne alphaviruses due to the high case fatality rate associated with clinical infections, reaching as high as 75% in humans and 90% in horses (Griffin DE 2007). In patients that survive, the neurologic sequelae are often devastating. Although natural infections are acquired by mosquito bite, EEEV is also highly infectious by aerosol, making it a potential agent of bioterrorism.

Currently, there are no FDA-licensed vaccines or therapeutics for EEEV for human use. We evaluated the immunogenicity and protective efficacy of three potential second-generation inactivated EEEV vaccines in mice administered by various routes and schedules. Both formalin-inactivated CVEV1219 (fCVEV1219) and gamma-irradiated CVEV1219 (gCVEV1219) provided partial to complete protection against an aerosol challenge when administered by different routes and schedules at various doses, while INA-inactivated CVEV1219 (iCVEV1219) was unable to provide substantial protection against an aerosol challenge by any route, dose, or schedule tested. The results of these studies suggest that both fCVEV1219 and gCVEV1219 should be evaluated further and considered for advancement as potential second-generation inactivated vaccines.

Introduction

The goal of vaccine development is to produce a product that closely mimics natural infection; thereby stimulating an appropriate and effective immune response. However, new vaccine candidates for EEEV should protect against both subcutaneous and mucosal exposure to virulent virus, which can be challenging. Previous published studies with inactivated vaccine candidates for Venezuelan equine encephalitis virus (VEEV) demonstrated complete protection against a subcutaneous challenge but only partial protection against an aerosol challenge (Martin, Bakken et al. 2010; Martin, Bakken et al. 2010; Sharma, Gupta et al. 2011).

We utilized a genetically modified strain of EEEV, CVEV1219, to create three second-generation EEEV vaccine candidates. This modified-live virus is similar to V3526, the furin cleavage deletion mutant of VEEV. The PE2 domain of V3526 has been shown to be immunogenic given that monoclonal antibodies directed to this domain protected mice from lethal VEEV challenge (Parker, Buckley et al. 2010). Additionally, this vaccine candidate showed great promise in animal studies and protected against multiple serotypes of VEEV, while circumventing the vaccine interference that is often observed with alphaviruses (Hart, Caswell-Stephan et al. 2000; Hart, Lind et al. 2001). However, when it was transitioned to phase 1 human clinical trials it induced unacceptable side effects and was not further pursued.

Inactivating an attenuated-live virus provides an additional layer of safety in the formulation of the vaccine candidate. We utilized formalin, 1,5-iodonaphthylazide (INA), and gamma-irradiation to inactivate CVEV1219. Formalin has historically been used in inactivated vaccines licensed by the FDA. Although it induces cross-linking of proteins, which could affect epitope immunogenicity, it has recently been used to

successfully inactivate both V3526 (Martin, Bakken et al. 2010) and Japanese encephalitis virus (JEV) (http://www.fda.gov/BiologicsBloodVaccines/Vaccines/ApprovedProducts/ucm142577.htm 2009). INA is another chemical compound that has recently been used to inactivate enveloped viruses. It is a hydrophobic photo-reactive probe that binds to transmembrane anchors of proteins upon photo-activation with UV light (Viard, Ablan et al. 2008). Traditionally, it has been used for labeling membrane proteins and evaluating their dynamics and fusion as well as for studying protein-membrane interactions (Raviv, Salomon et al. 1987). However, with far-UV irradiation (310-360 nm), INA alkylates the transmembrane domains of viral proteins, resulting in their inactivation, while maintaining the integrity of the external domains. INA is unique in that it preserves membrane protein structural integrity and therefore is potentially useful for vaccine applications. INA has recently been used inactivate V3000 (Sharma, Raviv et al. 2007), V3526 (Sharma, Gupta et al. 2011), HIV (Raviv, Viard et al. 2005), SIV (Raviv, Viard et al. 2005), influenza virus (Raviv, Blumenthal et al. 2008), and Ebola virus (Warfield, Swenson et al. 2007). Gamma-irradiation has also been used experimentally to inactivate enveloped viruses. Gamma-irradiation inactivates viruses by generating strand-breaks in the genetic material, with little impact on the antigenic structure and biological integrity of proteins and has been used successfully to inactivate V3526 (Martin, Bakken et al. 2010) and influenza A virus (Lowy, Vavrina et al. 2001; Alsharifi, Furuya et al. 2009; Furuya, Regner et al. 2010). Therefore we inactivated CVEV1219 by each of these methods and evaluated immunogenicity and protective efficacy in mice.

Materials and Methods

CVEV1219

CVEV1219 is a chimeric virus composed of the nonstructural proteins of VEEV and the structural proteins of EEEV. In addition, the site for furin cleavage was deleted; therefore, furin is unable to cleave E2 and E3 and they are transported to the cell surface as their precursor (PE2). PE2 then forms a heterodimer with E1 and these structures then trimerize, resulting in an extra surface projection. This is a lethal mutation; however, the rescued virus contains compensatory mutations which alter the glycoprotein interactions and resuscitate the virus.

Inactivated vaccine candidates

Three inactivated CVEV1219 candidates were evaluated: formalin-inactivated CVEV1219 (fCVEV1219), INA-inactivated (iCVEV1219), and gamma-irradiated CVEV1219 (gCVEV1219). CVEV1219 was inactivated by each of these methods and residual infectivity was determined *in vitro* and *in vivo* using a multisystem approach as described previously.

IND EEEV vaccine

Control mice received the investigational new drug (IND) EEEV vaccine, which formulated from the PE6 WRAIR strain of EEEV prepared in chick embryo tissue (The Salk Institute, Government Services Division, Swiftwater, PA). This vaccine was prepared by inactivation with formaldehyde and neutralized with sodium bisulfite. Neomycin sulfate equivalent to 50 µg/ml, neomycin base, and 0.25% human serum

albumin were added. The vaccine was dried and stored at -20°C until use. For use, the vaccine was reconstituted with 3 ml of sterile water and mice were given 0.5 ml subcutaneously (4 µg) as per manufacturer's instructions.

Mice

Specific pathogen free 6-8-week-old female BALB/c mice (NCI, Frederick, MD) were housed in cages equipped with microisolators and were provided food and water *ad libitum* throughout the study. The room temperature was 23 $\pm$ 1°C and periods of light and dark were maintained on a 12 h cycle. Mice were acclimated for 1 week before vaccination. Mice were observed daily and weighed every other day for 14 d post-vaccination. Three weeks after vaccination, mice were anesthetized by inhalation of Isoflurane (Webster Veterinary, Devens, MA) using the IMPAC^{6} (VetEquip, Pleasanton, CA) and bled from the retroorbital sinus. One to two days later, vaginal flushes were obtained as previously described (Hart, Pratt et al. 1997). Mice were restrained and douched with 100 µL of PBS. Both serum and vaginal flush samples were individually collected and stored at -80°C for further analysis.

For the portions of the study involving challenge of mice with wild type EEEV, mice were housed in a biosafety level 3 (BSL-3) facility. Research was conducted at the United States Army Medical Research Institute of Infectious Diseases (USAMRIID) under an IACUC approved protocol in compliance with the Animal Welfare Act and other Federal statutes and regulations relating to animals and experiments involving animals and adheres to principles stated in the Guide for the Care and Use of Laboratory

Animals, National Research Council, 1996. The facility is fully accredited by the Association for Assessment and Accreditation of Laboratory Animal Care International.

Vaccinations

In the first study, mice were vaccinated intranasally (IN), intramuscularly (IM) or subcutaneously (SC) with 0.1-5 µg of inactivated EEEV (iEEEV) vaccine candidate: CVEV1219 inactivated by formalin (fCVEV1219), INA (iCVEV1219), or gamma-irradiation (gCVEV1219) (Table 4.1). All mice were vaccinated on d0. Half of the mice received a second vaccination of equal dose on d28, while the other half of the mice were challenged by the aerosol route. Those mice that received a second vaccination were challenged 28d after the final vaccination. One group of control mice received the investigational new drug (IND) EEEV vaccine, following the manufacturer's instructions (4 µg per dose, on d0 and d28, subcutaneously), and were challenge by aerosol 28 d after the final vaccination.

In the second study, mice were vaccinated with 3 µg intranasally (IN), 5 µg subcutaneously (SC), or 1 µg intramuscularly (IM) with fCVEV1219 (Table 4.4). All mice were vaccinated on d0 and then half of the mice were challenged by aerosol on d63, while the other half of the mice received a second vaccination on d56 and were challenged 28d after the final vaccination.

Enzyme-linked immunosorbent assay (ELISA)

Optimum viral and antibody concentrations were determined by checkerboard titration, in which an ELISA was performed using varying concentrations of both the

viral antigen and each of the primary antibodies. Serum and vaginal flush antibody responses to the vaccine candidates were then evaluated by ELISA as previously described (Hart, Pratt et al. 1997; Hart, Caswell-Stephan et al. 2000; Martin, Bakken et al. 2010). Briefly, Costar EIA/RIA 96-well high-binding plates (Corning Inc., Corning, NY) were coated with 0.2 μg of sucrose purified EEEV strain FL93-939 per well and incubated overnight, or up to 1 week, at 4°C. The following day, plates were blocked with Dulbecco's phosphate buffered saline (DPBS) (GIBCO^{TM} Invitrogen Corp., Grand Island, NY) containing 0.05% Tween 20 (Sigma-Aldrick, St. Louis, MO) and 5% nonfat dry milk (Becton Dickinson and Co., Sparks, MD) (PBSTM) for 2 hours at 37°C. The plates were washed 3 times with PBST using the BioTek ELx405^{TM} microplate washer (BioTek Instruments, Inc., Winooski, VT). Mouse sera were diluted in PBSTM containing 1% heat inactivated fetal bovine serum (GIBCO^{TM} Invitrogen Corp., Grand Island, NY), added to the plate and serially diluted 1:2 and then incubated for 1-2 hours at 37°C. Plates were washed 3 times with PBST followed by the addition of one of five peroxidase-labeled goat anti-mouse Ig (IgG 1:50,000; IgG1 1:50,000; IgG2a 1:100,000; IgG2b 1:10,000; IgA 1:10,000) (Bethyl Laboratories, Inc., Montgomery, TX). The plates were incubated with the secondary antibody for 1 hr at 37°C and then washed 3 times with PBST. The ABST Peroxidase substrate (KPL, Gaithersburg, MD) was added to each well and color developed for approximately 20-30 min at which time the optical density (OD) at 410 nm was determined using a Spectramax M5 microplate reader (Molecular Devices, Sunnyvale, CA). Endpoint titers were determined as the highest two-fold dilution that produced an OD greater than the mean OD of the negative controls wells plus 3 standard deviations.

Plaque-reduction neutralization test (PRNT)

Virus-neutralizing antibody responses were titrated as previously described (Hart, Caswell-Stephan et al. 2000). Briefly, sera were serially diluted two-fold in Hank's Balanced Salt Solution (HBSS) containing HEPES red (USAMRIID, Fort Detrick, MD) and 2% FPB and incubated overnight with virus. The serum-virus mixture was then added in duplicate to 6-well plates containing a confluent monolayer of Vero cells (African green monkey kidney cells). Plates were incubated at 37°C for 1 hour, with rocking every 15 min. Following the incubation period, wells were overlaid with 0.5% agarose in EBME media (USAMRIID, Fort Detrick, MD) containing HEPES and 10% FBS, 1% L-glutamine, 1% NEAA, 1% penicillin-streptomycin sulfate, and 0.1% gentamicin was added, and plates were incubated at 37°C at 5% CO_2 for 24 hr. Thereafter, cells were stained by the addition of a second agarose overlay prepared as above containing 5% neutral red. The plates were incubated at 37°C at 5% CO_2 for 24 hr. Defined plaques (neutral red exclusion areas) were counted. The endpoint titer was determined to be the highest dilution with an 80% or greater reduction (PRNT 80) of the number of plaques observed in control wells.

Challenge Virus

EEEV strain FL93-939 sucrose purified working stock was prepared from seed stock through one passage in Vero cells as previously described. Virus titer was determined by standard plaque assay on Vero cell monolayers. Challenge virus was diluted in Eagle's minimum essential medium (EMEM) (USAMRIID, Fort Detrick, MD).

Aerosol Challenge

Aerosol exposures were conducted in a whole-body bioaerosol exposure system. A Collison nebulizer (BGI, Inc., Waltham, MA) was used to generate small (1μm mass median aerodynamic diameter) diameter particles for each acute 10 min exposure. Briefly, mice were place in wire cages, which were then placed into a chamber where they were exposed to aerosolized virus for 10 min. The 'presented' dose was estimated by calculating the respiratory minute volume (V_m) using Guyton's formula (Guyton 1947), expressed as $Vm = 2.10 \text{ x } W_b^{0.75}$ where W_b = body weight (gm) based on the average group weights the day of exposure. The presented dose was then calculated by multiplying the estimated total volume (V_t) of experimental atmosphere inhaled by each animal ($V_t = V_m$ x length of exposure) by the empirically determined exposure concentration (C_e) ('presented dose' = C_e x V_t). Exposure concentration, expressed in plaque-forming units (PFU)/L, was determined by isokinetic sampling of the chamber with an all-glass impinger (AGI) (Ace Glass, Vineland, NJ). AGI samples were titrated by standard plaque assay on Vero cell monolayers (Roy, Reed et al. 2009). Back titration of challenge virus preparations were determined by standard plaque assay using Vero cells.

Statistics

Fisher's exact tests with stepdown Bonferroni adjustment was used to compare survival rates. Logistic regression of survival by log_{10}-transformed immune response factors with backward elimination to select a set of statistically-significant covariates from among the covariates (vaccine candidate, dose, route, and schedule) was used to

determine odds ratios. Logistic regression by probit analysis of survival status by immune response factor was used to predict $\log_{10}$-transformed immune response factors that would yield a probability of survival of 90% and 99%.

Results

In the first study mice were vaccinated and challenged as described in Table 4.1, with one of three iEEEV vaccine candidates, formalin-inactivated CVEV1219 (fCVEV1219), INA-inactivated CVEV1219 (iCVEV1219), or gamma-irradiated CVEV1219 (gCVEV1219) at doses ranging from 5-0.1 μg by the IN, IM or SC route. Mice were monitored for weight loss and clinical illness for 14 days post-vaccination. While all groups lost a small amount of weight, less than 2%, 1 day post-vaccination, all groups quickly recovered and weighed more than their original weight by 3 days post-infection (dpi) (data not shown).

Animals were given 1 or 2 doses of an iEEEV vaccine candidate and were challenged by aerosol 28 days after the last vaccination. Generally, animals that were vaccinated by the IN route but were not protected against an aerosol challenge, clinical signs of disease and weight loss began at 3-4 dpi regardless of vaccine candidate, dose, or schedule (Figures 4.1-4.3). However, animals that were vaccinated by the IM route but were not protected against an aerosol challenge, clinical signs of disease and weight loss began at 2-3 dpi (Figures 4.4-4.6). In those animals that were vaccinated by the SC route but were not protected against an aerosol challenge, the onset of clinical signs of disease was more variable and occurred between 2-5 dpi (Figures 4.7-4.9). Overall, the majority of animals in which clinical signs of disease were observed succumbed to infection or were euthanized; however, a small percentage of animals in which minimal clinical signs,

Table 4.1. Study design for first study evaluating iEEEV candidates

Group	Dose	Route	Vaccination Schedule	Bleed, VF Schedule	Aerosol Challenge	# Mice
1	5 µg iEEEV	IM, SC, IN	D0	D21	D28	10
2	3 µg iEEEV	IM, SC, IN	D0	D21	D28	10
3	1 µg iEEEV	IM, SC, IN	D0	D21	D28	10
4	0.1 µg iEEEV	IM, SC, IN	D0	D21	D28	10
5	Sterile Saline	IM, SC, IN	D0	D21	D28	10
6	5 µg iEEEV	IM, SC, IN	D0, D28	D21, D49	D56	10
7	3 µg iEEEV	IM, SC, IN	D0, D28	D21, D49	D56	10
8	1 µg iEEEV	IM, SC, IN	D0, D28	D21, D49	D56	10
9	0.1 µg iEEEV	IM, SC, IN	D0, D28	D21, D49	D56	10
10	Sterile saline	IM, SC, IN	D0, D28	D21, D49	D56	10
11	EEEV IND	SC	D0, D28	D21, D49	D56	10

Table 4.1. Mice were vaccinated with one of three inactivated EEEV (iEEEV) vaccine candidates, formalin-inactivated CVEV1219 (fCVEV1219), INA-inactivated CVEV1219 (iCVEV1219), or gamma-irradiated CVEV1219 (gCVEV1219) according to the dose, route, and schedule listed. Serum and vaginal flush samples were collected 21 d after each vaccination. Mice were challenged with EEEV strain FL93-939 by aerosol 28 d after the last vaccination.

such as ruffled fur, were observed made a full recovery. Onset of clinical disease in saline control mice in each group was between 2-4 dpi, while the EEEV IND vaccine control mice showed signs of disease at 3 dpi. One animal in this group became sick, but recovered (Figure 4.9).

In mice given a single IN vaccination, only fCVEV1219 provided statistically significant partial protection against an aerosol challenge at the 3 µg dose (70%) (p=0.031), while both iCVEV1219 and gCVEV1219 provided no protection regardless of dose (Figure 4.10A, dark bars). In mice given two IN vaccinations, fCVEV1219 provided 90-100% protection against an aerosol challenge at the 1 µg dose or higher. However, both iCVEV1219 and gCVEV1219 did not provide significant partial
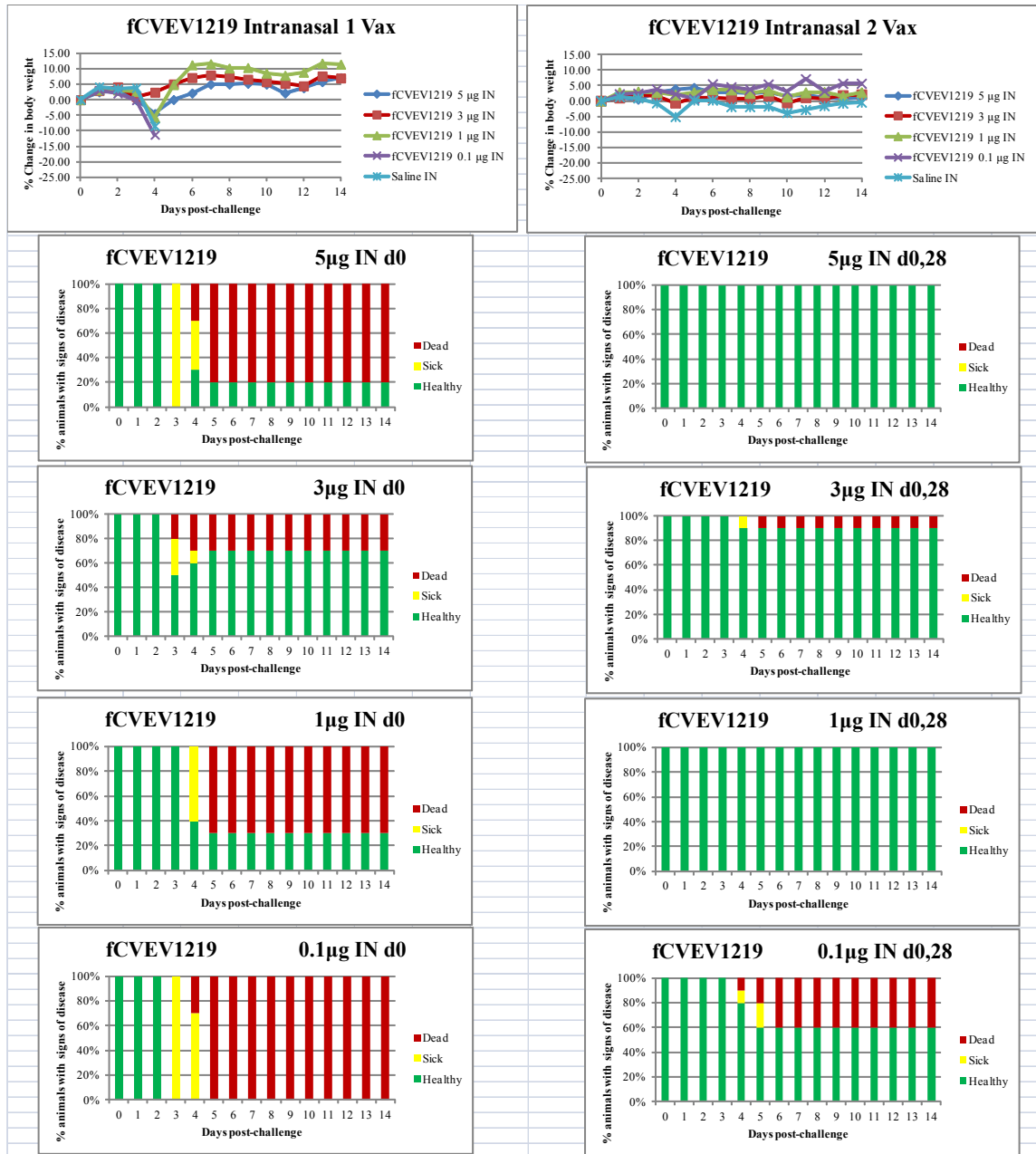
Figure 4.1. Percent change in body weight and onset of clinical signs in mice vaccinated with formalin-inactivated CVEV1219 (fCVEV1219) by the intranasal (IN) route with doses ranging from 5-0.1 µg. Mice received either a single vaccination on d0 and then were challenged on d28 or they received vaccinations on d0 and d28 and were challenged on d56. Mice were monitored for 28 d post-aerosol challenge; however, no changes were noted after 14 d.
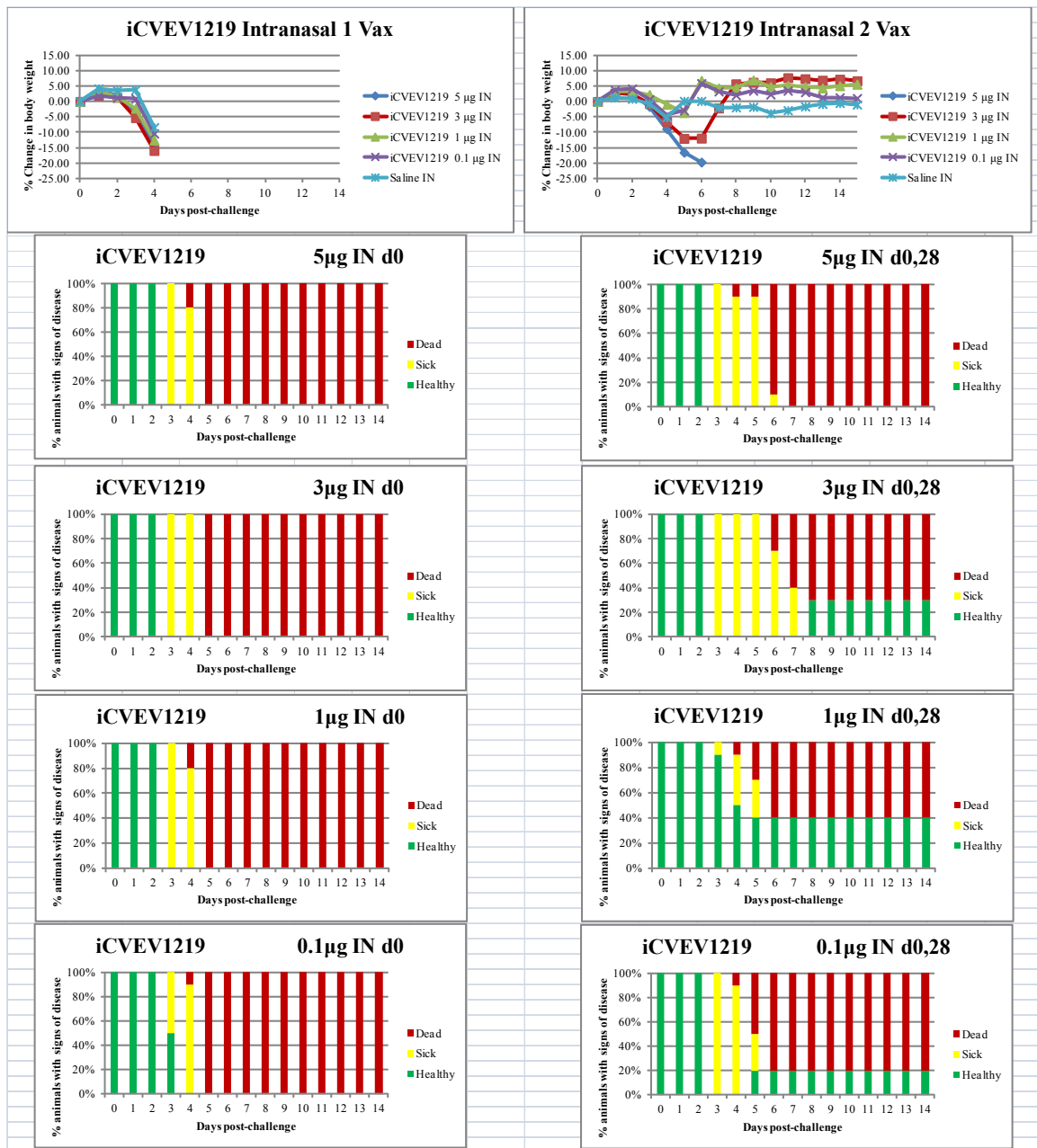
Figure 4.2. Percent change in body weight and onset of clinical signs in mice vaccinated with INA-inactivated CVEV1219 (iCVEV1219) by the intranasal (IN) route with doses ranging from 5-0.1 µg. Mice received either a single vaccination on d0 and then were challenged on d28 or they received vaccinations on d0 and d28 and were challenged on d56. Mice were monitored for 28 d post-aerosol challenge; however, no changes were noted after 14 d.
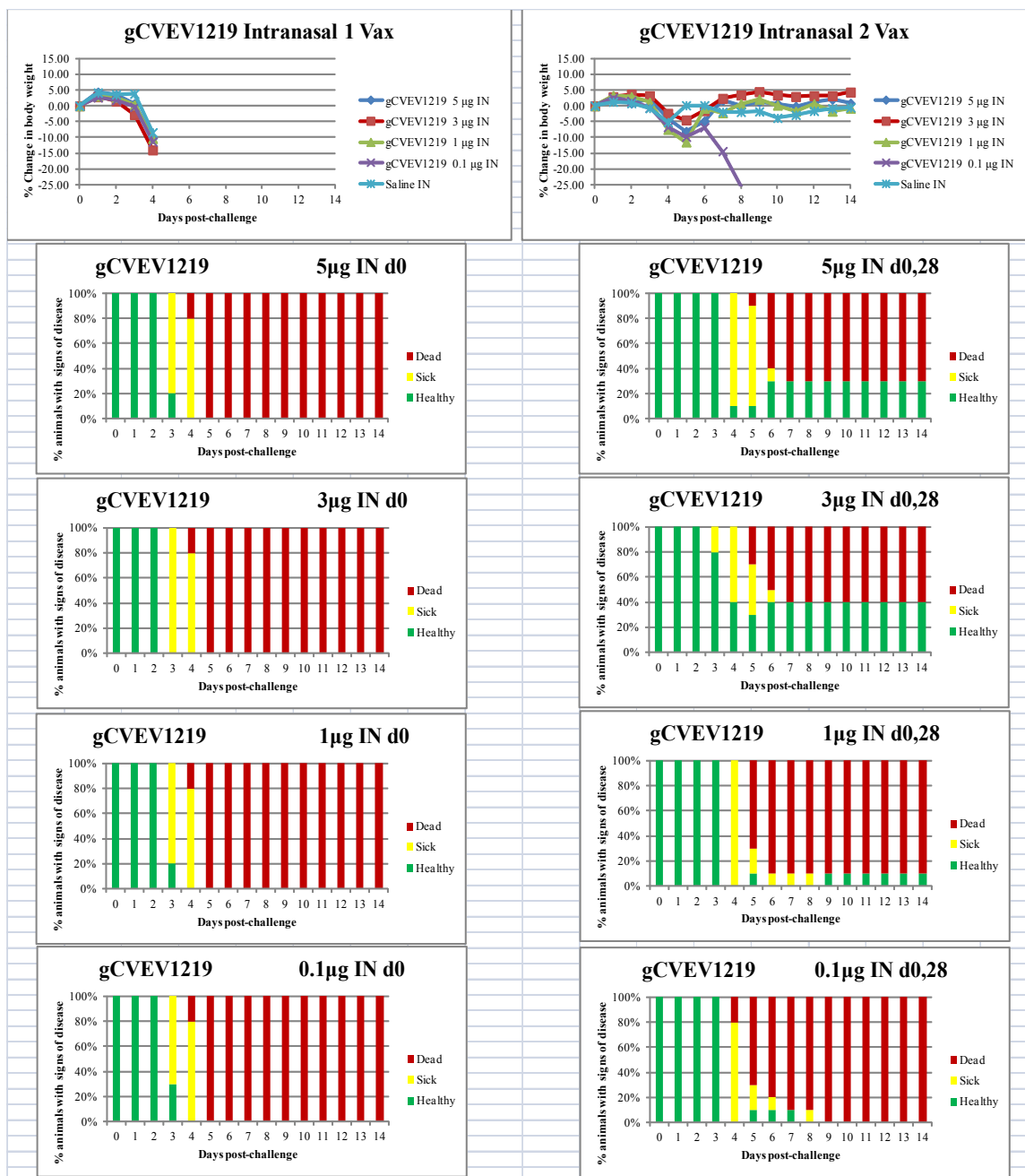
Figure 4.3. Percent change in body weight and onset of clinical signs in mice vaccinated with gamma-irradiated CVEV1219 (gCVEV1219) by the intranasal (IN) route with doses ranging from 5-0.1 µg. Mice received either a single vaccination on d0 and then were challenged on d28 or they received vaccinations on d0 and d28 and were challenged on d56. Mice were monitored for 28 d post-aerosol challenge; however, no changes were noted after 14 d.
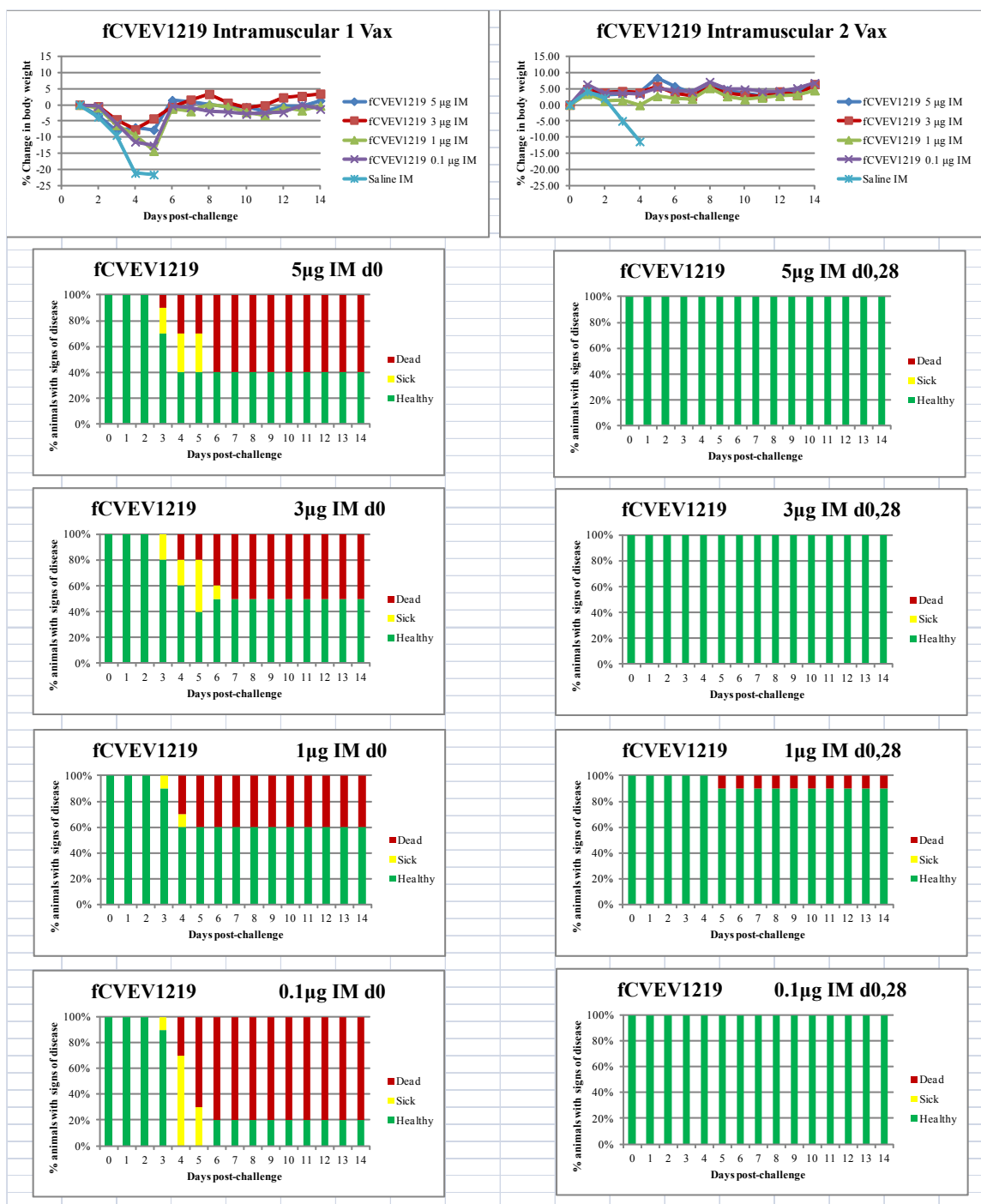
Figure 4.4. Percent change in body weight and onset of clinical signs in mice vaccinated with formalin-inactivated CVEV1219 (fCVEV1219) by the intramuscular (IM) route with doses ranging from 5-0.1 μg. Mice received either a single vaccination on d0 and then were challenged on d28 or they received vaccinations on d0 and d28 and were challenged on d56. Mice were monitored for 28 d post-aerosol challenge; however, no changes were noted after 14 d.
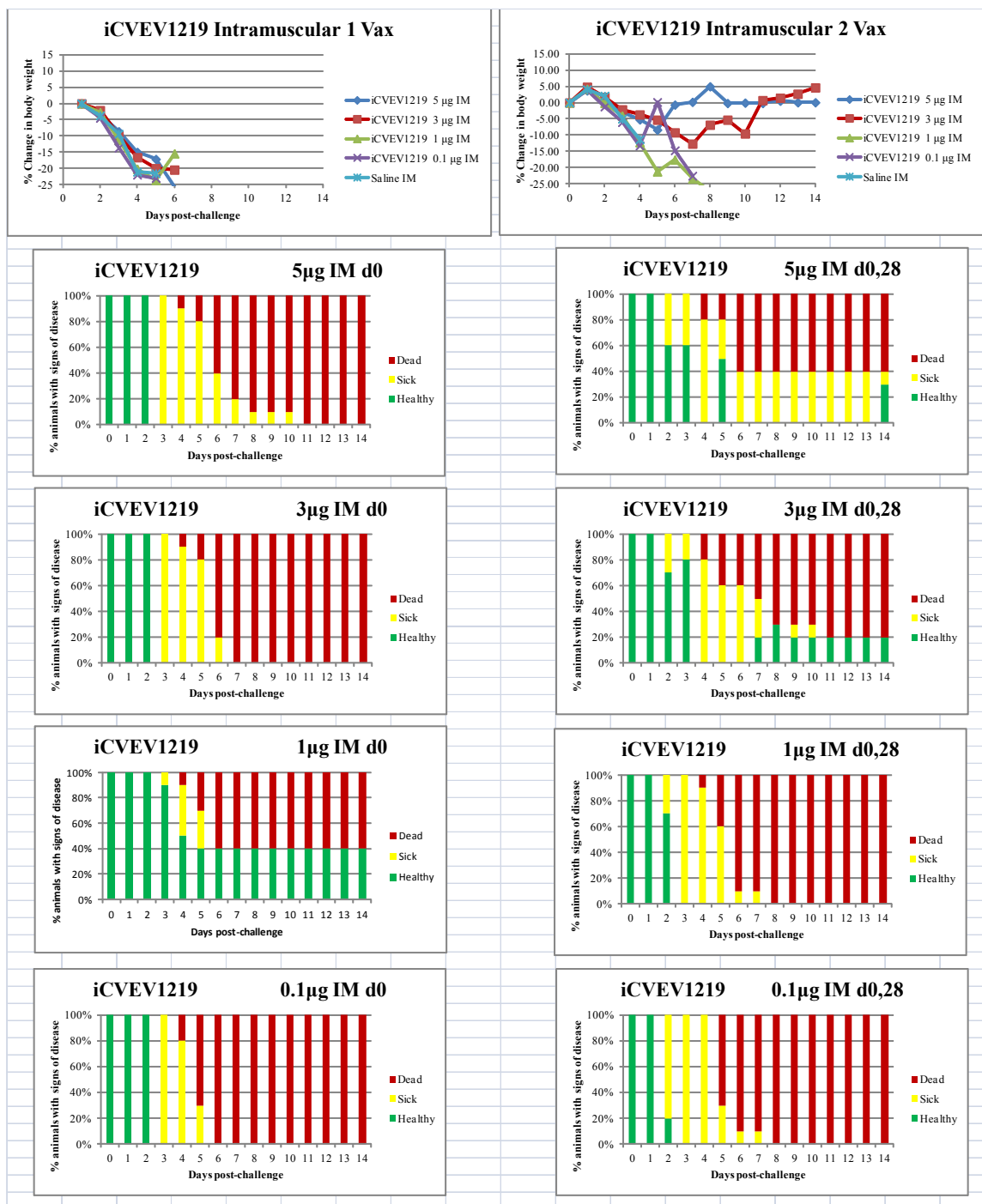
Figure 4.5. Percent change in body weight and onset of clinical signs in mice vaccinated with INA-inactivated CVEV1219 (iCVEV1219) by the intramuscular (IM) route with doses ranging from 5-0.1 µg. Mice received either a single vaccination on d0 and then were challenged on d28 or they received vaccinations on d0 and d28 and were challenged on d56. Mice were monitored for 28 d post-aerosol challenge; however, no changes were noted after 14 d.
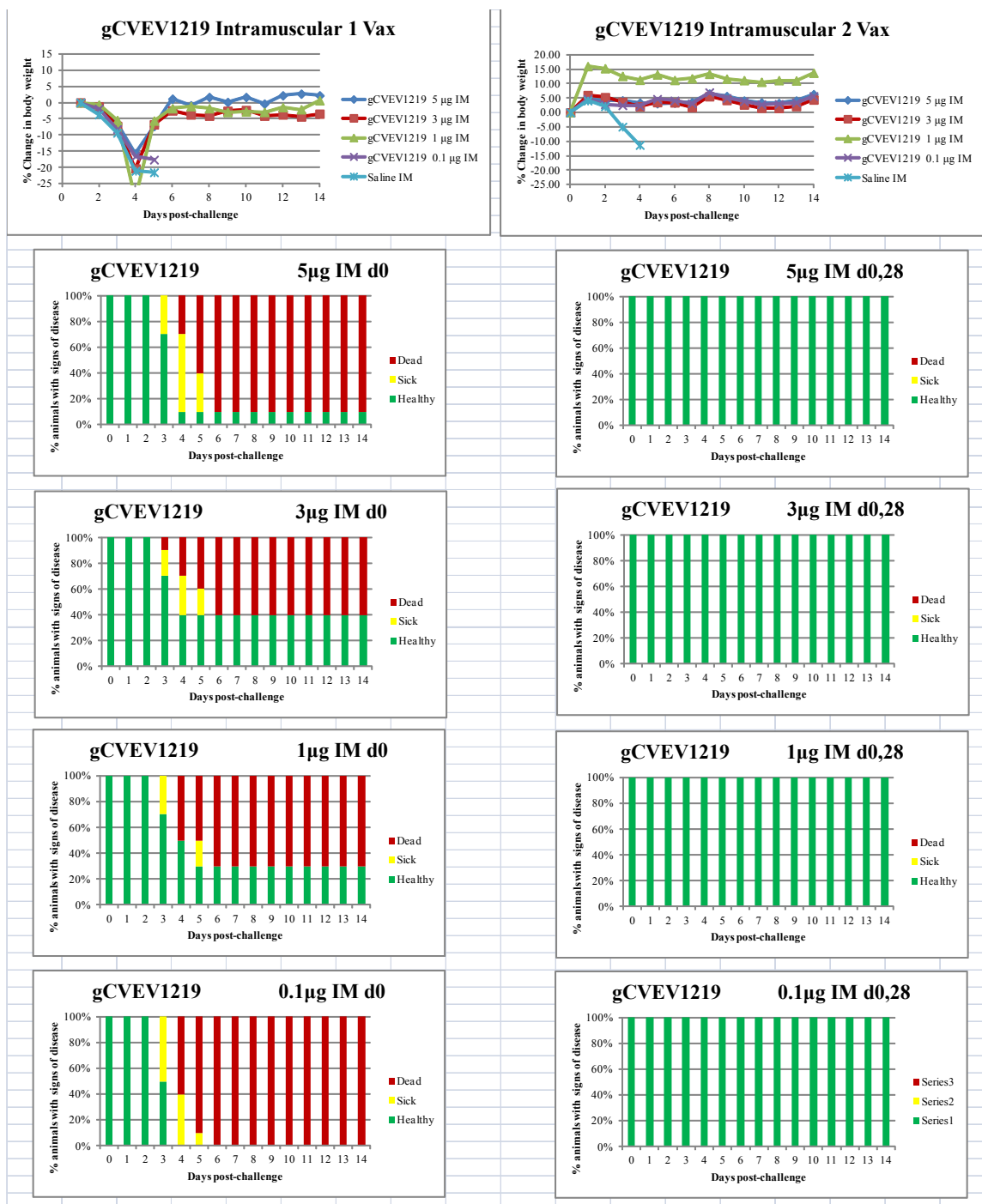
Figure 4.6. Percent change in body weight and onset of clinical signs in mice vaccinated with gamma-irradiated CVEV1219 (gCVEV1219) by the intramuscular (IM) route with doses ranging from 5-0.1 µg. Mice received either a single vaccination on d0 and then were challenged on d28 or they received vaccinations on d0 and d28 and were challenged on d56. Mice were monitored for 28 d post-aerosol challenge; however, no changes were noted after 14 d.
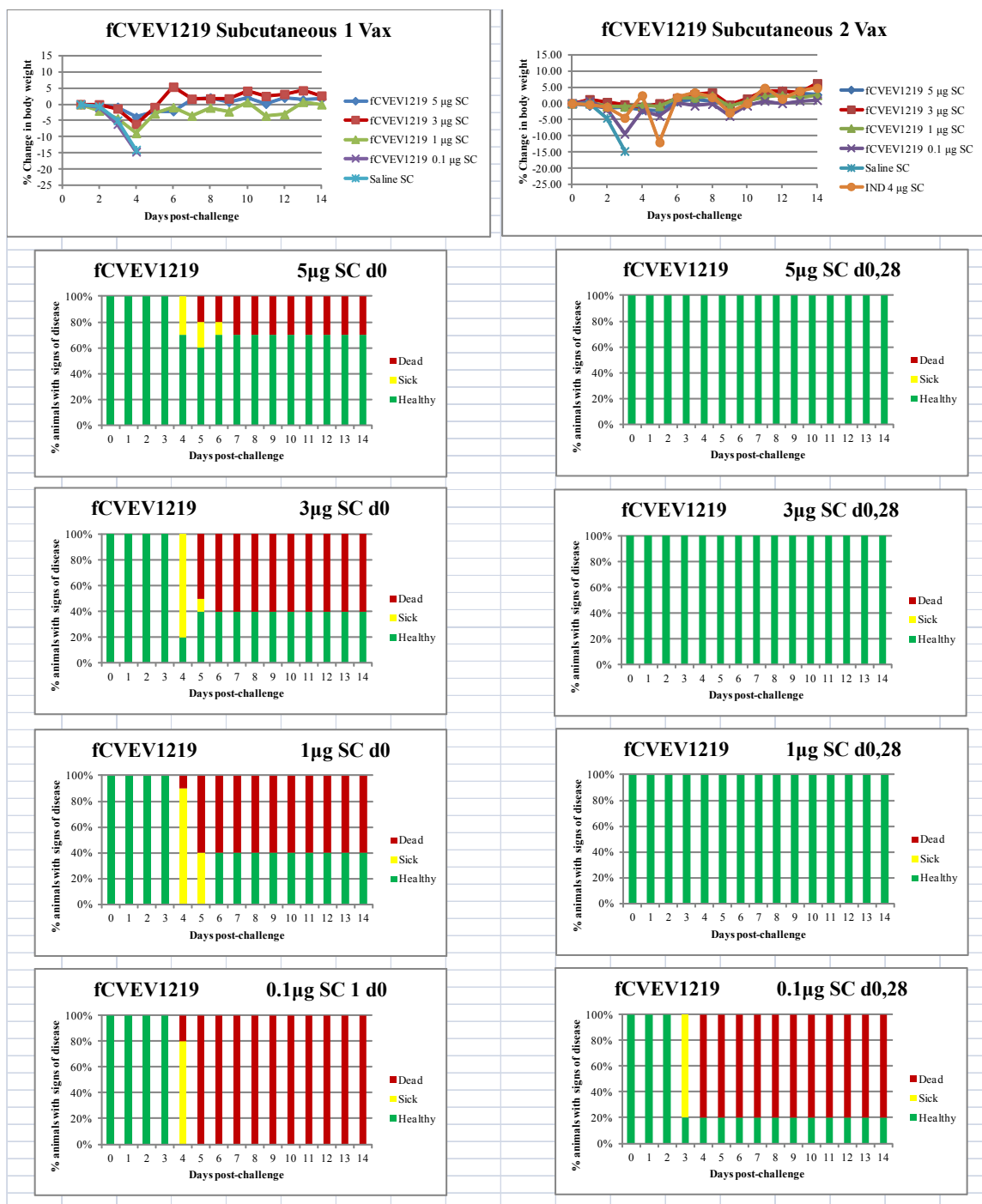
Figure 4.7. Percent change in body weight and onset of clinical signs in mice vaccinated with formalin-inactivated CVEV1219 (fCVEV1219) by the subcutaneous (SC) route with doses ranging from 5-0.1 µg. Mice received either a single vaccination on d0 and then were challenged on d28 or they received vaccinations on d0 and d28 and were challenged on d56. Mice were monitored for 28 d post-aerosol challenge; however, no changes were noted after 14 d.
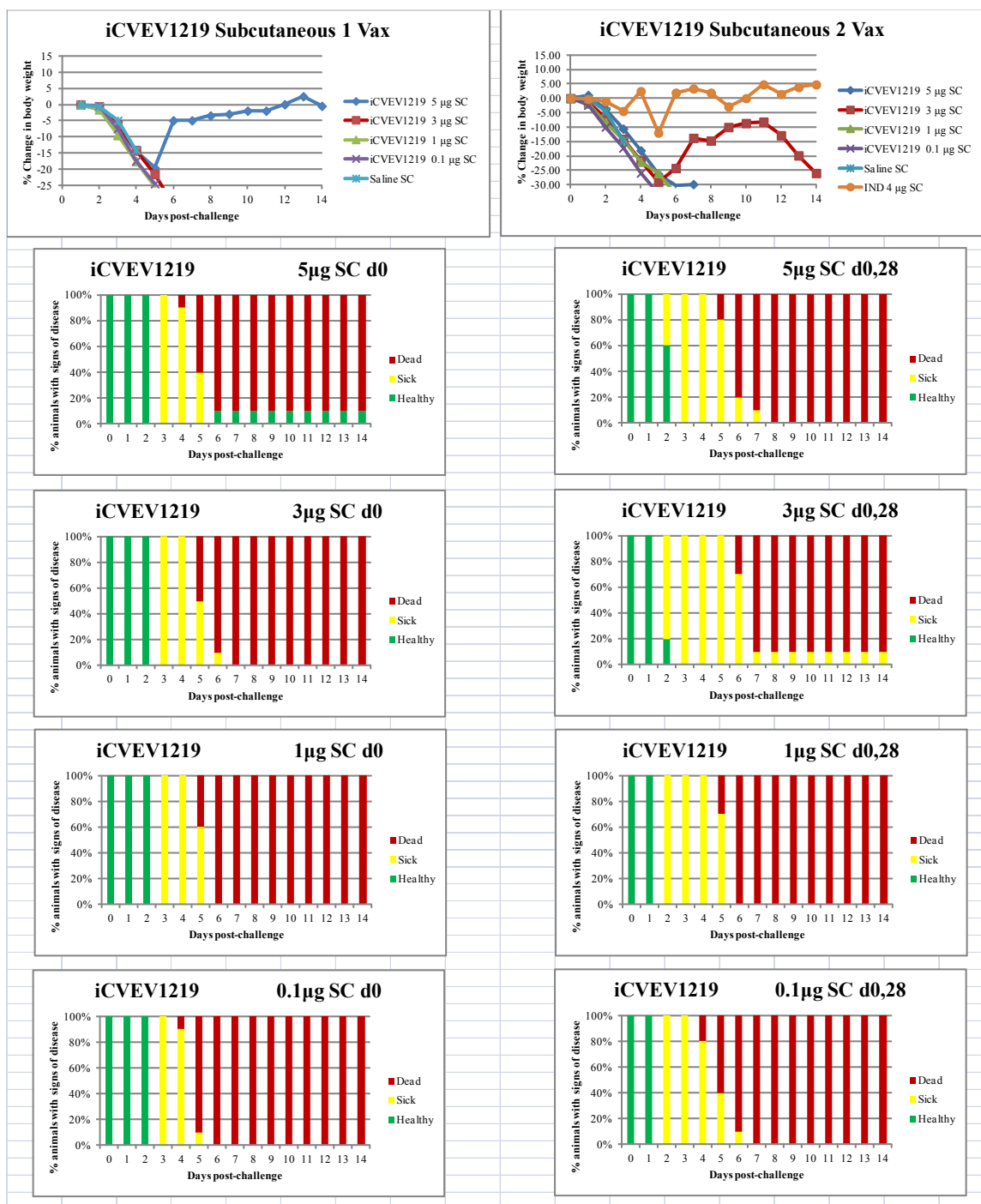
Figure 4.8. Percent change in body weight and onset of clinical signs in mice vaccinated with INA-inactivated CVEV1219 (iCVEV1219) by the subcutaneous (SC) route with doses ranging from 5-0.1 µg. Mice received either a single vaccination on d0 and then were challenged on d28 or they received vaccinations on d0 and d28 and were challenged on d56. Mice were monitored for 28 d post-aerosol challenge; however, no changes were noted after 14 d.
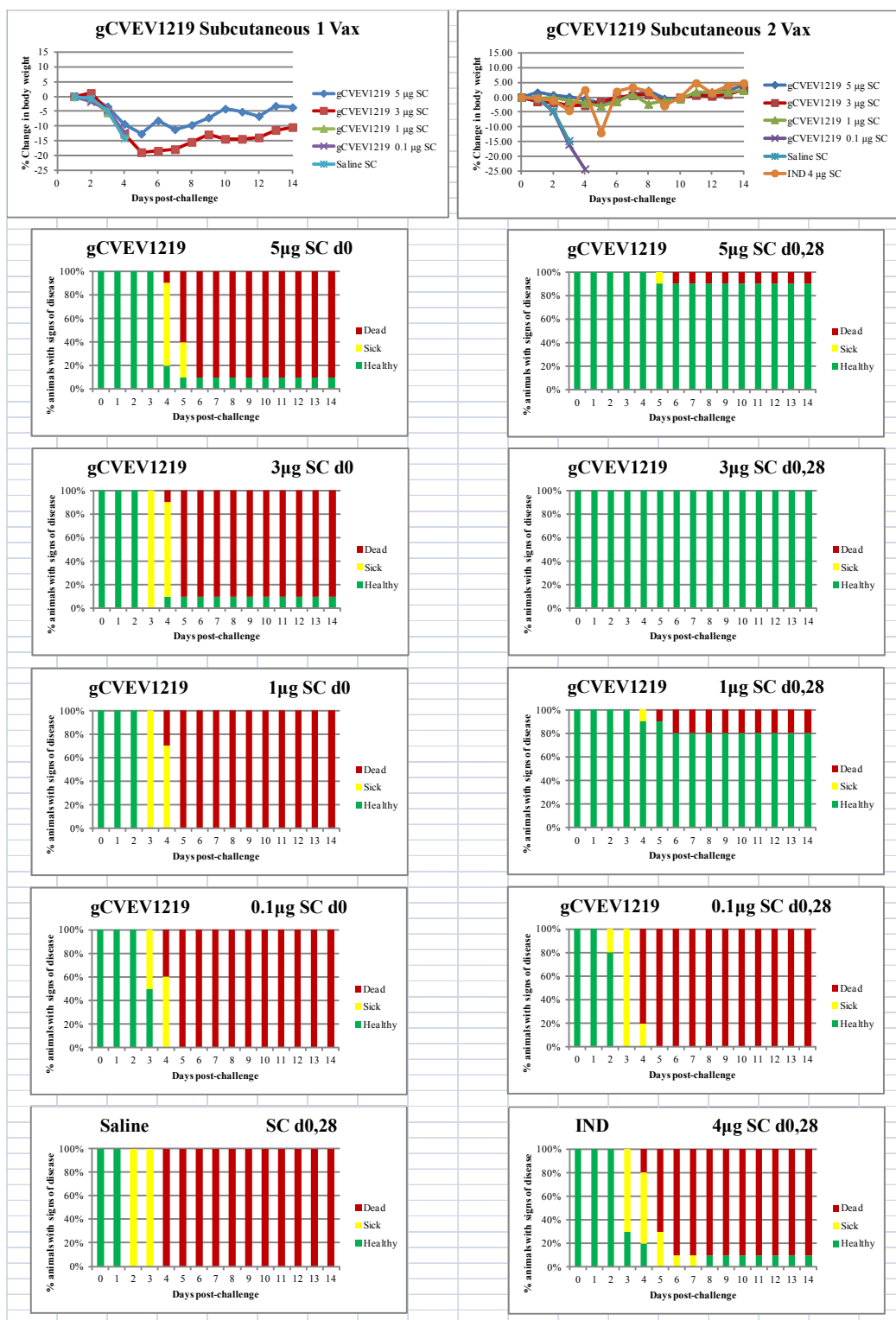
Figure 4.9. Percent change in body weight and onset of clinical signs in mice vaccinated with gamma-irradiated CVEV1219 (gCVEV1219) by the subcutaneous (SC) route with doses ranging from 5-0.1 µg. Mice received either a single vaccination on d0 and then were challenged on d28 or they received vaccinations on d0 and d28 and were challenged on d56. Mice were monitored for 28 d post-aerosol challenge; however, no changes were noted after 14 d.

protection at any dose (Figure 4.10A, light bars). For unknown reasons, 3/10 control

mice challenged on d56 survived aerosol challenge; however, fCVEV1219 groups which

were completely protected (5 µg and 1 µg doses) were still statistically significant

(p=0.031), using the Fisher's exact tests with stepdown Bonferroni adjustment for

multiple comparisons. Additionally, statistically significant differences in survival rates

were noted between mice that received 1 vaccination and mice that received two

vaccinations of fCVEV1219 IN at the 5, 1, and 0.1 µg doses (p<0.05). When comparing

the IN vaccination regime to the standard EEEV IND regime (2 doses, 4 µg per dose,

SC), the mice given fCVEV1219 in a 2 dose regime at 5, 3, or 1µg dose had statistically

higher survival rates than the mice that received the EEEV IND vaccine (p<0.05).

In mice given a single IM vaccination, both fCVEV1219 and gCVEV1219 provided

partial protection (30-60%) against aerosol challenge at multiple doses, but the level of

protection was not statistically significant (Figure 4.10B, dark bars). However, both

fCVEV1219 and gCVEV1219 provided 100% protection against aerosol challenge at

multiple doses when given in a two dose regimen (p<0.001) (Figure 4.10B, light bars).

iCVEV1219 was unable to provide significant protection in either the one or two dose

regimens. Statistically significant differences in survival rates were noted between mice

that received 1 vaccination and mice that received two vaccinations of either fCVEV1219

at the 5, 3, or 0.1 µg doses or gCVEV1219 at the 5, 3, 1, and 0.1 µg doses (p<0.05).

When comparing the IM vaccination regime to the standard EEEV IND regime (2 doses,

4 µg per dose, SC), the mice given fCVEV1219 or gCVEV1219 in a 2 dose regime at all

doses had statistically higher survival rates than the mice that received the EEEV IND

vaccine (p<0.05).

A.

B.

C.
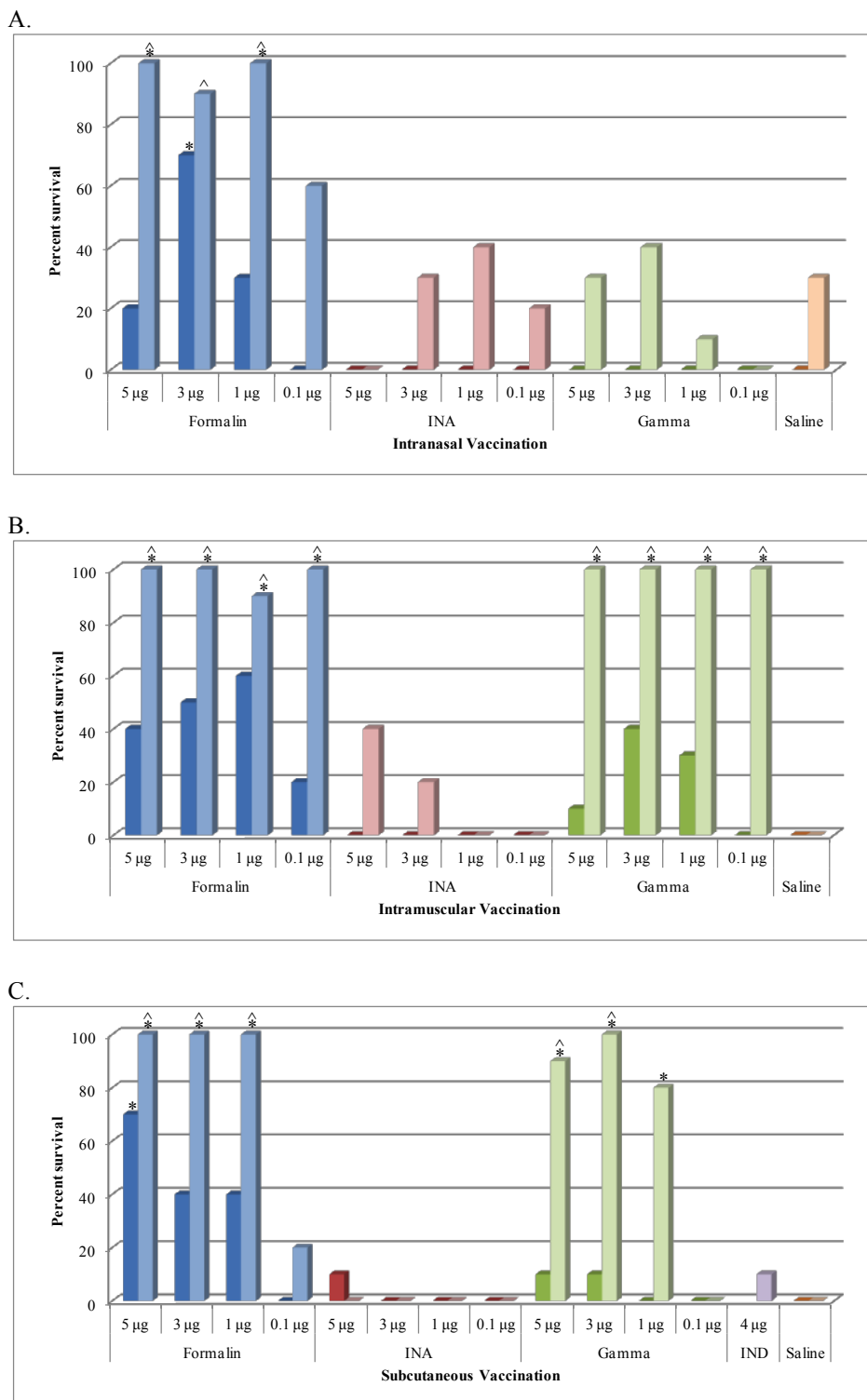
Figure 4.10. Protective efficacy of iEEEV vaccine candidates. Groups of BALB/c mice (n=10) were administered one (dark bars) or two doses (light bars) of iEEEV vaccine candidate at doses ranging from 5-0.1µg by IN, IM, or SC routes. Mice were challenged by aerosol with at least $100LD_{50}$ of EEEV strain FL93-939, 28 days after the final vaccination, and were monitored for 28 days for mortality and clinical signs of disease (* p-value <0.05 for pairwise comparison to saline group; ^ p-value<0.05 for pairwise comparison to IND vaccine group)

In mice given a single SC vaccination, only fCVEV1219 at the highest dose (5 µg) provided significant partial protection against an aerosol challenge (p=0.031) when compared to saline controls (Figure 4.1C, dark bars), while all other doses of fCVEV1219 and all doses of iCVEV1219 and gCVEV1219 did not. However, both fCVEV1219 and gCVEV1219 provided 100% protection at multiple doses when given in a two dose regime (p=0.001) (Figure 4.1C, light bars). Statistically significant differences in survival rates were also noted between those mice that received 1 vaccination and mice that received two vaccinations of either fCVEV1219 at the 1 and 3 µg doses or gCVEV1219 at the 5, 3, and 1 µg doses (p<0.01). When comparing the SC vaccination regime to the standard EEEV IND regime (2 doses, 4 µg per dose, SC), the mice given fCVEV1219 at the 5, 3, or 1 µg dose or gCVEV1219 at the 5 and 3 µg dose in a 2 dose regime had statistically higher survival rates than the mice that received the EEEV IND vaccine (p<0.05).

Neutralizing antibody responses and virus specific serum antibody levels were determined for all groups vaccinated once or twice the iEEEV vaccine candidates at doses ranging from 5-0.1 µg by the IN, IM, or SC routes. Neutralizing antibody responses as well as all immunoglobulins measured were greater after the second vaccination regardless of vaccine candidate, dose or method of inactivation (Figures 4.11-4.13). Levels of serum neutralizing antibody appeared to correlate with survival, while serum levels of virus-specific IgG appeared more similar within a given route and schedule regardless of inactivation method.
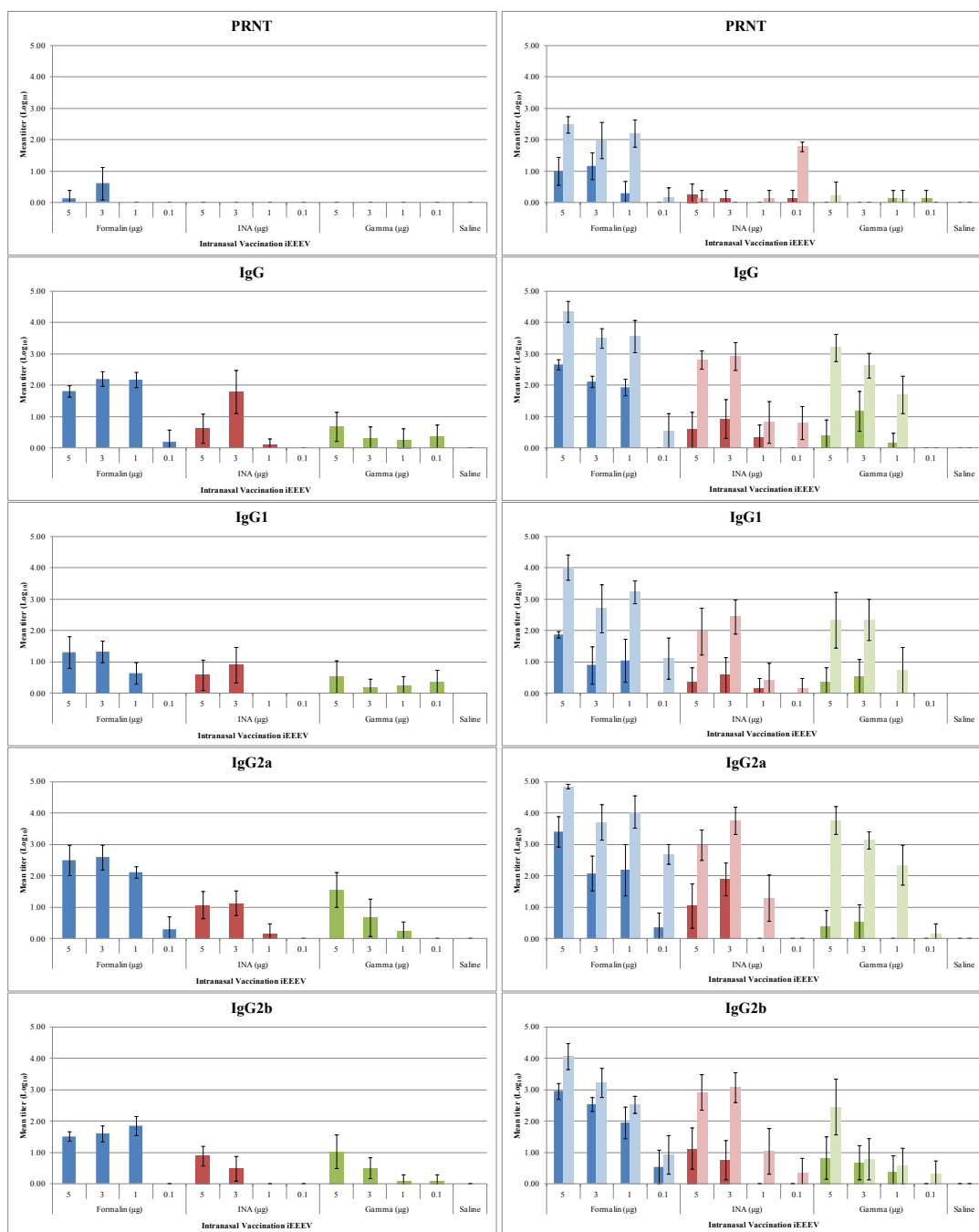
Figure 4.11. Serum antibody responses in mice vaccinated intranasally with iEEEV vaccine candidates. Groups of BALB/c mice (n=10) were vaccinated once (graphs on left) or twice (graphs on right) with one of three iEEEV vaccine candidates (formalin-inactivated, INA-inactivated, or gamma irradiated) at doses ranging from 5-0.1µg by the IN route. Serum was collected 21 d after each vaccination. Neutralizing antibody responses were determined by PRNT and serum antibody levels were determined by ELISA. In all graphs, dark bars represent the mean group titer 21 d after the first vaccination (n=10); light bars represent the mean group titer 21 d after the second vaccination (n=10). Standard error bars represent 2 times the SE of the mean (SE=SDxsqrt(n)).

Figure 4.12. Serum antibody responses in mice vaccinated intramuscularly with iEEEV vaccine candidates. Groups of BALB/c mice (n=10) were vaccinated once (graphs on left) or twice (graphs on right) with one of three iEEEV vaccine candidates (formalin-inactivated, INA-inactivated, or gamma irradiated) at doses ranging from 5-0.1µg by the IM route. Serum was collected 21 d after each vaccination. Neutralizing antibody responses were determined by PRNT and serum antibody levels were determined by ELISA. In all graphs, dark bars represent the mean group titer 21 d after the first vaccination (n=10); light bars represent the mean group titer 21 d after the second vaccination (n=10). Standard error bars represent 2 times the SE of the mean (SE=SDxsqrt(n)).
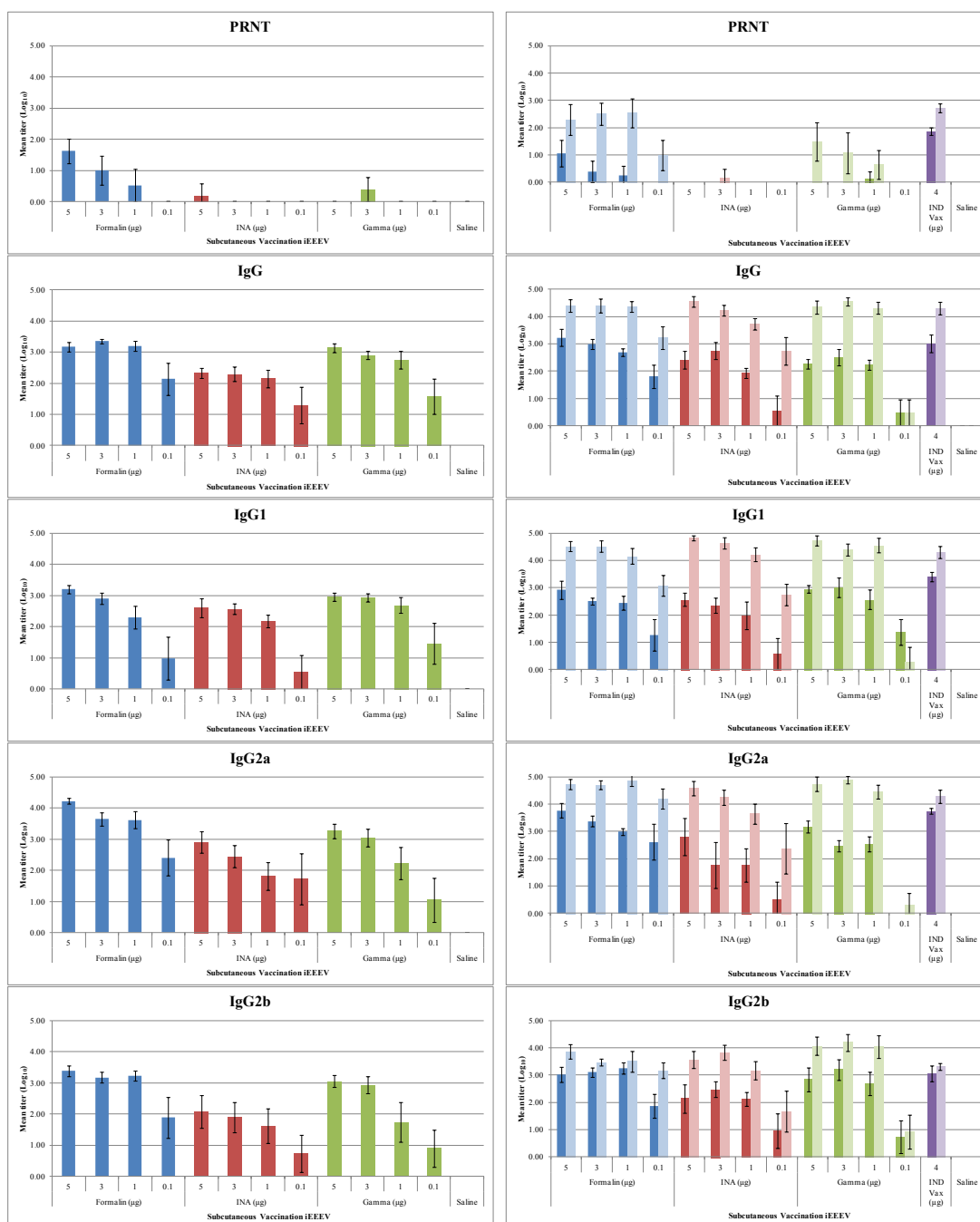
Figure 4.13. Serum antibody responses in mice vaccinated subcutaneously with iEEEV vaccine candidates. Groups of BALB/c mice (n=10) were vaccinated once (graphs on left) or twice (graphs on right) with one of three iEEEV vaccine candidates (formalin-inactivated, INA-inactivated, or gamma irradiated) at doses ranging from 5-0.1μg by the SC route. Serum was collected 21 d after each vaccination. Neutralizing antibody responses were determined by PRNT and serum antibody levels were determined by ELISA. In all graphs, dark bars represent the mean group titer 21 d after the first vaccination (n=10); light bars represent the mean group titer 21 d after the second vaccination (n=10). Standard error bars represent 2 times the SE of the mean (SE=SDxsqrt(n)).

Logistic regression was utilized to assess whether there was a significant increase in odds of survival for each unit increase in immune response factor. Table 4.2 contains the overall odds ratio for the odds of survival for each unit increase in immune response factor, the 95% confidence limits for the odds ratio, and p-value for each immune response parameter. For example, taking into account all methods of inactivation, routes of inoculation, and doses, for every unit increase (a ten-fold increase in titer) in serum neutralizing antibody immune response as measured by the PRNT after 2 vaccinations (at day 56) the animal would have over a 4-fold increase in odds of surviving an aerosol exposure; whereas, in the same animals, an increase in each unit of IgG, IgG2a or IgG2b would expect to increase the odds of survival by approximately 2-fold.

Logistic regression by probit analysis of survival status by immune response factor was used to predict $\log_{10}$-transformed immune response factors that would yield a probability of survival of 90% and 99% (Table 4.3). According to this analysis, regardless of dose, route, or inactivation method, a $\log_{10}$-transformed PRNT value of 1.57 after 1 vaccination or 2.20 after 2 vaccinations would protect 90% of mice from an aerosol challenge against EEEV strain FL93-939, while much higher titers of IgG, IgG1, IgG2a or IgG2b would be needed to protect the same number of animals. This analysis was also done to evaluate the various methods of inactivation as well as the route of inoculation and the vaccine regime. When evaluating the method of inactivation, it is clear that regardless of whether the animal received 1 vaccination (day 21) or 2 vaccinations (day 56), the lowest titers required to protect either 90% or 99% of the animals were the serum neutralizing antibody titers (PRNT) and that the gCVEV1219

Table 4.2. Odds ratios for each unit increase in immune response factor

Immune Response Parameter	Day*	Odds Ratio	OR 95% CI	p-value
IgG	21	1.099	(0.797, 1.515)	0.5667
	56	2.344	(1.489, 3.690)	**0.0002**
IgG1	21	1.784	(1.310, 2.430)	**0.0002**
	56	1.807	(1.236, 2.642)	**0.0023**
IgG2a	21	1.567	(1.189, 2.064)	**0.0014**
	56	2.013	(1.245, 3.254)	**0.0043**
IgG2b	21	2.247	(1.636, 3.087)	**<0.0001**
	56	2.094	(1.441, 3.043)	**0.0001**
PRNT	21	1.881	(1.240, 2.853)	**0.0029**
	56	4.249	(2.464, 7.326)	**<0.0001**
VF IgA	21	1.344	(0.829, 2.179)	0.2305
	56	1.474	(0.891, 2.438)	0.1309

Table 4.2. Odds ratio for the odds of survival for each unit increase in immune response factor, the 95% confidence limits for the odds ratio, and p-value for each immune response parameter. Groups of BALB/c mice (n=10) were vaccinated once (day 0) or twice (day 0, 28) with one of three iEEEV vaccine candidates (formalin-inactivated, INA-inactivated, or gamma irradiated) at doses ranging from 5-0.1µg by the IN, IM, or SC route. Serum and vaginal flush samples were collected 21 days after each vaccination.
* Data from all groups after 1 vaccination for day 21; data from mice receiving 2 vaccinations for day 56.

Table 4.3. Predicted titers required for 90% and 99% survival

		IgG		IgG1		IgG2a		IgG2b		PRNT	
	Day*	90%	99%	90%	99%	90%	99%	90%	99%	90%	99%
Overall	21	5.43	8.13	5.35	8.30	5.64	8.33	4.69	6.77	1.57	2.66
	56	6.19	9.29	7.04	11.34	5.89	8.41	5.65	8.64	2.20	3.65
Method of Inactivation											
Formalin	21	5.83	10.50	4.43	8.09	6.63	11.96	5.14	8.80	1.46	2.83
Gamma		5.20	7.83	4.32	6.36	4.83	7.02	4.03	5.59	1.01	1.79
INA		--	--	--	--	--	--	--	--	1.26	1.87
Formalin	56	3.59	6.55	3.32	5.56	4.12	6.03	3.33	6.10	1.77	3.16
Gamma		4.21	5.38	3.92	5.36	4.41	5.39	3.70	5.33	0.85	1.35
INA		--	--	--	--	--	--	--	--	--	--
Route											
IN	21	3.47	5.30	2.05	3.16	4.19	6.44	2.94	4.41	0.87	1.38
IM		4.04	5.18	3.03	3.73	4.33	5.53	3.74	4.63	1.01	1.73
SC		4.52	6.11	4.30	5.76	4.81	6.41	3.67	4.47	3.24	5.50
IN	56	6.26	10.17	4.58	7.30	6.60	10.35	5.85	9.74	2.72	4.65
IM		4.10	4.26	6.09	9.72	4.29	4.80	4.24	4.97	1.03	1.66
SC		4.93	5.73	5.98	7.85	4.74	5.01	4.21	4.90	2.68	4.25
Regime											
1 vaccination	21	5.04	6.52	6.03	8.49	5.40	6.94	5.47	7.38	1.62	2.40
2 vaccinations	56	3.85	5.99	3.88	6.38	4.24	6.62	3.80	5.73	1.37	2.62

Table 4.3. Predicted $\log_{10}$-transformed titer for each immune response factor that would yield a probability of survival of 90% and 99%. Groups of BALB/c mice (n=10) were vaccinated once (day 0) or twice (day 0, 28) with one of three iEEEV vaccine candidates (formalin-inactivated, INA-inactivated, or gamma irradiated) at doses ranging from 5-0.1µg by the IN, IM, or SC route. Serum was collected 21 days after each vaccination.
* Data from all groups after 1 vaccination for day 21; data from mice receiving 2 vaccinations for day 56.

vaccine candidate would require a lower PRNT compared to the fCVEV1219 vaccine candidate to protect the same percentage of animals. This method of analysis could not predict what titer would yield 90 or 99% survival for the INA method of inactivation (iCVEV1219) because there were so few survivors. When comparing the routes of inoculation without regard to dose or method of inactivation, again the lowest titers required to protect either 90% or 99% of the animals were the serum neutralizing antibody titers (PRNT). While the lowest titers required to protect either 90 or 99% of the animals after one vaccination were found in those animals vaccinated by the IN route (0.87 and 1.38, respectively), this did not hold true for those animals receiving two vaccinations, where the lowest titers required to protect 90 or 99% of the animals were found in the animals vaccinated by the IM route (1.03 and 1.66, respectively). However, the log_{10}-transformed serum neutralizing antibody titers required to protect either 90 or 99% of the animals from either the IN (0.87 and 1.38, respectively) and IM (1.01 and 1.73, respectively) routes were relatively low on day 21 compared to the SC (3.24 and 5.5, respectively) route. This was not consistent for the animals receiving 2 vaccinations (day 56), where the IM PRNT titers were the lowest (1.03 and 1.66, respectively) and the IN and SC titers were similar and were 1 to 3 logs higher than the IM. When comparing the vaccination regime without regard to dose, route, or method of inactivation, again the lowest titers required to protect either 90% or 99% of the animals were the serum neutralizing antibody titers (PRNT). The titers that would yield a probability of survival of 90 or 99% were low and similar between those animals receiving one or two vaccinations.

Vaginal flush (VF) samples were collected from all mice 21 days after each vaccination to assess virus specific mucosal IgA responses. As expected, those mice vaccinated by the IN route had significantly higher IgA levels than those vaccinated by either the IM or SC routes (Figure 4.14) with increased levels after the second vaccination. However, the odds ratios for the VF IgA samples, for both the day 21 and day 56 samples were among the lowest with wide variability between groups (Table 4.2). For this reason, the predicted $\log_{10}$-transformed VF IgA titer that would yield a 90% or 99% probability of survival against an aerosol challenge was not determined.
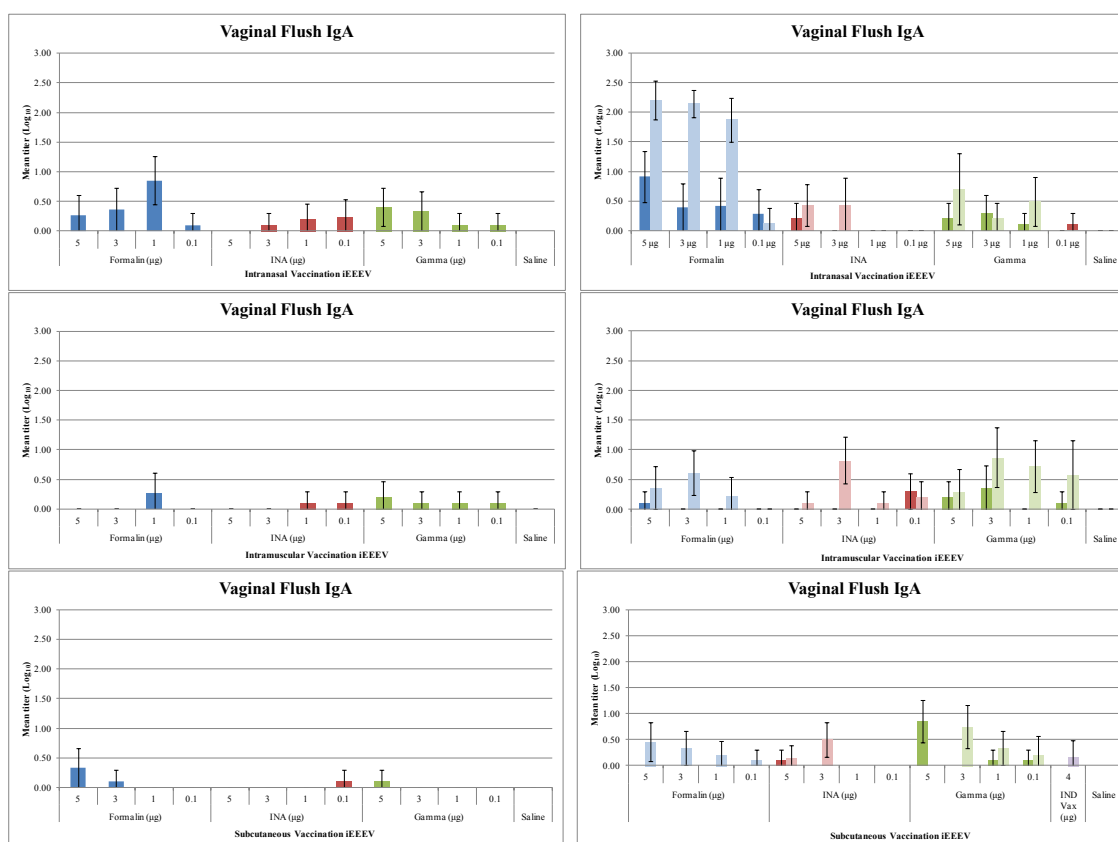
Figure 4.14. Vaginal flush IgA antibody responses in mice vaccinated with iEEEV vaccine candidates. Groups of BALB/c mice (n=10) were vaccinated once (graphs on left) or twice (graphs on right) with one of three iEEEV vaccine candidates (formalin-inactivated, INA-inactivated, or gamma irradiated) at doses ranging from 5-0.1µg by the IN, IM, or SC route. Vaginal flush samples were collected 21 d after each vaccination and virus specific IgA antibody levels were determined by ELISA. In all graphs, dark bars represent the mean group titer 21 days after the first vaccination (n=10); light bars represent the mean group titer 21 days after the second vaccination (n=10). Standard error bars represent 2 times the SE of the mean (SE=SDxsqrt(n)).

From the results of the intranasal vaccination study we chose to evaluate the

fCVEV1219 vaccine candidate in an extended vaccine regime and aerosol challenge

experiment. These mice were vaccinated and challenged as described in Table 4.4.

Serum samples were evaluated for neutralizing antibody responses using PRNT and for

virus-specific IgG using ELISA, while vaginal flush samples were evaluated for virus-

specific IgA levels using ELISA.

Table 4.4. Study design for second study evaluating iEEEV candidates

Group	Vaccine Candidate	Dose	Route	Vaccination Schedule	Blood, VF Collection	Aerosol Challenge	# Mice
1	fCVEV1219	5 µg	SC	D0	D21, D56	D63	10
2	fCVEV1219	3 µg	IN	D0	D21, D56	D63	10
3	fCVEV1219	1 µg	IM	D0	D21, D56	D63	10
4	No Vax	--	--	D0	D21, D56	D63	5
5	fCVEV1219	5 µg	SC	D0, D56	D21, D56, D77	D84	10
6	fCVEV1219	3 µg	IN	D0, D56	D21, D56, D77	D84	10
7	fCVEV1219	1 µg	IM	D0, D56	D21, D56, D77	D84	10
8	No Vax	--	--	D0, D56	D21, D56, D77	D84	5

Table 4.4. Mice were vaccinated with the formalin-inactivated CVEV1219 (fCVEV1219) vaccine candidate according to the dose, route, and schedule listed. Multiple serum and vaginal flush samples were collected and mice were challenged with EEEV strain FL93-939 by aerosol either 63 d or 28 d after the last vaccination depending on the vaccination schedule.

Similar to the results of the first study and to the unvaccinated controls, those

animals that received a single vaccine and were challenged 63 days post-vaccination but

were not protected from an aerosol challenge began to lose weight and show clinical

signs of disease by 3-4 dpi (Figure 4.15). All of the animals that showed clinical signs of

disease succumbed to infection or were euthanized. In contrast to the results of the first study, 100% of the animals that received a single vaccination of 5 μg fCVEV1219 by the SC route survived an aerosol challenge, when that challenge was delayed to 63 days post-vaccination as opposed to 28 days post-vaccination as in the first study (Figure 4.16). Additionally, 100% of animals that received 2 vaccinations (on day 0 and day 56), regardless of dose and route tested, survived an aerosol challenge when challenged 28 days after the second vaccination (Figure 4.16). Unvaccinated controls showed clinical signs of disease 3 days post-challenge and all succumbed to infection or were euthanized by 5 days post-challenge (Figure 4.15). Fischer's exact tests with stepdown Bonferroni adjustment were used to compare survival rates. As noted in Figure 4.16, the survival rate was statistically significantly different between the group that received a single SC vaccination (5 μg fCVEV1219) and both the unvaccinated controls and the mice in the first study that received the EEEV IND vaccine (p<0.001). Additionally, statistically significant differences in survival rates were observed between all groups of animals that received 2 vaccinations and both the unvaccinated controls and the mice from the first study that received the EEEV IND vaccine (p<0.0007). A statistically significant difference in the survival rate was noted between mice receiving either 1 or 2 vaccinations by the IN route (3 μg fCVEV1219) (p=0.037).

Neutralizing antibody responses and virus specific serum antibody levels were determined for all groups vaccinated once or twice with fCVEV1219 vaccine candidate at doses ranging from 5-1 μg by the IN, IM, or SC routes. For those mice receiving the fCVEV1219 vaccine candidate by any route, both the neutralizing antibody responses as

Figure 4.15. Percent change in body weight and onset of clinical signs in mice vaccinated with formalin-inactivated CVEV1219 (fCVEV1219) by IN, IM, or SC route with doses ranging from 5-1 µg. Mice received either a single vaccination on day 0 and were challenged on day 56 or they received vaccinations on day 0 and day 56 and were challenged on day 84. Mice were monitored for 28 days post-aerosol challenge; however, no changes were noted after 14 days.
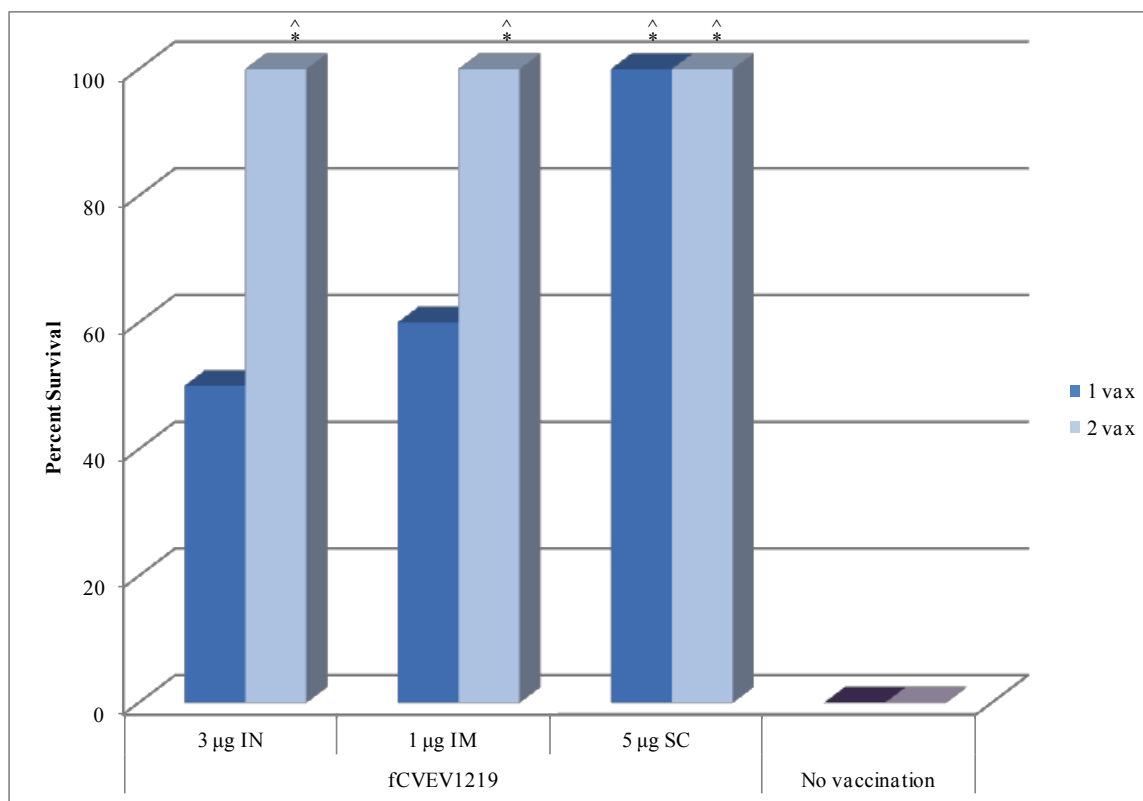
Figure 4.16. Protective efficacy of fCVEV1219 vaccine candidate when administered on an extended vaccination schedule with aerosol challenge. Groups of BALB/c mice (n=10) were administered one (dark bars) or two doses (light bars) of fCVEV1219 at doses ranging from 5-1µg by IN, IM, or SC routes. Half of the mice were challenged by aerosol, with at least $100LD_{50}$ of EEEV strain FL93-939, 63 days after the first vaccination, while the other half were challenged 28 days after the second vaccination (d84). Mice were monitored for 28 days post-challenge for mortality and clinical signs of disease (* p-value <0.05 for pairwise comparison to control group; ^ p-value<0.05 for pairwise comparison to IND vaccine group from the first study)

well as all immunoglobulins measured generally increased over time and were the highest after the second vaccination (Figures 4.17). Levels of serum neutralizing antibody appeared to correlate with survival. The 5 µg SC fCVEV1219 group had the highest titer following the single vaccination. The virus-specific serum IgG levels appeared more similar regardless of dose or route of inoculation. Interestingly, and in contrast to the data in the first vaccine study, the levels of virus-specific IgA in the vaginal flush samples appeared more similar in the groups receiving fCVEV1219 either by the IN or SC routes.
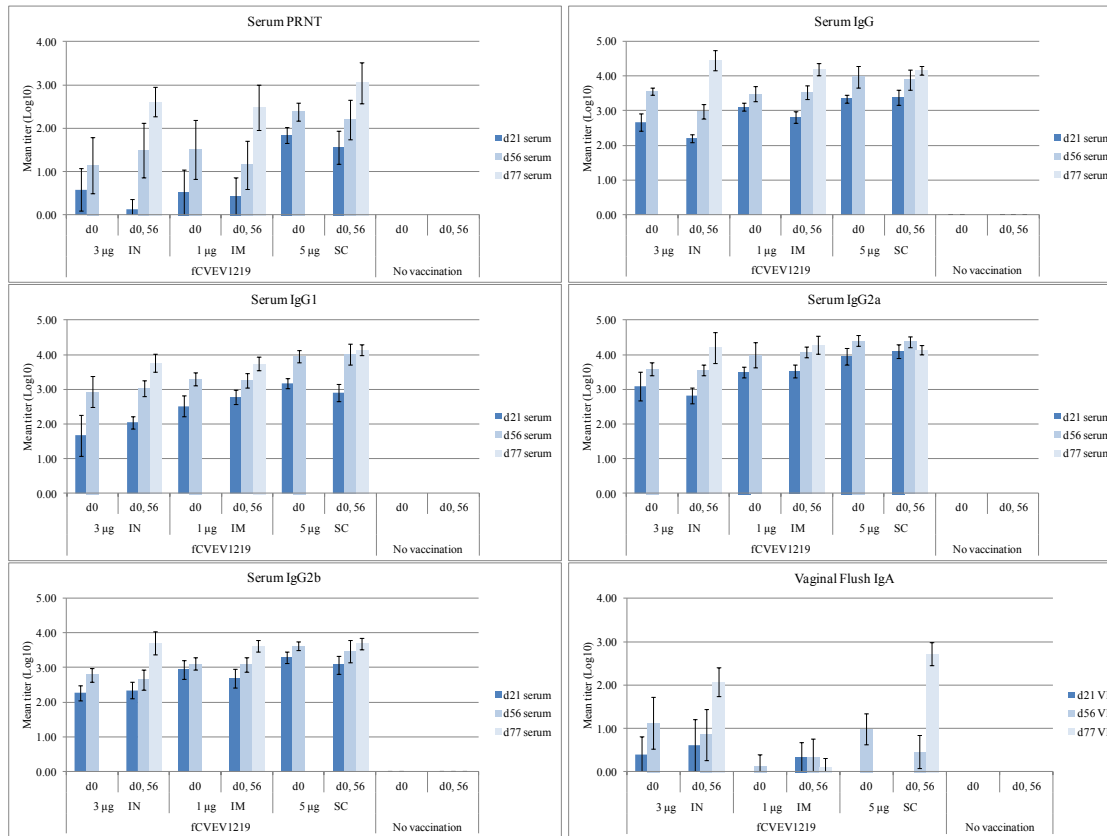
Figure 4.17. Serum and vaginal flush antibody responses in mice vaccinated with fCVEV1219 vaccine candidate. Groups of BALB/c mice (n=10) were vaccinated once (d0) or twice (d0, 56) with fCVEV1219 at doses ranging from 5-1µg by the In, IM, or SC route. Serum and vaginal flush samples were collected on day 21, 56, and 77 post-vaccination. Neutralizing antibody responses were determined by PRNT and serum and vaginal flush antibody levels were determined by ELISA. Dark bars represent the mean group titer 21 days after the first vaccination (n=10); medium bars represent the mean group titer 56 days after the first vaccination (n=10); light bars represent the mean group titer 21 days after the second vaccination (day 77, n=10). Standard error bars represent 2 times the SE of the mean (SE=SDxsqrt(n)).

Logistic regression by probit analysis was utilized to assess whether there was a significant increase in odds of survival for each unit increase in immune response factor. However, unlike the results of the first vaccine study, only the odds ratio for IgG1 on day 21 (2.5) and the odds ratio for PRNT on day 56 (3.6) were significant and reproducible (p<0.05) (data not shown). There was insufficient data for the day 77 samples for analysis by logistic regression; therefore, this data set was not analyzed.

Logistic regression by probit analysis of survival status by immune response factor was used to predict $\log_{10}$-transformed immune response factors that would yield a probability of survival of 90% and 99% (Table 4.5). According to this analysis, regardless of dose or route, a $\log_{10}$-transformed PRNT value of 1.84 21 days after the first vaccination or a $\log_{10}$-transformed PRNT value of 2.22 56 days after 1 vaccination would protect 99% of mice from an aerosol challenge against EEEV strain FL93-939, while much higher titers of IgG, IgG1, IgG2a or IgG2b would be needed to protect the same number of animals. The data was insufficient to calculate the probability of survival for the day 77 samples.

Table 4.5. Predicted titers required for 90% and 99% survival

	Day*	IgG		IgG1		IgG2a		IgG2b		PRNT	
		90%	99%	90%	99%	90%	99%	90%	99%	90%	99%
Overall	21	3.15	4.69	2.47	3.42	3.64	5.04	2.86	3.93	0.93	1.84
	56	3.82	5.43	3.36	4.05	4.07	5.04	3.22	4.28	1.56	2.22

Table 4.5. Predicted $\log_{10}$-transformed titer for each immune response factor that would yield a probability of survival of 90% and 99%. Groups of BALB/c mice (n=10) were vaccinated once (day 0) or twice (day 0, 56) with fCVEV1219 vaccine candidate doses ranging from 5-1µg by the IN, IM, or SC route. Serum was collected from all animals (n=60) on days 21 and 56 after the first vaccination.
* Data from all groups after 1 vaccination for day 21 and 56

T-tests with stepdown Bonferroni adjustment for multiple comparisons were utilized to assess whether there were statistically significant differences in the immune response factors between the various groups. For all groups, whether they received 1 or 2 vaccinations, regardless of dose or route, the levels of virus-specific serum antibody levels of IgG, IgG1, IgG2a and IgG2b were significantly higher in vaccinated mice versus unvaccinated controls at all time points (p<0.0001) (data not shown). The same was true for the PRNT values for all groups at day 56 and day 77 when comparing

vaccinated to unvaccinated animals (p<0.05). However, when evaluating the levels of virus-specific IgA in the vaginal flush samples, only those mice receiving either 1 or 2 vaccinations by the IN or SC routes had significantly higher levels than the unvaccinated controls (p<0.05) (data not shown). While there were significant differences in the amount of virus specific IgG, IgG1, IgG2a and IgG2b found in those mice receiving 1 or 2 vaccines intranasally at 21 and 56 days post-vaccination (p<0.0007), this was not the case for those mice receiving 1 or 2 vaccines intramuscularly or subcutaneously for any of the immunoglobulins measured at any timepoint (data not shown).

Conclusion

The goal of vaccine development is to produce a product that closely mimics natural infection; thereby stimulating an appropriate and effective immune response. However, because EEEV is a NIAID Category B agent due to its virulence and potential use as a biological weapon, new vaccine candidates should protect against both subcutaneous and mucosal exposure to virulent virus, which can be challenging.

Modified live vaccines often induce a stronger and longer lasting immune response; nonetheless, they are not without problems, as was recently seen when V3526 was tested in phase I clinical trials. V3526 protected mice from both subcutaneous and aerosol challenge (Hart, Caswell-Stephan et al. 2000). Additionally, V3526 provided protection within one week of vaccination and protection persisted for at least one year against both homologous and heterologous VEEV (Hart, Lind et al. 2001). However, when it was transitioned to phase 1 human clinical trials it induced unacceptable side effects and was not further pursued.

Inactivating an attenuated-live virus provides an additional layer of safety in the formulation of the vaccine candidate. Since there is no virus replication during immunization with inactivated vaccines, the virus cannot revert to virulence, as is sometimes seen with modified-live vaccines. In this study we evaluated the protective efficacy and immunogenicity of three iEEEV vaccine candidates administered by various routes, schedules, and doses. We utilized a genetically modified strain of EEEV (CVEV1219), similar to V3526, and inactivated it using formalin (fCVEV1219), INA (iCVEV1219), or gamma-irradiation (gCVEV1219). Formalin inactivation was chosen because it has been used to develop safe and effective human and veterinary vaccines since 1955 (Furesz, 2006, Biologicals), and it has recently been used to successfully inactivate both V3526 (Martin, Bakken et al. 2010), and Japanese encephalitis virus (JEV) (http://www.fda.gov/BiologicsBloodVaccines/Vaccines/ApprovedProducts/ucm142577.htm 2009). We also inactivated CVEV1219 using INA, a hydrophobic photo-reactive probe that inactivates enveloped viruses by alkylating the transmembrane domains of viral proteins upon photo-activation with far-UV irradiation (310-360 nm). INA has recently been used inactivate V3000 (Sharma, Raviv et al. 2007), V3526 (Sharma, Gupta et al. 2011), HIV (Raviv, Viard et al. 2005), SIV (Raviv, Viard et al. 2005), influenza virus (Raviv, Blumenthal et al. 2008), and Ebola virus (Warfield, Swenson et al. 2007). The last method we used to inactivate CVEV1219 was gamma-irradiation. Gamma-irradiation inactivates viruses by generating strand-breaks in the genetic material, with little impact on the antigenic structure and biological integrity of proteins and has been used successfully to inactivate other enveloped viruses such as V3526 (Martin, Bakken et

al. 2010) and influenza A virus (Lowy, Vavrina et al. 2001; Alsharifi, Furuya et al. 2009; Furuya, Regner et al. 2010).

In this study, we compared the efficacy of iEEEV vaccine candidates (fCVEV1219, iCVEV1219, gCVEV1219) at varying doses, schedules and routes of administration against an aerosol challenge. In the first study, BALB/c mice were administered one or two doses of the inactivated candidates by the intranasal (IN), intramuscular (IM), or subcutaneous (SC), routes and subsequently challenged by the aerosol route 28 days after the final vaccination. A single-dose administration of the fCVEV1219 vaccine candidate provided partial protection (20-70%) in mice when administered at doses ranging from 1-5 µg by any route, while gCVEV1219 resulted in protection rates ranging from 10-40% when administered IM or SC as a single vaccination at either the 3 or 5 µg doses. However, when mice received 2 vaccinations 80-100% were protected against an aerosol challenge when vaccinated with fCVEV1219 vaccine candidate by any route or the gCVEV1219 vaccine candidate by the IM or SC routes at doses from 1-5 µg. INA-inactivated CVEV1219 was unable to provide substantial protection against an aerosol challenge by any route, dose or schedule tested. Overall, both fCVEV1219 and gCVEV1219 given in the 2 dose regime intramuscularly provided excellent protection (90-100%) against an aerosol challenge at all doses. When evaluating correlates of protection, this data suggests that the level of serum neutralizing antibodies may be a useful tool in predicting survival and that only a ten-fold increase in titer would increase the odds of survival by more than 4 fold.

Due to the increased protective efficacy seen following two vaccinations of the fCVEV1219 vaccine candidate regardless of route or dose, we investigated whether

extending the time between vaccination and challenge would allow for development of a more mature and hence more effective immune response that would increase the protective efficacy of the vaccine following a single dose. While there was no significant change in the protective efficacy when the vaccine was administered intranasally or intramuscularly, there was noteworthy increases in survival when then vaccine was administered subcutaneously, with survival increasing from 40% to 100% following the extended vaccination schedule. And importantly, we achieved 100% protection from an aerosol challenge by all doses and routes evaluated when the vaccine was given in an extended 2-dose regime. As in the first study, the data from this study suggests that the level of serum neutralizing antibody may be a useful tool in predicting survival.

In both studies, vaginal flush virus-specific IgA levels were measured in order to determine if this would be a useful correlate of protection against an aerosol challenge. However, this did not appear to be the case in these studies. As expected, the intranasal route of inoculation typically induced the greatest IgA responses, especially in the 2-dose regimen and these animals typically survived aerosol challenge. However, the protective efficacy of fCVEV1219 and gCVEV1219 vaccine candidates administered IM or SC, as a 2 dose regimen, were equally high but the vaginal IgA responses were much lower. As noted by the standard error bars, there was significant inter-animal variation, not only in IgA levels, but in the IgG and PRNT levels as well. This variability can make group effect determinations difficult.

Currently, there are no FDA-licensed vaccines or therapeutics for EEEV for human use. In this study, the IND EEEV vaccine, which is presently used for at risk personnel, only protected 10% of the mice against an aerosol challenge with North American EEEV

strain FL93-939. These experiments are the first to show that a second-generation inactivated vaccine for EEEV was able to provide 100% protection from an aerosol challenge using different methods of inactivation, doses, routes of inoculation and schedules. The use of adjuvants may be able to boost and/or sustain the immune response, which will be important as these products are moved forward. Future studies will examine the onset and duration of immunity with these potential second-generation inactivated EEEV vaccines with and without the use of adjuvants.

REFERENCES

Alsharifi, M., Y. Furuya, et al. (2009). "Intranasal flu vaccine protective against seasonal and H5N1 avian influenza infections." PLoS One **4**(4): e5336.

Furuya, Y., M. Regner, et al. (2010). "Effect of inactivation method on the cross-protective immunity induced by whole 'killed' influenza A viruses and commercial vaccine preparations." J Gen Virol **91**(Pt 6): 1450-1460.

Griffin DE (2007). Alphaviruses. Fields Virology. Knipe DM, Griffin DE, Lamb RAet al. Philadelphia, Lippincott Williams & Wilkins**:** 1024-1067.

Guyton, A. C. (1947). "Measurement of the respiratory volumes of laboratory animals." Am J Physiol **150**(1): 70-77.

Hart, M. K., K. Caswell-Stephan, et al. (2000). "Improved mucosal protection against Venezuelan equine encephalitis virus is induced by the molecularly defined, live-attenuated V3526 vaccine candidate." Vaccine **18**(26): 3067-3075.

Hart, M. K., C. Lind, et al. (2001). "Onset and duration of protective immunity to IA/IB and IE strains of Venezuelan equine encephalitis virus in vaccinated mice." Vaccine **20**(3-4): 616-622.

Hart, M. K., W. Pratt, et al. (1997). "Venezuelan equine encephalitis virus vaccines induce mucosal IgA responses and protection from airborne infection in BALB/c, but not C3H/HeN mice." Vaccine **15**(4): 363-369.

http://www.fda.gov/BiologicsBloodVaccines/Vaccines/ApprovedProducts/ucm142577.htm. (2009). "Japanese Encephalitis Virus Vaccine, Inactivated, Adsorbed Approval Letter."   Retrieved November, 29, 2011, 2011.

Lowy, R. J., G. A. Vavrina, et al. (2001). "Comparison of gamma and neutron radiation inactivation of influenza A virus." Antiviral Res **52**(3): 261-273.

Martin, S. S., R. R. Bakken, et al. (2010). "Comparison of the immunological responses and efficacy of gamma-irradiated V3526 vaccine formulations against subcutaneous and aerosol challenge with Venezuelan equine encephalitis virus subtype IAB." Vaccine **28**(4): 1031-1040.

Martin, S. S., R. R. Bakken, et al. (2010). "Evaluation of formalin inactivated V3526 virus with adjuvant as a next generation vaccine candidate for Venezuelan equine encephalitis virus." Vaccine **28**(18): 3143-3151.

Parker, M. D., M. J. Buckley, et al. (2010). "Antibody to the E3 glycoprotein protects mice against lethal venezuelan equine encephalitis virus infection." J Virol **84**(24): 12683-12690.

Raviv, Y., R. Blumenthal, et al. (2008). "Hydrophobic inactivation of influenza viruses confers preservation of viral structure with enhanced immunogenicity." J Virol **82**(9): 4612-4619.

Raviv, Y., Y. Salomon, et al. (1987). "Selective labeling of proteins in biological systems by photosensitization of 5-iodonaphthalene-1-azide." Proc Natl Acad Sci U S A **84**(17): 6103-6107.

Raviv, Y., M. Viard, et al. (2005). "Inactivation of retroviruses with preservation of structural integrity by targeting the hydrophobic domain of the viral envelope." J Virol **79**(19): 12394-12400.

Roy, C. J., D. S. Reed, et al. (2009). "Pathogenesis of aerosolized Eastern Equine Encephalitis virus infection in guinea pigs." Virol J **6**(1): 170.

Sharma, A., P. Gupta, et al. (2011). "Safety and protective efficacy of INA-inactivated Venezuelan equine encephalitis virus: implication in vaccine development." Vaccine **29**(5): 953-959.

Sharma, A., Y. Raviv, et al. (2007). "Complete inactivation of Venezuelan equine encephalitis virus by 1,5-iodonaphthylazide." Biochem Biophys Res Commun **358**(2): 392-398.

Viard, M., S. D. Ablan, et al. (2008). "Photoinduced reactivity of the HIV-1 envelope glycoprotein with a membrane-embedded probe reveals insertion of portions of the HIV-1 Gp41 cytoplasmic tail into the viral membrane." Biochemistry **47**(7): 1977-1983.

Warfield, K. L., D. L. Swenson, et al. (2007). "Ebola virus inactivation with preservation of antigenic and structural integrity by a photoinducible alkylating agent." J Infect Dis **196 Suppl 2**: S276-283.

Chapter 5

Systemic and Mucosal Immunogenicity of fCVEV1219

Abstract

Eastern equine encephalitis virus (EEEV), an arbovirus, is an important human and veterinary pathogen belonging to one of seven antigenic complexes in the genus *Alphavirus*, family *Togaviridae*. EEEV is considered the most deadly of the mosquito-borne alphaviruses due to the high case fatality rate associated with clinical infections, reaching as high as 75% in humans and 90% in horses (Griffin DE 2007). In patients that survive, the neurologic sequelae are often devastating. Although natural infections are acquired by mosquito bite, EEEV is also highly infectious by aerosol, making it a potential agent of bioterrorism.

Currently, there are no FDA-licensed vaccines or therapeutics for EEEV for human use. However, in studies completed as part of this thesis, we demonstrated successful inactivation of a genetically modified strain of EEEV, CVEV1219, and that two inactivation methods in particular, formalin-inactivation (fCVEV1219) and gamma-irradiated (gCVEV1219), provided 80-100% protective efficacy against an aerosol challenge when given as a 2-dose regimen either intramuscularly or subcutaneously at doses ranging from 1-5 μg. Additionally, immunogenicity studies revealed that serum neutralizing antibody titers correlated with survival; however, vaginal flush virus specific IgA responses were varied. To further evaluate the immune response to fCVEV1219, mice were vaccinated either once or twice intranasally and various mucosal samples as well as the spleen were collected. The mucosal samples were evaluated for virus-specific IgA levels while the spleen was processed and evaluated for B and T cell responses.

While serum neutralizing antibody titers, serum virus-specific IgG and mucosal IgA increased with the number of vaccinations, there was no significant difference between vaccination schedules. We were unable to detect differences in any of the splenic T and B cell populations when comparing vaccinated versus unvaccinated mice. The results of these studies suggest that serum neutralizing antibody titers correlate with the number of vaccines given but not the vaccination schedule per se, that measuring vaginal flush virus-specific IgA levels provides a good estimate of virus-specific IgA at other mucosal sites, and that *in vitro* restimulation of both B and T cells is necessary to appreciate differences in splenic cell populations.

Introduction

The goal of vaccine development is to produce a product that closely mimics natural infection; thereby stimulating an appropriate and effective immune response. However, because EEEV is recognized as a potential bioweapon that is likely to be aerosolized, new vaccine candidates for EEEV must protect against both subcutaneous and mucosal exposure to virulent virus. In order for a second-generation vaccine candidate to protect against aerosolized EEEV, an effective immune response at the site of infection, the nasal mucosa, is thought to be essential. Therefore, the evaluation of virus-specific serum IgG as well as mucosal IgA will likely be helpful in determining the effectiveness of a vaccine candidate.

It is now well established that the innate immune system, which has limited specificity and no memory, plays an essential role in shaping the adaptive immune response, which is characterized by high specificity and variable memory. However, it is also known that induction of memory does not ensure protection from a second infection

(Campos and Godson 2003; Woodland and Kohlmeier 2009), but this failure to protect is often related to the pathogenesis of the infection and the biological limitations of the immune system and not to the failure to induce a specific immune response. For example, it is known that it takes a significantly longer time to generate effector cells from naive B and T cells after the first encounter than it does to generate them from memory B and T cells upon subsequent exposure. Depending on the type of infection and the pathogenesis, this time lag may be crucial and ultimately determine whether the host becomes ill. The goal of any vaccine is to induce immune memory such that if the host encounters the pathogen in the future, the memory cells will be present, expand quickly and effectively, and differentiate into effector cells and ultimately eliminate the pathogen (Campos and Godson 2003).

In order to better characterize the systemic and mucosal immune response to fCVEV1219 after one or two intranasal vaccinations, we evaluated serum neutralizing antibody responses, serum virus-specific IgG and mucosal IgA responses, and splenic T and B cell populations in vaccinated and unvaccinated mice.

Materials and Methods

CVEV1219

CVEV1219 is a chimeric virus composed of the nonstructural proteins of VEEV and the structural proteins of EEEV. In addition, the site for furin cleavage was deleted; therefore, furin is unable to cleave E2 and E3 and they are transported to the cell surface as their precursor (PE2). PE2 then forms a heterodimer with E1 and these structures then trimerize, resulting in an extra surface projection. This is a lethal mutation; however, the

rescued virus contains compensatory mutations which alter the glycoprotein interactions and resuscitate the virus.

Inactivated vaccine candidate

Sucrose purified CVEV1219 virus stock was inactivated using formalin (fCVEV1219) and residual infectivity was determined *in vitro* and *in vivo* using a multisystem approach as described previously.

Mice

Specific pathogen free 6-8-week-old female BALB/c mice (NCI, Frederick, MD) were housed in cages equipped with microisolators and were provided food and water *ad libitum* throughout the study. The room temperature was $23 \pm 1^{o}C$ and periods of light and dark were maintained on a 12 h cycle. Mice were acclimated for 1 week before vaccination and were housed in a biosafety level 3 (BSL-3) facility. Research was conducted at the United States Army Medical Research Institute of Infectious Diseases (USAMRIID) under an IACUC approved protocol in compliance with the Animal Welfare Act and other Federal statutes and regulations relating to animals and experiments involving animals and adheres to principles stated in the Guide for the Care and Use of Laboratory Animals, National Research Council, 1996. The facility is fully accredited by the Association for Assessment and Accreditation of Laboratory Animal Care International.

Experimental Design

Mice were vaccinated according to the schedule listed in Table 5.1 and tissue and fluid samples were collected 7-14 days post-vaccination. Mice were briefly anesthetized with isoflurane using an integrated multi-patient anesthesia machine (IMPAC[6]) (VetEquip, Pleasanton, CA) and were given 3 μg fCVEV1219 in a 20 μL volume (10 μL per nostril). Mice were vaccinated on day 0 and samples collected on day 14 or mice were vaccinated on day 0 and 28 or day 0 and 56 and samples were collected 7 days after the last vaccination. At the time of sample collection, mice were anesthetized with mouse KAX, a combination containing 50 mg ketamine (100 mg/ml, Fort Dodge Animal Health, Fort Dodge, IA), 0.5 mg acepromazine 10 mg/ml (Boehringer Ingelheim, Ridgefield, CT), and 5.5 mg xylazine 20 mg/ml (Lloyd Laboratories, Walnut, CA), given intraperitoneally at a dose of 0.2 ml per 20 gm. A bronchoalveolar lavage (BAL) and nasopharyneal flush (NF) were performed using 0.5 ml of sterile PBS for each. Briefly, the trachea was exposed and an 18-g needle was inserted toward the lower or upper respiratory tract, respectively. PBS was flushed into the lungs and aspirated for BALs or through the nares and/or oropharynx for nasopharyneal flushes. Mice were euthanized by exsanguination via cardiac puncture and serum was collected for immunoglobulin analysis. Vaginal flushes were obtained as previously described (Hart, Pratt et al. 1997), by douching with 100 μL of PBS. Gastrointestinal flushes were collected by removing the proximal small intestine and flushing it with 0.5 ml of PBS. Fecal pellets were collected by opening the distal colon and removing 3-5 fecal pellets and mixing them with 0.5 ml of PBS. All samples were individually collected and stored at -80°C until further analysis .

Table 5.1. Experimental design using IN fCVEV1219

Group	Inoculum	Dose	Route	Vaccination Schedule	Day of Harvest	# of Mice
1	fCVEV1219	3 µg	IN	D0	D14	10
2	fCVEV1219	3 µg	IN	D0, D28	D35	10
3	fCVEV1219	3 µg	IN	D0, D56	D63	10
4-1 → 4-3	PBS	--	IN	D0	D14	3
4-4 → 4-6	PBS	--	IN	D0, D28	D35	3
4-7 → 4-10	PBS	--	IN	D0, D56	D63	4

Table 5.1. Mice were vaccinated with formalin-inactivated CVEV1219 (fCVEV1219) according to the dose, route, and schedule listed. Serum and mucosal samples were collected and spleens harvested 7-14 days after the vaccination.

Enzyme-linked immunosorbent assay (ELISA)

Optimum viral and antibody concentrations were determined by checkerboard titration, in which an ELISA was performed using varying concentrations of both the viral antigen and each of the primary antibodies. Serum and vaginal flush antibody responses to the vaccine candidates were then evaluated by ELISA as previously described (Hart, Pratt et al. 1997; Hart, Caswell-Stephan et al. 2000; Martin, Bakken et al. 2010). Briefly, Costar EIA/RIA 96-well high-binding plates (Corning Inc., Corning, NY) were coated with 0.2 µg of sucrose purified EEEV strain FL93-939 per well and incubated overnight, or up to 1 week, at 4°C. The following day, plates were blocked with Dulbecco's phosphate buffered saline (DPBS) (GIBCO^{TM} Invitrogen Corp., Grand Island, NY) containing 0.05% Tween 20 (Sigma-Aldrick, St. Louis, MO) and 5% nonfat dry milk (Becton Dickinson and Co., Sparks, MD) (PBSTM) for 2 hours at 37°C. The plates were washed 3 times with PBST using the BioTek ELx405^{TM} microplate washer

(BioTek Instruments, Inc., Winooski, VT). Mouse sera were diluted in PBSTM

containing 1% heat inactivated fetal bovine serum (GIBCO^{TM} Invitrogen Corp., Grand

Island, NY), added to the plate and incubated for 1-2 hours at 37°C. Plates were washed

3 times with PBST followed by the addition of one of five peroxidase-labeled goat anti-

mouse Ig (IgG 1:50,000; IgG1 1:50,000; IgG2a 1:100,000; IgG2b 1:10,000; IgA

1:10,000) (Bethyl Laboratories, Inc., Montgomery, TX). The plates were incubated with

the secondary antibody for 1 hr at 37°C and then washed 3 times with PBST. The ABST

Peroxidase substrate (KPL, Gaithersburg, MD) was added to each well and color

developed for approximately 20-30 min at which time the optical density (OD) at 410 nm

was determined using a Spectramax M5 microplate reader (Molecular Devices,

Sunnyvale, CA). Endpoint titers were determined as the highest two-fold dilution that

produced an OD greater than the mean OD of the negative controls wells plus 3 standard

deviations.

Plaque-reduction neutralization test (PRNT)

Virus-neutralizing antibody responses were titrated as previously described (Hart,

Caswell-Stephan et al. 2000). Briefly, sera were serially diluted two-fold in Hank's

Balanced Salt Solution (HBSS) containing HEPES red (USAMRIID, Fort Detrick, MD)

and 2% FPB and incubated overnight with virus. The serum-virus mixture was then

added in duplicate to 6-well plates containing a confluent monolayer of Vero cells

(African green monkey kidney cells). Plates were incubated at 37°C for 1 hour, with

rocking every 15 min. Following the incubation period, wells were overlaid with 0.5%

agarose in EBME media (USAMRIID, Fort Detrick, MD) containing HEPES and 10%

FBS, 1% L-glutamine, 1% NEAA, 1% penicillin-streptomycin sulfate, and 0.1%

gentamicin was added, and plates were incubated at 37°C at 5% CO_2 for 24 hr.

Thereafter, cells were stained by the addition of a second agarose overlay prepared as

above containing 5% neutral red. The plates were incubated at 37°C at 5% CO_2 for 24 hr.

Defined plaques (neutral red exclusion areas) were counted. The endpoint titer was

determined to be the highest dilution with an 80% or greater reduction (PRNT 80) of the

number of plaques observed in control wells.

Splenocyte analysis

Spleens were harvested aseptically immediately after euthanasia and pooled into

groups of 3-4 in 10 mls of cold RPMI-1640 media containing 10% FBS, 2% L-glutamine,

2% HEPES buffer, and 0.1% gentamicin and kept on ice throughout the processing steps.

Spleens were cut into small pieces and homogenized using medicons and the

MediMachine (BD Biosciences, San Diego, CA). Homogenates were then filtered

through a 50 µm Filcon filter (BD Biosciences, San Diego, CA) and filtered cell

suspensions were centrifuged at 1700 rpm for 5-7 min. The pellets were then suspended

in 3 mls RBC lysis buffer (Sigma-Aldrich, St. Louis, MO) and incubated at room

temperature for 5-7 min. Lysis buffer was removed by the addition of 45 mls of media

and centrifugation at 1700 rpm for 5-7 min. For intracellular cytokine staining (ICC), the

cells were suspended in media to a concentration of 1E+7 cells/ml. Cells were seeded on

a 96 well plate (Costar, Corning Inc., Corning, NY) at 100 µL/well and incubated with

media containing GogliPlug (Brefeldin A) (BD Biosciences, San Diego, CA) and IL-2 for

4 hours at 37°C, 5% CO_2. After incubation, cells were pelleted by centrifugation at 1700

rpm for 2 min and then washed 3 times with cold PBS containing 1% FBS and then cells

were suspended in 50 µL of cold PBS containing 1% FBS and FcBlock (BD Biosciences,

San Diego, CA) and incubated for 30 min at 4^oC. Cells were then washed in cold PBS

containing 1% FBS and centrifuged at 1700 rpm for 2 min and suspended in 50 µL of

ICC surface antibodies for T cell panel 1 (Table 5.2). Cells were incubated for 30 min in

the dark at 4^oC and then washed with cold PBS containing 1% FBS and centrifuged at

1700 rpm for 2 min. Cells were then suspended in 100 µL of Fix/Perm buffer (BD

Biosciences, San Diego, CA), incubated for 30 min in the dark at 4^oC, and then

centrifuged at 1700 rpm for 2 min. Cells were washed 1 time with 175 µL of 1X Perm

Wash buffer, centrifuged at 1700 rpm for 2 min and then suspended in50 µL of ICC

cytokine antibodies for T cell panel 1 (Table 5.2). Cells were incubated for 30 min in the

dark at 4^oC and then washed with cold PBS and 1% FBS, centrifuged at 1700 rpm and

suspended in 20 µL PBS containing 1% FBS. Cells were stored in the dark at 4^oC until

analysis was complete. For surface marker antibody staining, remaining cells were

pelleted, suspended in 3 mls of cold PBS containing 1% FBS and FcBlock (1:100), and

incubated on ice for 30 min. Cells were then washed with cold PBS containing 1% FBS

and suspended at a concentration of 1E+7 cells/ml and seeded (100 µL/well) on a 96-well

round bottom plate. Cells were centrifuged at 1700 rpm for 2 min and suspended in 50

µL/well of surface marker antibodies (Table 5.2) and incubated for 30 min in the dark at

4^oC. Cells were washed in 175 µL of cold PBS containing 1% FBS and centrifuged at

1700 rpm for 2 min. Cells were suspended in cytofix (BD Biosciences, San Diego, CA)

and stored in the dark at 4^oC until analyzed. Cells were analyzed using a BD FACS

Canto II flow cytometer with DIVA software platform (BD Biosciences, San Diego, CA).

The analysis was done using FlowJo (Tree Star Inc, Ashland, OR).

Table 5.2. Antibodies used to detect intracellular cytokines and surface markers

	Marker	Fluorescent label	Dilution	Source	Cat#
T cell panel 1	CD4 (RM4-5)	V450	1:250	BD	560468
	CD8 (53-6.7)	PE-Cy7	1:750	BD	552877
	CD44 (IM7)	APC	1:100	BD	559250
	IFN gamma (XMG1.2)	FITC	1:100	eBio	11-7311-82
	TNF alpha (MP6-XT22)	PE	1:100	eBio	12-7321-82
T cell panel 2	CD4 (RM4-5)	V450	1:250	BD	560468
	CD28 (37.51)	APC			
	CD95 (Jo2)	FITC	1:250	BD	554257
T cell panel 3	CD8 (53-6.7)	PE-Cy7	1:750	BD	552877
	CD11b (M1/70)	PE	1:1500	eBio	12-0112-85
B cell panel 1	CD19 (1D3)	V450	1:500	BD	560375
	MHCII (M5/114.15.2)	PE-Cy5	1:1000	eBio	15-5321-82
	IgA (C10-3)	FITC	1:25	BD	559354
B cell panel 2	CD19 (1D3)	V450	1:500	BD	560375
	MHCII (M5/114.15.2)	PE-Cy5	1:1000	eBio	15-5321-82
	IgG1 (A85-1)	FITC	1:25	BD	553443
B cell panel 3	CD19 (1D3)	V450	1:500	BD	560375
	MHCII (M5/114.15.2)	PE-Cy5	1:1000	eBio	15-5321-82
	IgG2a (R19-15)	FITC	1:25	BD	553390

Table 5.2. Antibodies used to detect intracellular cytokines and surface markers in splenocyte analysis. Splenocytes were isolated and prepared as described above and incubated with various antibodies to detect intracellular cytokines and surface markers using the fluorescent labels and dilutions listed above. Cells were analyzed using a BD FACSCanto II flow cytometer and software. (BD = BD Biosciences, San Diego, CA; eBio = eBioscience, San Diego, CA)

Results

The study had two main goals, first was to analyze the mucosal immune response at various sites to an intranasal vaccine using a variety of vaccine schedules. The second goal was to analyze B and T cell responses in the spleen, specifically effector cells using antibodies to detect various intracellular cytokines and surface markers using flow cytometry.

Serum neutralizing antibody responses were greater in mice that received 2 vaccinations regardless of schedule. No significant difference was observed in the amount of serum neutralizing antibody present in mice vaccinated on day 0 and 28 as compared to those that were vaccinated on day 0 and 56 (Figure 5.1). Similar findings were noted when virus-specific serum IgG levels were evaluated. For total IgG, as well as the various isotypes measured, there were increased antibody titers in mice that received two vaccinations as compared to those that received a single vaccination. Again, there were no significant differences in IgG levels when comparing mice that were vaccinated on day 0 and 28 to those that were vaccinated on day 0 and 56 (Figure 5.2).

In order to compare virus-specific serum IgA levels to those found at various mucosal sites, samples were collected from 5 different areas: nasal flush (upper airway), bronchoalveolar lavage (lower airway), GI flush (proximal small intestine), fecal pellets (distal large intestine), and vaginal flush (genital tract). Because the mice were vaccinated using the intranasal route, it was expected that more virus-specific IgA would be found in the nasal flush and BAL; however, there were no significant differences in the levels of IgA when comparing the various mucosal sites for a given group (Figure

5.3). As with IgG, there was generally more IgA at all sites in mice that received 2

vaccinations as compared to those that only received a single vaccination. There were no

significant differences between the mice vaccinated on day 0 and 28 compared to those

vaccinated on day 0 and 56. Interestingly, generally there was more virus-specific IgA in

the serum than at any of the mucosal sites. This may be due to variations in levels of

serum versus secretory IgA or due to the fact that the level of IgA in the serum was

measured directly, whereas the IgA measured at the various mucosal sites was collected

by flushing the site, thereby potentially diluting the amount of antibody present.

Additionally, it is important to note that there was significant inter-animal variability

which resulted in large standard errors in some groups.
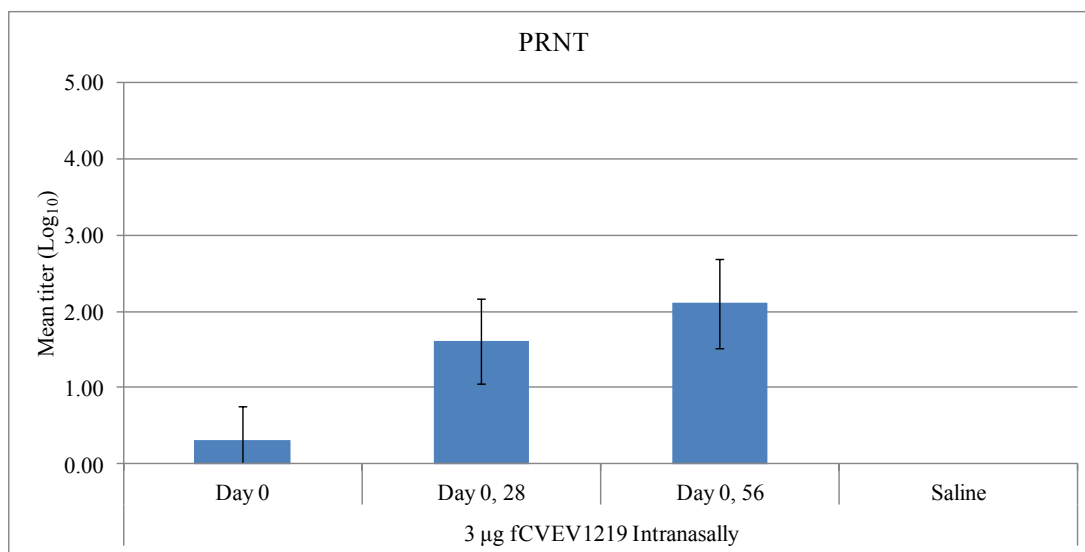
Figure 5.1. Neutralizing serum antibody responses in mice vaccinated with formalin-inactivated CVEV1219 (fCVEV1219) vaccine candidate. Groups of BALB/c mice (n=10) were vaccinated intranasally once or twice with 3µg fCVEV1219. Serum was collected 7-14 d after each vaccination. Neutralizing antibody responses were determined by PRNT. Standard error bars represent 2 times the SE of the mean (SE=SDxsqrt(n)).
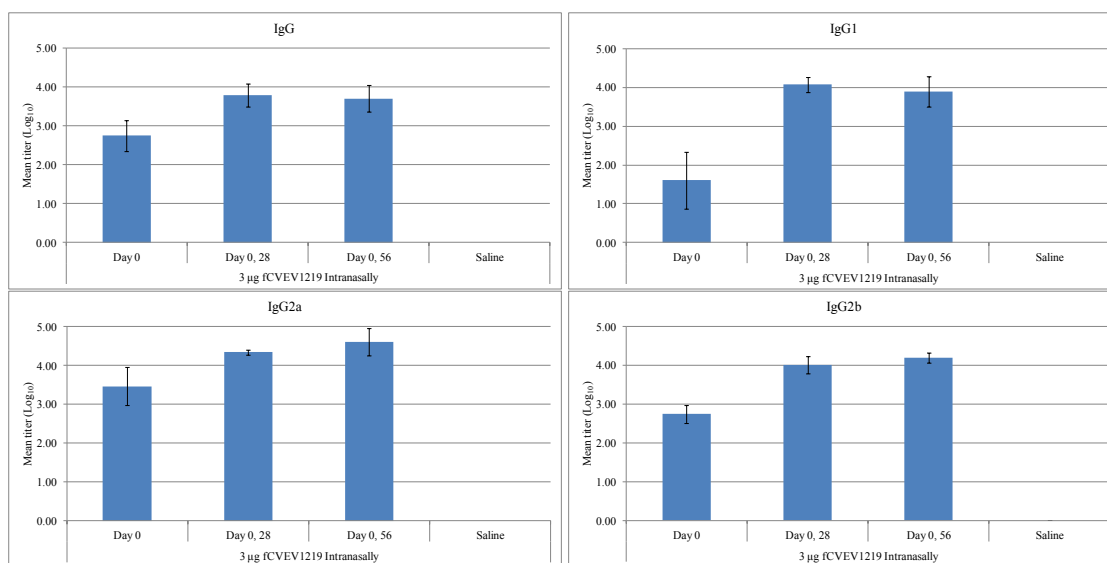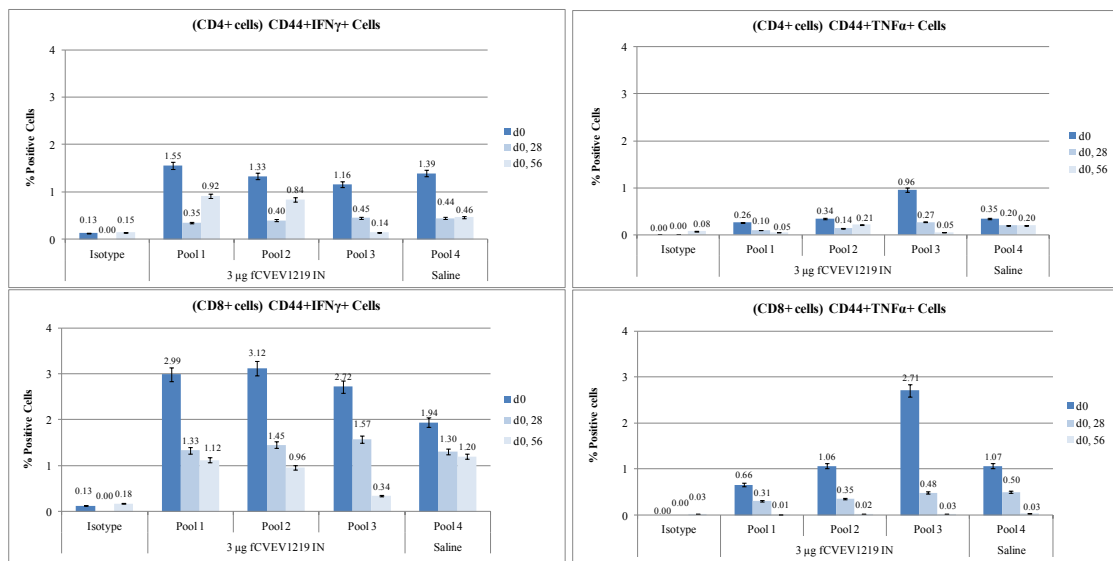
Figure 5.2. Virus-specific serum antibody responses in mice vaccinated with formalin-inactivated CVEV1219 (fCVEV1219) vaccine candidate. Groups of BALB/c mice (n=10) were vaccinated intranasally once or twice with 3µg fCVEV1219. Serum was collected 7-14 d after the last vaccination. Virus specific serum antibody levels were determined by ELISA. Standard error bars represent 2 times the SE of the mean (SE=SDxsqrt(n)).
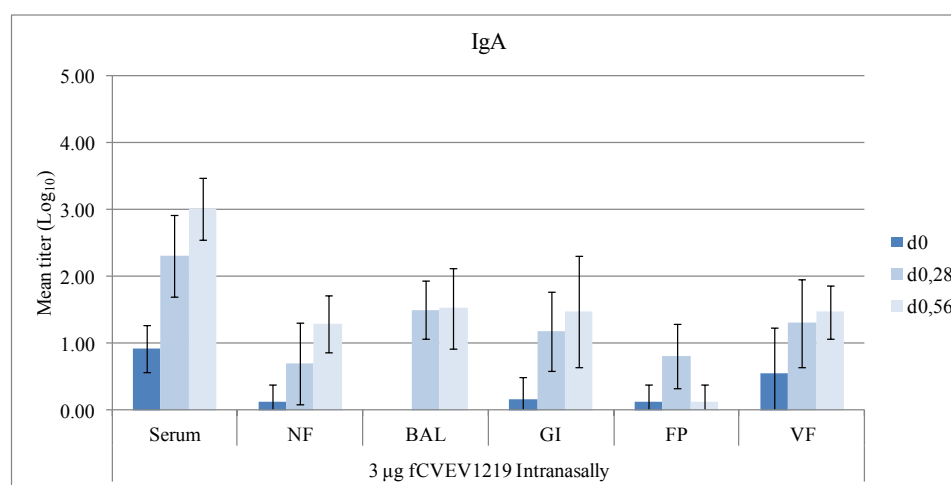
Figure 5.3. Virus-specific IgA antibody responses in mice vaccinated with formalin-inactivated CVEV1219 (fCVEV1219) vaccine candidate. Groups of BALB/c mice (n=10) were vaccinated intranasally once or twice with 3µg fCVEV1219. Samples were collected 7-14 d after each vaccination. Virus specific IgA antibody levels were determined by ELISA. Standard error bars represent 2 times the SE of the mean (SE=SDxsqrt(n)). Sample abbreviations: NF = nasal flush; BAL = bronchoalveolar lavage; GI = proximal small intestinal flush; FP = fecal pellets; VF = vaginal flush.

In order to evaluate the systemic immune response, splenocytes were harvested, processed, and labeled using a variety of fluorescent-labeled antibodies to detect both intracellular cytokines and cell surface markers. Treatment with phorbol myristate actetate (PMA) with ionomicin to non-specifically stimulate T cells resulted in the detection of high levels of both CD4+ and CD8+ T cells, indicating these cells could be stimulated *in vitro* (data not shown). Additionally, in all cases, the detection of isotype control antibodies was very low, indicating minimal background interference.

CD4+ T lymphocytes may be divided into either central memory or effector memory cells, based on their homing capacity and effector functions. Central memory T cells home to lymphoid organs whereas effector memory T cells migrate to the peripheral tissues. Additionally, central memory T cells have little effector function, but have a high capacity to proliferate, whereas effector memory T cells exhibit effector function, but have a low capacity to proliferate (Sun, Schmitz et al. 2005). We evaluated the percentage of effector memory T cells, as indicated by the presence of CD44 and activation by expression of either IFN-γ or TNF-α. No significant differences in activated effector memory CD4+ or CD8+ cells populations were observed when comparing the vaccinated mice (by any schedule) to the saline controls (Figure 5.4).

CD4+ T cells were evaluated to determine the percentage of central memory T cells by using CD28 and CD95 as markers. Naive CD4+ T cells are identified by intermediate expression of CD28 and lack of expression of CD95, whereas memory CD4+ T cells express CD95 and can be separated into central memory and effector memory subset

depending on CD28 expression (Sun, Schmitz et al. 2005). CD95, also known as the Fas

receptor, has a dual-function exerting either pro- or anti-apoptotic effects depending on

Figure 5.4. CD4 and CD8 T cell responses in mice vaccinated with formalin-inactivated CVEV1219 (fCVEV1219) vaccine candidate. Groups of BALB/c mice (n=10) were vaccinated intranasally once or twice with 3µg fCVEV1219. Spleens were harvested 7-14 d after each vaccination and 3-4 spleens were pooled for analysis. CD4 and CD8 cell responses were measured using various fluorescent-labeled antibodies to detect intracellular cytokines and surface markers followed by flow cytometric analysis. Standard error bars represent 2 times the SE of the mean (SE=SDxsqrt(n)).

the cellular content, and activation state (Paulsen, Valentin et al. 2011) and is used as a

marker for memory CD4+ T cells. In this study, the majority of CD4+ cells were either

CD28+ or CD95+; however there were very few CD4+ cells that were CD28+CD95+

(central memory CD4+ T cells). Additionally, there were no differences between our

vaccinated and unvaccinated groups (Figure 5.5).

Mac-1 (CD11b) is a member of the β2-integrin family of adhesion molecules and is

expressed on monocytes, peritoneal B-1 cells, CD8+ dendritic cells, NK cells, and a

subset of CD8+ T cells. Mac-1 expression on CD8+ T cells is used as a marker to

differentiate recently activated effector cells from resting memory cells. While there
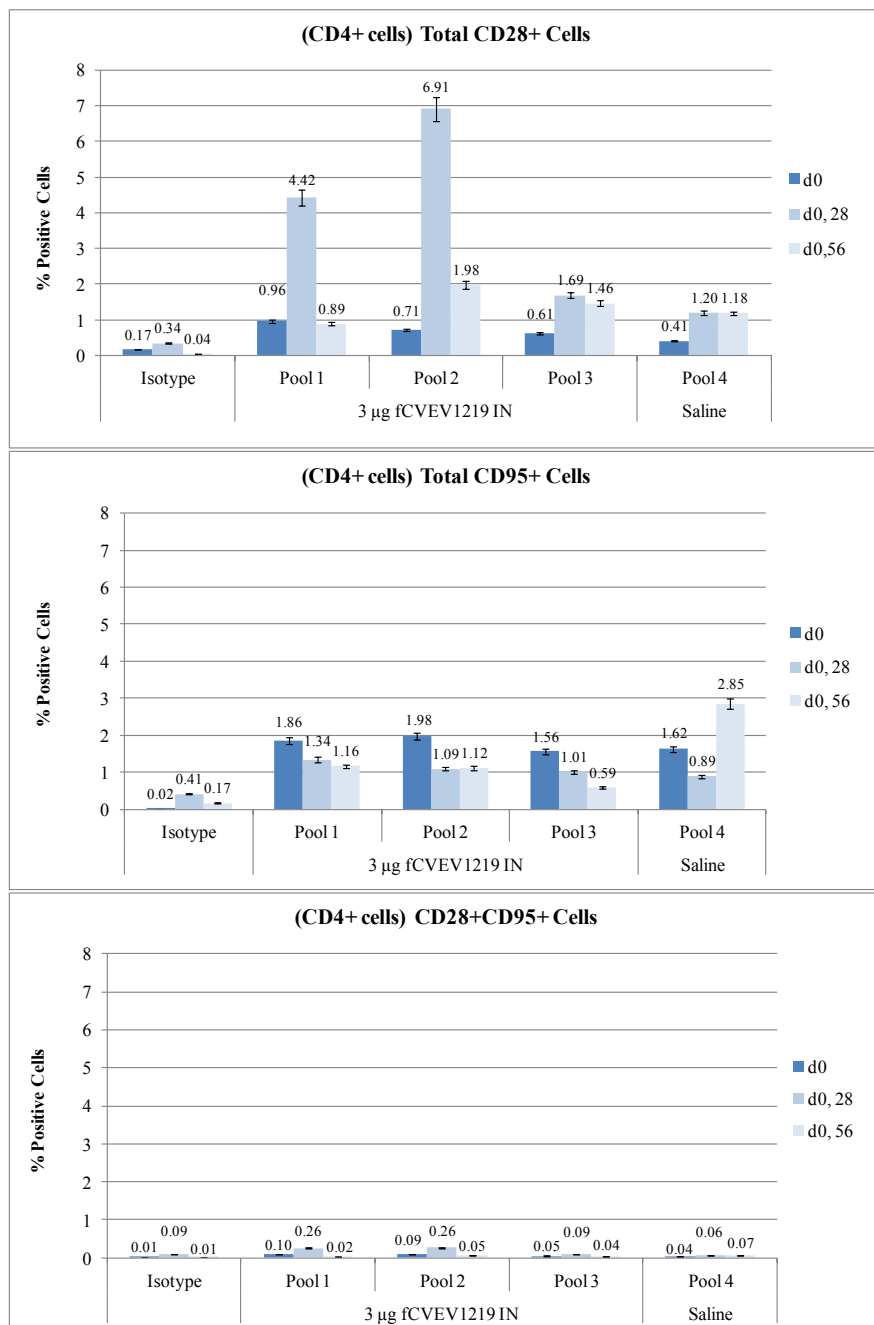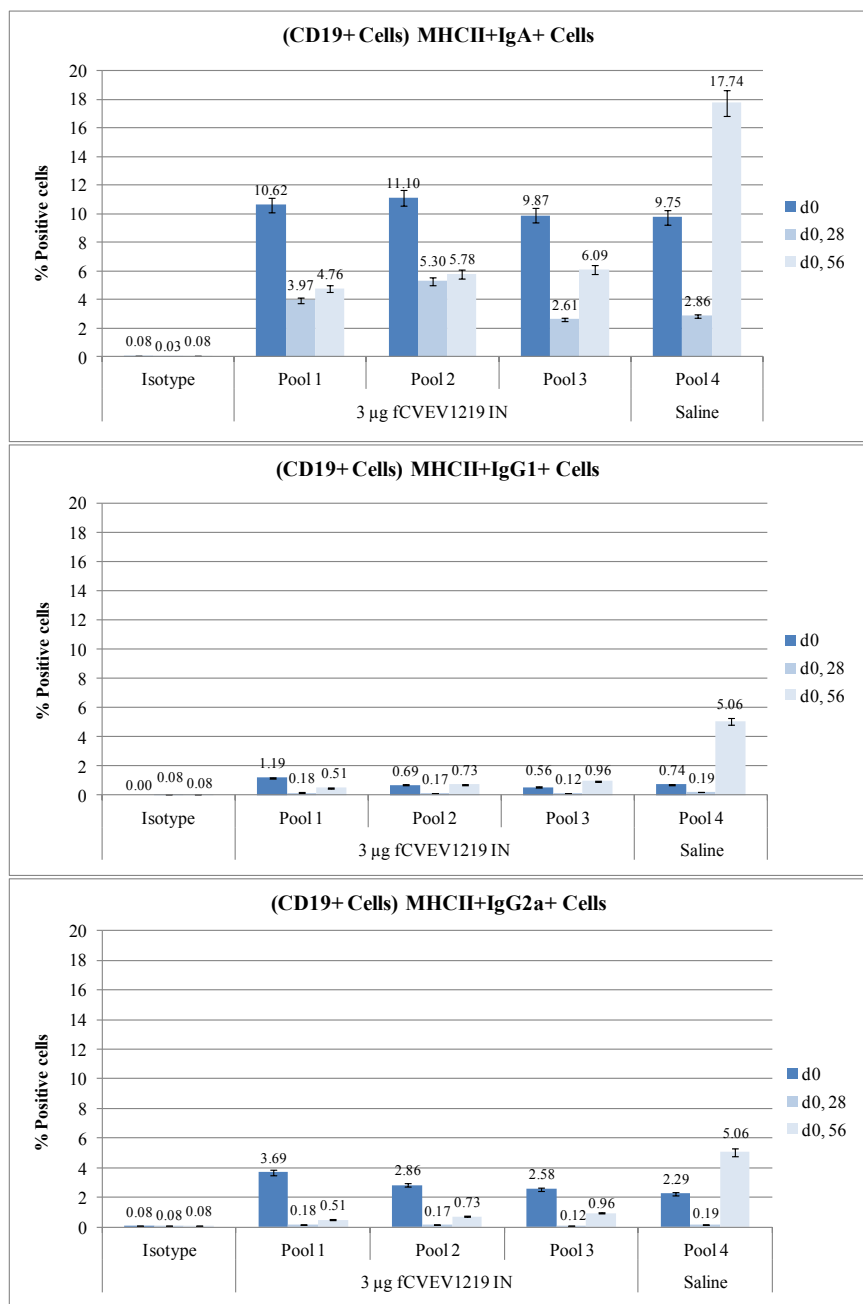
Figure 5.5. CD4 T cell responses in mice vaccinated with formalin-inactivated CVEV1219 (fCVEV1219) vaccine candidate. Groups of BALB/c mice (n=10) were vaccinated intranasally once or twice with 3µg fCVEV1219. Spleens were harvested 7-14 d after each vaccination and 3-4 spleens were pooled for analysis. CD4 cell responses were measured using various fluorescent-labeled antibodies to detect intracellular cytokines and surface markers followed by flow cytometric analysis. Standard error bars represent 2 times the SE of the mean (SE=SDxsqrt(n)).
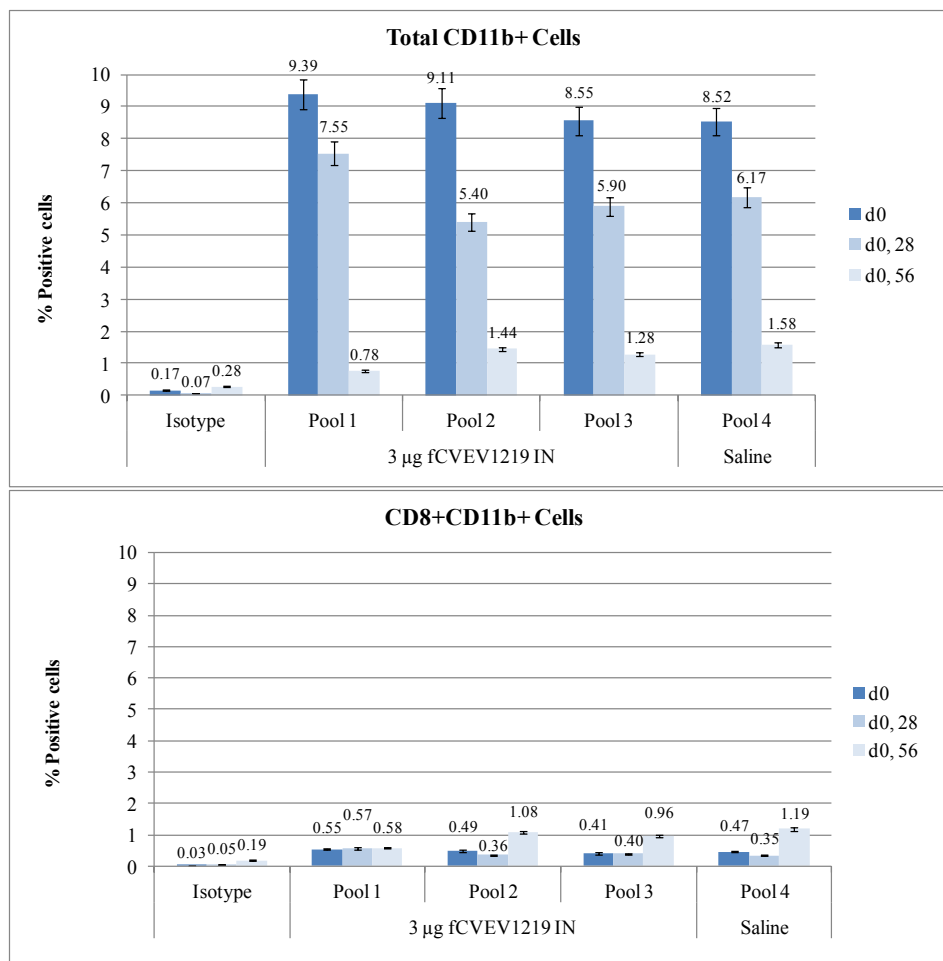
Figure 5.6. CD8 T cell responses in mice vaccinated with formalin-inactivated CVEV1219 (fCVEV1219) vaccine candidate. Groups of BALB/c mice (n=10) were vaccinated intranasally once or twice with 3μg fCVEV1219. Spleens were harvested 7-14 d after each vaccination and 3-4 spleens were pooled for analysis. CD8 cell responses were measured using various fluorescent-labeled antibodies to detect intracellular cytokines and surface markers followed by flow cytometry analysis. Standard error bars represent 2 times the SE of the mean (SE=SDxsqrt(n)).

were relatively high percentages of total CD11b+ cells, there were very low percentages

of CD8+ CD11b+ cells in all groups, vaccinated and unvaccinated and no differences

between groups (Figure 5.6).

In this experiment, B cells were also analyzed to determine the percentage of cells

producing various immunoglobulins. CD19 is a general marker used to identify B cells

and was used in this study to identify which B cells were producing IgA, IgG1 or IgG2a.

Of the B cells measured, IgA-producing B cells were the most predominant, followed by

IgG2a-producing cells. There were very few IgG1-producing B cells noted in this study

(Figure 5.7). These results are in contrast our findings based on ELISA; however it is

important to note that the cells analyzed here were isolated from the spleen and virus-

specific immunoglobulins were not differentiated in this assay; whereas, the cells

analyzed by ELISA were from the serum and the immunoglobulins titered were only the

virus-specific immunoglobulins.

Figure 5.7. B cell responses in mice vaccinated with formalin-inactivated CVEV1219 (fCVEV1219) vaccine candidate. Groups of BALB/c mice (n=10) were vaccinated intranasally once or twice with 3μg fCVEV1219. Spleens were harvested 7-14 d after each vaccination and 3-4 spleens were pooled for analysis. B cell responses were measured using various fluorescent-labeled antibodies to detect intracellular cytokines and surface markers followed by flow cytometric analysis. Standard error bars represent 2 times the SE of the mean (SE=SDxsqrt(n)).

Conclusion

The goal of vaccine development is to produce a product that closely mimics natural infection; thereby stimulating an appropriate and effective immune response. However, because EEEV is a NIAID Category B agent due to its virulence and potential use as a biological weapon, new vaccine candidates should protect against both subcutaneous and aerosol exposure to virulent virus, which can be challenging.

The most significant threat from EEEV comes from its potential use as an aerosolized bioweapon. Our pathogenesis studies revealed that when mice were exposed to aerosolized EEEV, the virus entered the brain through the olfactory mucosa. Therefore an effective vaccine must be able to prevent or limit the infection of the olfactory mucosa and subsequent spread to the brain. While vaccines given parentally can induce a mucosal response, generally vaccines given at the expected site of infection induce a stronger local immune response. By inactivating an attenuated-live virus an additional layer of safety is built into the formulation of the vaccine candidate. Since there is no virus replication during immunization with inactivated vaccines, the virus cannot revert to virulence, as is sometimes seen with modified-live vaccines. In the vaccine studies described in this thesis, 100% protection from an aerosol challenge was achieved when mice were vaccinated with a formalin-inactivated genetically modified strain of EEEV (CVEV1219) intranasally.

In this study we evaluated the systemic and mucosal immune response of an inactivated EEEV vaccine candidate based on different vaccination schedules. We utilized a genetically modified strain of EEEV (CVEV1219), similar to V3526, which was then formalin-inactivated (fCVEV1219). The levels of serum neutralizing antibody

responses were significantly higher in mice receiving two vaccinations versus those only receiving a single vaccination; however, there was no difference between those that were vaccinated on day 0 and 28 and those that were vaccinated at day 0 and 56. Similar results were seen in virus-specific serum IgG levels and IgA levels from all sample sites. The level of virus-specific IgA in the vaginal flush samples were similar to those seen in the nasal flush and bronchoalveolar lavage; therefore, vaginal flush samples are helpful in estimating IgA responses at various mucosal sites in studies where animal survival is desired. However, dilutional effects that occur during collection need to be taken into consideration. Additionally, there was a fair amount of virus-specific IgA in the serum; however, this may represent both the secretory and circulating forms. Importantly, there were significant inter-animal variations in most immunoglobulins measured which resulted in large standard errors in some groups. This is also an important consideration, especially when transitioning products into nonhuman primates where group size may be more limited.

No significant differences were observed in any T or B cells parameters measured when comparing vaccinated and unvaccinated mice. This could be explained by any one of several reasons. First, the splenocytes were not specifically stimulated *in vitro* following collection. Subsequent studies in our lab have shown that a 7-9 day *in vitro* stimulation with either virus or virus-specific peptides may be required to appreciate differences in these cell populations. Secondly, it may be necessary to collect the draining lymph node, as well as the spleen, as cell populations may vary from the localized site to the spleen. Lastly, samples were harvested at times expected for peak immune responses post-vaccination. However, it may be necessary to harvest at various

time points post-vaccination to ensure evaluations of the cell populations are made during

the peak immune response. Nonetheless, these experiments provide the foundation for

future studies examining the mechanism of protection induced by inactivated vaccines.

REFERENCES

Campos, M. and D. L. Godson (2003). "The effectiveness and limitations of immune memory: understanding protective immune responses." Int J Parasitol **33**(5-6): 655-661.

Griffin DE (2007). Alphaviruses. Fields Virology. Knipe DM, Griffin DE, Lamb RAet al. Philadelphia, Lippincott Williams & Wilkins**:** 1024-1067.

Hart, M. K., K. Caswell-Stephan, et al. (2000). "Improved mucosal protection against Venezuelan equine encephalitis virus is induced by the molecularly defined, live-attenuated V3526 vaccine candidate." Vaccine **18**(26): 3067-3075.

Hart, M. K., W. Pratt, et al. (1997). "Venezuelan equine encephalitis virus vaccines induce mucosal IgA responses and protection from airborne infection in BALB/c, but not C3H/HeN mice." Vaccine **15**(4): 363-369.

Martin, S. S., R. R. Bakken, et al. (2010). "Comparison of the immunological responses and efficacy of gamma-irradiated V3526 vaccine formulations against subcutaneous and aerosol challenge with Venezuelan equine encephalitis virus subtype IAB." Vaccine **28**(4): 1031-1040.

Paulsen, M., S. Valentin, et al. (2011). "Modulation of CD4+ T-cell activation by CD95 co-stimulation." Cell Death Differ **18**(4): 619-631.

Sun, Y., J. E. Schmitz, et al. (2005). "Dysfunction of simian immunodeficiency virus/simian human immunodeficiency virus-induced IL-2 expression by central memory CD4+ T lymphocytes." J Immunol **174**(8): 4753-4760.

Woodland, D. L. and J. E. Kohlmeier (2009). "Migration, maintenance and recall of memory T cells in peripheral tissues." Nat Rev Immunol **9**(3): 153-161.

Chapter 6

Conclusion and Future Directions

Eastern equine encephalitis virus (EEEV) is considered the most deadly of the mosquito-borne alphaviruses due to the high case fatality rate associated with clinical infections, reaching as high as 75% in humans and 90% in horses. It is also listed as a category B agent by the NIAID due to its virulence, its potential use as a biological weapon, and the lack of a licensed vaccine or effective antiviral treatment for human infections. Recently a NA EEEV strain FL93-939 has been used in several studies because of its uniform virulence in adult mice. However, little is known about the early events in the pathogenesis of this strain, which are important to understand before it is used extensively to challenge animal models in vaccine development protocols.

We evaluated the pathogenesis of NA EEEV strain FL93-939 in BALB/c mice by three routes of infection, intranasal, aerosol, and subcutaneous. It is clear from these studies that EEEV enters the brain through the olfactory system when mice are exposed either by the intranasal or aerosol route. The mechanism and rapidity in which the virus enters the brain has important vaccine and therapeutic implications. First, for a vaccine to be effective, it must prevent the virus from infecting olfactory neurons. Since the nasal cavity is a mucosal surface, it would be reasonable to expect that an effective vaccine would induce the production of neutralizing IgA as well as IgG. Secondly, since virus was present in the brain within 6 hpi after aerosol exposure, any therapeutic developed would have a very narrow therapeutic window and would need to easily cross the blood-

brain-barrier. These are not insurmountable tasks; however, after years of research, there is still no licensed vaccine or therapeutic available for human use.

Important future directions include further elucidation of the molecular pathogenesis of this virus. This could include such analysis as global gene expression in the brain and target cells using microarray technology, as well as laser capture microdissection (LCM) to differentially select virally-infected and uninfected neurons for further analysis including RNA profiles, miRNA expression, and host protein and signal pathway analysis. The results of these studies will provide a more complete understanding of the early molecular events in the pathogenesis of EEEV and will play an important role in the development of potential therapeutic targets.

While the mouse is a convenient animal model for these types of studies, further characterization of other animal models is needed. There is little information regarding the pathogenesis of aerosolized EEEV in other animal species, if or how the pathogenesis of aerosolized EEEV correlates with subcutaneous exposure, and if these models are truly representative of disease seen in humans. There have been no reported cases of laboratory exposure to aerosolized EEEV and the incidence of natural infection is low; therefore, there is no means to provide for a human clinical trial in an endemic area. Consequently predictive animal models are essential for licensure under the U.S. Food and Drug Administration (FDA) Animal Rule.

To address the lack of an FDA licensed vaccine for EEEV, we optimized several methods of inactivating a genetically-modified strain of EEEV (CVEV1219). Inactivation of a genetically-modified, attenuated strain of EEEV was selected in order to add an additional layer of safety. The protective efficacy studies demonstrated that both

formalin-inactivated and gamma-irradiated CVEV1219 provided 100% protection in mice against an aerosol challenge when administered by various doses, routes, and schedules. Furthermore, the immunogenicity studies with these vaccine candidates provided important information regarding minimal serum neutralizing antibody and serum IgG titers required to protect 90% and 99% of mice against an aerosol challenge. While both fCVEV1219 and gCVEV1219 proved to be viable second-generation vaccine candidates, iCVEV1219 did not. This was somewhat surprising given the success seen in the mouse model using INA-inactivated V3526. The differences noted in these studies may be due to inherent viral differences between EEEV and VEEV.

Important future directions will include determining the duration of immunity as well as the effects of various adjuvants. In order to determine which adjuvants may improve the protective efficacy of future vaccine candidates we must first understand the importance of the innate and adaptive (humoral and cell-mediated) immunity in post-exposure survival. Ideally, a second-generation EEEV vaccine candidate will protect against an aerosol exposure with a single vaccination, the onset of protection will be rapid, the duration of protection will be at least 1 year, and it will be able to be combined with VEEV and WEEV in a trivalent vaccine with minimal interference.

EEEV has received little attention in the medical research and biodefense communities; however, it is an important pathogen to study for two reasons. First, despite a relatively low incidence of natural infection in the U.S., the resultant encephalitis can be deadly and those that survive often have significant neurologic sequelae. Secondly, the pathogen characteristics and lethality make this virus an important agent to consider as a potential biological weapon. While there are still

significant gaps in the understanding of the pathogenesis of this virus in various species and routes of infection, these studies provided important first steps in developing a knowledge base from which to move forward.

REFERENCES

(2006). "Eastern equine encephalitis--New Hampshire and Massachusetts, August-September 2005." MMWR Morb Mortal Wkly Rep **55**(25): 697-700.

Adams, A. P., J. F. Aronson, et al. (2008). "Common marmosets (Callithrix jacchus) as a nonhuman primate model to assess the virulence of eastern equine encephalitis virus strains." J Virol **82**(18): 9035-9042.

Aguilar PV, Adams AP, et al. (2008). "Structural and nonstructural protein genome regions of eastern equine encephalitis virus are determinants of interferon sensitivity and murine virulence." J Virol **82**(10): 4920-4930.

Aguilar, P. V., S. Paessler, et al. (2005). "Variation in interferon sensitivity and induction among strains of eastern equine encephalitis virus." J Virol **79**(17): 11300-11310.

Aguilar, P. V., R. M. Robich, et al. (2007). "Endemic eastern equine encephalitis in the Amazon region of Peru." Am J Trop Med Hyg **76**(2): 293-298.

Alsharifi, M., Y. Furuya, et al. (2009). "Intranasal flu vaccine protective against seasonal and H5N1 avian influenza infections." PLoS One **4**(4): e5336.

Arrigo, N. C., A. P. Adams, et al. (2010). "Evolutionary patterns of eastern equine encephalitis virus in North versus South America suggest ecological differences and taxonomic revision." J Virol **84**(2): 1014-1025.

Bauer, R. W., M. S. Gill, et al. (2005). "Naturally occurring eastern equine encephalitis in a Hampshire wether." J Vet Diagn Invest **17**(3): 281-285.

Brault, A. C., A. M. Powers, et al. (1999). "Genetic and antigenic diversity among eastern equine encephalitis viruses from North, Central, and South America." Am J Trop Med Hyg **61**(4): 579-586.

Calisher, C. H. (1994). "Medically important arboviruses of the United States and Canada." Clin Microbiol Rev **7**(1): 89-116.

Campos, M. and D. L. Godson (2003). "The effectiveness and limitations of immune memory: understanding protective immune responses." Int J Parasitol **33**(5-6): 655-661.

Charles PC, Walters E, et al. (1995). "Mechanism of neuroinvasion of Venequelan equine encephalitis virus in the mouse." Virology 208: 662-671.

Cheng RH, Kuhn RJ, et al. (1995). "Nucleocapsid and glycoprotein organization in an enveloped virus." Cell **80**(4): 621-630.

Corniou, B., P. Ardoin, et al. (1972). "First isolation of a South American strain of Eastern Equine virus from a case of encephalitis in Trinidad." Trop Geogr Med **24**(2): 162-167.

Day, J. F. and L. M. Stark (1996). "Transmission patterns of St. Louis encephalitis and eastern equine encephalitis viruses in Florida: 1978-1993." J Med Entomol **33**(1): 132-139.

Del Piero, F., P. A. Wilkins, et al. (2001). "Clinical, pathologic, immunohistochemical, and virologic findings of eastern equine encephalomyelitis in two horses." Vet Pathol **38**(4): 451-456.

Deresiewicz, R. L., S. J. Thaler, et al. (1997). "Clinical and neuroradiographic manifestations of eastern equine encephalitis." N Engl J Med **336**(26): 1867-1874.

DeTulleo L and K. T (1998). "The clathrin endocytic pathway in viral infection." EMBO J **17**(16): 4585-4593.

Ding M and S. MJ (1989). "Evidence that Sindbis virus nsP2 is an autoprotease which processes the virus nonstructural polyprotein." Virology **171**: 280-284.

Dremov, D. P. and R. G. Solianik (1977). "[Use of rabbits for study of the neurovirulence of attenuated variants of eastern equine encephalomyelitis virus]." Virologie **28**(4): 263-269.

Dremov, D. P., R. G. Solyanik, et al. (1978). "Attenuated variants of eastern equine encephalomyelitis virus: pathomorphological, immunofluorescence and virological studies of infection in Syrian hamsters." Acta Virol **22**(2): 139-145.

Dunbar, M. R., M. W. Cunningham, et al. (1998). "Seroprevalence of selected disease agents from free-ranging black bears in Florida." J Wildl Dis **34**(3): 612-619.

Dyce, K. M., W. O. Sack, et al. (1987). Textbook of Veterinary Anatomy. Philadelphia, W.B. Saunders Company.

Elmore, S. (2007). "Apoptosis: a review of programmed cell death." Toxicol Pathol 35(4): 495-516.

Elvinger, F., A. D. Liggett, et al. (1994). "Eastern equine encephalomyelitis virus infection in swine." J Am Vet Med Assoc **205**(7): 1014-1016.

Espinosa, B. J., S. C. Weaver, et al. (2009). "Susceptibility of the Aotus nancymaae owl monkey to eastern equine encephalitis." Vaccine **27**(11): 1729-1734.

Farrar, M. D., D. L. Miller, et al. (2005). "Eastern equine encephalitis in dogs." J Vet Diagn Invest **17**(6): 614-617.

Festjens, N., T. Vanden Berghe, et al. (2006). "Necrosis, a well-orchestrated form of cell demise: signalling cascades, important mediators and concomitant immune response." Biochim Biophys Acta 1757(9-10): 1371-1387.

Fiers, W., R. Beyaert, et al. (1999). "More than one way to die: apoptosis, necrosis and reactive oxygen damage." Oncogene 18(54): 7719-7730.

Frolov I and S. S (1996). "Translation of Sindbis virus mRNA: analysis of sequences downstream of the initiating AUG codon that enhance translation." J Virol **70**: 1182-1190.

Furuya, Y., M. Regner, et al. (2010). "Effect of inactivation method on the cross-protective immunity induced by whole 'killed' influenza A viruses and commercial vaccine preparations." J Gen Virol **91**(Pt 6): 1450-1460.

Gaedigk-Nitschko K and S. MJ (1990). "The Sindbis virus 6K protein can be detected in virions and is acylated with fatty acids." Virology **175**(1): 274-281.

Gardner, C. L., C. W. Burke, et al. (2008). "Eastern and Venezuelan equine encephalitis viruses differ in their ability to infect dendritic cells and macrophages: impact of altered cell tropism on pathogenesis." J Virol **82**(21): 10634-10646.

Gardner, C. L., G. D. Ebel, et al. (2011). "Heparan sulfate binding by natural eastern equine encephalitis viruses promotes neurovirulence." Proc Natl Acad Sci U S A 108(38): 16026-16031.

Gardner, C. L., J. Yin, et al. (2009). "Type I interferon induction is correlated with attenuation of a South American eastern equine encephalitis virus strain in mice." Virology **390**(2): 338-347.

Garman, R. H. (2011). "Histology of the central nervous system." Toxicol Pathol 39(1): 22-35.

Glomb-Reinmund S and K. M (1988). "The role of low pH and disulfide shuffling in the entry and fusion of Semliki Forest virus and Sindbis virus." Virology **248**(2): 372-381.

Goldfield, M., J. N. Welsh, et al. (1968). "The 1959 outbreak of Eastern encephalitis in New Jersey. 5. The inapparent infection:disease ratio." Am J Epidemiol **87**(1): 32-33.

Golstein, P. and G. Kroemer (2007). "Cell death by necrosis: towards a molecular definition." Trends Biochem Sci 32(1): 37-43.

Gottdenker, N. L., E. W. Howerth, et al. (2003). "Natural infection of a great egret (Casmerodius albus) with eastern equine encephalitis virus." J Wildl Dis **39**(3): 702-706.

Griffin DE (2007). Alphaviruses. Fields Virology. Knipe DM, Griffin DE, Lamb RAet al. Philadelphia, Lippincott Williams & Wilkins**:** 1024-1067.

Griffin, D. E., B. Levine, et al. (1994). "Age-dependent susceptibility to fatal encephalitis: alphavirus infection of neurons." Arch Virol Suppl 9: 31-39.

Guy, J. S., T. D. Siopes, et al. (1995). "Experimental transmission of eastern equine encephalitis virus and Highlands J virus via semen of infected tom turkeys." Avian Dis **39**(2): 337-342.

Guyton, A. C. (1947). "Measurement of the respiratory volumes of laboratory animals." Am J Physiol 150(1): 70-77.

Hardy RW and S. JH (1988). "Processing of the nonstructural polyproteins of Sindbis virus: study of the kinetics in vivo using monospecific antibodies." J Virol **62**: 998-1007.

Hart, M. K., K. Caswell-Stephan, et al. (2000). "Improved mucosal protection against Venezuelan equine encephalitis virus is induced by the molecularly defined, live-attenuated V3526 vaccine candidate." Vaccine **18**(26): 3067-3075.

Hart, M. K., C. Lind, et al. (2001). "Onset and duration of protective immunity to IA/IB and IE strains of Venezuelan equine encephalitis virus in vaccinated mice." Vaccine **20**(3-4): 616-622.

Hart, M. K., W. Pratt, et al. (1997). "Venezuelan equine encephalitis virus vaccines induce mucosal IgA responses and protection from airborne infection in BALB/c, but not C3H/HeN mice." Vaccine **15**(4): 363-369.

Helenius A, Kartenbeck J, et al. (1980). "On the entry of Semliki Forest virus into BHK-21 cells." J Cell Biol **84**: 404-420.

Hotchkiss, R. S., A. Strasser, et al. (2009). "Cell death." N Engl J Med 361(16): 1570-1583.

http://www.fda.gov/BiologicsBloodVaccines/Vaccines/ApprovedProducts/ucm142577.htm. (2009). "Japanese Encephalitis Virus Vaccine, Inactivated, Adsorbed Approval Letter." Retrieved November, 29, 2011, 2011.

Hurst, E. W. (1936). "Infection of the rhesus monkey (Macaca mulatta) and the guinea-pig with the virus of equine encephalomyelitis." J Path Bact **42**: 371-402.

Kuhn RJ (2007). Togaviridae: The viruses and their replication. Fields Virology. Knipe DM, Griffin DE, Lamb RAet al. Philadelphia, Lippincott Williams & Wilkins**:** 1001-1022.

Labrada, L., X. H. Liang, et al. (2002). "Age-dependent resistance to lethal alphavirus encephalitis in mice: analysis of gene expression in the central nervous system and identification of a novel interferon-inducible protective gene, mouse ISG12." J Virol 76(22): 11688-11703.

Letson, G. W., R. E. Bailey, et al. (1993). "Eastern equine encephalitis (EEE): a description of the 1989 outbreak, recent epidemiologic trends, and the association of rainfall with EEE occurrence." Am J Trop Med Hyg **49**(6): 677-685.

Liu, C., D. W. Voth, et al. (1970). "A comparative study of the pathogenesis of western equine and eastern equine encephalomyelitis viral infections in mice by intracerebral and subcutaneous inoculations." J Infect Dis **122**(1): 53-63.

Lowy, R. J., G. A. Vavrina, et al. (2001). "Comparison of gamma and neutron radiation inactivation of influenza A virus." Antiviral Res **52**(3): 261-273.

Marsh M, Bolzau E, et al. (1983). "Penetration of Semliki Forest virus from acidic prelysosomal vacuoles." Cell **32**: 931-940.

Martin, S. S., R. R. Bakken, et al. (2010). "Comparison of the immunological responses and efficacy of gamma-irradiated V3526 vaccine formulations against subcutaneous and aerosol challenge with Venezuelan equine encephalitis virus subtype IAB." Vaccine **28**(4): 1031-1040.

Martin, S. S., R. R. Bakken, et al. (2010). "Evaluation of formalin inactivated V3526 virus with adjuvant as a next generation vaccine candidate for Venezuelan equine encephalitis virus." Vaccine **28**(18): 3143-3151.

Mathews, J. H. and J. T. Roehrig (1989). "Specificity of the murine T helper cell immune response to various alphaviruses." J Gen Virol **70 (Pt 11)**: 2877-2886.

McBride, M. P., M. A. Sims, et al. (2008). "Eastern equine encephalitis in a captive harbor seal (Phoca vitulina)." J Zoo Wildl Med **39**(4): 631-637.

McLean, R. G., W. J. Crans, et al. (1995). "Experimental infection of wading birds with eastern equine encephalitis virus." J Wildl Dis **31**(4): 502-508.

Monath, T. P., M. S. Sabattini, et al. (1985). "Arbovirus investigations in Argentina, 1977-1980. IV. Serologic surveys and sentinel equine program." Am J Trop Med Hyg **34**(5): 966-975.

Morgan, I. M. (1941). "INFLUENCE OF AGE ON SUSCEPTIBILITY AND ON IMMUNE RESPONSE OF MICE TO EASTERN EQUINE ENCEPHALOMYELITIS VIRUS." J Exp Med **74**(2): 115-132.

Nathanson, N., P. D. Stolley, et al. (1969). "Eastern equine encephalitis. Distribution of central nervous system lesions in man and Rhesus monkey." J Comp Pathol **79**(1): 109-115.

Nolen-Walston, R., D. Bedenice, et al. (2007). "Eastern equine encephalitis in 9 South American camelids." J Vet Intern Med **21**(4): 846-852.

Orvedahl, A. and B. Levine (2008). "Autophagy and viral neurovirulence." Cell Microbiol 10(9): 1747-1756.

Orvedahl, A., S. MacPherson, et al. (2010). "Autophagy protects against Sindbis virus infection of the central nervous system." Cell Host Microbe 7(2): 115-127.

Paessler, S., R. Z. Fayzulin, et al. (2003). "Recombinant sindbis/Venezuelan equine encephalitis virus is highly attenuated and immunogenic." J Virol **77**(17): 9278-9286.

Paessler, S., P. Aguilar, et al. (2004). "The hamster as an animal model for eastern equine encephalitis--and its use in studies of virus entrance into the brain." J Infect Dis **189**(11): 2072-2076.

Paredes AM, Brown DT, et al. (1993). "Three-dimensional structure of a membrane-containing virus." Proc Natl Acad Sci USA **90**(19): 9095-9099.

Parker, M. D., M. J. Buckley, et al. (2010). "Antibody to the E3 glycoprotein protects mice against lethal venezuelan equine encephalitis virus infection." J Virol **84**(24): 12683-12690.

Paulsen, M., S. Valentin, et al. (2011). "Modulation of CD4+ T-cell activation by CD95 co-stimulation." Cell Death Differ **18**(4): 619-631.

Pratt, W., M. K. Hart, et al. (2006). Alphaviruses. Biodefense Research Methodology and Animal Models. J. R. Swearengen. Boca Raton, Florida, CRC Taylor & Francis**:** 181-206.

Przelomski, M. M., E. O'Rourke, et al. (1988). "Eastern equine encephalitis in Massachusetts: a report of 16 cases, 1970-1984." Neurology **38**(5): 736-739.

Pursell, A. R., F. E. Mitchell, et al. (1976). "Naturally occurring and experimentally induced eastern encephalomyelitis in calves." J Am Vet Med Assoc **169**(10): 1101-1103.

Pursell, A. R., J. C. Peckham, et al. (1972). "Naturally occurring and artificially induced eastern encephalomyelitis in pigs." J Am Vet Med Assoc **161**(10): 1143-1147.

Raviv, Y., R. Blumenthal, et al. (2008). "Hydrophobic inactivation of influenza viruses confers preservation of viral structure with enhanced immunogenicity." J Virol **82**(9): 4612-4619.

Raviv, Y., Y. Salomon, et al. (1987). "Selective labeling of proteins in biological systems by photosensitization of 5-iodonaphthalene-1-azide." Proc Natl Acad Sci U S A **84**(17): 6103-6107.

Raviv, Y., M. Viard, et al. (2005). "Inactivation of retroviruses with preservation of structural integrity by targeting the hydrophobic domain of the viral envelope." J Virol **79**(19): 12394-12400.

Reed, D. S., M. G. Lackemeyer, et al. (2007). "Severe encephalitis in cynomolgus macaques exposed to aerosolized Eastern equine encephalitis virus." J Infect Dis **196**(3): 441-450.

Reed, D. S., T. Larsen, et al. (2005). "Aerosol exposure to western equine encephalitis virus causes fever and encephalitis in cynomolgus macaques." J Infect Dis **192**(7): 1173-1182.

Reichert, E., A. Clase, et al. (2009). "Alphavirus antiviral drug development: scientific gap analysis and prospective research areas." Biosecur Bioterror **7**(4): 413-427.

Ross, W. A. and J. B. Kaneene (1996). "Evaluation of outbreaks of disease attributable to eastern equine encephalitis virus in horses." J Am Vet Med Assoc **208**(12): 1988-1997.

Roy, C. J., D. S. Reed, et al. (2009). "Pathogenesis of aerosolized Eastern Equine Encephalitis virus infection in guinea pigs." Virol J **6**(1): 170.

Ryzhikov, A. B., E. I. Ryabchikova, et al. (1995). "Spread of Venezuelan equine encephalitis virus in mice olfactory tract." Arch Virol 140(12): 2243-2254.

Schmitt, S. M., T. M. Cooley, et al. (2007). "An outbreak of Eastern equine encephalitis virus in free-ranging white-tailed deer in Michigan." J Wildl Dis **43**(4): 635-644.

Sharma, A., P. Gupta, et al. (2011). "Safety and protective efficacy of INA-inactivated Venezuelan equine encephalitis virus: implication in vaccine development." Vaccine **29**(5): 953-959.

Sharma, A., Y. Raviv, et al. (2007). "Complete inactivation of Venezuelan equine encephalitis virus by 1,5-iodonaphthylazide." Biochem Biophys Res Commun **358**(2): 392-398.

Simmons DT and S. JH (1972). "Replication of Sindbis virus. I. Relative size and genetic content of the 26S and 49S RNA." J Mol Biol **71**: 599-613.

Spalding, M. G., R. G. McLean, et al. (1994). "Arboviruses in water birds (Ciconiiformes, Pelecaniformes) from Florida." J Wildl Dis **30**(2): 216-221.

Steele, K. E., K. J. Davis, et al. (1998). "Comparative neurovirulence and tissue tropism of wild-type and attenuated strains of Venezuelan equine encephalitis virus administered by aerosol in C3H/HeN and BALB/c mice." Vet Pathol 35(5): 386-397.

Steele, K. E. and N. Twenhafel (2010). "Review paper: Pathology of animal models of alphavirus encephalitis." Vet Pathol **45**(7): 790-805.

Strizki, J. M. and P. M. Repik (1995). "Differential reactivity of immune sera from human vaccinees with field strains of eastern equine encephalitis virus." Am J Trop Med Hyg **53**(5): 564-570.

Sun, Y., J. E. Schmitz, et al. (2005). "Dysfunction of simian immunodeficiency virus/simian human immunodeficiency virus-induced IL-2 expression by central memory CD4+ T lymphocytes." J Immunol **174**(8): 4753-4760.

Tate, C. M., E. W. Howerth, et al. (2005). "Eastern equine encephalitis in a free-ranging white-tailed deer (Odocoileus virginianus)." J Wildl Dis **41**(1): 241-245.

Tenbroeck, C., E. W. Hurst, et al. (1935). "EPIDEMIOLOGY OF EQUINE ENCEPHALOMYELITIS IN THE EASTERN UNITED STATES." J Exp Med **62**(5): 677-685.

Tuttle, A. D., T. G. Andreadis, et al. (2005). "Eastern equine encephalitis in a flock of African penguins maintained at an aquarium." J Am Vet Med Assoc **226**(12): 2059-2062, 2003.

Van den Broeck, W., A. Derore, et al. (2006). "Anatomy and nomenclature of murine lymph nodes: Descriptive study and nomenclatory standardization in BALB/cAnNCrl mice." J Immunol Methods 312(1-2): 12-19.

Veazey, R. S., C. C. Vice, et al. (1994). "Pathology of eastern equine encephalitis in emus (Dromaius novaehollandiae)." Vet Pathol **31**(1): 109-111.

Viard, M., S. D. Ablan, et al. (2008). "Photoinduced reactivity of the HIV-1 envelope glycoprotein with a membrane-embedded probe reveals insertion of portions of the HIV-1 Gp41 cytoplasmic tail into the viral membrane." Biochemistry **47**(7): 1977-1983.

Vogel P, Kell WM, et al. (2005). "Early events in the pathogenesis of eastern equine encephalitis virus in mice." Am J Pathol **166**(1): 159-171.

Wang YF, Sawicki SG, et al. (1991). "Sindbis virus nsP1 functions in negative-strand RNA synthesis." J Virol **65**: 985-988.

Warfield, K. L., D. L. Swenson, et al. (2007). "Ebola virus inactivation with preservation of antigenic and structural integrity by a photoinducible alkylating agent." J Infect Dis **196 Suppl 2**: S276-283.

Webster, L. T. and F. H. Wright (1938). "RECOVERY OF EASTERN EQUINE ENCEPHALOMYELITIS VIRUS FROM BRAIN TISSUE OF HUMAN CASES OF ENCEPHALITIS IN MASSACHUSETTS." Science **88**(2283): 305-306.

White J, K. J, et al. (1980). "Fusion of Semliki Forest virus with the plasma membrane can be induced by low pH." J Cell Biol **87**(264-272).

Williams, S. M., R. M. Fulton, et al. (2000). "Diagnosis of eastern equine encephalitis by immunohistochemistry in two flocks of Michigan ring-neck pheasants." Avian Dis **44**(4): 1012-1016.

Woodland, D. L. and J. E. Kohlmeier (2009). "Migration, maintenance and recall of memory T cells in peripheral tissues." Nat Rev Immunol **9**(3): 153-161.

Zeiss, C. J. (2003). "The apoptosis-necrosis continuum: insights from genetically altered mice." Vet Pathol 40(5): 481-495.

Zong, W. X. and C. B. Thompson (2006). "Necrotic death as a cell fate." Genes Dev 20(1): 1-15.

ABBREVIATIONS

AE	Aerosol
ARIMA	Autoregressive integrated moving average
BAL	Bronchoalveolar lavage
BHK	Baby hamster kidney
BSL-3	Biosafety level-3
CBC	Complete blood count
CD62E	E-selectin
CD62L	L-selectin
CDC	Centers for Disease Control
CMI	Cell mediated immunity
CNS	Central nervous system
CPE	Cytopathic effect
CVEV1219	Genetically modified strain of EEEV
DAB	Diaminobenzidine
DPBS	Dulbecco's phosphate buffered saline
EBME	Basal medium eagle with earle's salts
EDTA	Ethylenediamenetetraacetic acid
EEEV	Eastern equine encephalitis virus
EEE	Eastern equine encephalitis
EEE-HMAF	EEE hyperimmune mouse acites fluid
ELISA	Enzyme-linked immunosorbent assay
EMEM	Eagle's minimum essential medium
FBS	Fetal bovine serum
fCVEV1219	Formalin-inactivated CVEV1219
FDA	Food and Drug Administration
gCVEV1219	Gamma-irradiated CVEV1219
G-CSF	Granulocyte colony stimulating factor
GM-CSF	Granulocyte-monocyte colony stimulating factor
HBSS	Hank's balanced salt solution
HIV	Human immunodeficiency virus
iCVEV1219	INA-inactivated CVEV1219
iEEEV	Inactivated EEEV
IFA	Immunofluorescent assay
IFN	Interferon
IHC	Immunohistochemistry
IM	Intramuscular
IMPAC[6]	Integrated multi-patient anesthesia machine
IN	Intranasal
INA	1,5-iodonaphthylazide
IND	Investigational new drug
JEV	Japanese encephalitis virus
LCM	Laser capture microdissection
LD_{50}	Lethal dose 50
LD_{99}	Lethal dose 99
MCP-1	Macrophage chemoattractant protein
MIG	Monokine induced by IFN-γ
MIP	Macrophage inflammatory protein
MTTD	Mean time to death
NA	North American
NEAA	Non-essential amino acids
NF	Nasophargyneal flush
NIAID	National Institute of Allergy and Infectious Diseases
NK	Natural killer

PBS	Phosphate buffered saline
PBST	PBS with Tween 20
PBSTM	PBS with Tween 20 and nonfat dry milk
PFU	Plaque forming unit
PRNT	Plaque-reduction neutralization test
RANTES	Regulated upon activation, normal T-cell expressed and secreted
SA	South American
SC	Subcutaneous
SD TTD	Standard deviation time to death
SFV	Semliki-forest virus
SINV	Sindbis virus
SIV	Simian immunodeficiency virus
TNF	Tumor necrosis factor
USAMRIID	United States Army Medical Research Institute of Infectious Diseases
UTMB	University of Texas Medical Branch
V3526	Genetically modified strain of VEEV
VEEV	Venezuelan equine encephalitis virus
WBC	White blood count
WEEV	Western equine encephalitis virus